

Advanced oxidation of fluoroquinolone antibiotics in water by heterogeneous photocatalysis

ir. Xander Van Doorslaer

2014

Advanced Oxidation TiO_2

of

Fluoroquinolone Antibiotics in water

by

Heterogeneous Photocatalysis

ir. Xander VAN DOORSLAER

ISBN 978-9-0598970-2-1



9 789059 897021



FACULTEIT BIO-INGENIEURSWETENSCHAPPEN



Promotors: Prof. dr. ir. Jo Dewulf
Prof. dr. ir. Kristof Demeestere
Research group EnVOC
Department of Sustainable Organic Chemistry and Technology
Faculty of Bioscience Engineering
Ghent University

Dean: Prof. dr. ir. Guido Van Huylenbroeck

Rector: Prof. dr. Anne De Paepe

ir. Xander Van Doorslaer

Advanced oxidation of fluoroquinolone antibiotics in water
by heterogeneous photocatalysis

Thesis submitted in fulfillment of the requirements
for the degree of Doctor (PhD) in Applied Biological Sciences

Dutch translation of the title: Geavanceerde oxidatie van fluorchinolon antibiotica in water door middel van heterogene fotokatalyse.

Cover: naar een ontwerp van Xander Van Doorslaer

Printed: University Press, info@universitypress.be

Van Doorslaer X. 2014 Advanced oxidation of fluoroquinolone antibiotics in water by heterogeneous photocatalysis

ISBN-number: 978-90-5989-702-1

The author and the promotors give the authorisation to consult and to copy parts of this work for personal use only. Every other use is subject to the copyright laws. Permission to reproduce any material contained in this work should be obtained from the author.

Woord Vooraf

Herman van Veen had gelijk. We moeten rennen, springen, vliegen, duiken, vallen, opstaan en WEER DOORGAAN. Een evidentie voor wetenschappers, want onderzoek blijft onderzoek en loopt niet steeds van een leien dakje. Het verblijf in Taiwan was tegelijk leerrijk maar ook ontnuchterend.

Mijn grootste dank gaat dan ook uit naar mijn beide promotoren Jo Dewulf en Kristof Demeestere die mij met raad en daad bijstonden en mij steeds hebben gemotiveerd om er te blijven voor gaan. Het was een zeer aangename en leerrijke samenwerking.

Daarenboven voelde doctoreren niet eens aan als werken. Dit is te danken aan de collega's bij EnVOC, maar ook de mensen van dé Synthese mochten er wezen. De losse sfeer, de desk volleyball, de regelmaat in pintjes, de geniale kerstfeestjes, maar vooral de deugddoende koffiepauzes maakten het zeer aangenaam vertoeven op de werkvloer.

Minstens even belangrijk was de hulp van vrienden; dit zowel op het thuisfront als de bio-ingenieur kliek. Echt bedankt voor de vele mopjes over *'doctoraatstudentjes'* en *'werken'* aan de Universiteit.

Bedankt mama en papa om me de kans te geven deze studies aan te gaan en met succes te voltooien. Jullie steun en trots was onvermoeibaar. Ook gaat er dank naar de schoonfamilie en dan vooral “den bompa” die vol ongeduld heeft gewacht op dit moment.

Als laatste maar niet de minste, wil ik Emilie bedanken. De laatste maanden zag je me typen tijdens het opstaan, tijdens het eten, tijdens het tv kijken en tijdens het slapengaan. Ja, zelfs op snowboardreis was het typen. Bedankt voor je eindeloze geduld, begrip en - ik moest het er expliciet bij vermelden, beste lezer - de was, de boodschappen, het koken, de kuis en alle andere huishoudelijke taken die je de laatste maanden op jou nam. Ik mag met zekerheid zeggen dat jij op 23-08-2014 van mij een dikke ‘JA, IK WIL’ krijgt.

Xander VAN DOORSLAER, 2014

Table of Contents

Abbreviation index.....	vii
Notation index.....	x
Introduction, Outline, and Research objectives	1
Part I Literature review: Fluoroquinolones as emerging environmental pollutants, and heterogeneous photocatalysis as an innovative treatment technique	
1.0 Introduction	13
1.1 Fluoroquinolones as emerging micropollutants	14
1.1.1 Introduction.....	14
1.1.2 Chemical structure and therapeutic use.....	17
1.1.3 Physical-chemical properties relevant for environmental FQ behavior.....	20
1.1.4 Sources.....	27
1.1.4.1 Sources from human applications.....	27
1.1.4.2 Sources from veterinary applications	31
1.1.5 Pathways.....	33
1.1.5.1 WWTPs.....	33
1.1.5.2 Landfills.....	40
1.1.6 Occurrence in the environment.....	41
1.1.6.1 Aqueous matrices	41
1.1.6.2 Sediment and soil.....	44
1.1.6.3 Biota	45

1.1.7	Environmental fate and behavior.....	47
1.1.7.1	Partitioning in the environment.....	47
1.1.7.2	Conversion in the environment.....	49
1.1.7.3	Bioaccumulation.....	50
1.1.8	Ecological effects.....	51
1.1.9	Conclusions.....	55
1.2	Heterogenous photocatalysis: an AOP for innovative environmental technology.....	58
1.2.1	Introduction.....	58
1.2.2	Advanced Oxidation Processes.....	58
1.2.3	Heterogeneous photocatalysis.....	60
1.2.3.1	Definition and principles.....	60
1.2.3.2	Photocatalysts.....	62
1.2.3.3	Applications: heterogeneous photocatalysis for the removal of pharmaceutical residues.....	64
Part II	Photocatalytic removal of moxifloxacin: adsorption, effect of process parameters, and reactive species	
2.0	Introduction.....	67
2.1	UV-A and UV-C induced photolytic and photocatalytic degradation of aqueous ciprofloxacin and moxifloxacin: effect of pH and role of adsorption.....	68
2.1.1	Materials and methods.....	68
2.1.1.1	Chemicals and experimental setup.....	68
2.1.1.2	Analytic methods.....	70
2.1.1.3	Degradation kinetics.....	70
2.1.1.4	Partitioning of FQs between an aqueous phase and TiO ₂	71
2.1.2	Results and Discussion.....	74
2.1.2.1	Photolysis.....	74
2.1.2.2	Heterogeneous photocatalysis.....	78
2.1.2.3	Adsorption and estimation of the partition ratios.....	81
2.1.3	Conclusions.....	85
2.2	TiO ₂ mediated heterogeneous photocatalytic degradation of moxifloxacin: operational variables and scavenger study.....	86
2.2.1	Materials and methods.....	86

2.2.1.1	Chemicals and experimental setup	86
2.2.1.2	Effect of radical inhibitors.....	86
2.2.1.3	Analytic methods.....	87
2.2.2	Results and Discussion	87
2.2.2.1	Initial MOX concentration	87
2.2.2.2	Catalyst concentration and stirring speed	91
2.2.2.3	Oxygen concentration	96
2.2.2.4	Temperature	97
2.2.2.5	Effect of radical inhibitors.....	99
2.2.3	Conclusions.....	103
 Part III Identification of moxifloxacin photocatalytic degradation products		
3.1	Introduction	107
3.2	Material and methods.....	108
3.2.1	Chemicals and experimental setup	108
3.2.2	Analytic methods.....	109
3.2.2.1	TOC and MOX determination	109
3.2.2.2	Degradation product identification	109
3.3	Results and Discussion.....	110
3.3.1	Degree of MOX mineralization.....	110
3.3.2	Identification of degradation products.....	111
3.4	Conclusions.....	119
 Part IV Biological endpoints: residual antibacterial activity and algal growth inhibition		
4.0	Introduction	123
4.1	Residual antibacterial activity of a MOX solution after photocatalytic treatment	125
4.1.1	Materials and methods	125
4.1.1.1	Chemicals and experimental setup	125
4.1.1.2	Antibacterial activity	125
4.1.2	Results and Discussion	126
4.1.3	Conclusions.....	132

4.2	Ecotoxicity of a MOX solution after photocatalytic treatment towards a green alga non-target organism	133
4.2.1	Materials and methods.....	133
4.2.1.1	Chemicals	133
4.2.1.2	Algal toxicity of MOX and its photocatalytic degradation mixture: growth inhibition tests	133
4.2.1.3	Calculations and statistics.....	135
4.2.2	Results and Discussion	136
4.2.2.1	Test validity and internal quality control.....	136
4.2.2.2	Algal toxicity of pure MOX and CIP.....	137
4.2.2.3	Photocatalytic degradation: moxifloxacin removal and algal growth inhibition	139
4.2.2.4	Identified degradation products: structural characteristics and possible impact on biological activity and cell permeation	141
4.2.3	Conclusions.....	142

Part V Heterogeneous photocatalysis of moxifloxacin in hospital effluent: effect of selected matrix constituents

5.1	Introduction	145
5.2	Materials and methods.....	146
5.2.1	Chemicals and experimental setup	146
5.2.2	Analytical methods.....	148
5.2.3	Experimental approach.....	149
5.3	Results and Discussion.....	152
5.3.1	Photocatalytic degradation of MOX in (un)filtered hospital effluent water.....	152
5.3.2	Effect of inorganic constituents.....	154
5.3.3	Effect of organic constituents	157
5.3.3.1	Effect of humic acid	157
5.3.3.2	Effect of different types of DOM	162
5.3.4	Combined effect of inorganic and organic constituents	163
5.4	Conclusions	166

Part VI General Discussion and Perspectives

6.1	Scientific overview, Progress & Discussion	169
6.2	Photocatalytic mechanisms: adsorption and reactive species	173
6.2.1	Adsorption-desorption equilibrium	173
6.2.2	Reactive species.....	175
6.3	Photocatalytic degradation of MOX: effect of process parameters	176
6.4	Degradation products.....	178
6.5	Biological endpoints	179
6.6	From synthetic to real environmental matrices: degradation in the effluent of a hospital WWTP	181
6.7	Challenges.....	185
6.8	Perspectives.....	189
	Summary.....	195
	Samenvatting	201
	Addenda	207
	Bibliography	223
	Curriculum Vitae	261

Abbreviation index

AOP	Advanced oxidation process
AOX	Adsorbable organohalogens
BAF	Bioaccumulation factor
BET	Brunauer-Emmett-Teller
BHI	Brain hearth infusion
BOD	Biochemical oxygen demand
BSA	Bovine serum albumin
CB	Conduction band
CCAP	Culture Collection of Algae and Protozoa
CEC	Cation exchange capacity
CI	Confidence interval
CIP	Ciprofloxacin
CLINA	Clinafloxacin
COD	Chemical oxygen demand
Comp	Component
DANO	Danofloxacin
DBE	Double bond equivalent
DI	Difloxacin
DNA	Desoxyribonucleinic acid
DOM	Dissolved organic matter
DP	Degradation product
EC	European Commission
EC-50	Median effect concentration
ECDC	European Center for Disease Prevention and Control
ENRO	Enrofloxacin

ESAC	European Surveillance of Antimicrobial Consumption
ESI	Electrospray ionization
EU	European Union
FA	Fulvic acid
FLU	Flumequine
FQ	Fluoroquinolone
FWHM	Full width at half maximum
GATI	Gatifloxacin
Gen	Generation
HA	Humic acid
HPLC	High performance liquid chromatography
HQ	Hazard quotient
HRMS	High resolution mass spectrometry
Hum	Human
IC	Inorganic carbon
ISC	Inter system crossing
ISO	Isopropanol
KI	Potassium iodide
LEVO	Levofloxacin
LOD	Limit of detection
LOME	Lomefloxacin
LOQ	Limit of quantification
LRMS	Low resolution mass spectrometry
MARBO	Marbofloxacin
MEC	Measured environmental concentration
MF	Microfiltration
MOX	Moxifloxacin
MW	Molecular weight
NA	Nutrient agar
NCR	Non-captured radicals
NHE	Normal hydrogen electrode
NOR	Norfloxacin
OECD	Organisation for Economic Cooperation and Development
OFL	Ofloxacin
PDA	Photodiode array detector
PEFL	Pefloxacin

PEG	Polyethylene glycol
PET	Polyethylene terephthalate
PNEC	Predicted no effect concentration
PZC	Point of zero charge
RE	Removal efficiency
RO	Reverse osmosis
ROS	Reactive oxygen species
rps	Rotations per second
RSSQ	Residual sum of squares
S/N	Signal-to-noise ratio
SARA	Sarafloxacin
SODIS	Solar disinfection
SPAR	Sparfloxacin
SPM	Suspended particulate matter
SRNOM	Suwannee river natural organic matter
TOC	Total organic carbon
TSA	Tryptone soy agar
UF	Ultrafiltration
UV	Ultraviolet
VB	Valence band
VDW	Van der Waals
Vet	Veterinary
WFD	Water Framework Directive
WWTPs	Wastewater treatment plants

Notation index

\underline{b}	Estimated parameter vector	dep.
B	Algal cell density	cells mL ⁻¹
C	Concentration	mol L ⁻¹
		mol kg _{cat} ⁻¹
C ₀	Initial concentration	mol L ⁻¹
D	pH dependent octanol-water partition coefficient	L L ⁻¹
F	Fisher's F value	-
I	Growth rate inhibition	%
J =	Jacobian matrix	-
k	Bimolecular rate constant	L mol ⁻¹ s ⁻¹
k ₁	Apparent first-order reaction rate constant	min ⁻¹
K'	Partition ratio	mol mol ⁻¹
K/K _d	Solid-water partition coefficient	L kg ⁻¹
K _{LH}	Langmuir-Hinshelwood adsorption coefficient	L μmol ⁻¹
K _{oc}	Organic carbon normalized solid-water partition coefficient	L kg ⁻¹
K _{ow}	Octanol-water partition coefficient	L L ⁻¹
k _r	Rate coefficient according to Langmuir-Hinshelwood equation	L mol ⁻¹ min ⁻¹
n	Number of observations / repetitions	-
n _{resp}	Number of responses	-
pK _a	Dissociation constant	-
P _{ow}	Octanol-water partition coefficient	L L ⁻¹
r ₀	Initial degradation rate	μmol L ⁻¹ min ⁻¹

r_0^*	Initial degradation rate based on total moles in reaction solution	$\mu\text{mol L}^{-1} \text{min}^{-1}$
R^2	Coefficient of determination	-
S	Adsorbed fraction	mol mol^{-1}
S^*	Objective function	-
T	Temperature	$^{\circ}\text{C}$ or K
t	Reaction time	min
$t_{1/2}$	Half-life time	min
t_R	Retention time	min
V	Volume	L
$\underline{\underline{V(b)}}$	Covariance matrix	-
\emptyset	Diameter	mm

Greek symbols

α	Significance level	-
β	Estimated parameter vector	-
γ	Ratio of scavenger concentration to MOX concentration	mol mol^{-1}
$\delta_{i,j}$	Substitution factor Eq. 2.6	
ΔE_g	Band gap energy	eV
ΔH°	Adsorption enthalpy	kJ mol^{-1}
θ	Theta angle	$^{\circ}$
κ	Ratio of degradation rate	mol mol^{-1}
μ	Specific growth rate	d^{-1}
λ	Wavelength	nm
$\rho_{i,j}$	Correlation between parameter i and j	-
φ	Nominator in Eq. 2.4 and Fig. 2.5	-

Abbreviated Superscript/Subscript

ad	Adsorbed
app	Apparent

aq	Aqueous
C	Control
calc	Calculated
cat	Catalyst
d	Day
eq	Equilibrium
F	Filtered
l	Liquid phase
L	Langmuir
LH	Langmuir-Hinshelwood
max	Maximum
NF	Not filtered
ow	Octanol-water
resp	Response
sig	Significance
T	Test solution
tab	Tabulated
Z/0	Zwitterion and uncharged molecule



Introduction, Outline, and Research objectives

At date, more than one-third of the Earth's accessible renewable freshwater is used for agricultural, industrial, and domestic purposes. Water withdrawals are predicted to increase by 50% by 2025 in developing countries, and 18% in developed countries due to the continuous growth of the human population (Schwarzenbach et al., 2006; UNEP, 2007). Moreover, in 60% of the European cities with more than 100,000 inhabitants, groundwater is already used at a faster rate than it can be replenished (UNwater).

Human related activities, like industry, agriculture, and domestic use, cause an increased water pollution, resulting in the occurrence of different inorganic and organic compounds in environmental waters, with potential hazard for both humans and ecosystems. Therefore, the European Union Water Framework Directive (WFD; 2000/60/EC) classified 33 pollutants as priority substances in 2001 for which environmental quality standards are layed down in 2008 (EU Directive 2008/105/EC). These compounds are from a divergent nature such as polycyclic aromatic hydrocarbons, biocides, metals and flame retardants. Moreover, in the proposal for amending the list of priority substances, the European Commission (EC) has included for the first time three pharmaceutical

compounds, namely diclofenac, estradiol, and ethinylestradiol (EC, 2012). Although they were not included yet, they are put on a 'watch-list' for further evaluation (EC, 2013).

Pharmaceuticals constitute a large group of healthcare products and reports show that the production and consumption has been steadily increasing in recent years, both globally and in the European Union (EU) (Efpia, 2013). Despite their benefits for human health, pharmaceuticals are regarded as emerging contaminants of concern due to their continuous release into the environment and persistence. Even at very low concentrations as ng L^{-1} to $\mu\text{g L}^{-1}$, there is a risk for adverse effects on the environment (Kümmerer, 2009a; Santos et al., 2010; Verlicchi et al., 2012a).

A study performed by Santos et al. (2010) showed that among the wide variety of pharmaceutical classes detected in the environment, antibiotics have the highest detection frequency. The concern associated with antibiotics is the development of multi-resistant bacteria, which can compromise public health by complicating treatment effectiveness. The latter is frequently reported in newspapers and media reporting the risks associated with overconsumption of antibiotics in both human and veterinary applications (De Morgen, 2012; De Standaard, 2012; EOS, 2012; Het Nieuwsblad, 2012a; Het Nieuwsblad, 2012b; HLN, 2012).

Among antibiotics, fluoroquinolone (FQ) compounds are of great interest for a number of reasons. First of all, they are a fully synthetic group of wide spectrum antibacterials and are the third largest group of consumed antibiotics, accounting for 17% of the global market share with a sell of 7.1 billion US \$ in 2009 (Hamad, 2010). Second, due to the increasing intake, a significant FQ resistance formation for the bacteria *E. coli*, *K. pneumoniae* and *P. aeruginosa* has been observed by the

European Center for Disease Prevention and Control (ECDC) for 28 European countries in a time span of 2007 to 2010 (ECDC, 2010). Third, due to the limited biodegradability of these antibiotics, an incomplete removal is attained in conventional wastewater treatment plants (WWTP), resulting in a continuous release into the environment.

As a result, numerous FQ antibiotics can be found in surface waters causing adverse effects on aquatic organisms (Robinson et al., 2005; Larsson et al., 2007). The concern is not as much the acute effect of these FQs but rather the long-term chronic effect of low concentrations in surface waters. The presence of these concentrations may induce selective pressure in microbial populations leading to quinolone resistant pathogens (Kümmerer and Henninger, 2003; Adam et al., 2007) and/or impose chronic toxicity on aquatic organisms (Carlsson et al., 2009; Ebert et al., 2011).

To prevent resistance formation and toxic effects, the removal of these antibiotics by physical-chemical technologies is required prior to discharge in the environment. Recently, research on Advanced Oxidation Processes (AOP) like heterogeneous photocatalysis, ozonation and sonification is performed to evaluate the removal potential for these biorecalcitrant compounds (De Witte et al., 2008; De Bel et al., 2009; Homem and Santos, 2011; Tong et al., 2012; Wang and Xu, 2012).

This PhD focuses on TiO₂ mediated heterogeneous photocatalysis since it is a promising technology, capable of degrading many environmental pollutants of concern today without the use of extra consumables (H₂O₂, iron) or toxic reactants such as ozone (Herrmann, 2005; Tong et al., 2012).

Moxifloxacin (MOX) is selected as a model compound based on the fact that it is one of the latest generation FQs, its increasing consumption (81.3% of the European third generation quinolone outpatient consumption in 2009), and the lack of literature concerning its degradation with AOPs (Adriaenssens et al., 2011). Ciprofloxacin (CIP) is an older (2nd generation) FQ compound and is, at some times, used as a benchmark for the results obtained with MOX.

The main objective of this dissertation is to obtain a better understanding of the FQ photocatalytic degradation with respect to several research aspects, like (i) the adsorption on a TiO₂ catalyst, (ii) the effect of operational variables, (iii) the formation of photocatalytic degradation products, (iv) the residual biological activity, and (v) the application in a real effluent matrix.

In **Part I** of this study, general information on the FQ structure and physical-chemical properties is given with a discussion on their occurrence in different environmental matrices. In addition, the basic principles of the AOP heterogeneous photocatalysis are described.

Scientific research performed in this work is structured according to different research topics, which are summarized in Table 0.1 combined with the experimental conditions applied. **Parts II to V** describe the setup and results of the experimental work.

Table 0.1 Experimental strategy and operational conditions applied in this PhD study during photolytic and photocatalytic degradation

Research topic	Part	Degradation technique	Matrix	Light source	Comp ^a	C _{FQ} ^b (μM)	C _{buffer} ^c (mM)	C _{cat} ^d (g L ⁻¹)	pH	Sparging gas (60 mL min ⁻¹)	Rps ^e	Temperature (K)
Adsorption and	Part II (2.1)	Photolysis	Demineralized water	UV-A/C	MOX	37.4	10	- ^f	3, 7, 10	O ₂	7.9	298
			Demineralized water	UV-A/C	CIP	45.3	10	-	3, 7, 10	O ₂	7.9	298
		Photocatalysis	Demineralized water	UV-A/C	MOX	37.4	10	0.5	3, 7, 10	O ₂	7.9	298
			Demineralized water	UV-A/C	CIP	45.3	10	0.5	3, 7, 10	O ₂	7.9	298
Degradation mechanism	Part II (2.2)	Photocatalysis	Demineralized water	UV-A	MOX	12.5-124.6	10	5	7	air	13.2	298
			Demineralized water	UV-A	MOX	37.4	10	0.25-8	7	air	2.3-13.2	298
			Demineralized water	UV-A	MOX	37.4	10	5	7	O ₂ , air, N ₂	13.2	298
			Demineralized water	UV-A	MOX	37.4	10	5	7	air	13.2	278-338
		Photocatalysis	Demineralized water ^g	UV-A	MOX	37.4	10	1	7	air	13.2	298
Degradation products	Part III	Photocatalysis	Demineralized water	UV-A	MOX	124.6	10	1	3, 7, 10	air	13.2	298
Biological activity	Part IV (4.1)	Photocatalysis	Demineralized water	UV-A	MOX	37.4	10	1	3, 7, 10	air	13.2	298
	Part IV (4.2)	Photocatalysis	Demineralized water	UV-A	MOX	124.6	10	1	7	air	13.2	298
Effluent water	Part V	Photocatalysis	Demineralized water ^h Hospital effluent	UV-A	MOX	37.4	10 ⁱ	1	7	air	13.2	298

^a component; ^b initial FQ concentration; ^c buffer concentration; ^d catalyst concentration; ^e rotations per second; ^f no catalyst addition; ^g scavenger addition; ^h inorganic carbon, chloride and organic matter addition; ⁱ no buffer addition for effluent matrices.

The first objective in **Part II** was to study the adsorption mechanism of two FQ compounds, CIP and MOX, on a TiO₂ catalyst. Therefore, adsorption experiments are performed at different pH levels to calculate partition coefficients for the different FQ species. In a next step, a main focus is set on the photocatalytic degradation where it is compared with photolysis, and the effect of different process parameters is evaluated on both the adsorption-desorption equilibrium and the degradation rate. At last, the goal was to gain new insights on the photocatalytic degradation mechanism by tentatively quantifying the contribution of the main reactive species during photocatalytic reaction of MOX using radical scavengers.

Since complete mineralization using an AOP is not strived after for economic reasons (Doll and Frimmel, 2004), a second research target was to investigate photocatalytic degradation products (DP) formation, and, to evaluate the effect of pH on this matter (**Part III**). Separation and detection of the different DPs is performed using liquid chromatography (LC) coupled to low resolution mass spectrometry (LRMS), and identification of the detected photocatalytic DPs is performed using high resolution mass spectrometry (HRMS) analysis. Moreover, to gain insights in the photocatalytic reaction pathway of MOX, structural differences of the identified DPs are compared.

Given that FQs are biologically active molecules, a third point of interest is to study antibacterial activity and ecotoxicity as biological endpoints during photocatalytic treatment of a MOX solution (**Part IV**). Residual antibacterial activity is investigated by means of agar diffusion tests for a set of relevant bacterial species, and algal growth inhibition tests are performed to assess ecotoxicity on the green alga *Pseudokirchneriella subcapitata*. A particular focus is

set on evaluating the contribution of both MOX and its photocatalytic DPs to the overall reaction solutions' residual biological activity.

To evaluate the application potential of heterogeneous photocatalysis as a tertiary treatment step, research in real effluent matrices is necessary. Therefore, in a last research part, the photocatalytic degradation of MOX is investigated in a hospital effluent matrix with a systematic effect evaluation of the main inorganic and organic wastewater components on both the adsorption-desorption equilibrium and photocatalytic degradation rate (**Part V**).

General conclusions, discussion, scientific progress, and future research perspectives are outlined in **Part VI**.

The interconnection of the different research topics and chapters in this study is visualized in Fig. 0.1.

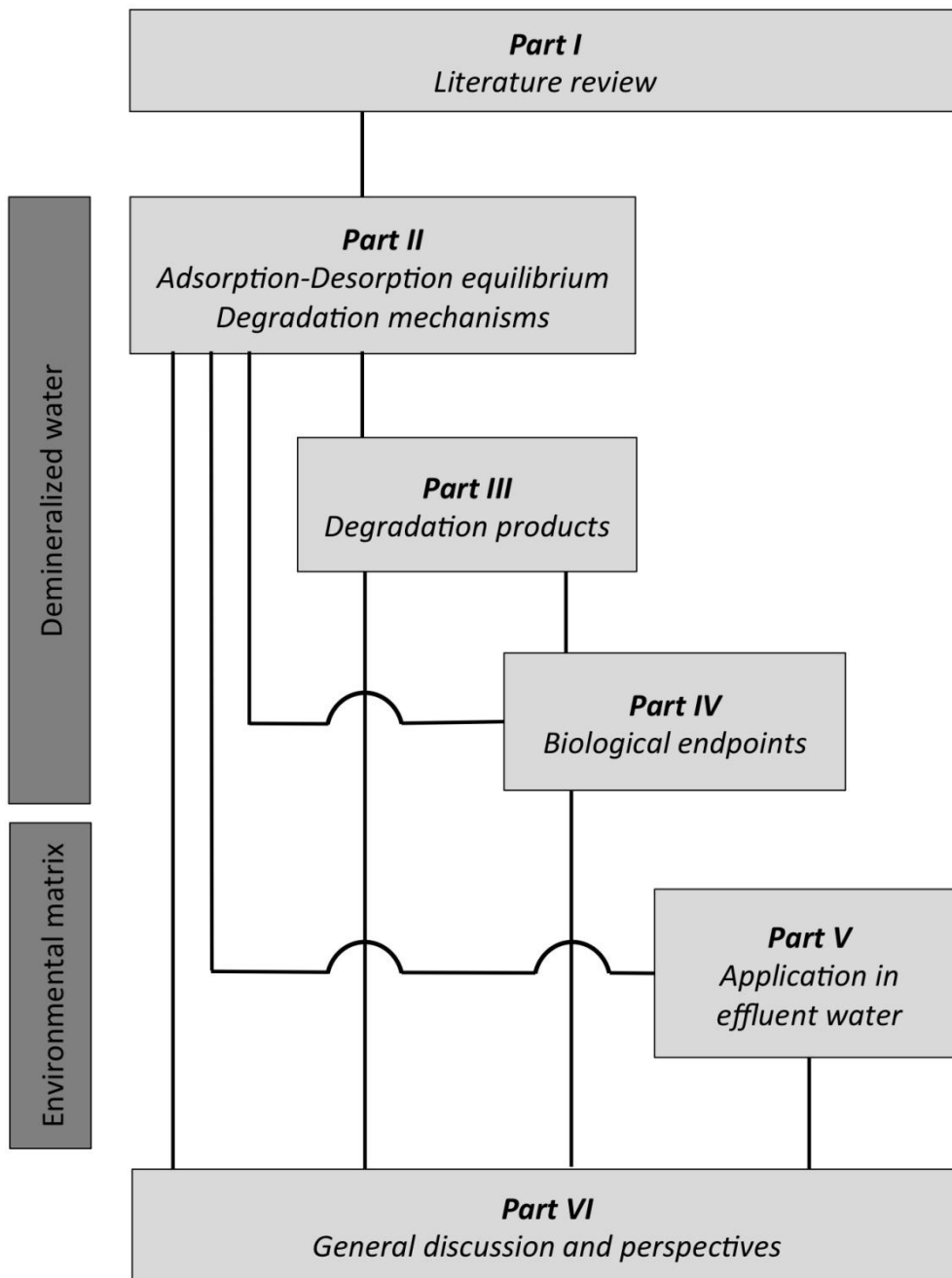


Fig. 0.1 Schematic outline of the research topics focused in this PhD.

Acknowledgements

The research was conducted at the EnVOC research group:

Research Group Environmental Organic Chemistry and Technology.

Department of Sustainable Organic Chemistry and Technology.

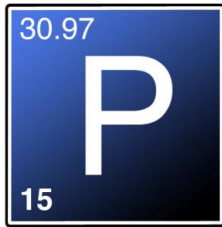
Faculty of Bioscience Engineering, Ghent University.

Coupure Links 653, 9000 Ghent.

Tel: +32 9 264 59 50

Fax: +32 9 264 62 43

URL: <http://www.envoc.ugent.be/>



art I

Literature review

Fluoroquinolones as emerging environmental pollutants, and heterogeneous photocatalysis as an innovative treatment technique

1.0 Introduction

Part I consists of literature data, which provide background information on (i) FQs as antimicrobial compounds with environmental concern, and (ii) heterogeneous photocatalysis as an advanced oxidation technique. Throughout this chapter, the FQ compound names are represented by their acronyms, which are listed in Table 1.1.

In **Chapter 1.1**, the main goal is to bring forward a critical overview of literature data on physical-chemical properties of FQ antibiotics, as well as their sources, use, and occurrence in different environmental matrices. Also, ecotoxicity risks associated with FQ contamination are evaluated, by linking literature toxicity data with environmental occurrence data.

In **Chapter 1.2**, the advanced oxidation technology heterogeneous photocatalysis is presented as a possible treatment technique to degrade micropollutants from water matrices. The basic principles, applications, and reaction steps of this technology are briefly presented.

1.1 Fluoroquinolones as emerging micropollutants

1.1.1 Introduction

At date, more than 5000 different pharmaceutical compounds intended for human and veterinary applications are used worldwide (Dorival-García et al., 2013a). Despite their benefits, a growing concern about potential adverse impacts on biota and human health has emerged as a result of their continuous release into the environment (Jones et al., 2004; Fent et al., 2006; Kümmerer, 2009a; Allen et al., 2010; Michael et al., 2013; Rizzo et al., 2013; Tijani et al., 2013).

Pharmaceuticals are a broad group of compounds divided into different classes, such as analgesics and anti-inflammatory drugs, antibiotics, anti-epileptics, beta-blockers, contrast media, cytostatics, hormones, antidepressants, disinfectants and antiseptics, among others. Recent reviews provide a general overview on the exposure routes and the occurrence of pharmaceutical residues in the environment (Gavrilescu and Caliman, 2009; Kümmerer, 2009a; Fatta-Kassinos et al., 2011; Tijani et al., 2013), and WWTPs (Miège et al., 2009; Verlicchi et al., 2012a)

Other reviews particularly focus on one specific class of pharmaceuticals, such as antiviral drugs (Jain et al., 2013), psychiatric pharmaceuticals (Calisto and Esteves, 2009), anti-inflammatory and analgesic pharmaceuticals (Ziylan and Ince, 2011), and antibiotics (Thiele-Bruhn, 2003; Kemper, 2008; Kümmerer, 2009b; Kümmerer, 2009c; Segura et al., 2009; Seifrtová et al., 2009; Du and Liu, 2012; Michael et al., 2013) covering different topics, including detection techniques, occurrence in the environment, ecotoxicity, and treatment by biological systems.

Antibiotics are more and more a focus point of research due to their high detection frequency in the environment, and the increasing bacterial resistance formation (Kümmerer, 2009b; Kümmerer, 2009c; Bouki et al., 2013; Rizzo et al., 2013). Reviews on one specific subgroup of antibiotics are scarce. Hruska and Franek (2012) recently discussed the environmental occurrence of sulfonamides, and Speltini et al. (2010) mainly focused on sample preparation and detection methods for FQs in environmental matrices. To date, no recent comprehensive review on the occurrence of FQs in different environmental matrices has been published. A last update has been presented by Sukul and Spittler (2007), who present a broad overview including a brief description of the environmental occurrence of FQ compounds.

FQs are of interest, since they are wide spectrum antibacterials with an increasing use in hospitals, households, and veterinary applications (Adriaenssens et al., 2011; BelVetSac, 2011; Grave et al., 2012). Moreover, they are the third largest group of consumed antibiotics in the world (Hamad, 2010).

FQ antibiotics are excreted unmetabolized up to 70% and, when released in the environment, they can promote resistance formation on microbial populations. A significant increase in FQ bacterial resistance between 2007 and 2010 is observed by the European Surveillance for Antimicrobial Consumption (ESAC) (ESAC, 2010). Moreover, the presence of these pseudo-persistent compounds in the environment can induce toxic effects on aquatic organisms (Robinson et al., 2005). The lack of biodegradation and high adsorption affinity results in long residence times in the environment, with reported half-life times of 10.6 days in surface water (Andreozzi et al., 2003) and up to 580 days in soil matrices (Rosendahl et al., 2012).

The main goal of this chapter is to compile a comprehensive review on the FQ structure, use, classes, sources, pathways, occurrence, fate and behavior, and ecotoxicity of these emerging micropollutants in different environmental matrices. An extensive literature data survey is performed, including manuscripts from 1998 to mid 2013, which report physical-chemical parameters, FQ concentrations above the limit of quantification (LOQ), and removal efficiencies (RE) after wastewater treatment, yielding a dataset of 4100 data points from over 204 references.

The chapter is structured as follows. First, the chemical structure and therapeutic use of the FQs detected in the environment is presented in **Section 1.1.2**. **Section 1.1.3** summarizes published information on physical-chemical properties relevant for the fate and behavior of FQs in the environment. Main sources and pathways of FQ compounds to the environment are discussed in **Section 1.1.4** and **Section 1.1.5**, respectively, where **Section 1.1.6** deals with the occurrence of FQs in different environmental matrices. The environmental fate and behavior of FQs is presented in **Section 1.1.7**, while the final section (**Section 1.1.8**) deals with ecological effects of FQs in both solid and aqueous matrices.

A schematic outline and the link between the different sections included in this chapter are presented in Fig. 1.1.

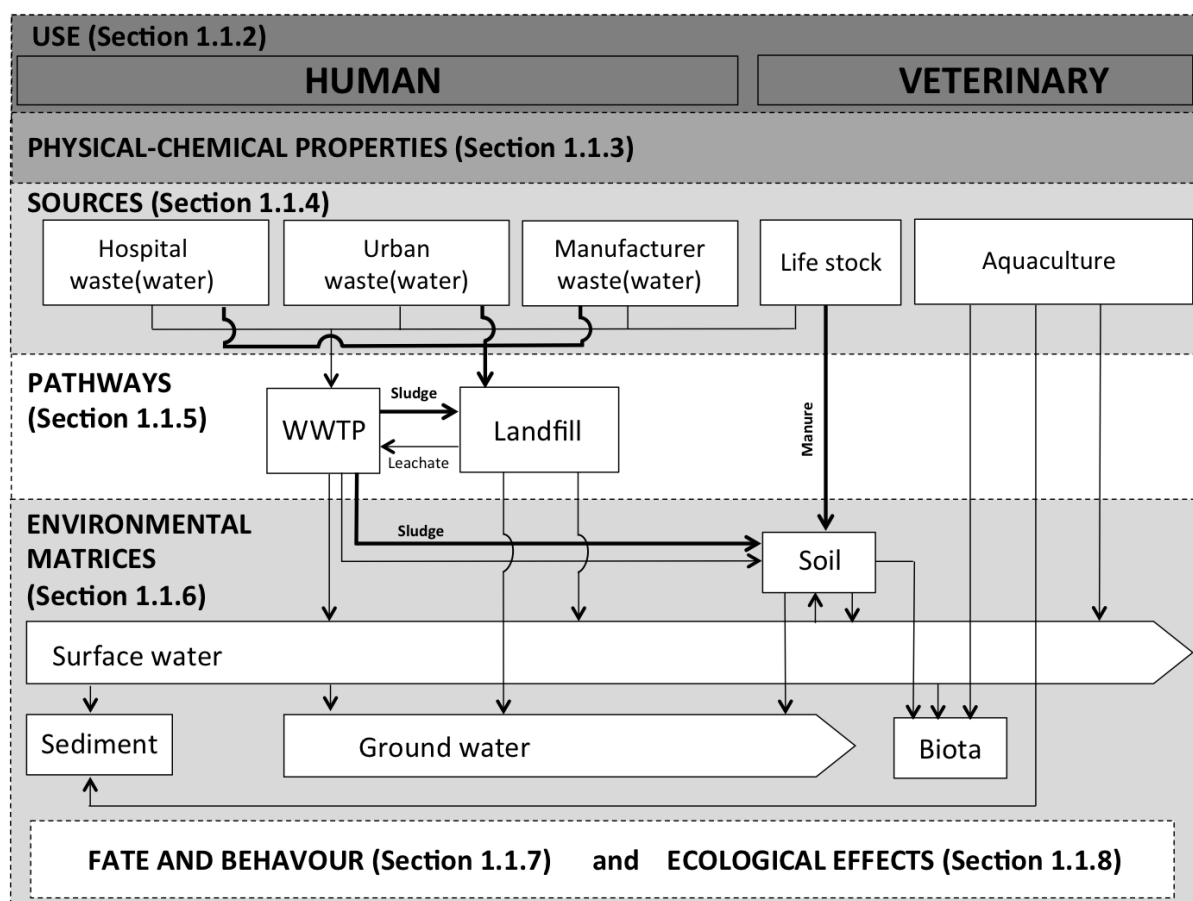


Fig. 1.1 Schematic outline of this chapter including the different sources, pathways, occurrence, fate, behavior and ecological effects of FQ antibiotics in the environment. Based on Santos et al. (2010), and Homem and Santos (2011). Bold lines represent solid waste streams.

1.1.2 Chemical structure and therapeutic use

Nalidixic acid, discovered in 1962 as a by-product of anti-malaria research, is the parent compound of the quinolone antibiotic class and has a narrow antibacterial spectrum. Until the development of FLU, none of the earlier synthesized compounds had offered any significant therapeutic improvements (Appelbaum and Hunter, 2000).

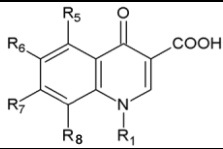
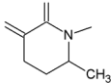
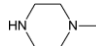
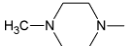
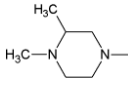

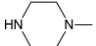
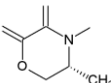
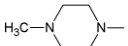
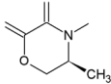
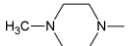

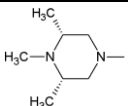

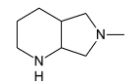

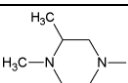

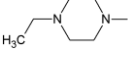

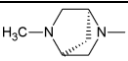
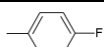
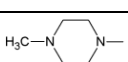

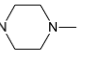
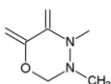
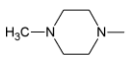
FLU is the first monofluorinated quinolone, from which the subgroup of the FQs has been arisen. The addition of fluorine resulted into an increased antibacterial

spectrum, indicating that a structural modification of the '4-quinolone' skeleton (Table 1.1 Top) could improve the activity. This marked the beginning of intensive chemical synthesis efforts to refine structure-activity relationship, optimize pharmacokinetics, and reduce toxicity and drugs interactions. The addition of different R₁, R₇ and R₈ groups created new and more effective FQ compounds with broader antibacterial spectra (Table 1.1). In the case of FLU, OFL, LEVO and MARBO an extra ring structure is created on the quinolone base structure, hereby bridging the R₁ and R₈ substituent.

The use of FQ compounds in animal husbandry creates an important source of antimicrobial-resistant bacteria. Some studies suggested that the majority of antibiotic-resistant *E. coli* carried by people may have originated in food animals, especially chickens (Collignon et al., 2009).

To mitigate human health risks associated with antibiotic usage in veterinary applications, the World Health Organization ranked antibiotics according to their importance in human medicine, with FQs being '*critically important*' (Collignon et al., 2009). Therefore, the EU has divided the use of FQ compounds in human (Hum) and veterinary (Vet) applications (Table 1.1). FQs used for human infection treatment are not allowed for veterinary applications, except MOX. However, this is an uncommon practice (EMA; Papich, 2010). Moreover, it is known that CIP is frequently used off-label in companion animal treatment (Pallo-Zimmeman, 2010).

Table 1.1 Structures, generation and use of FQs detected in the natural environment

Basic quinolone structure									
									
Gen ^a	MW ^c	Use	Compound		R ₈	R ₁	R ₅	R ₆	R ₇
1	261.30	Vet ^d	Flumequine	FLU			H	F	H
1	319.34	Hum ^e	Norfloxacin	NOR	H	-CH ₂ -CH ₃	H	F	
2	333.36	Hum	Pefloxacin	PEFL	H	-CH ₂ -CH ₃	H	F	
2	351.35	Hum	Lomefloxacin	LOME	F	-CH ₂ -CH ₃	H	F	
2	331.35	Hum	Ciprofloxacin	CIP	H		H	F	
2	361.37	Hum	Ofloxacin	OFL			H	F	
2	361.37	Hum	Levofloxacin	LEVO			H	F	
2	392.41	Hum	Sparfloxacin *	SPAR	F		H	F	
3	401.43	Hum	Moxifloxacin	MOX	-O-CH ₃		H	F	
3	375.39	Hum	Gatifloxacin *	GATI	-O-CH ₃		H	F	
- ^b	359.46	Vet	Enrofloxacin	ENRO	H		H	F	
-	357.37	Vet	Danofloxacin	DANO	H		H	F	
-	399.39	Vet	Difloxacin	DI	H		H	F	
-	385.36	Vet	Sarafloxacin	SARA	H		H	F	
-	362.36	Vet	Marbofloxacin	MARBO			H	F	

* no sales in EU in 2010-2012 (electronic communication ECDC); ^a generation according to ECDC classification (Adriaenssens et al., 2011); ^b no classification mentioned according to ECDC (Adriaenssens et al., 2011); ^c molecular weight; ^d veterinary use; ^e human use.

In addition, FQs are also classified into different generations based on their antibacterial spectrum, with more recent generations having a wider antibacterial spectrum. However, there is no consensus on the distinction between generations for FQs used in human applications. American authors mainly report four different generations based on Andriole (1999) and Owens and Abrose (2000), while the ECDC, formerly known as ESAC, classifies FQs only in three different generations based on Ball (2000). This hampers transparency for FQ consumption data comparison, since this is frequently reported on a generation basis (Adriaenssens et al., 2011). Literature data on generation determination for veterinary FQs is lacking, and so far, only one reference is found which states that veterinary FQs observed in Table 1.1 are positioned in the second generation (Giguère et al., 2013).

1.1.3 Physical-chemical properties relevant for environmental FQ behavior

The tendency of a chemical to partition from the aqueous phase to the atmosphere is expressed by the Henry's law constant, while its affinity to adsorb on solids is frequently evaluated by the octanol-water partition constant, $\log K_{ow}$, which is also often reported as $\log P_{ow}$ (Kümmerer, 2008). FQ compounds have very low Henry's law constants at ambient temperature, $< 10^{-15} \text{ atm}\cdot\text{m}^3 \text{ mol}^{-1}$ (Dorival-García et al., 2013b), resulting in a negligible volatilization. Literature data on K_{ow} values for FQs detected in the natural environment are presented in Table 1.2.

Table 1.2 Selected physical-chemical properties of FQs detected in the environment

Comp	Log (octanol-water)	pK _{a1}	pK _{a2}	pK _{a3}	pK _{a4}	K _{d, soil} (L kg ⁻¹)	K _{d, sediment} (L kg ⁻¹)	K _{d, sludge} (L kg ⁻¹)
FLU	0.97; 1.72/1.46 (n = 6) ^a	na ^d	na	6.29 (n = 11)	na	-	-	-
NOR	-3.78; 1.45/-1.17 (n = 39)	3.10 (n = 2) ^b	5.55 (n = 2)	6.27 (n = 21)	8.71 (n = 22)	41; 335633/29876 (n = 44)	30; 75/54 (n = 2)	686; 3530/1829 (n = 3)
CIP	-2.82; 2.30/-0.81 (n = 48)	3.32 (n = 3)	5.59 (n = 2)	6.14 (n = 28)	8.85 (n = 27)	74; 1277874/21099 (n = 104)	794; 18620/7000 (n = 3)	367; 5123/1804 (n = 8)
PEFL	-2.29; 1.34/-0.38 (n = 25)	-	-	6.11 (n = 7)	7.46 (n = 6)	-	-	-
LOME	-1.28; 2.31/-0.76 (n = 19)	-	5.00 (n = 1)	5.87 (n = 6)	9.23 (n = 6)	-	-	-
OFL	-3.35; 1.52/-0.58 (n = 48)	-	5.20 (n = 1)	5.98 (n = 15)	8.00 (n = 16)	309; 4325/2205 (n = 9)	2982 (n = 1)	872; 3746/1905 (n = 3)
LEVO	-2.00; 1.30/-0.72 (n = 9)	-	-	5.19 (n = 3)	7.07 (n = 3)	-	-	-
SPAR	-0.86; 4.53/0.66 (n = 6)	-	-	6.09 (n = 3)	8.79 (n = 3)	-	-	-
GATI	-1.14; 2.27/0.03 (n = 5)	-	-	5.83 (n = 2)	8.93 (n = 2)	-	-	-
MOX	-1.33; 2.49/-0.09 (n = 11)	-	-	6.13 (n = 6)	9.61 (n = 7)	-	-	516; 3018/1419 (n = 3)
SARA	-1.26; 0.84/-0.67 (n = 7)	-	-	5.91 (n = 5)	9.07 (n = 5)	-	-	-
DANO	1.78 (n = 1)	-	-	6.18 (n = 4)	8.78 (n = 4)	848; 255644/43631 (n = 13)	-	-
ENRO	-0.83; 4.70/1.10 (n = 10)	3.88 (n = 2)	6.19 (n = 1)	6.20 (n = 16)	8.13 (n = 14)	54; 251430/16244 (n = 42)	-	-
MARBO	- ^c	-	-	5.69 (n = 1)	8.02 (n = 1)	2500 (n = 1)	-	-
DI	-0.59; 0.89/0.38 (n = 7)	-	-	5.88 (n = 4)	7.42 (n = 4)	-	-	-

^a min; max/average (n = number of observations), depending on reference denoted as K_{ow}, P_{ow}, P_{app}, D; ^b average; ^c not reported; ^d not applicable; Data obtained from Ross et al. (1992), Takács-Novák et al. (1992), Torniaainen et al. (1996), Drakopoulos and Ioannou (1997), Howard and Meylan (1997), Huang et al. (1997), Nowara et al. (1997), Volmer et al. (1997), MacGowan (1999), Schmitt-Kopplin et al. (1999), Kan and Petz (2000), Stuer-Lauridsen et al. (2000), Tolls (2001), Park et al. (2002), Golet et al. (2003), Lin et al. (2004), Qiang and Adams (2004), Renew and Huang (2004), Drillia et al. (2005), Hari et al. (2005), Langlois et al. (2005), Michot et al. (2005), Neugebauer et al. (2005), Babić et al. (2006), Martinez et al. (2006), De Witte et al. (2007), Neves et al. (2007), Segura et al. (2007), Lorenzo et al. (2008), Park and Choi (2008), Uslu et al. (2008), Feitosa-Felizzola and Chiron (2009), Muñoz et al. (2009), Tamtam et al. (2009), Vasudevan et al. (2009), Williams et al. (2009), Xu et al. (2009), Babić et al. (2010), Conkle et al. (2010), Figueroa-Diva et al. (2010), Li and Zhang (2010), Rosal et al. (2010), Ebert et al. (2011), Vazquez-Roig et al. (2011), Dalkmann et al. (2012), Dorival-García et al. (2012), Jia et al. (2012), Ratola et al. (2012), Rosendahl et al. (2012), Rusu et al. (2012), Sturini et al. (2012a), Vazquez-Roig et al. (2012), Völgyi et al. (2012), Dorival-García et al. (2013b), Leal et al. (2013), Li et al. (2013), Olofsson et al. (2013), Senta et al. (2013), Yan et al. (2013), Drugbank, FDA, LogKOW.

Two main points need to be addressed. First, a large variability, up to 5.5 log units, is observed and second, median log K_{ow} values for the different FQs are smaller than 2.5, which would indicate that FQs have a low sorption potential (Verlicchi et al., 2012a). However, it is observed that FQs have a high affinity for sludge, soils and sediments (Golet et al., 2003; Picó and Andreu, 2007; Vieno et al., 2007; Yang et al., 2010a), which would normally be expected for compounds with a log K_{ow} above 3 or 4 (Kümmerer, 2009a).

A first reason for the large variation on literature log K_{ow} values is that reported values include both modeled and experimental data. A more in-depth analysis revealed that the log K_{ow} values obtained via simulation software are at least 1 log unit higher than the experimentally determined values (Schmitt-Kopplin et al., 1999; Jia et al., 2012). Moreover, also among the experimental data, a clear variability is observed most probably due to a varying solution temperature and because of a pH dependent partitioning, as is reported for MOX, PEFL, NOR, and OFL (Takács-Novák et al., 1992; Langlois et al., 2005). The latter is a result of the amphoteric nature of FQ compounds. They can occur in different speciations, which are related by dissociation constants, pK_a values (Fig. 1.2).

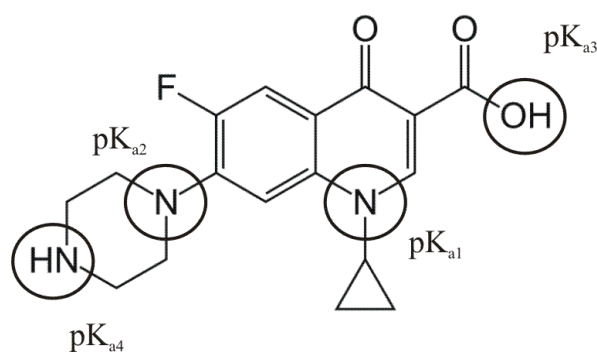


Fig. 1.2 Position of the different ionisable groups of CIP as a model compound for which most pK_a values are available.

Literature data on the dissociation constants for the carboxylic group (pK_{a3}) and the N_4 of the piperazinyl rings (pK_{a4}) of FQs are available, but data for pK_{a1} and pK_{a2} are scarce with contradictory results (Table 1.2). Rusu et al. (2012) published negative pK_{a2} values meaning that the FQ^{2+} speciation would only occur at pH levels below 1 (negative pK_{a2} values are not presented in Table 1.2), with no further protonation to FQ^{3+} . This is in contrast with several authors who reported positive pK_{a1} values, defining the equilibrium between FQ^{2+} and FQ^{3+} (Lin et al., 2004; De Witte et al., 2007; Senta et al., 2013). Even though no consensus on the dissociation at lower pH values is obtained, calculations of FQ speciation at environmental conditions can be performed since the pK_{a3} and pK_{a4} values determine the relevant FQ species at environmental conditions.

This speciation might be an important factor explaining the variability of the reported octanol-water partition coefficients, since depending on the pH, the FQ compound occurs as a mixture of neutral and/or differently charged species, which all may contribute to the partitioning process (Kümmerer, 2008), while the $\log K_{ow}$ value only reflects the partitioning of the neutral form. Therefore, for ionisable compounds, it is considered to be more relevant to use $\log D$, in some cases labeled as $\log P_{app}$, which takes this speciation into account by including the pK_a values in the calculation of the octanol-water partition coefficient (Langlois et al., 2005). However, $\log D$ ($\log P_{app}$) values for FQ compounds are seldomly observed in literature (Ross et al., 1992; Takács-Novák et al., 1992; Vazquez et al., 2001; Langlois et al., 2005; Segura et al., 2007; Feitosa-Felizolla and Chiron, 2009; Vazquez-Roig et al., 2012), and in fact, $\log K_{ow}$, $\log P_{ow}$, $\log P_{app}$ and $\log D$ values are used throughout each other explaining the observed variability in reported octanol-water partition coefficients.

Apart from the large variability, the high sorption of FQs on different solid environmental matrices shows that octanol-water partitioning determinations come short for evaluating the adsorption behavior of FQs. Moreover, some investigators have reported their doubts over the usefulness of $\log K_{ow}$ to predict the environmental partitioning of ionisable compounds due to the fact that, next to hydrophobic partitioning, electrostatic interactions play a significant role in the sorption process (Tolls 2001; Golet et al., 2003; Wegst-Uhrich et al., 2014). In fact, it is suggested by several researchers that the latter is the main sorption mechanism of FQ compounds on solid matrices (Golet et al., 2003; Lindberg et al., 2006; Batt et al., 2007; Zorita et al., 2009). Due to the limitations of $\log K_{ow}$ to account for electrostatic interactions, more realistic partition coefficients ($\log K_d$) have to be determined. K_d demonstrates the FQ sorption behavior on a real solid medium of interest like soils, sediments, and WWTP sludge, replacing the octanol phase. So far, only few researchers determined FQ K_d values for these matrices, which are presented in Table 1.2.

Among the experimentally determined FQ **soil** K_d values, a high variability is observed ranging from 41 up to 1,277,874 L kg⁻¹. This can be the result of different reasons, such as experimental setup and the properties of the test soils used during adsorption experiments. A first factor that can influence partition coefficient determination in soils is the ionic strength of the groundwater (Avisar et al., 2009). Adsorption experiments are mainly performed according to the OECD test guideline 106, which states that a 0.1 M CaCl₂ solution should be applied to mimic background groundwater ionic strength (Drillia et al., 2005; Uslu et al., 2008; Williams et al., 2009; Conckle et al., 2010; OECD, 2000; Sturini et al., 2012a). However, it is observed that other researchers also used demineralized water without ionic strength correction (Nowara et al., 1997), or applied buffers

for pH control (Vasudevan et al., 2009; Figueroa-Diva et al., 2010).

Next to ionic strength, the cation exchange capacity (CEC), soil composition and the pH of the groundwater are of importance. According to several researchers, the cation exchange capacity and soil texture are the soil factors with the greatest influence on FQ adsorption (Vasudevan et al., 2009; Figueroa-Diva et al., 2010; Leal et al., 2013). Soils with a high CEC and clay content have higher K_d values, while the occurrence of sand results in decreased K_d values due to its lower affinity for FQ compounds (Vasudevan et al., 2009; Leal et al., 2013). The pH of the groundwater influences FQ adsorption due to the pH dependent FQ speciation, and according to Leal et al. (2013), tropical soils have a higher affinity for FQs (K_d values $> 15,000 \text{ L kg}^{-1}$) due to their low pH levels, resulting in a higher amount of FQ cationic species. A variation in K_d values can also originate from differences in the applied experimental setup. A decreasing trend in K_d values is observed with higher initial FQ dosages due to the non-linear concentration dependent sorption of these compounds. Moreover, during FQ mixture soil adsorption experiments competition effects are observed that decreased K_d values of the individual FQ compounds (Uslu et al., 2008; Williams et al., 2009; Conkle et al., 2010).

To reduce the variability between K_d data of antibiotic compounds in different soils, organic carbon normalization is frequently employed, resulting in the organic carbon partition coefficients (K_{oc}) (Nowara et al., 1997; Tolls, 2001; Drillia et al., 2005; Cordova-Kreylos and Scow, 2007; Xu et al., 2009; Brooks and Huggett, 2013). This approach may be used for neutral compounds where adsorption is mainly driven by hydrophobic interactions with the soil organic fraction. However, for FQs it is shown that the organic carbon content is not a dominant adsorption factor (Vasudevan et al., 2009; Figueroa-Diva et al., 2010), and that

adsorption also occurs on inorganic clays and metal oxides like TiO_2 (Nowara et al., 1997; Part II). Therefore, organic carbon normalizing of partition coefficients cannot be universally applied to all antimicrobials, particularly those that have ionisable groups (Tolls, 2001; Cordova-Kreylos and Scow, 2007; Wegst-Uhrich et al., 2014).

Sediment adsorption studies are performed similar to soil adsorption experiments using 0.01 M CaCl_2 for fresh water sediments (Hari et al., 2005; Cordova-Kreylos and Scow, 2007), or using real seawater for marine sediments (Xu et al., 2009). A high affinity of CIP ($K_d = 7000 \text{ L kg}^{-1}$) and OFL (mean K_d value of 2982 L kg^{-1}) towards saltwater sediments is observed in Cordova-Kreylos and Scow (2007) and Xu et al. (2009). However, Hari et al. (2005) reported a low affinity of NOR for fresh water sediments, with K_d values that are on the average 40 to 600 times lower compared to NOR adsorption on soil and sludge matrices, respectively.

FQ partition coefficients for **WWTP sludge** show a much smaller range between 367 and 5123 L kg^{-1} (Table 1.2), and are determined in batch scale adsorption experiments where the biological activity of the sludge is inhibited by either sterilization or the addition of NaN_3 (Li and Zhang, 2010; Dorival-García et al., 2012; Dorival-García et al., 2013b). Next to a decreased FQ adsorption with increasing temperature, salinity of the water phase is of importance during sludge-water partitioning. Reported partition coefficients for CIP in saline sewage water (367 to 665 L kg^{-1}) are at least 3 times lower compared to CIP partition coefficients obtained in freshwater sewage water (2257 - 5123 L kg^{-1}).

1.1.4 Sources

There are different sources of FQs to the environment due to the use in both human and veterinary applications (Fig. 1.1). Waste streams originating from residential areas, hospitals and animal farms contain FQ compounds, since the administered FQ dose is only partially metabolized. Excretion ratios range between 30% for NOR, up to 70% for OFL (Kümmerer and Henninger, 2003). However, ENRO is completely metabolized but into CIP by de-ethylation (Andreu et al., 2007). The focus of this review is on 'mother compounds', since to the author's best knowledge, there are no quantitative data reported for FQ metabolites in environmental matrices.

1.1.4.1 Sources from human applications

Pollution resulting from human applications can occur by discharging FQ containing effluent water, or through the disposal of unused FQ containing medication. With respect to the first, three different sources are of interest, i.e. (i) hospital wastewater, (ii) urban wastewater, and (iii) bulk drug producer wastewater.

Hospital FQ wastewater concentrations range between 3 ng L⁻¹ and 240 µg L⁻¹, with more than 60% of the dataset (n = 148) exceeding 1 µg L⁻¹ (Fig. 1.3). The most frequently detected FQs are CIP, NOR, and OFL with average concentrations of 21 µg L⁻¹, 5 µg L⁻¹, and 11 µg L⁻¹, respectively. Although it is expected that in hospital wastewater only FQs for human applications are detected, ENRO is reported in 7 out of the 148 data points at concentrations below 250 ng L⁻¹ (Lin et al., 2009; Watkinson et al., 2009; Sim et al., 2011).

Next to hospital wastewater, **urban wastewater** can contain significant amounts of FQ pollution. When no remarks were made concerning the presence of hospitals, bulk drug producers, or other non-urban sources, reported WWTP influents are considered to be urban wastewater. Urban FQ wastewater concentrations range between 2 ng L⁻¹ and 14 µg L⁻¹, with only 16% of the data points (n = 410) exceeding 1 µg L⁻¹ (Fig. 1.3).

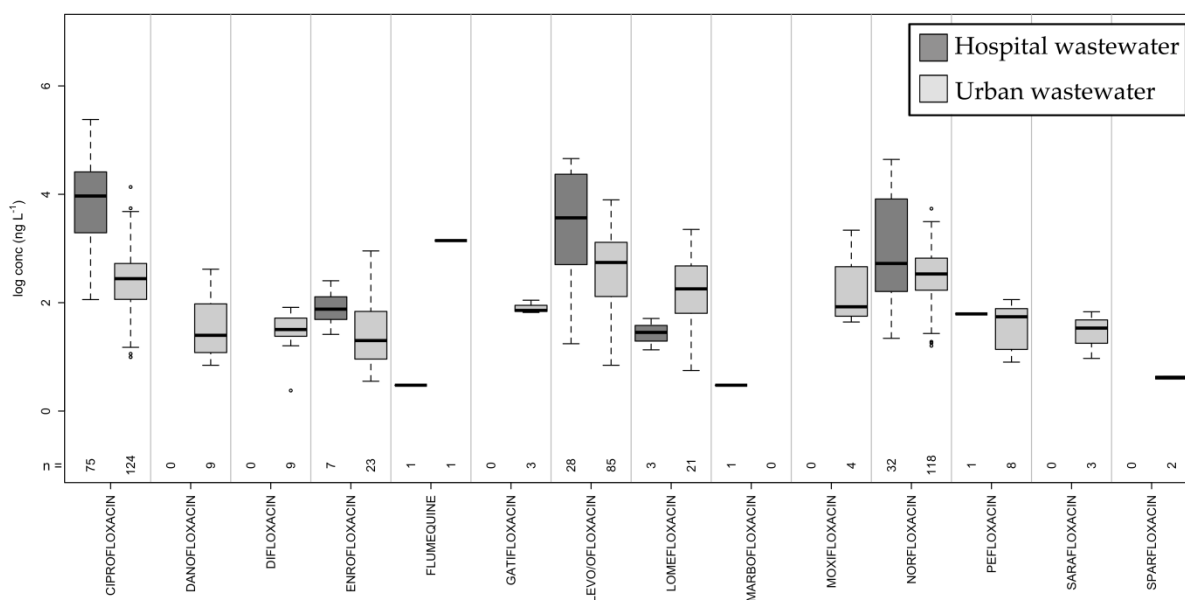


Fig. 1.3 Boxplots of FQ concentrations (ng L⁻¹) in hospital wastewater (dark grey), and urban wastewater (light grey) (n = number of observations). Data obtained from Hartmann et al. (1998), Golet et al. (2001), Golet et al. (2002a), Golet et al. (2003), Ohlsen et al. (2003), Reverté et al. (2003), Jarnheimer et al. (2004), Lindberg et al. (2004), Costanzo et al. (2005), Ferdig et al. (2005), Lindberg et al. (2005), Alexy et al. (2006), Brown et al. (2006), Karthikeyan and Meyer (2006), Mitani and Kataoka (2006), Peng et al. (2006), Vieno et al. (2006), Yasojima et al. (2006), Batt et al. (2007), Segura et al. (2007), Thomas et al. (2007), Vieno et al. (2007), Watkinson et al. (2007), Xu et al. (2007a), Duong et al. (2008), Gulkowska et al. (2008), Lin et al. (2008), Martins et al. (2008), Seifrtová et al. (2008), Senta et al. (2008), Spongberg and Witter (2008), Terzić et al. (2008), Xiao et al. (2008), Ghosh et al. (2009), Gros et al. (2009), Li et al. (2009), Lin et al. (2009), Lu et al. (2009), Miège et al. (2009), Shi et al. (2009), Walraven and Laane (2009), Watkinson et al. (2009), Zorita et al. (2009), Rosal et al. (2010), Sim et al. (2010), Teijon et al. (2010), Bernabeu et al. (2011), Cui et al. (2011), Deblonde et al. (2011), Sim et al. (2011), Takasu et al. (2011), Tong et al. (2011a), Yang et al. (2011), Dolar et al. (2012), Gao et al. (2012a), Gracia-Lor et al. (2012), Jia et al. (2012), Leung et al. (2012), Verlicchi et al. (2012a), Verlicchi et al. (2012b), Blair et al. (2013), Li et al. (2013), Senta et al. (2013), Tewari et al. (2013).

Comparing urban wastewater with hospital wastewater, three main points need to be addressed. First, urban wastewater is more intensively studied, since a higher amount of FQ detections are observed in literature for urban than for hospital wastewaters. Second, FQ concentrations in hospital wastewaters are, as might be expected, higher compared to concentrations observed in urban wastewater, with median concentrations of CIP, NOR and LEVO/OFL up to 30 times higher (Fig. 1.3). In a recent literature review on pharmaceuticals in wastewaters, a similar observation is made where mean antibiotic concentrations in urban wastewater were 5-10 times lower compared to concentrations in hospital wastewaters (Verlicchi et al., 2010). Third, taking into account the wastewater flows, next to the reported concentrations, FQ daily loads are obtained, which nuances the previously observed differences between both wastewaters.

A total load of FQs in hospital wastewater of 0.3-29 g d⁻¹ are reported for Chinese, Swiss and Norwegian hospitals (Alder et al., 2004; Thomas et al., 2007; Duong et al., 2008), while a total FQ load of 216 g d⁻¹ to 1228 g d⁻¹ in urban wastewater was calculated for Chinese WWTPs serving 100,000 to 2,400,000 people (Gao et al., 2012a; Jia et al., 2012; Li et al., 2013). Also in Europe, high FQ loads are reported, ranging from 190 to 326 g FQ d⁻¹ to WWTPs from Zagreb and Zürich (Golet et al., 2003; Senta et al., 2013). Even for small WWTPs serving only 2100-22,000 inhabitants, substantial FQ urban wastewater loads (0.3-8.1 g d⁻¹) are observed (Golet et al., 2002a; Alexy et al., 2006; Karthikeyan and Meyer, 2006; Lin et al., 2009). A Swiss study showed that 62% of the pharmaceutical load entering a WWTP originates from household use, and that the other 38% was consumed in hospitals (Escher et al., 2011). Verlicchi et al. (2012b) reported that respectively 5%, 15% and 67% of the NOR, CIP and OFL load entering the WWTP originates from hospital use, and Santos et al. (2013) calculated the contribution of four large

hospitals to the overall influent load of FQs to a WWTP in Coimbra, Spain, at 49%. This indicates that the importance of hospital loads to the overall FQ load is situation specific, and that both sources are of importance, with hospital wastewaters as point source and urban wastewater as a more disperse source of FQ pollution.

Apart from urban and hospital wastewater, FQs enter the environment also through **bulk drug** producing activities, with FQ wastewater concentrations ranging from 6 ng L⁻¹ up to 31 mg L⁻¹ (Lin et al., 2008; Walraven and Laane, 2009; Babić et al., 2010; Sim et al., 2011). Average concentrations of OFL, NOR, and CIP in production facility wastewaters amount 103 µg L⁻¹, 270 µg L⁻¹ and 4.9 mg L⁻¹, respectively, being higher compared to their hospital and urban wastewaters concentrations. Considering the wastewater flows from Korean pharmaceutical producers, an average daily load of 10 kg pharmaceuticals d⁻¹ of which 6.5 kg d⁻¹ are antimicrobials is obtained (Sim et al., 2011). An extreme situation is observed in India, where 90 bulk drug producing manufacturers discharge a total FQ load of over 46 kg d⁻¹ consisting out of CIP, NOR, LOME and OFL (Larsson et al., 2007). According to Kümmerer (2009a), the significant contribution of manufacturing plant wastewater to the total inlet load of a sewage treatment plant is not restricted to Asian countries, but also occurs in developed countries.

Next to aqueous waste streams, the **incorrect disposal** of excess or overdue medicines by households and pharmacists is of major concern. A UK survey performed in 2003 revealed that only 4% of the questioned households disposed unused drugs via sink or toilet, while 71% of the households discard them with municipal waste that is either landfilled or incinerated (Bound and Voulvoulis, 2005). Reports also indicate incorrect disposal of pharmaceutical waste in

pharmacies (Tong et al., 2011b). A survey of New-Zealand community pharmacies revealed that, although the most common route of disposal for unused solid formulations like tablets, capsules, and semi-solid preparations is via third-party contractors, still 34% of the community pharmacists reported the incorrect disposal of solids with urban waste. Liquid medicines however, are predominantly (> 66%) disposed via toilet or sink (Tong et al., 2011b).

1.1.4.2 Sources from veterinary applications

Waste originating from livestock applications can be separated in wastewater and manure. Literature data on FQ pollution of livestock wastewater is scarce and, so far, only Sim et al. (2011) and Zhou et al. (2013) reported the presence of ENRO, NOR, OFL, and CIP at concentrations ranging from 63 ng L⁻¹ to 585 ng L⁻¹.

On the other hand, the occurrence of FQs in **manure** is reported by several researchers, with concentrations ranging from 5.3 µg kg⁻¹ up to 1.4 g kg⁻¹ (Martínez-Carballo et al., 2007; Karci and Balcioglu, 2009; Hu et al., 2010; Zhao et al., 2010; Leal et al., 2012; Zhou et al., 2013). Average FQ concentrations in chicken, pig, and cow manures from eight provinces in China ranged between 1 and 5 mg kg⁻¹ (Zhao et al., 2010). However, FQ manure concentrations of a swine farm from a common Chinese province are at least 2 orders of magnitude lower (Zhou et al., 2013). This is, according the researchers, attributed to the low observed concentration of FQs in the animal feed, e.g. ENRO at 2.7 µg kg⁻¹ feed. Martínez-Carballo et al. (2007) reported that ENRO is particularly observed in chicken and turkey manure, with maximum concentration levels of 2.8 and 8.3 mg kg⁻¹, respectively. Leal et al. (2012) found similar ENRO concentrations in Brazilian chicken dung (6.7 mg kg⁻¹), but also reported the occurrence of other FQs such as NOR and CIP at 2.6 mg kg⁻¹ and 1.4 mg kg⁻¹, respectively.

Next to livestock applications, FQs are widely used in aquaculture facilities with NOR, ENRO, and FLU the most commonly used FQ compounds (Sapkota et al., 2008). In many cases, they are used for disease prevention instead of disease treatment, and this goes for both intensive and extensive applications (Holmström et al., 2003). Shrimp farmers often use homemade feeds mixed with antibiotics bought on the market, or use illegal feeds, which make it difficult to know which compounds, and at what quantity are dosed. For adult shrimp, NOR is frequently used, and concentrations in shrimp feeds are reported to be in the range of 0.5 to 6 g kg⁻¹ feed. The application of medicated feeds results in the direct pollution of shrimp pond waters with FQ compounds. Shrimp pond surface waters sampled at 16 intensive and extensive Vietnamese shrimp farms resulted in an average NOR concentration of 1 mg L⁻¹ (Le and Munekage, 2004). FQs used in larvae ponds during the shrimp development period, resulted in FQ pond water concentrations ranging between 0.3-1.2 mg L⁻¹ (Thuy et al., 2011; Thi et al., 2012).

FQ polluted waters are discharged into the natural environment, but literature data on FQ concentrations in aquaculture effluent is scarce, and reported concentrations are 3 orders of magnitude lower compared to the pond water concentrations. OFL and NOR are the two dominant FQ compounds observed in effluent waters from fish nurseries and breeding farms in the Bohai Bay region, with OFL concentrations ranging up to 7.9 µg L⁻¹ (Zou et al., 2011). Aquaculture activities in developed countries also contribute to FQ pollution, with a reported FLU concentration of 64 µg L⁻¹ in the effluent water of a Dutch ornamental fish farm (Walraven and Laane, 2009).

In the case of aquaculture activity in open waters, a direct contamination of the environment occurs with the application of medicated feed. However, FQ concentrations in the vicinity of Chinese cage-culture fisheries were below the

limit of detection (LOD), indicating the strong dilution after application of FQ feed additives (He et al., 2012).

1.1.5 Pathways

FQ compounds used in veterinary applications are in many cases directly released into the environment (Fig. 1.1). For human wastewater and solid waste, two important intermediate treatment steps are observed, i.e. WWTPs and landfills.

1.1.5.1 WWTPs

Wastewaters from human activities in hospitals, residential areas, and manufacturer plants are transported via sewerage systems to WWTPs where they are, in most cases, biologically treated. Typically, WWTPs contain a primary sedimentation followed by a nitrification/denitrification step. The biologically treated wastewater is finally clarified, yielding a secondary effluent.

1.1.5.1.1 Influent and effluent FQ concentrations and removal efficiencies

Boxplots of the FQ influent, secondary effluent and tertiary (see Section 1.1.5.1.3) effluents concentrations of WWTPs are presented in Fig. 1.4a. It should be noted that the concentrations of the chiral FQ compounds OFL and LEVO are merged, since it was not always clear to which of both chiral compounds was referred to in some manuscripts.

A high variation in influent and effluent concentrations can be observed for the different FQ compounds, with influent concentrations ranging from 2 ng L⁻¹ up to 8 µg L⁻¹, and effluent concentrations from 0.3 ng L⁻¹ up to 31 µg L⁻¹.

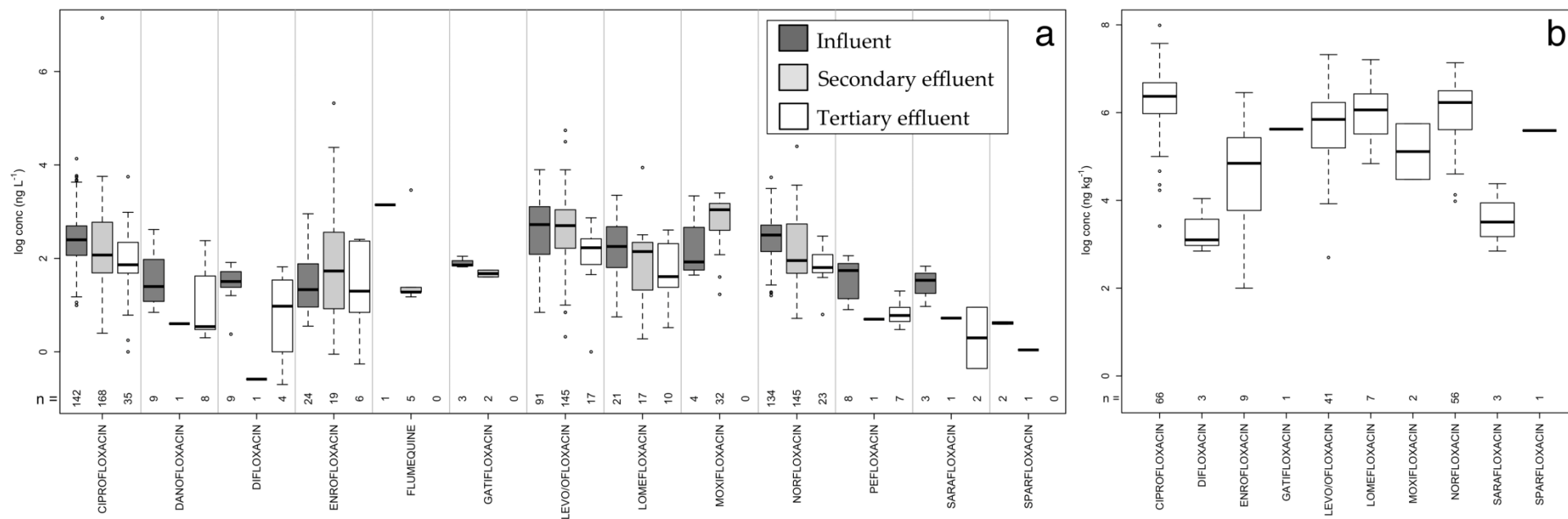


Fig. 1.4 Boxplots of FQ concentrations (ng L^{-1}) in (a) WWTP influent (dark grey), secondary effluent (grey) and tertiary effluent (white); (b) WWTP sludge concentrations (ng kg^{-1}) (n = number of observations). Data obtained from Golet et al. (2001), Golet et al. (2002a), Golet et al. (2002b), Andreozzi et al. (2003), Golet et al. (2003), Reverté et al. (2003), Miao et al. (2004), Renew and Huang (2004), Batt and Aga (2005), Castiglioni et al. (2005), Costanzo et al. (2005), Ferdig et al. (2005), Lindberg et al. (2005), Nakata et al. (2005), Zuccato et al. (2005), Aga et al. (2006), Alexy et al. (2006), Babić et al. (2006), Brown et al. (2006), Karthikeyan and Meyer (2006), Lindberg et al. (2006), Mitani and Kataoka (2006), Peng et al. (2006), Vieno et al. (2006), Yasojima et al. (2006), Batt et al. (2007), Martinez Bueno et al. (2007), Segura et al. (2007), Thomas et al. (2007), Vieno et al. (2007), Watkinson et al. (2007), Xu et al. (2007a), Gulkowska et al. (2008), Lin et al. (2008), Seifrtová et al. (2008), Senta et al. (2008), Spongberg and Witter (2008), Terzić et al. (2008), Xiao et al. (2008), Coetsier et al. (2009), Fick et al. (2009), Ghosh et al. (2009), Gros et al. (2009), Li et al. (2009), Lillenberg et al. (2009), Lin et al. (2009), Lu et al. (2009), Miège et al. (2009), Minh et al. (2009), Muñoz et al. (2009), Okuda et al. (2009), Radjenović et al. (2009), Shi et al. (2009), Walraven and Laane (2009), Watkinson et al. (2009), Zorita et al. (2009), Gros et al. (2010), Lillenberg et al. (2010), López-Serna et al. (2010), McClellan and Halden (2010), Morash et al. (2010), Rosal et al. (2010), Teijon et al. (2010), Walters et al. (2010), Bernabeu et al. (2011), Cui et al. (2011), Deblonde et al. (2011), Köck-Schulmeyer et al. (2011), Sim et al. (2011), Tong et al. (2011a), Yang et al. (2011), Al Aukidy et al. (2012), Cabeza et al. (2012), De la Cruz et al. (2012), Dolar et al. (2012), Gao et al. (2012a), Gottschall et al. (2012), Gracia-Lor et al. (2012), Jia et al. (2012), Leung et al. (2012), Montesdeoca-Esponda et al. (2012), Prieto-Rodríguez et al. (2012), Tang et al. (2012), Verlicchi et al. (2012a), Blair et al. (2013), Dorival-García et al. (2013a), Li et al. (2013), Olofsson et al. (2013), Prieto-Rodríguez et al. (2013), Senta et al. (2013), Tewari et al. (2013).

An exception is a study performed by Fick et al. (2009) where CIP, ENRO, LOME, NOR, and LEVO/OFL are detected up to several mg L⁻¹ in secondary effluents of a WWTP that receives wastewater from over 90 bulk drug producers. However, no influent data is reported for that specific study site. The most frequently reported FQ compounds are CIP, NOR, and LEVO/OFL, and combine more than 80% of the data points for influent and effluent waters. Of the 451 influent FQ concentration data points used in Fig. 1.4a, 46 (10%) are from veterinary origin, indicating that wastewaters from veterinary applications are of lesser importance.

FQ removal efficiencies (RE) for WWTPs are presented in Table 1.3. Tabulated RE are not calculated from Fig. 1.4a but are an overview of the in literature reported values. A high variation in RE (47-77% on the average) is observed, being in agreement with data for other antibiotic compounds like tetracycline and sulfamethoxazole (Verlicchi et al., 2012a).

Table 1.3 Literature data on WWTP fluoroquinolone removal efficiencies

Compound	RE ^a		
	min	max	average
FLU			- ^b
NOR	-16	96	68 (n = 52) ^c
CIP	20	100	74 (n = 68)
PEFL	11	96	77 (n = 9)
LOME	-60	100	71 (n = 21)
ENRO	0	90	49 (n = 11)
LEVO/OFL	-66	98	53 (n = 37)
DANO	-44	97	61 (n = 10)
MARBO			-
GATI	43	50	47 (n = 2)
DI	63	100	81 (n = 7)
MOX	40	61	51 (n = 2)
SARA	44	100	77 (n = 3)
SPAR			75 (n = 1)

^a removal efficiency; ^b no data; ^c n = number of observations. Data obtained from Golet et al. (2002a), Golet et al. (2003), Lindberg et al. (2005), Castiglioni et al. (2006), Karthikeyan and Meyer (2006), Lindberg et al. (2006), Peng et al. (2006), Batt et al. (2007), Radjenović et al. (2007), Vieno et al. (2007), Watkinson et al. (2007), Xu et al. (2007a), Gulkowska et al. (2008), Seifrtová et al. (2008), Xiao et al. (2008), Ghosh et al. (2009), Li et al. (2009), Lu et al. (2009), Miège et al. (2009), Shi et al. (2009), Zorita et al. (2009), Rosal et al. (2010), Bernabeau et al. (2011), Gao et al. (2012a), Jia et al. (2012), Leung et al. (2012), Li et al. (2013), Senta et al. (2013), Tewari et al. (2013).

Some researchers reported that WWTPs reduced FQ influent concentrations below LOD levels (Karthikeyan and Meyer, 2006; Lu et al., 2009; Gao et al., 2012a), while others observed higher effluent than influent concentrations (Gulkowska et al., 2008; Li et al., 2009; Gao et al., 2012a). A possible explanation proposed by Xu et al. (2007a) is the exclusion of influent particulate matter, which may lead to an underestimation of the influent concentrations. Also the deconjugation of FQ metabolites in raw influent during the water treatment process might explain the higher effluent concentrations (Xu et al., 2007a; Plósz et al., 2010; Verlicchi et al., 2012a).

The FQ removal in a WWTP can be influenced by the composition of the influent (industrial versus urban), type of treatment process, and process parameters like solid retention time, hydraulic retention time and temperature (Gao et al., 2012a; Tang et al., 2012). Although it is not yet fully understood which are the detrimental factors, it is suggested by a few authors that solid retention time and hydraulic retention time are of main importance for FQ removal (Batt et al., 2007; Gao et al., 2012a; Li et al., 2013).

1.1.5.1.2 FQ removal mechanisms

Possible FQ removal mechanisms during wastewater treatment are biodegradation and sorption on activated sludge. However, the role of biodegradation in the removal of FQs is not yet clear, with variable results found in literature on this regard. Negligible biodegradation (< 10%) of FQs is observed by Jia et al. (2012), Li and Zhang (2010), and Verlicchi et al. (2012a). However, biodegradation tests performed by Halling-Sørensen et al. (2000) in an activated sludge reactor showed a 50% reduction of the initially spiked CIP ($250 \mu\text{g L}^{-1}$) after 2.5 days of biodegradation. It is also reported that membrane reactors operating under nitrifying conditions improved FQ biodegradation up to 60%

removal (Senta et al., 2011; Dorival-García et al., 2013b). In saline sewage sludge, biodegradation of CIP, OFL and NOR reached up to 40% removal after 48 h, which might be due to a different microbial community compared to fresh water sludge (Li and Zhang, 2010). Although the importance of biodegradation is not fully understood, it is suggested by several authors that the predominant removal mechanism for FQ compounds is sorption to sludge, rather than biodegradation (Golet et al., 2003; Conkle et al., 2010; Jia et al., 2012).

1.1.5.1.3 Tertiary treatment

Comparing CIP, NOR, and LEVO/OFL influent and secondary effluent concentrations, it can be observed that conventional WWTPs remove these FQ compounds to a low extent, with a decrease of 53%, 72%, and 5% of the median influent concentrations, respectively (Fig. 1.4a). Due to the incomplete removal, 15 out of the 82 manuscripts reported an additional tertiary treatment to increase the removal of the FQ compounds. After tertiary treatment, CIP, NOR and LEVO/OFL median concentrations decreased with 71%, 80%, and 68% compared to the influent median concentrations, indicating that tertiary treatments are an efficient way to reduce FQ pollution.

In this data survey, the most frequently applied tertiary treatments are filtration techniques like sand filters (Nakata et al., 2005; Aga et al., 2006; Batt et al., 2007; Zorita et al., 2009), contact filtration (Golet et al., 2003; Shi et al., 2009; Teijon et al., 2010), membrane filters (Yang et al., 2011; Cabeza et al., 2012; Li et al., 2013), and biofilters (Renew et al., 2004; Lu et al., 2009), but also the use of activated carbon (Renew et al., 2004; Yang et al., 2011) is observed.

In literature, the application of microfiltration (MF) and ultrafiltration (UF) as a tertiary treatment technique for FQ removal shows a wide range in removal

efficiencies. Yang et al. (2011) and Li et al. (2013) observed a negligible contribution of MF and UF to the FQ removal from secondary effluents, while Watkinson et al. (2007) reported a 55% FQ removal efficiency after MF of a secondary WWTP effluent. The latter authors contribute this relatively high FQ removal to their sorption onto larger particles since MF pore sizes are unlikely to withhold solubilized molecules. The negligible removal observed in the first two studies can be the result of a low residual amount of suspended particulate material after the secondary clarifier, reducing the contribution of MF and UF in the total FQ removal. A tertiary sand filtration is reported to contribute up to 17% in FQ removal (Batt et al., 2007). Similar contributions are observed for granular activated carbon, with 18% of CIP and 30% of LEVO/OFL removal (Yang et al., 2011). Biofiltration, however, is according to Lu et al. (2009), of no importance for improving FQ removal.

The application of AOPs like ozonation is described by Li et al. (2013), Renew et al. (2004), and Yang et al. (2011). Ozonation of the secondary WWTP effluents with ozone dosages between 1 and 5 mg L⁻¹ increased FQ removal efficiencies from 44-86% during conventional wastewater treatment to 85-98% (Li et al., 2013), and reduced CIP concentrations from 23 ng L⁻¹ down to 1 ng L⁻¹ (Yang et al., 2011). Some WWTPs perform an additional disinfection step such as chlorination and/or UV light irradiation, which can decrease the effluent FQ concentrations even more (Renew et al., 2004; Batt et al., 2007). An increase of CIP removal efficiency from 50% to 71% is observed in the Lackawana WWTP after chlorination of the secondary effluent (Batt et al., 2007). In the same study, it is shown that, although FQ antibiotics absorb in the UV region, no significant photolytic degradation is attained during UV mediated disinfection (wavelength not reported).

1.1.5.1.4 WWTP sludge

As a result of the high affinity of FQ compounds towards sludge (Table 1.2), concentrations of different FQ compounds range from 100 ng kg⁻¹ up to 98 mg kg⁻¹ (mean = 3.2 mg kg⁻¹), with more than 97% of the reported sludge concentrations higher than 1 µg kg⁻¹ (Fig. 1.4b). Moreover, only 8% of the in total 178 data points are for veterinary FQs like ENRO, SAR, and DI having concentrations not exceeding 470 µg kg⁻¹.

According to the Sludge Directive 86/278/EEC, EU membership states can decide if they allow the application of excess WWTP sludge as a fertilizer on agricultural soils. In most of the EU membership states, this is applied only to a limited extent with less than 100,000 tons of sludge used on an annual basis over a time span 1999-2009. However, a significant use in sludge has been observed for Spain, UK, France, and Germany with amounts up to 1 million tons per year (EUROSTAT).

Sludge must be treated before application in agriculture, but the member states may authorize the use of untreated sludge if it is injected, or worked into the soil (Sludge Directive). In most cases, sludge is anaerobically digested before it is used as fertilizer (Stasinakis, 2012). Removal of FQ compounds under methanogenic (anaerobic) conditions in sludge digesters is not well described. So far, only 2 manuscripts report the behavior of the FQs during sludge treatment with RE of 10-14% for NOR, and 10-42% for CIP (Golet et al., 2003; Lindberg et al., 2006). After treatment, biosolids are often subjected to a storage period before land application. Chenxi et al. (2008) observed that storing treated sludge for 2 months under aerobic and anaerobic conditions did not result in a noticeable CIP removal. Indications of thermal degradation during digested sludge pelleting are reported by Lindberg et al. (2006).

An American study calculated the annual FQ load by the application of sludge onto US agricultural land for both OFL and CIP at 18,000-23,000 kg year⁻¹, and for NOR at 970-1200 kg year⁻¹ (McClellan and Halden, 2010). For Sweden, a ten times lower total FQ load (1872 kg year⁻¹) is calculated from data obtained by Olofsson et al. (2013) with the assumption that 60% of the excess sludge is reused as fertilizer (Swedish EPA, 2002). To compare FQ loads of sludge fertilization with loads from WWTPs, a total FQ (CIP + OFL + NOR) load of 50,000 kg year⁻¹ is assumed for the entire US based on the data obtained from McClellan and Halden (2010). The latter is equivalent to 137 kg d⁻¹ and is on the average 1000 times higher compared to total FQ load in a typical WWTP effluent, ranging between 19 g d⁻¹ and 510 g d⁻¹ (Golet et al., 2003; Gao et al., 2012a; Jia et al., 2012). Taking into account that, in 2011, USA had 17,000 working WWTPs, a similar total FQ load for WWTP effluents is obtained (WWTP USA, 2011). This shows that, next to effluent waters, sludge fertilization can also significantly contribute to the FQ pollution of the environment.

1.1.5.2 Landfills

Sludge, which is not used as fertilizer is either incinerated or landfilled together with household waste. In 2009, landfilling of sludge did not exceed 10,000 tons for most EU countries, except for Poland (80,000 tons) and Greece (110,000 tons) (EUROSTAT). If the landfill site has no effluent collection, FQ contamination of surface and groundwater can occur due to leaching or run-off. Modern landfills, however, are equipped with protective barriers and leachate collection systems. Landfill leachate is treated before discharge into the environment (Foo and Hameed, 2009), and recent research performed on biologically treated landfill leachate from a Belgian landfill site reports the occurrence of the FQ compound MOX among 9 other pharmaceuticals, but no quantification was performed (Oloibiri, 2013). A study performed by Musson and Townsend (2009) on a US

landfill “grab sample” revealed a CIP content of 6.5 g in solid formulations after sorting, which was equal to a load of 71 mg CIP kg⁻¹ waste. The latter indicates that landfills have a large amount of FQ containing solid formulations, which are a potential source of pollution.

1.1.6 Occurrence in the environment

1.1.6.1 Aqueous matrices

There is a growing concern regarding FQ pollution in the aquatic environment, resulting in an increase of scientific papers screening for FQ compounds in different aqueous matrices.

FQ pollution of **surface waters** can occur due to (i) run-off by rain from agricultural fields fertilized with FQ contaminated manure or sludge, (ii) discharge of FQ containing WWTP effluent waters or treated landfill leachate, and (iii) direct contamination by dosing FQ containing feeds in aquaculture applications (Fig. 1.1).

In this data survey, 47 articles are included that report FQ concentrations in surface waters of both fresh and marine origin. They are published in a time span of 2002-2013, with more than 80% of them released after 2007. Surface water analysis for FQs is mainly performed in Europe and Eastern Asia, with only a few measuring campaigns performed in American and Australian surface waters (Kolpin et al., 2002; Costanzo et al., 2005; Conley et al., 2008; Watkinson et al., 2009). An overview of the in literature reported FQ surface water concentrations is presented in Fig. 1.5a.

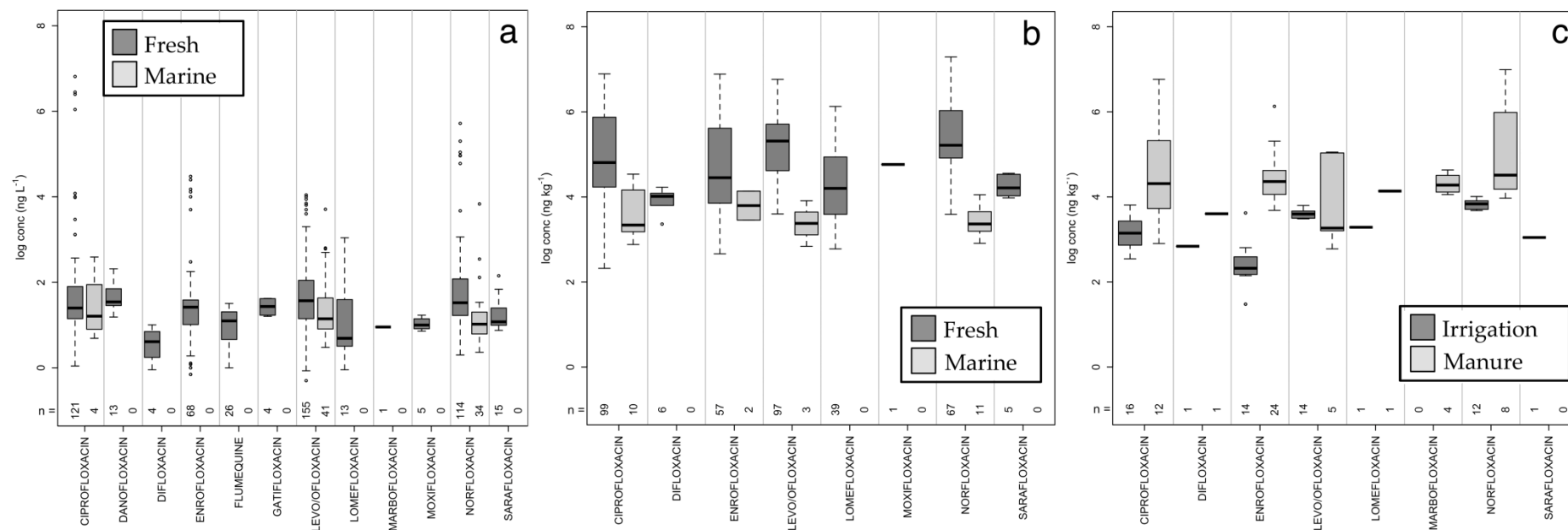


Fig. 1.5 FQ concentration boxplots in (a) fresh surface waters (dark grey) and marine surface waters (light grey) (ng L^{-1}), (b) fresh water sediments (dark grey) and marine sediments (light grey) (ng kg^{-1}), and (c) soils irrigated with WWTP effluent (dark grey) and fertilized with manure (light grey) (ng kg^{-1}) (n = number of observations). Data obtained from Golet et al. (2002a), Kolpin et al. (2002), Calamari et al. (2003), Christian et al. (2003), Morales-Muñoz et al. (2004), Costanzo et al. (2005), Ferdig et al. (2005), Zuccato et al. (2005), Vieno et al. (2006), Gros et al. (2007), Gulkowska et al. (2007), Martínez-Carballo et al. (2007), Pena et al. (2007), Xu et al. (2007b), Conley et al. (2008), Nageswara et al. (2008), Tamtam et al. (2008), Uslu et al. (2008), Xiao et al. (2008), Coetsier et al. (2009), Feitosa-Felizzola and Chiron (2009), Fick et al. (2009), Gros et al. (2009), Karci and Balcioglu (2009), Minh et al. (2009), Sturini et al. (2009), Tamtam et al. (2009), Walraven and Laane (2009), Watkinson et al. (2009), Xu et al. (2009), Ginebreda et al. (2010), Gros et al. (2010), Hu et al. (2010), López-Serna et al. (2010), Sturini et al. (2010), Yang et al. (2010a), Vazquez-Roig et al (2010), Cui et al. (2011), Dinh et al. (2011), Köck-Schulmeyer et al. (2011), Li et al. (2011), López-Serna et al. (2011), Luo et al. (2011), Mompelat et al. (2011), Takasu et al. (2011), Tong et al. (2011a), Valcárel et al. (2011), Vazquez-Roig et al. (2011), Vulliet and Cren-Olivé (2011), Zou et al. (2011), Al Aukidy et al. (2012), Dalkmann et al. (2012), Gao et al. (2012b), He et al. (2012), Hu et al. (2012), Leal et al. (2012), Li et al. (2012a), Montesdeoca-Esponda et al. (2012), Okay et al. (2012), Shi et al. (2012), Sturini et al. (2012a), Tang et al. (2012), Vazquez-Roig et al. (2012), Adachi et al. (2013), Tewari et al. (2013), Yan et al. (2013), Zhou et al. (2013).

The occurrence of FQs in marine waters is less frequently reported compared to fresh water. Marine surface water concentrations presented in Fig. 1.5a mainly originate from samples taken in coastal regions (Gulkowska et al., 2007; Xu et al., 2007b; Minh et al., 2009; Xu et al., 2009; Zou et al., 2011) and range between 2 ng L^{-1} and $7 \text{ } \mu\text{g L}^{-1}$ (median: 12 ng L^{-1} , 75th percentile: 32 ng L^{-1} , 25th percentile: 8 ng L^{-1}). Although there is a limited amount of data ($n = 79$), lower median concentrations of CIP, NOR, and LEVO/OFL are observed compared to fresh surface water.

FQ concentrations in the latter range between 0.5 ng L^{-1} and 6.5 mg L^{-1} , with approximately 80% of the concentrations below 100 ng L^{-1} . In surface waters a higher amount of veterinary FQ compounds is reported compared to WWTP influent (Section 1.1.5.1), $\pm 20\%$ of the data points, which could be the result of aquaculture activities. Most of the outliers depicted in Fig. 1.5a originate from rivers in the Pantacheru region in India, which receive treated effluent water originating from 90 pharmaceutical bulk drug producers (Fick et al., 2009). Excluding the outliers reported by Fick et al. (2009), a median fresh FQ surface water concentration of 26 ng L^{-1} ($n = 501$; 75th percentile: 59 ng L^{-1} ; 25th percentile: 11 ng L^{-1}) is obtained. The high variability can be the result of different factors like sampling location (e.g. close to an effluent discharge or upstream sampling), different river flows (e.g. dilution factors), seasonal influences, etc. (Batt et al., 2006; Tamtam et al., 2008; López-Serna et al., 2010; Al Aukidy et al., 2012; Gao et al., 2012a; Gao et al., 2012b).

Next to surface water, **groundwater** is threatened by FQ pollution due to (i) percolation from sludge or manure fertilized acres into the deeper soil layers, (ii) landfill leachate if there are no collection barriers, and (iii) via FQ polluted surface waters (Fig. 1.1). Extreme CIP groundwater pollution ($0.7\text{-}14 \text{ } \mu\text{g L}^{-1}$) is

observed in the Pantacheru region in India, where also high CIP surface water concentrations are detected (Fick et al., 2009). Densely populated areas are also vulnerable for FQ groundwater pollution, as is observed by Teijon et al. (2010) and López-Serna et al. (2013), where FQ concentrations up to $0.5 \mu\text{g L}^{-1}$ are reported in the region of the metropolis of Barcelona. However, data are much more scarce than for surface water.

1.1.6.2 Sediment and soil

Once FQs are released into the aquatic environment, partitioning between surface water and **sediment** matrices occurs (Fig. 1.1). Concentrations of FQ antibiotics in fresh water sediments are detected from 210 ng kg^{-1} up to 20 mg kg^{-1} , with an average concentration of $760 \mu\text{g kg}^{-1}$ ($n = 371$) (Fig. 1.5b). Concentrations of FQs in marine sediments are three orders of magnitude lower compared to fresh water sediments, ranging from $0.8\text{-}34 \mu\text{g kg}^{-1}$, although experimentally determined partition coefficients in Section 1.1.3 indicated that marine sediments have a higher affinity towards FQ compounds.

Other solid matrices vulnerable for FQ pollution are **soils**, which can be contaminated due to (i) direct excretion of life stock onto fields, (ii) application of contaminated manure, (iii) irrigation with secondary effluent or polluted river water, and (iv) the application of WWTP sludge as fertilizer (Fig. 1.1). Although no literature is observed regarding direct manure excretion, reported FQ concentrations in soils after manure fertilization range between 600 ng kg^{-1} and 9.8 mg kg^{-1} , with an average of $511 \mu\text{g kg}^{-1}$ ($n = 55$) (Fig. 1.5c). Irrigation of agricultural fields with WWTP secondary effluent waters, however, resulted in a lower FQ pollution compared to manure fertilization, with concentrations up to $10 \mu\text{g kg}^{-1}$ (Fig. 1.5c). Moreover, more than 75% of the manure treated soil sample data points exceed $9 \mu\text{g kg}^{-1}$, indicating that manure fertilization is of more

importance for FQ soil pollution than effluent irrigation. Studies evaluating the FQ pollution soils treated with WWTP sludge are scarce and, so far, only experimental field studies are reported (Golet et al., 2002b; Gottschall et al., 2012). Average CIP and NOR concentrations of 400 and 300 $\mu\text{g kg}^{-1}$ respectively, are observed on experimental fields in Zürich 8 months after sludge fertilization, with no observed decrease during the following 13 months (Golet et al., 2002b). These concentrations are similar compared to the mean FQ concentration after manure application. A study performed by Gottschall et al. (2012) revealed a minor leaching of FQ compounds applied by sludge fertilization to the soil matrix. Moreover, after one year of application, 60-70% of the dosed FQs were still present in the sludge cores due to their high affinity for sludge.

1.1.6.3 Biota

FQ polluted surface waters and sediments are the habitat of different **aquatic organisms**, which can result in the uptake of FQ compounds by these species (Fig. 1.6).

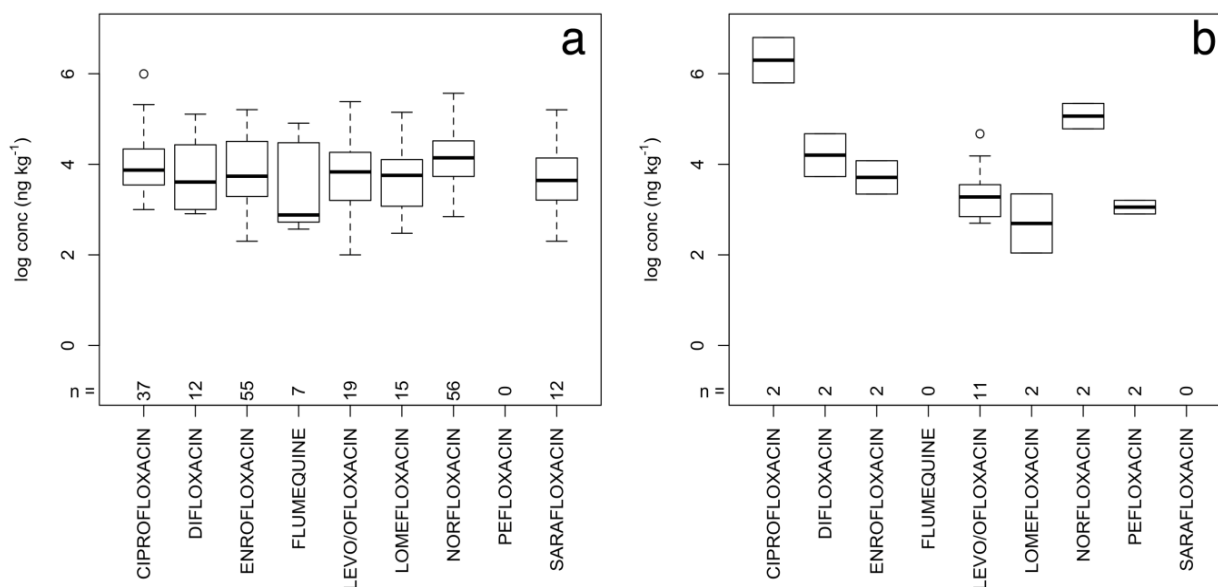


Fig. 1.6 Boxplots of FQ concentrations (ng kg^{-1}) observed in (a) animals and (b) plants (n = number of observations). Data obtained from Dufresne et al. (2007), Juan-García et al. (2007), Tittlemier et al. (2007), Zhao et al. (2007), Hu et al. (2010), Takeda et al. (2011), Gao et al. (2012b), He et al. (2012), Li et al. (2012a), Li et al. (2012b), Turnipseed et al. (2012).

From Fig. 1.6a, it can be observed that median FQ concentrations in animal species are for most compounds around $10 \mu\text{g kg}^{-1}$. FQ detections are predominantly reported for aquaculture and farm animals. CIP concentrations up to $21 \mu\text{g kg}^{-1}$ are reported for aquacultured shrimps (Zhao et al., 2007), and ENRO residues were observed in aquacultured frog legs at an average concentration of $29 \mu\text{g kg}^{-1}$ (Turnipseed et al., 2012). In mollusks from the Bohai Sea, China, eight different FQ compounds were detected at concentrations of 830 ng kg^{-1} up to $370 \mu\text{g kg}^{-1}$ (Li et al., 2012b). Also liver and muscle tissue of nine kinds of marine bred fish from the Pearl River Delta contained NOR, CIP, and ENRO at concentrations ranging from $3 \mu\text{g kg}^{-1}$ to $250 \mu\text{g kg}^{-1}$ (He et al., 2012). An Australian survey performed in 2007 on 100 imported aquaculture products reported FQ concentrations in Thai (FLU: $3.4 \mu\text{g kg}^{-1}$) and Chinese (FLU: $2.7\text{-}16 \mu\text{g kg}^{-1}$, CIP: $3.1 \mu\text{g kg}^{-1}$, ENRO: $33\text{-}130 \mu\text{g kg}^{-1}$) prawns, and in Indonesian (FLU: $2.0 \mu\text{g kg}^{-1}$) and Vietnamese fish (FLU: $8.3 \mu\text{g kg}^{-1}$) (AQIS 2007). ENRO is also detected in bovine meat samples taken from Valencian slaughterhouses, reaching at least $58 \mu\text{g kg}^{-1}$ (Juan-García et al., 2007). Zhao et al. (2007) reported similar concentrations for NOR ($1.1\text{-}43 \mu\text{g kg}^{-1}$), CIP ($1.0\text{-}74 \mu\text{g kg}^{-1}$) and ENRO ($2.0\text{-}161 \mu\text{g kg}^{-1}$) in Chinese chicken and swine muscle tissues.

Apart from cultured animals, FQ compounds are also observed in wildlife. Li et al. (2012a) reported that crustacean, fish, reptiles and birds residing in and near the FQ polluted Baiyangdian Lake in China, contain mean FQ concentrations ranging from $1.8\text{-}24 \mu\text{g kg}^{-1}$, with NOR the most prominent one.

FQ compounds are also observed in food products derived from animals. LEVO/OFL, CIP and NOR residues were detected in Chinese honey at concentrations ranging from $12 \mu\text{g kg}^{-1}$ to $56 \mu\text{g kg}^{-1}$, and DI was detected once at a concentration of $47 \mu\text{g kg}^{-1}$ (Zhou et al., 2009). Moreover, FQ compounds

MARBO, DANO, ENRO and CIP are observed up to $19 \mu\text{g L}^{-1}$ in raw Czech cow milk (Navrátilová et al., 2011).

Next to animals and animal derived products, FQs are detected in plants (Fig. 1.6b). Although few data is available on this matter, it is noticed that there is a higher variability in FQ concentrations compared to animals, and concentrations range from 100 ng kg^{-1} up to 6 mg kg^{-1} . Hydrophyte plants from the Baiyangdian Lake contain at least $8.4 \mu\text{g kg}^{-1}$ of FQs, with CIP the dominant compound (Li et al., 2012a). In agriculture crops, LEVO/OFL concentrations up to $3.6 \mu\text{g kg}^{-1}$ are measured in stalks and leafs of rape, radish, celery and coriander crops grown on manure fertilized agricultural fields (Hu et al., 2010).

1.1.7 Environmental fate and behavior

1.1.7.1 Partitioning in the environment

During surface water sampling campaigns in the aquatic environment, some researchers determined FQ concentrations in both sediments and the surrounding waters. This enabled them to calculate concentration ratios, presented in Table 1.4. Although few data are available, it can be observed that concentration ratios calculated for real samples are higher compared to the partition coefficients (K_d) determined in lab conditions (Table 1.2).

The same is true for FQ concentration ratios between WWTP sludge and water. Average concentration ratios are at least 10 times higher compared to experimentally determined partition ratios (K_d) in Table 1.2, even though in both scenarios, the FQ sludge-water partitioning is considered at equilibrium (Pomiès et al., 2013). Also other antibiotic compounds like roxithromycin, sulfamethoxazole and trimethoprim show higher concentration ratios in the real

environment than the K_d values determined in lab scale batch sorption tests (Halling-Sørensen et al., 2000; Joss et al., 2005; Carballa et al., 2008; Barron et al., 2009; Li et al., 2013).

Table 1.4 Reported concentration ratios for FQs detected in sediment and sludge matrices

Compound	Measured concentration ratios $\left(\frac{\text{mg}/\text{kg}_{\text{sediment/sludge}}^{\text{DS}}}{\text{mg}/\text{L}_{\text{water}}} \right)$					
	Sediment/Water			Sludge/Water		
	min	max	average	min	max	average
FLU			- ^a			-
NOR	9360	68065	36673 (n = 4) ^b	158	630957	79696 (n = 10)
CIP	264	14176	7220 (n = 2)	398	501187	67857 (n = 10)
PEFL			-			-
LOME			39838 (n = 1)	4602	17600	12076 (n = 4)
ENRO	362	8128	4245 (n = 2)	1000	39000	21575 (n = 6)
OFL	2280	33973	18127 (n = 2)	2836	398107	79827 (n = 6)
LEVO			-	2512	6310	4411 (n = 2)
DANO			-			-
MARBO			-			-
GATI			-	10800	19100	14733 (n = 3)
DI			-			11919 (n = 1)
MOX			-	14000	17000	15300 (n = 3)
SARA			2268 (n = 1)			1613 (n = 1)
SPAR			-	31900	45800	37667 (n = 3)

^a not reported; ^b n = number of observations; Data obtained from Stuer-Lauridsen et al. (2000), Golet et al. (2003), Okuda et al. (2009), Yang et al. (2010a), Peng et al. (2011), Gao et al. (2012b), Jia et al. (2012), Li et al. (2012a), Li et al. (2013), Senta et al. (2013).

This could be due to the fact that lab experiments use inactivated sludge to determine partition coefficients, while concentration ratios in the real environment are determined at operating conditions. Although Stevens-Garmon et al. (2011) reported that chemical inactivation (e.g. sodium azide) of sludge can alter partition coefficients by affecting the aqueous composition or sludge surface characteristics, there is yet no consensus on this matter (Hyland et al., 2012).

1.1.7.2 Conversion in the environment

In environmental matrices, FQs can be degraded by different processes, of which photolysis, biodegradation, and oxidation by mineral oxides are of main importance.

FQs present in **surface waters** are primarily degraded via photolysis (Ge et al., 2010a; Sturini et al., 2012b; Babić et al., 2013). However, this is a slow process resulting in long environmental residence times. Half-life times of 3-12 d under sunlight irradiation are observed for OFL in surface waters (Xu et al., 2009), and of 1.9-2.3 d for FLU in shrimp pond water (Lai and Lin, 2009). Mesocosm spiked with ENRO (25 $\mu\text{g L}^{-1}$) and irradiated with different sunlight regimes showed half-life times from 0.8 d under full illumination to 72 d under near-complete shading conditions (Knapp et al., 2005).

Photolytic degradation of FQ compounds sorbed to aquatic **sediments** can only occur at the sediment surface and in the first millimeters of depth (Xu et al., 2009). As a result, FQ photolysis in sediments is rather slow, with reported half-life times ranging from 6 d up to 34 d (Lai and Lin, 2009; Xu et al., 2009). Next to photolytic degradation, it is reported that iron oxides, commonly present in aquatic sediments, are capable of oxidizing FQ compounds (Zhang and Huang, 2007). Biodegradation, however, showed to be of negligible importance for FQs sorbed on sediments sampled from aquaculture ponds (Lai and Lin, 2009).

FQ compounds present in **soils** are susceptible to oxidation by manganese oxides, commonly found in soils (Zhang and Huang, 2005), but also photolysis can have an impact on FQ degradation as is reported by Sturini et al. (2012a). Moreover, strong electrostatic sorption, as well as chemical aging, which is the migration of

molecules into very small sites within the soil matrix (e.g., nanopores), make FQs inaccessible for biodegradation (Alexander, 2000). A FQ biodegradation study performed by Mougin et al. (2013) recorded less than 0.01% CIP mineralization after 84 d of incubation. Remarkably, biodegradation of CIP was improved up to 5-8 times by the addition of earthworms, which modified the antibiotic distribution within the soil profile. Despite these possible FQ degradation mechanisms, environmental half-life times of FQs sorbed on soil matrices are, compared to sediment matrices, up to 200 times longer. Half-life times between 1-3 years of CIP and NOR are reported in a mesocosm soil study performed by Walters et al. (2010), revealing a high resistance towards biotic and abiotic degradation. In accordance, half-life times of more than 217 d are observed in experimental field studies with sludge and manure fertilized agricultural soils (Gottschall et al., 2012; Rosendahl et al., 2012). These long half-life times are a clear indication for the persistent nature of FQ antibiotic compounds in soil matrices.

1.1.7.3 Bioaccumulation

Limited information is available on FQ, bioaccumulation factors (BAF) defined as the ratio of the concentration in biotic tissue over the concentration in the surrounding water. According to Kelly and Gobas (2001), chemicals are bioaccumulative when their BAF is higher than 5000 L kg⁻¹, and potentially bioaccumulative if their BAF ranges between 2000-5000 L kg⁻¹ (Gao et al., 2012b). So far, only two references reported FQ BAFs. For aquatic animals residing in and near the Baiyangdian lake, FQ BAFs ranged between 125 and 16,700 L kg⁻¹, and only ENRO was bioaccumulated in shrimp and river snails with mean BAFs of 16,700 and 6140 L kg⁻¹, respectively. ENRO, CIP, and SAR were potentially bioaccumulative for crabs and 3 different carp species (Gao et al., 2012b; Li et al., 2012a).

Mean BAFs for FQs in hydrophyte plants ranged between 653 and 170,000 L kg⁻¹, with only bioaccumulation of CIP (Li et al., 2012a). This is possibly due to the fact that plants are able to metabolize ENRO into its metabolite CIP, which might also partially explain the lower observed BAFs for ENRO in comparison with animals (Li et al., 2012a). Recently, Thi et al. (2012) indicated the potential of bioaccumulation to be used in phytoremediation by showing the accumulation of FQs in shrimp pond waters by the hydrophyte plant species *C. demersum* and *C zizanioides*.

1.1.8 Ecological effects

The long environmental residence times of FQ compounds in soil matrices can affect the composition and activity of soil microbial communities, which is demonstrated for CIP at 200 µg kg⁻¹ by Girardi et al. (2011). Also fresh water sediments are affected by the presence of FQs, with microbial community composition changes observed after a repeated exposure of 540 µg kg⁻¹ and 80 µg kg⁻¹ CIP (Maul et al., 2006). Naeslund et al. (2008) reported that the lowest effect concentration of CIP on a marine sediment bacterial community was 0.1 µg kg⁻¹. The latter is at least 2 times lower than the concentrations measured in marine and fresh water sediments (Fig. 1.5b), indicating the potential ecotoxicity of FQ polluted sediments.

Next to the toxicity in soils and sediments, the combination of a continuous FQ discharge and long surface water residence times can create toxic conditions for aquatic organisms. FQ median effect concentrations (EC-50) for different aquatic organisms like cyanobacteria, bacteria, green algae, aquatic plants, and animals are summarized in Table A.1. It is noticed that EC-50s are situated in the µg L⁻¹ to mg L⁻¹ range, with cyanobacteria being the most sensitive aquatic organisms

(0.005-0.465 mg L⁻¹), and algae and plants (0.022-38.5 mg L⁻¹) more sensitive than invertebrates and fish (0.53-477 mg L⁻¹).

To evaluate the environmental risk of FQs, hazard quotients (HQ) are calculated (Fig. 1.7), expressing the measured environmental concentration (MEC) divided by the predicted no effect concentration (PNEC) (Robinson et al., 2005; Li et al., 2012a; Martins et al., 2012). The latter is frequently determined by applying an assessment factor to the lowest EC-50 of a test organism group encompassing three trophic levels, usually fish, crustaceans and algae (Länge and Dietrich, 2002; Park and Choi, 2008; Li et al., 2012a; Martins et al., 2012). A commonly used ranking criterion to assess ecological risk is presented by Verlicchi et al. (2012a). HQ < 0.1 represent a low risk to aquatic organisms, 0.1 < HQ < 1 indicate a medium risk, and HQs higher than 1 reveal a high ecological risk. From Table A.1, it is observed that FQ ecotoxicological data are relatively scarce. Therefore, HQs of FQs which lack ecotoxicity data for three trophic levels are marked with an asterisk (Fig. 1.7) and are calculated by selecting the most sensitive test organisms.

HQs are calculated for the reported saline and fresh surface water concentrations (MECs) from Fig. 1.5a. For marine organisms, few ecotoxicological data are reported, and *V. fischeri* showed to be the most sensitive investigated test organism (Table A.1). To assess environmental risk in fresh surface waters, different test organisms are selected based on sensitivity and data availability. CIP, NOR, and FLU are evaluated using *M. aeruginosa*, LEVO/OFL and LOME using *L. gibba*, and SARA, ENRO, and MOX using the algal species *D. subcapitatus* and *P. subcapitata* (Table A.1).

From Fig. 1.7a it can be observed that the risk of CIP pollution in **marine surface water** is low for *V. fisheri*. However, LEVO/OFL and NOR HQs exceed the threshold value of 1 for 54% and 24% of the data points, respectively. HQs up to 375 are calculated, indicating the extreme ecotoxicological risks in certain marine areas (Robinson et al., 2005; Zou et al., 2011).

Fresh water aquatic organisms are threatened by CIP, LEVO/OFL, SARA, and ENRO pollution (Fig. 1.7b). The reported CIP surface water concentrations in Fick et al. (2009) pose an extreme ecological risk for aquatic organisms, with calculated HQs for cyanobacteria of at least 2000. However, this is an exceptional situation and the high FQ concentrations reported in that study (up to 6.5 mg L⁻¹ CIP) are therefore omitted during further discussion. More than 85% of the calculated CIP and LEVO/OFL HQs are higher than 1, with HQs ranging up to 1932 and 1110 for CIP and LEVO/OFL, respectively. This shows that CIP and LEVO/OFL surface water concentrations may pose a high ecological risk for cyanobacteria and *L. gibba*. This is in agreement with Grung et al. (2008) and Li et al. (2012a), reporting CIP and OFL HQ values ranging from 1.5 up to 52 for the cyanobacterium *M. aeruginosa*. Also the veterinary FQs SARA and ENRO pose a risk in about 40% of the reported concentrations. Only 1% of NOR HQs are higher than 1, and no high ecotoxicological risk is observed for LOME, FLU, and MOX, although for the latter compound no ecotoxicological data are available for more sensitive test organism species.

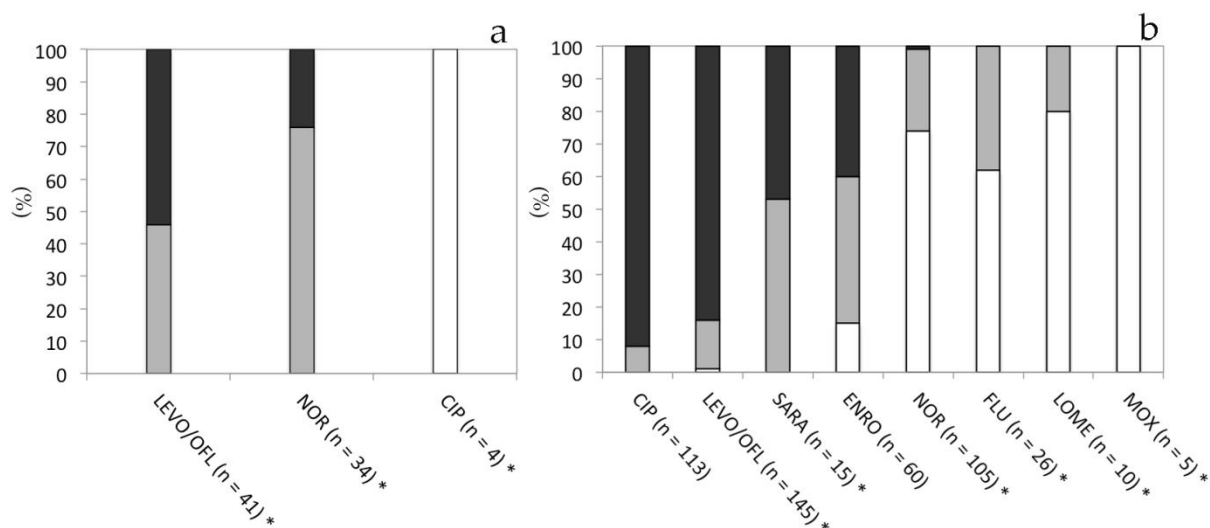


Fig. 1.7 (a) Procentual representation of the calculated FQ HQs for marine surface waters using *V. fischeri* as target organism; (b) Procentual representation of the calculated FQ HQs for fresh surface seawater using the reported EC-50s of the most sensitive target organisms. Dark grey represents HQs equal or higher than 1, light grey shows the fraction of HQs between 1 and 0.1, and the white fraction shows HQs lower than 0.1 (n = number of data points). * Risk assessment is performed on a limited amount of ecotoxicity data, using the most sensitive target organism reported in Table A.1.

Overall, the results depicted in Fig. 1.7 indicate that FQ compounds pose a potential environmental risk towards aquatic organisms like *V. fischeri*, cyanobacteria *M. aeruginosa*, and sensitive aquatic plant species. In addition, crustacea and higher aquatic organisms like fish are not likely at risk due to the higher EC-50 values for these species (Table A.1; Li et al., 2012a). However, current approaches and knowledge have limitations.

First, due to the scarcity of ecotoxicological data, a full environmental risk assessment cannot be properly executed for most FQs. Therefore, more ecotoxicological research is needed on different trophic levels of fresh water and especially marine organisms, where a greater sensitivity distribution is expected due to a higher species diversity (Fisk, 2013). Second, the use of single compound PNEC values in risk assessment is questionable, since concentrations of FQs lower than the PNEC value can contribute to the overall mixture ecotoxicity

(Backhaus et al., 2000). Therefore, a more complete assessment of the potential risk resulting from FQ (and other micropollutant) mixtures in surface waters is required. A possible approach is summing the MEC/PNEC values of the different detected FQs, as performed in Kümmerer and Henninger (2003) with the assumption that synergetic effects are negligible. This is, however, not clear since synergism is reported by Yang et al. (2008) and Gonzalez-Pleiter et al. (2013) during algal growth inhibition tests with *Pseudokirchneriella subcapitata*. Third, although acute toxicity towards higher organisms occurs at FQ concentrations higher than environmental ones, negative effects by prolonged exposure at low concentrations cannot be ruled out, suggesting more research on chronic toxicological effects (Fent et al., 2006; Santos et al., 2010; Martins et al., 2012).

1.1.9 Conclusions

Environmental FQ pollution is a problem that is expected to gain even more attention in the coming years, since FQ antimicrobial consumption is still increasing.

FQ pollution encompasses different environmental matrices with CIP, NOR, and OFL/LEVO being the most frequently reported FQs. Although it could be assumed that this is most likely due to the higher consumption of these compounds, FQ consumption is quite difficult to assess since consumption data are gathered on a country specific basis, and are hard to obtain. This is especially true for FQ consumption in agricultural applications. For human (FQ) antibiotics, Europe has set a first step towards uniformity by collecting consumption data of all its membership states through one authorization, i.e. the ECDC.

Environmental research on FQs belonging to the latest generation, e.g. MOX, is scarce. However, since a shift in consumption towards these newer generations of

FQs is observed by ECDC, it is advisable that researchers include more recently developed FQ compounds in their target compound scanning list during sample analysis to increase the knowledge on FQ occurrence in WWTPs and the natural environment.

This chapter clearly shows that conventional WWTPs are not fully capable in removing FQ compounds. Therefore, actions are necessary to diminish the discharge of these emerging organic micropollutants. The authors propose four courses of action.

First, **prevention and sensibilization** campaigns are of importance to inform the public on the risks involved with excess use of antibiotic compounds. The increasing bacterial resistance formation calls for urgent matters and a decrease in antibiotic consumption is advised to halt this resistance formation. Moreover, a controlled disposal and treatment of overdue and excess drugs is necessary. In agriculture applications, where anti-infectives are also regularly used, further actions are needed to control and regulate the use of antibiotics in live-stock and aquaculture applications.

Second, improved **treatment** of polluted wastewaters is necessary to prevent the discharge of these biorecalcitrant compounds into the environment. Therefore, the performance of existing WWTPs should be optimized for the removal of FQ and other micropollutants by implementing tertiary treatment techniques. This should be combined with an ongoing research for new and more innovative water treatment techniques.

Third, it is observed that **sludge and manure fertilization** are sources of FQ pollution towards agricultural soils and, in some cases, crops harvested from these fields. Therefore, strict and uniform regulations on the application of urban

WWTP sludge and livestock manure as fertilizers during agriculture activities is advisable.

Final, more research is needed that focuses on the ecotoxicological risks associated with pharmaceutical pollution, especially for chronic effects in environmental mixtures. These experimental data will help policy makers to decide which compounds pose a threat to the aquatic environment and need to be included in the priority substance lists defined in **legislative frameworks** like the Directive 2008/105/EC, which is a daughter Directive of the Water Framework Directive 2000/60/EC. Ecotoxicological data can be used to define Environmental Quality Standards for monitoring of ambient water, sediments, and biota. The EU has set a first step towards environmental pharmaceutical regulation by adding three pharmaceuticals on the 'watch list' (EC, 2013). Although they are not included in the priority substance list yet, this is a first acknowledgment of the environmental problems associated with pharmaceutical pollution.

1.2 Heterogenous photocatalysis: an AOP for innovative environmental technology

1.2.1 Introduction

As shown in Chapter 1.1, many pharmaceuticals including FQs are not efficiently removed by conventional WWTPs, resulting in the occurrence of these micropollutants in environmental waters. In the last decade, a lot of research has been addressed to additionally treat secondary effluent waters using oxidation techniques defined as Advanced Oxidation Processes. A literature survey on Web of Knowledge using “advanced oxidation process” and “wastewater” as key words resulted in 1543 publications since 2000 implying that this research area is of great interest for water treatment applications.

1.2.2 Advanced Oxidation Processes

The concept of “advanced oxidation processes” was established by Glaze et al. (1987). They are based on the production of highly reactive and non-selective hydroxyl radicals leading to the destruction of organic pollutants in a gaseous or aqueous phase (Andreozzi et al., 1999; Demeestere et al., 2007). Key AOPs, typically performed at ambient temperature and pressure, include heterogeneous and homogeneous photocatalysis, electrolysis, ozonation, the Fenton's reaction, sonication, and wet air oxidation (Klavarioti et al., 2009).

AOPs are intensively investigated for their application in wastewater treatment. They are recommended when wastewater contains components with a high

chemical stability and low biodegradability. An AOP treatment can result in the transformation of the refractory or toxic compounds into less complex compounds, with the aim to reduce toxicity and/or increase biodegradability. Recent reviews discuss the application of AOPs for the removal of different kinds of hazardous pollutants like pesticides, aromatic compounds, dyes, etc. in industrial wastewaters (Chiron et al., 2000; Han et al., 2009; Chong et al., 2010; Ahmed et al., 2011; Kim and Ihm, 2011). One AOP application which gains more and more interest is the removal of emerging micropollutants like pharmaceutical residues in WWTP effluent waters. Among the different AOP techniques, ozonation and heterogeneous photocatalysis are the most intensively investigated (Esplugas et al., 2007; Kassinos et al., 2009; Klavarioti et al., 2009; Homem and Santos, 2011; Tong et al., 2012) (Fig. 1.8).

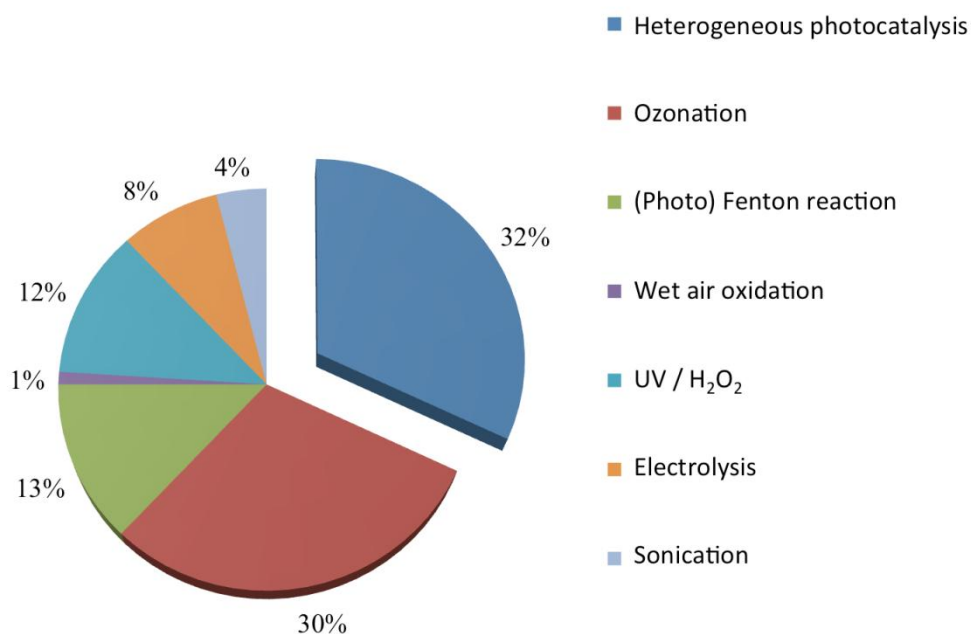


Fig. 1.8 Distribution of AOPs investigated for pharmaceutical residue degradation in wastewater, from 1998-2008 (number of scientific papers = 99) (Klavarioti et al., 2009).

On a scientific research level, ozonation and heterogeneous photocatalysis are the two main investigated AOP technologies for pharmaceutical residues

degradation. Looking at operating full-scale AOP installations, it is observed that homogeneous AOP techniques such as ozonation (and in few cases UV/H₂O₂ and photo-Fenton reaction) are mainly used for disinfection purposes rather than for micropollutant remediation (Singh, 2012; Hey, 2013) but full-scale applications for micropollutant removal are on the rise (Pills, 2009; MicroPoll, 2010; Hey, 2013). On a pilot-scale level, a more diverse use of AOPs for organic pollutant removal is observed with some treatment facilities investigating the application of heterogeneous photocatalysis for secondary effluent remediation (Miranda-García et al., 2011; Mozia et al., 2012; Sousa et al., 2012; Hey, 2013).

Here, we briefly explain the main principles and applications of heterogeneous photocatalysis, given the scope of this PhD work.

1.2.3 Heterogeneous photocatalysis

1.2.3.1 Definition and principles

Heterogeneous photocatalysis is defined by Palmisano and Sclafani (1997) as “a catalytic process during which one or more reaction steps occur by means of electron-hole pairs photogenerated on the surface of semiconducting materials illuminated by light of suitable energy.” A heterogeneous photocatalytic degradation process can be decomposed into five consecutive steps (Herrmann, 2010):

- 1: Transfer of the reactants from the liquid phase to the catalyst surface
- 2: Adsorption of the reactants
- 3: Reaction of the adsorbed compounds on the catalyst surface
- 4: Desorption of the reaction product(s)
- 5: Transfer of the degradation products to the bulk solution

The difference with classic heterogeneous catalysis lies in step 3, including (i) the activation of the catalyst through absorption of photons, (ii) formation and migration of reactive species, and (iii) the electron transfer reactions. Catalyst activation is based on semiconductor photochemistry, and can be presented by the 'band-gap' model (Fig. 1.9).

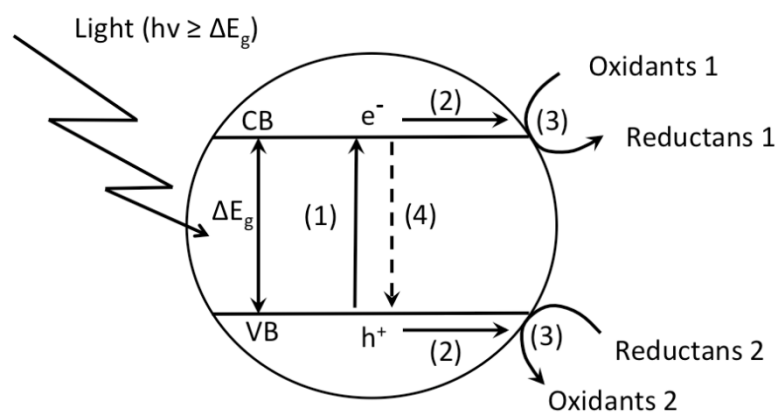


Fig. 1.9 Schematic representation of the semiconductor 'band gap model'. (1) photo-induced electron-hole separation, (2) charge migration to the surface, (3) oxidation/reduction reactions, (4) electron-hole recombination. VB: valence band, CB: conduction band, ΔE_g : band gap.

Semiconductors are materials with an electronic structure characterized by a band gap (ΔE_g), which is defined as the energy (eV) needed to excite an electron from the valence band (VB) to the conduction band (CB). The VB is considered as the highest energy level completely filled with electrons, whereas the CB is the lowest energy band without electrons. The excitation of an electron from the VB to the CB occurs when the catalyst absorbs photons with an energy content equal to or higher than the band gap energy, generating electron-hole pairs (1). Both reactive species can migrate to the catalyst surface (2), and react with electron donors (e.g., target compound and/or H_2O and hydroxyl ions) and acceptors (e.g., oxygen) adsorbed on the semiconductor surface (3). Redox reactions can occur if the redox potential of the adsorbates is suitable. In the case for VB 'holes', oxidation can

proceed if the redox potential of the VB is more positive than that of the adsorbed compounds; and for CB electrons, a more negative reduction potential is needed. Photo-induced 'holes' are capable of oxidizing pollutants by direct oxidation, or in an indirect way through the formation of hydroxyl radicals created by the oxidation of water and hydroxyl ions. If no reaction occurs within the required time scale span (typically less than 1 μ s) (Mohamed and Bahnemann, 2012), CB electrons and VB 'holes' can recombine and dissipate the input energy as heat (4).

A more elaborate discussion on the different photocatalytic degradation mechanisms occurring in the liquid phase and on the catalyst surface is given in Chapter 2.1.

1.2.3.2 Photocatalysts

Common photocatalysts investigated for their application in water remediation are (i) metal oxides like TiO_2 , ZnO , ZrO_2 , CeO_2 ... and (ii) sulfides like ZnS , CdS , CdSe , CdTe , ... (Herrmann, 1999). Band gaps, VB and CB edges of some of these semiconductors are presented in Fig. 1.10.

TiO_2 is by far the most investigated photocatalyst for a wide range of environmental applications due to its chemical inertness, low toxicity, well positioned VB and CB edges, commercial availability, and low purchase price (about 20 € kg^{-1}) (Carp et al., 2004; Muñoz, 2006). From Fig. 1.10, it can be observed that TiO_2 based photocatalysts have more suitable band edges compared to other photocatalysts, since VB redox potentials are more positive than the ($\cdot\text{OH}/\text{OH}$) redox couple, resulting in the oxidation of adsorbed water molecules and hydroxyl ions to hydroxyl radicals.

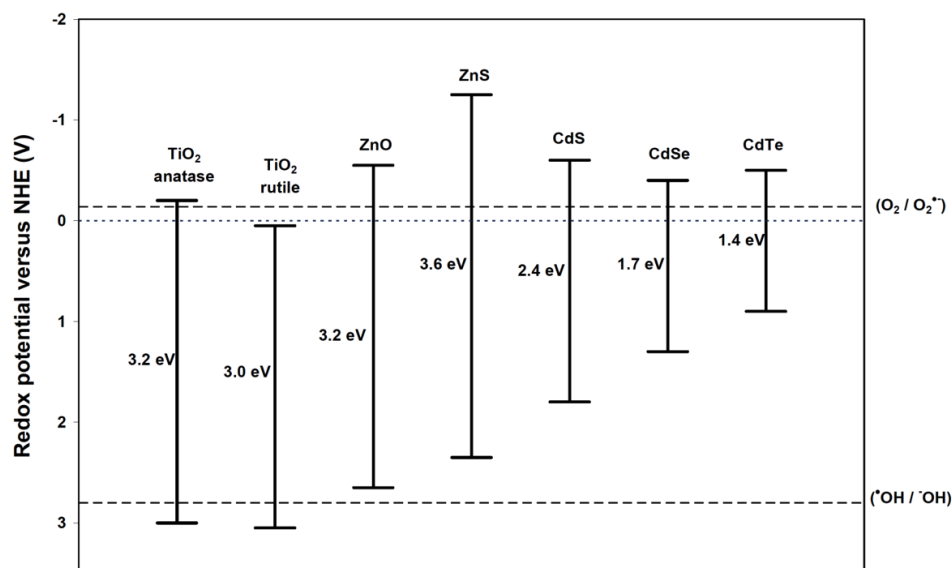


Fig. 1.10 Band gaps, VB and CB edges of common semiconductors and standard redox potentials (versus NHE: normal hydrogen electrode) of the $O_2/O_2^{\bullet-}$ and $^{\bullet}OH/{}^{\bullet}OH$ redox couple (Demeestere et al., 2007).

Activation of TiO_2 anatase occurs when irradiated light is absorbed with an energy higher than 3.2 eV, which corresponds to a wavelength lower than 388 nm. Rutile is activated at wavelengths lower than 413 nm due to its smaller band gap. Although anatase has a higher band gap energy, it is reported to contain a higher photoactivity compared to rutile (Herrmann, 1999). This can be explained by the fact that anatase is capable in reducing oxygen towards superoxide radicals with CB electrons, resulting in longer electron-hole separation (Fig. 1.10).

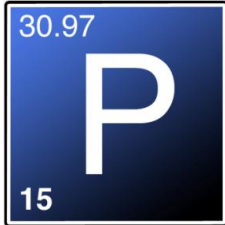
Apart from the use of a pure rutile or anatase photocatalyst, a mixture of both crystalline phases can improve catalyst activity due to a better electron-hole separation, and thus a reduced recombination speed (Hurum et al., 2003). The most commonly used and commercially available TiO_2 photocatalyst is Aeroxide P25, formerly known as Degussa P25, which contains anatase and rutile at reported ratios typically between 70:30 or 80:20 (Ohtani et al., 2010). Actually, it

is not easy to find a photocatalyst with a higher activity than that of P25, resulting in the fact that P25 has been used as a de-facto standard titania based photocatalyst. Using the scientific search engine Web of Knowledge, more than 1400 papers are found since 1990, which describe the use of P25 for photocatalytic reactions, showing the importance of this catalyst for the photocatalytic research domain.

1.2.3.3 Applications: heterogeneous photocatalysis for the removal of pharmaceutical residues

The application of heterogeneous photocatalysis for the treatment of wastewater with pharmaceutical residues is intensively investigated, with antibiotics and anti-inflammatory drugs receiving the most attention (Yurdakal et al., 2007; Klamerth et al., 2009; Miranda-García et al., 2010; Homem and Santos, 2011; Tong et al., 2012).

Antibiotics are target compounds of interest due to their persistence towards biodegradation in conventional WWTPs. Photocatalytic degradation is reported for tetracyclines, β -lactams, and sulfonamide antibiotics (Palominos et al., 2009; Klauson et al., 2010; Tong et al., 2012). However, few manuscripts discuss heterogeneous photocatalysis of FQ antibiotics, especially for the newer FQ generations. Therefore, and given the environmental relevance of FQs (see Chapter 1.1), Parts II-V of this PhD focus on a systematic and in-depth research dealing with different aspects of heterogeneous photocatalysis for FQ removal in (waste)water.



art II

Photocatalytic removal of moxifloxacin: adsorption, effect of process parameters, and reactive species

Redrafted from:

Van Doorslaer, X., Demeestere, K., Heynderickx, P.M., Van Langenhove, H., Dewulf, J., 2011. Applied Catalysis B-Environmental, 101, 540-547.

and

Van Doorslaer, X., Heynderickx, P.M., Demeestere, K., Debevere, K., Van Langenhove, H., Dewulf, J., 2012. Applied Catalysis B-Environmental, 111-112, 150-156.

2.0 Introduction

The application of heterogeneous photocatalysis for the removal of FQ antibiotics from a water matrix is only scarcely investigated. Although first insights have been gained in Haque and Muneer (2007), Paul et al. (2007), Calza et al. (2008), and Palominos et al. (2008), literature data on the photocatalytic removal of the recently developed FQ compound MOX is lacking. Therefore, in this first experimental part, the heterogeneous photocatalysis of MOX is investigated with a twofold scope.

In Chapter 2.1, the effect of pH and irradiation conditions on both the photolytic and TiO₂ mediated photocatalytic removal of CIP and MOX in aqueous solutions are studied. The degradation of CIP is used as a benchmark for the results obtained with MOX. In heterogeneous photocatalysis, adsorption is a key step in the degradation mechanism (Herrmann, 2010), but quantitative data on the adsorption-desorption process are lacking for CIP and MOX. Therefore, equilibrium partition ratios for the different CIP and MOX species are quantified, and linked to the photocatalytic degradation rates.

Chapter 2.2 deals in a first part with the optimization of Degussa P25 mediated photocatalytic degradation of MOX through a systematic investigation of the effect of different operational variables such as initial FQ concentration, catalyst concentration, stirring speed, oxygen concentration in the gas flow sparged through the reaction solution, and reaction temperature. Secondly, the goal is to obtain a better understanding of the contribution of some major reactive species in the photocatalytic degradation mechanism by the addition of selective reactive species scavengers at different concentrations

2.1 UV-A and UV-C induced photolytic and photocatalytic degradation of aqueous ciprofloxacin and moxifloxacin: effect of pH and role of adsorption

2.1.1 Materials and methods

2.1.1.1 Chemicals and experimental setup

Demineralized water ($< 0.2 \mu\text{S cm}^{-1}$) used during the photolytic and photocatalytic experiments is prepared from tap water with ion exchange cartridges (Aquadem[®], Werner, Germany). The following compounds are spiked to the demineralized water: (i) the target FQ compounds ciprofloxacin and moxifloxacin (ciprofloxacin.HCl; moxifloxacin.HCl (BAY12-80369) provided by MP Biomedicals Inc. and the Bayer corporation, respectively), and (ii) a phosphate buffer (10 mM) using H_3PO_4 (Merck, 85%), KH_2PO_4 (Sigma Aldrich, 99%), K_2HPO_4 (Acros, $\geq 98\%$) and K_3PO_4 (Sigma Aldrich, $\geq 98\%$). Small amounts of NaOH (Acros, extra pure) and HCl (Fiers, 37%) are dosed for pH adjustment. No further modifications of the aqueous matrix are performed.

As a photocatalyst, commercial Degussa P25 TiO_2 (Evonik, Antwerp, Belgium) is used with a BET specific surface area of $48.3 \pm 0.7 \text{ m}^2 \text{ g}^{-1}$ (TRISTAR Micromeritics, Aachen, Germany), $86.7 \pm 0.6\%$ of anatase and primary anatase and rutile particle sizes of $18.7 \pm 0.1 \text{ nm}$ and $23.3 \pm 1.2 \text{ nm}$, respectively (Siemens D5000 scintillation counter, Bruker, Karlsruhe, Germany, $\theta = 0.02^\circ$) (Spurr and Myers, 1957).

Photolytic and photocatalytic degradation experiments are performed in a lab scale batch reactor of 300 mL (Fig. 2.1), using the reaction conditions summarized in Table 0.1. The reaction temperature is controlled at a constant value of 298 ± 1 K by immersing the reactor in a water bath.

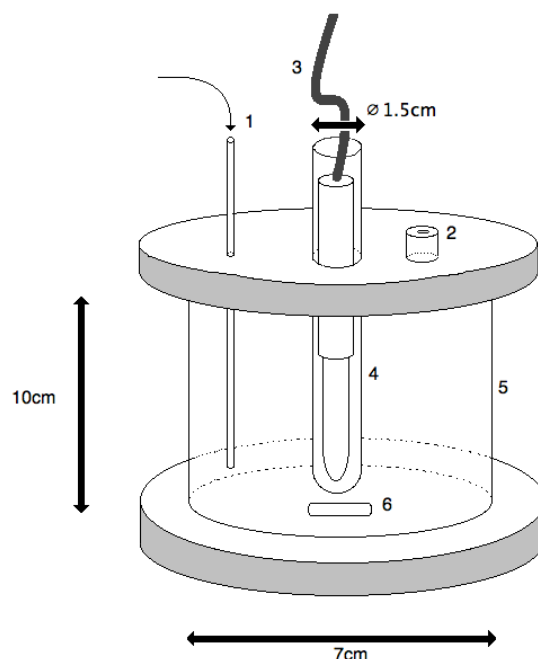


Fig. 2.1 Experimental setup with gas flow inlet (1), sampling port (2), UV Pen ray lamp (3), quartz tube (4), reaction vessel (5) and stir bar (6).

UV-A (300-440 nm with main peak at 365 nm) and UV-C (main peak at 254 nm with four minor peaks around 400 nm) pen rays are used as a light source and positioned axially in the reactor. The first is provided by UVP (United Kingdom), the latter by Ningbo Sunfine UV lighting co. (China). By means of actinometry measurements performed according to Hatchard and Parker (1956), photon irradiance for both illumination sources were determined to be 0.52 mW cm^{-2} ($1.6 \cdot 10^{-9} \text{ Einstein s}^{-1} \text{ cm}^{-2}$) and 0.93 mW cm^{-2} ($2.0 \cdot 10^{-9} \text{ Einstein s}^{-1} \text{ cm}^{-2}$) (calculated for outer reactor surface), respectively.

The CIP and MOX solutions (with and without TiO₂ catalyst) are stirred under darkness and sparged with pure oxygen for 30 min prior to irradiation. During irradiation, suspensions are continuously stirred and sparged. Aliquots of 2 mL are collected with a spinal needle syringe and filtered over a Whatman 0.22 µm Spartan mini disk filter to remove the residual TiO₂ before analysis.

2.1.1.2 Analytic methods

CIP and MOX concentrations are measured by liquid chromatography (HPLC) coupled to a photodiode array detector (PDA, Surveyor, Thermo Scientific, USA). A Luna C18(2) column (150 mm × 3.0 mm, 3 µm, Phenomenex, USA) with a mobile phase containing water (HiPerSolv CHROMANORM, HPLC grade with 0.1% formic acid (Fluka, ≥ 98%) and acetonitrile (HiPerSolv CHROMANORM, HPLC grade) is used for the chromatographic analysis of CIP and MOX. Quantification of CIP takes place at 278.0 ± 4.5 nm and MOX at 296.0 ± 4.5 nm. The CIP and MOX chromatographic peak areas are plotted as a function of time relatively to the peak area corresponding to the initial concentration, giving C/C₀ versus time graphics.

2.1.1.3 Degradation kinetics

Photolytic and photocatalytic degradation kinetics of CIP and MOX are described using an apparent first-order degradation rate model, Eq. 2.1:

$$\frac{C}{C_0} = \exp(-k_1 t) \quad (2.1)$$

The apparent first-order reaction rate constant, k_1 (min⁻¹), is for each experiment determined by regression of at least 24 experimental data points, obtained in Section 2.1.1.1, to Eq. 2.1, using ODRpack (Boggs et al., 1987).

2.1.1.4 Partitioning of FQs between an aqueous phase and TiO₂

2.1.1.4.1 Experimental

The fraction of the initially added amount of both FQs adsorbed on the catalyst surface is determined in the same setup and experimental conditions as described in Section 2.1.1.1 at pH values 3.0, 5.0, 7.0, 8.5 and 10.0. Therefore, aqueous samples are analyzed for CIP and MOX before and 30 min after catalyst addition. Preliminary experiments revealed that adsorption-desorption equilibrium is attained after 5 min for both FQ compounds (data not shown), confirming results mentioned by (Paul et al., 2010). The adsorbed FQ fraction S (mol mol⁻¹) on the catalyst surface is defined by Eq. 2.2:

$$S = \frac{C_{A,ad}}{C_{A,0}} \frac{m_{cat}}{V} \quad (2.2)$$

with both FQs denoted as 'A' in the following calculations.

2.1.1.4.2 Governing equations

Partition ratios for the different FQ species are estimated from the experimentally determined adsorbed FQ fraction S on the catalyst surface. A detailed calculation is provided in Addendum B. Due to the amphoteric nature of both FQs, the defined adsorbed FQ fraction can be expanded to the different FQ species which are related by pK_a values (Fig. 2.2 and Fig. B.1).

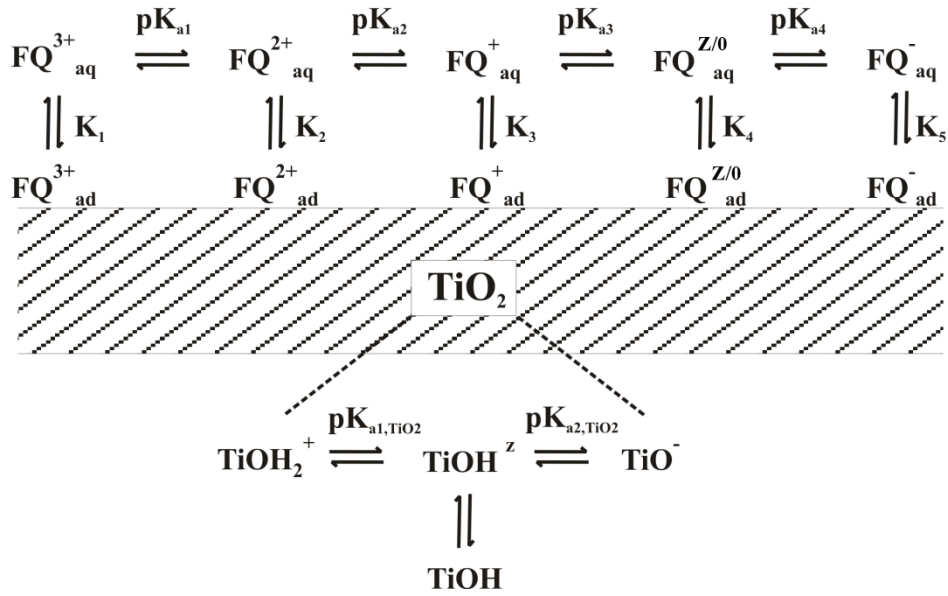


Fig. 2.2 Schematic overview of the FQ interaction with the TiO_2 surface expressed as K values and the shift in charge due to the solution pH expressed as pK_a values.

Therefore, Eq. 2.2 can be expanded to Eq. 2.3:

$$S = \frac{C_{A_{ad}^{3+}} + C_{A_{ad}^{2+}} + C_{A_{ad}^{+}} + C_{A_{ad}^{Z/0}} + C_{A_{ad}^{-}}}{C_{A,0}} \frac{m_{cat}}{V} \quad (2.3)$$

As seen in Fig. 2.2, the adsorbed FQ species concentration ($\text{mol kg}_{\text{cat}}^{-1}$) is related to its aqueous concentration (mol L^{-1}) with a partition ratio K ($\text{L kg}_{\text{cat}}^{-1}$) in Eq. 2.4:

$$K_q = \frac{C_{A_{ad}^{\varphi}}}{C_{A_{aq}^{\varphi}}} \quad \text{with } \varphi = 3+, 2+, +, Z/0, - \text{ and } q = 1-5 \quad (2.4)$$

Using the general mol balance of the adsorption process in Fig. 2.2, vide Eq. 2.5, and substitution of $K'_q = \frac{m_{cat}}{V} K_q$ with $q = 1-5$ and $\delta_{i,j} = 10^{\text{pH}_i - \text{pK}_{a,j}}$ with $j = 1-4$, give linear Eqs. 2.6, $i = 1-5$, in the unknown partition ratios K'_1, K'_2, K'_3, K'_4 and K'_5 :

$$VC_{A,0} = V(C_{A_{aq}^{3+}} + C_{A_{aq}^{2+}} + C_{A_{aq}^+} + C_{A_{aq}^{Z/0}} + C_{A_{aq}^-}) + m_{cat}(C_{A_{ad}^{3+}} + C_{A_{ad}^{2+}} + C_{A_{ad}^+} + C_{A_{ad}^{Z/0}} + C_{A_{ad}^-}) \quad (2.5)$$

$$\frac{K'_1}{\delta_{i,1}\delta_{i,2}} + \frac{K'_2}{\delta_{i,2}} + K'_3 + \delta_{i,3}K'_4 + \delta_{i,3}\delta_{i,4}K'_5 = \frac{S_i}{1-S_i} \left(\frac{1}{\delta_{i,1}\delta_{i,2}} + \frac{1}{\delta_{i,2}} + 1 + \delta_{i,3} + \delta_{i,3}\delta_{i,4} \right) \quad (2.6)$$

The partition ratios K are obtained by multiplying the solution vector \underline{K}' by the factor $\frac{V}{m_{cat}}$. A volume of $2.0 \cdot 10^{-1}$ L and an applied catalyst mass of $1.0 \cdot 10^{-4}$ kg_{cat} gives a factor of $2.0 \cdot 10^3$ L kg_{cat}⁻¹.

2.1.1.4.3 Estimation of partition ratios

Five partition ratios, as given in Fig. 2.2, are obtained by regression of Eq. 2.6 to the experimental adsorption data, obtained in Section 2.1.1.4.1., using ODRpack. Three replicate experiments are performed at five pH levels, so that fifteen responses ($n_{resp} = 15$) are applied in the fitting procedure. The objective function is defined by Eq. 2.7, with L_l and R_l the left and the right hand side in Eq. 2.6 for every experimental point l . Due to the difference in order of magnitude of \underline{R}_l , normalisation is performed by setting $w_l = R_l^{-2}$ (Himmelblau, 1970):

$$S^* = \sum_{l=1}^{n_{resp}} w_l (R_l - L_l)^2 \quad (2.7)$$

Details on the estimation of the partition ratios are given in Addendum B.

2.1.2 Results and Discussion

In this chapter, experiments are performed at a constant pH obtained by the addition of a buffer. During the adsorption experiments (Section 2.1.2.3) a constant pH is observed for the investigated pH range (3.0-10.0). However, this was not the case during photolytic and photocatalytic degradation experiments at pH 5.0 and 8.5. Therefore, results for these pH levels are omitted in the following discussion. Preliminary experiments showed that storing the FQ solutions in the dark gives no significant loss of both FQs (data not shown), indicating that microbiological, thermal, or hydrolytic decay is negligible and that the absorbed UV light initiates the photodegradation.

2.1.2.1 Photolysis

The relative concentrations plotted over time for the photolytic degradation of CIP and MOX at pH 7.0 (open symbols) are presented in Fig. 2.3 (see Fig. B.2 for pH 3.0 and 10.0). Both FQs can be degraded with UV-light and follow an apparent first-order degradation ($R^2 \geq 0.97$, $n \geq 24$) at the selected pH values.

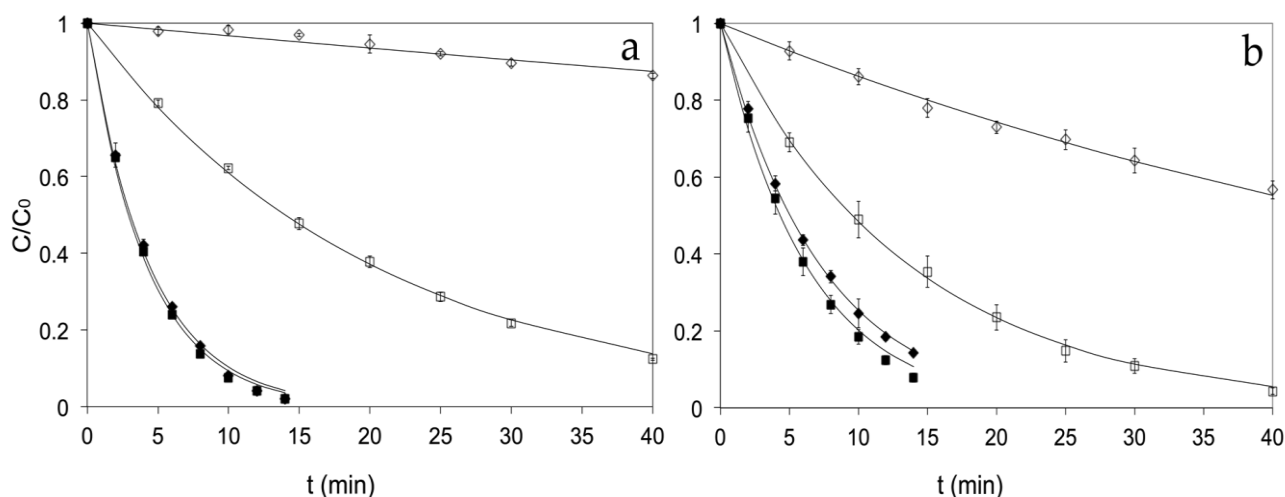


Fig. 2.3 Photolytic and photocatalytic degradation of (a) MOX and (b) CIP with UV-A (◇), UV-C (□), UV-A TiO_2 (◆) and UV-C TiO_2 (■) at pH 7.0 ($n = 3$). Full lines are obtained by regression of Eq. 2.1 to the experimental data.

The possible photochemical reactions of FQs in an aqueous solution are given in Fig. 2.4a. Incident light can excite a FQ molecule in solution to its singlet state (1). Through inter system crossing (ISC) a singlet state FQ can go to its triplet state (2). According to the Jablonski diagram (Cosa, 2004) the singlet and triplet state of a molecule are the energy levels with the highest probability to undergo a photo-induced chemical reaction. For FQs in particular, it is reported that photo-induced oxidation is mainly dependent on the photo-generation of the FQ triplet state (Mella et al., 2001; Monti et al., 2001; Albini and Monti, 2003).

Two main mechanisms of triplet state FQ degradation are reported: direct oxidation with the formation of DPs as a result of defluorination, decarboxylation and side-chain degradation (3) and quenching with oxygen yielding reactive oxygen species (ROS), e.g., $^1\text{O}_2$, $\text{O}_2^{\bullet-}$ and $\bullet\text{OH}$ (Boelsteri, 2003; Agrawal et al., 2007; Lorenzo et al., 2008). Quenching can proceed by energy transfer via type II photodynamic reaction with the formation of singlet oxygen $^1\text{O}_2$ (step 4a), electron transfer via type I photodynamic reaction to form $\text{O}_2^{\bullet-}$ and $\text{FQ}^{\bullet+}$ (step 4b), homolytic degradation with the formation of FQ^{\bullet} and $\bullet\text{OH}$ (step 4c) and physical quenching (step 4d). These produced ROS can react with FQs and create DPs, which is called self-sensitized oxidation (Ge et al., 2010b).

Apparent first-order photolytic reaction rates are plotted as a function of pH and illumination source in Fig. 2.5.

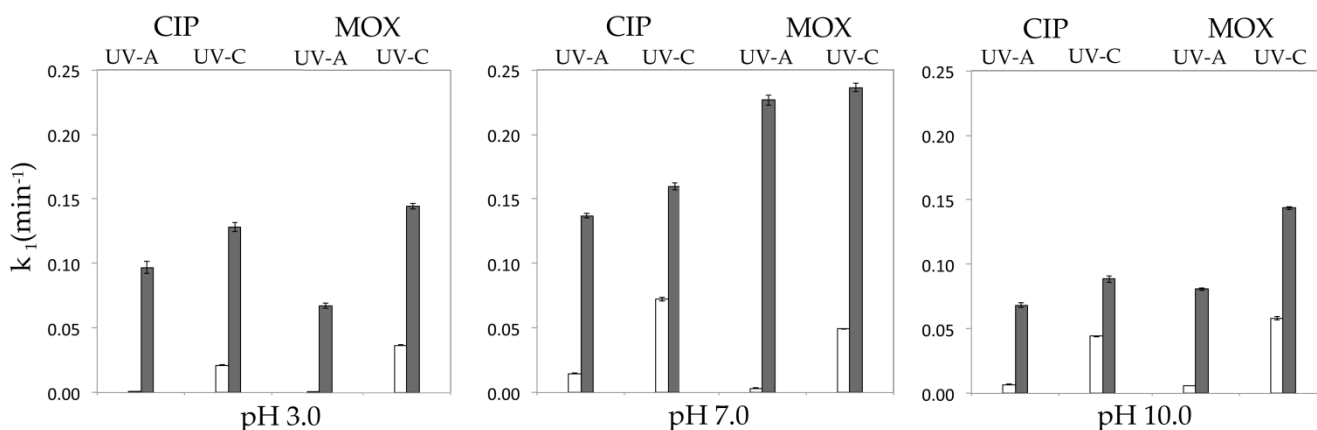


Fig. 2.5 Apparent first-order degradation constants k_1 (min⁻¹) with 95% confidence intervals for photolytic (white) and photocatalytic degradation (grey) of CIP and MOX under UV-A/UV-C irradiation at pH 3.0, 7.0 and 10.0 ($n = 3$).

Three points of interest can be stressed. First, significantly higher degradation rates are achieved with UV-C for both FQs, probably due to the higher absorption and photonic energy of UV-C light when comparing to UV-A (Hernández-Borrell and Montero, 1997; Langlois et al., 2005). Second, as reported for other FQs, e.g., DI, SARA, and GATI (Prabhakaran et al., 2009; Ge et al., 2010a), a pH dependency of the photolytic degradation rates for both CIP and MOX is observed. CIP photolytically degrades better at pH 7.0 ($k_{1,CIP,UV-A} = 0.015$ min⁻¹; $k_{1,CIP,UV-C} = 0.073$ min⁻¹) and has a maximal photostability at pH 3.0 ($k_{1,CIP,UV-A} =$ negligibly small; $k_{1,CIP,UV-C} = 0.021$ min⁻¹). The same tendency was noticed by Tornainen et al. (1996) under UV-B irradiation (313 nm), Avisar et al. (2010) with a UV spectrum 200-300 nm, and Vasconcelos et al. (2009a) with a broad spectrum (200-600 nm). The degradation rate of MOX is slow at pH 3.0 ($k_{1,MOX,UV-A} =$ negligibly small; $k_{1,MOX,UV-C} = 0.037$ min⁻¹) and increases with a maximum at pH 10.0 ($k_{1,MOX,UV-A} = 0.006$ min⁻¹; $k_{1,MOX,UV-C} = 0.058$ min⁻¹).

The shift in absorption spectra of both FQs, due to a pH change, may account for the pH dependency of the photolytic reactions (Hernández-Borrell and Montero, 1997; Langlois et al., 2005). Third, comparing both FQs reveals that MOX degrades slower than CIP under UV-A irradiation with no significant degradation for both FQs at pH 3.0. The apparent first-order degradation constants of CIP are 4.4 and 1.1 times higher at pH 7.0 and 10.0, respectively. The higher photostability of MOX under UV-A illumination is probably due to the addition of a methoxy group (OMe) at position 8 on the quinolone backbone (Matsumoto et al., 1992; Rosen et al., 1997). Under UV-C irradiation MOX has in comparison with CIP, a 1.7 and 1.3 times higher degradation rate constant at pH 3.0 and 10.0, but it is 1.5 times smaller at pH 7.0.

Comparing CIP and MOX to other members of the FQ family indicates a higher photostability for both FQs as a result of the lesser production of active oxygen species (Van Bambeke and Tulkens, 2009).

2.1.2.2 Heterogeneous photocatalysis

The photocatalytic degradation at pH 7.0 of both FQs as a function of time (full symbols) is presented in Fig. 2.3 (see Fig. B.2 for pH 3.0 and 10.0). As for photolysis, an apparent first-order degradation is observed ($R^2 \geq 0.95$, $n \geq 24$) and the reaction rates are plotted as a function of pH and illumination source in Fig. 2.5.

Four points gain attention. First, it can be noticed that the TiO_2 mediated heterogeneous photocatalysis is significantly faster for both FQs than photolysis due to the addition of a catalyst.

Second, looking at the photocatalysis of both FQs a significantly faster degradation is achieved with UV-C irradiation than with UV-A. The increase in

the degradation rate of CIP was smaller than 30% at the selected pH values. The degradation rate coefficients of MOX increase with a factor 2 at pH 3.0 and 10.0 but a negligible increase is noticed at pH 7.0. The faster degradation under UV-C illumination is probably due to the higher absorbance at 254 nm of the TiO₂-P25 catalyst and enhanced photolytic effect (Vijayabalan et al., 2009).

Third, a pH dependency is noticed for the photocatalytic reaction of both FQs. The photocatalytic degradation rates are higher for CIP and MOX at pH 7.0 than at pH 3.0 or 10.0. This trend is confirmed for CIP by (An et al., 2010a) under UV-A ($\lambda_{\text{max}} = 365 \text{ nm}$) and (Paul et al., 2007) under visible light ($\lambda > 400 \text{ nm}$) irradiation. This variation in degradation rate is probably the result of a pH dependent adsorption on the catalyst surface of FQ molecules (Table 2.1).

Fourth, comparing both FQs shows that the degradation rate coefficients of MOX are at least 15% higher than CIP at similar conditions, with an exception at pH 3.0 under UV-A irradiation.

Table 2.1 Photocatalytic apparent first-order degradation constant k_1 (min^{-1}) of both FQs and the amount of FQs adsorbed, denoted as S (mol mol^{-1}), as a function of pH. Standard deviations on adsorbed fractions, based on triplicate measurements, and 95% confidence intervals ($n \geq 24$) of the apparent first-order degradation constant are mentioned

pH	CIP			MOX		
	$k_{1,\text{UV-A}}$	$k_{1,\text{UV-C}}$	$10^2 S$	$k_{1,\text{UV-A}}$	$k_{1,\text{UV-C}}$	$10^2 S$
3.0	0.097 ± 0.005	0.128 ± 0.004	1.73 ± 0.26	0.069 ± 0.002	0.146 ± 0.002	1.78 ± 0.06
5.0	n.d. ^a	n.d.	10.46 ± 1.67	n.d.	n.d.	13.33 ± 2.20
7.0	0.137 ± 0.002	0.163 ± 0.003	8.48 ± 0.34	0.227 ± 0.004	0.236 ± 0.003	13.24 ± 0.56
8.5	n.d.	n.d.	2.87 ± 0.03	n.d.	n.d.	3.93 ± 0.03
10.0	0.068 ± 0.002	0.089 ± 0.003	0.94 ± 0.14	0.081 ± 0.001	0.144 ± 0.001	1.53 ± 0.10

^a not determined

Results in Table 2.1 indicate that the difference in degradation rate between MOX and CIP is the result of a higher adsorption of MOX on the catalyst surface. This positive relation between adsorption on the catalyst surface and the photocatalytic degradation rates shows that surface reactions in heterogeneous photocatalysis are more dominant than photocatalytically induced radical reactions in solution (Fig. 2.4b) (Ishibashi et al., 2000).

Three different kinds of surface reactions are reported in literature. First is the 'charge transfer' surface reaction (Fig. 2.4c), which is the dominant decay mechanism of CIP in a UV-A TiO₂ system according to Paul et al. (2010). The different steps in this mechanism are the complexation between FQ and the photocatalyst surface, photo-excitation of the surface-complex, the excited-state FQ molecule returns to the ground state by transferring an electron into the TiO₂ CB, the electron either recombines with the FQ molecule or is transferred to an adsorbed electron acceptor, and the formed radical cation of the FQ is further transformed into DPs. The second surface reaction is the 'direct oxidation' of an adsorbed FQ with a produced 'hole' in the VB of the semiconductor (Fig. 2.4d) (Ishibashi et al., 2000; Palominos et al., 2008). The third surface reaction is called the '·OH/O₂^{•-} mediated surface reaction' (Fig. 2.4e). Positive 'holes' produced in the VB migrate to the surface of the catalyst and form a trapped 'hole' (≡Ti^{IV}O•), usually described as an adsorbed hydroxyl anion (Chen et al., 2005). This trapped 'hole' can react with an adsorbed FQ and forms DPs.

2.1.2.3 Adsorption and estimation of the partition ratios

Since adsorption is a determining step in the heterogeneous photocatalytic degradation of FQs, it is interesting to gain more insights in this process. The pH dependent adsorption (Table 2.1) can be explained by taking into consideration the properties of both the catalyst and the FQs at different pH (Fig. 2.6).

For TiO_2 , as pH increases, the overall surface charge changes from positive ($\text{pK}_{\text{a1,TiO}_2} : 2.4-4.5$) to negative ($\text{pK}_{\text{a2,TiO}_2} : 8-9$) (Kormann et al., 1991; Vargas and Núñez, 2009; Elmolla and Chaudhuri, 2010) with a point of zero charge (PZC) at pH 6 (Silva et al., 2006). The zwitterion of TiO_2 is in equilibrium with a non-charged TiO_2 form (Vargas and Núñez, 2009).

According to Kormann et al. (1991) the non-charged TiO_2 is the main species in a pH range from 2-11. This means that adsorption is possible through different kinds of van der Waals (VDW) interactions (Demeestere et al., 2003). However, since pH shows to be a major parameter in the FQ adsorption process (Table 2.1), our results indicate that electrostatic interactions rather than VDW are a determining factor. The interaction between the TiO_2 surface charges and the FQs are a crucial factor in the adsorption and - as a result - the degradation rate. FQs are amphoteric of nature and change from positive charge at acidic pH to negative charge at alkaline pH, see Fig. 2.6.

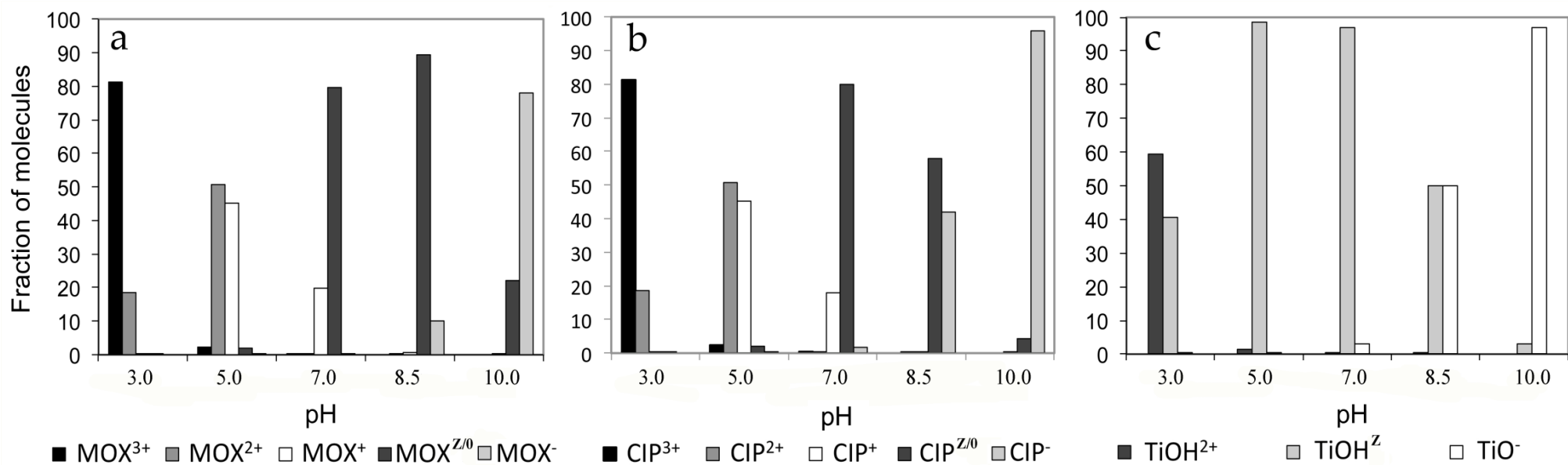


Fig. 2.6 Fraction of (a) MOX and (b) CIP species at pH 3.0, 5.0, 7.0, 8.5 and 10.0 based on the pK_a values mentioned in Fig. B.1. Surface charge of TiO₂ at different pH (c) based on average pK_a values mentioned in Kormann et al. (1991), Vargas and Núñez (2009), Elmolla and Chaudhuri (2010).

In an acidic solution (pH 3.0), the FQ ions are 3 and 2 times positively charged and the TiO_2 is present as a positive and zwitterion. Due to the attraction between the latter and the two positively charged FQ ions, a relatively small adsorption is achieved for the positive FQ species. In a neutral environment (pH 7.0), the adsorption of CIP and MOX increases by a factor 5 and 7, respectively, due to a greater variety of charge-charge interactions between the FQ ion species and the TiO_2 surface charges. The lower adsorption of CIP is probably the result of the higher amount of non-charged FQ present for CIP than for MOX (Hernández-Borrell and Montero, 1997; Langlois et al., 2005). At pH 10.0, both the catalyst and FQs become mainly negatively charged and the repulsion forces inhibit the adsorption on the catalyst surface.

Estimating the partition ratios for the different FQ species can provide knowledge on the affinity towards the TiO_2 catalyst. The five partition ratios for CIP and MOX are estimated according to the five parameter model in Fig. 2.2. All five parameters are significantly estimated, except partition ratio K_2 , which is negative. A possible reason for this negative value is the correlation between partition ratio K_1 and K_2 ($|\rho|_{\text{CIP}} = 0.987$, $|\rho|_{\text{MOX}} = 0.995$). A significantly negatively estimated partition ratio has no physical-chemical meaning, so K_2 is not estimated but set equal to K_1 (Seber and Lee, 2003). From the catalyst point of view, it can be supposed that the FQ^{2+} ion has an approximately similar adsorption behavior to the FQ^{3+} ion, since the third positive charge is positioned on the nitrogen connected to the mobile cyclopropyl group, see Table 1.1, hindering interaction with the catalyst. This proposition mechanistically corresponds to $K_1 = K_2$ and a four-parameter model (CIP-4, MOX-4) for the interaction of the aqueous ion with the catalyst is constructed. The estimation results are listed in Table 2.2.

Table 2.2 Parameter estimates with their 95% confidence intervals obtained by regression of the experimental data, see Section 2.1.1.4, with Eq. 2.6

Species	Parameter	Unit	CIP-4	t_{CIP}	MOX-4	t_{MOX}
3+	K_1	$\text{L kg}_{\text{cat}}^{-1}$	$38.7 \pm$	18.3	34.9 ± 6.7	11.6
2+	K_2	$\text{L kg}_{\text{cat}}^{-1}$	$= K_1$		$= K_1$	
+	K_3	$\text{L kg}_{\text{cat}}^{-1}$	$526.8 \pm$	20.3	690.5 ± 116.2	13.2
Z/0	K_4	$\text{L kg}_{\text{cat}}^{-1}$	$67.8 \pm$	19.4	95.7 ± 16.9	12.6
-	K_5	$\text{L kg}_{\text{cat}}^{-1}$	5.3 ± 3.7	3.2	12.7 ± 8.8	3.2
	S^*	-	0.259		0.617	
	$ \rho_{\text{max}} $	-	0.624		0.572	

For the sets CIP-4 and MOX-4, all parameters possess positive and significantly estimated values, and the four parameter model is globally significant ($F_{\text{calc}} = 100$). The similarity of the estimated parameters for CIP and MOX indicates that both FQs behave similarly in the presence of TiO_2 P25 photocatalyst, probably due to the similar chemical structure. The small K value of the 3+ and 2+ charged FQ species results from the repulsion with the positively charged TiO_2 at acidic conditions, see Fig. 2.6. Single positively charged FQ species have a greater partition ratio due to the favored attraction with the mainly zwitterionic form of TiO_2 . The partition ratio of the FQ zwitterion/non-charged form is lower than the K value of the single positively charged FQ ion. This is probably due to the higher projected area of the horizontally adsorbed zwitter FQ ions in comparison to the vertically adsorbed single charged FQ ions. Negatively charged FQ ions undergo great repulsion forces with the negatively charged TiO_2 catalyst and have therefore a small K value.

2.1.3 Conclusions

Both photolysis and photocatalysis are capable of degrading MOX in an aqueous solution with the most promising results obtained with UV-C mediated heterogeneous photocatalysis. Three main conclusions can be drawn from the experimental work in this chapter. First, the pH plays a significant role in photolytic and heterogeneous photocatalytic reactions with the fastest degradation observed at pH 10.0 and 7.0, respectively. Second, the photocatalytic degradation rate is strongly determined by the pH dependent FQ adsorption on the TiO₂ catalyst surface, favored at neutral conditions. Third, when comparing MOX with CIP, it is observed that MOX is more susceptible for photocatalytic degradation than CIP, exemplified by the first-order degradation constants being up to a factor of 1.6 higher. A new and deeper understanding of the FQ adsorption process is achieved by estimating partition ratios for the different FQ species. Results show that the single positively charged and zwitterions/non-charged FQs mainly determine the amount of FQs adsorbed on the TiO₂ catalyst surface.

2.2 TiO₂ mediated heterogeneous photocatalytic degradation of moxifloxacin: operational variables and scavenger study

2.2.1 Materials and methods

2.2.1.1 Chemicals and experimental setup

Isopropanol (ISO) is purchased from Fisher Scientific (Geel, Belgium, $\geq 99.5\%$) and potassium iodide (KI) from Sigma Aldrich (Bornem, Belgium, $\geq 99.5\%$). Oxygen (purity $\geq 99.9995\%$ O₂), pure air ($20 \pm 1\%$ O₂) and nitrogen (purity $\geq 99.8\%$ N₂) are purchased from Air Liquide (Luik, Belgium). Other chemicals are presented in Chapter 2.1.

The effect of pH on the photocatalytic degradation of MOX is discussed in Chapter 2.1, where it is concluded that neutral conditions are preferred above acid or alkaline pH. Therefore, pH 7.0 is applied for all the photocatalytic degradation experiments in this chapter, which are performed with the same experimental setup as described in Section 2.1.1.1 Other reaction conditions are summarized in Table 0.1.

2.2.1.2 Effect of radical inhibitors

An estimate of the contribution of hydroxyl radicals (HO[•]) and positive 'holes' (h⁺) during the heterogeneous photocatalytic degradation of MOX is determined by separately adding different concentrations of ISO (37.4-187,000 $\mu\text{mol L}^{-1}$) and KI (3.74-7480 $\mu\text{mol L}^{-1}$) to the reaction solution. Adsorption experiments were

performed to determine if the added scavenger affected the MOX adsorption on the catalyst surface. If scavenger addition did not influence MOX adsorption degradation reactions are performed.

2.2.1.3 Analytic methods

MOX analysis is performed using the HPLC-PDA procedure described in Chapter 2.1.

2.2.2 Results and Discussion

2.2.2.1 Initial MOX concentration

The effect of the initial MOX concentration ($C_{\text{MOX},0}$) was studied in the range 12.5-124.6 $\mu\text{mol L}^{-1}$ at 5 g L^{-1} TiO_2 loading. From the total amount of MOX added, a part is adsorbed on the TiO_2 surface until adsorption-desorption equilibrium is attained. By measuring the aqueous concentrations, ($C_{\text{MOX},\text{l,eq},0}$) at adsorption-desorption equilibrium after the addition of different initial MOX concentrations, an adsorption isotherm is determined (Fig. 2.7), which fits the Langmuir adsorption model well ($R^2 = 0.998$). The Langmuir adsorption isotherm shows that under the highest initial FQ concentration applied, no monolayer of adsorbed MOX is attained on the catalyst surface ($K = 0.051 \pm 0.004 \text{ L } \mu\text{mol}^{-1}$; $C_{\text{max}} = 8.96 \pm 0.31 \mu\text{mol g}_{\text{cat}}^{-1}$). The amount of MOX adsorbed at monolayer formation is represented by the dashed asymptotic line.

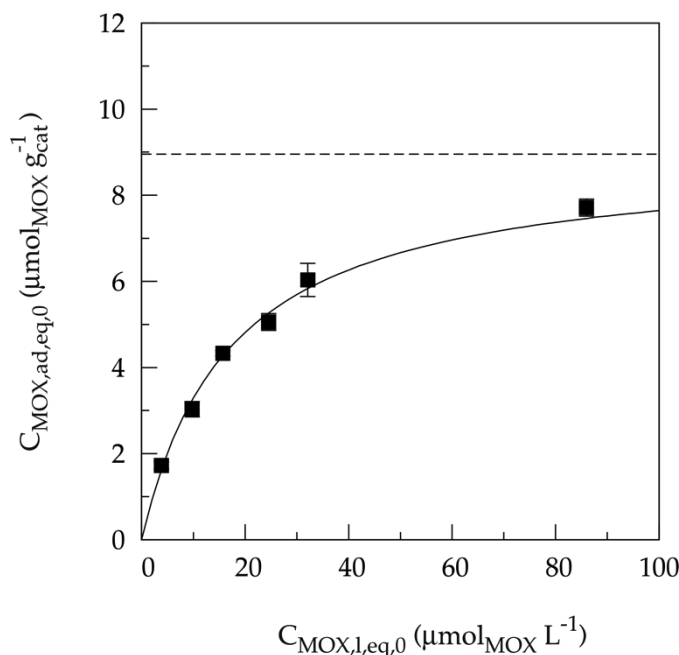


Fig. 2.7 Adsorption isotherm of MOX on a TiO_2 catalyst surface. Quantity of adsorbed MOX, $C_{\text{MOX},\text{ad},\text{eq},0}$ ($\mu\text{mol g}_{\text{cat}}^{-1}$) as a function of MOX concentration in solution after adsorption-desorption equilibrium, $C_{\text{MOX},l,\text{eq},0}$ ($\mu\text{mol L}^{-1}$) ($n = 3$).

The total photocatalytic degradation time is longer at higher initial MOX concentrations, see Fig. 2.8a. As the oxidation reaction proceeds, a smaller fraction of the TiO_2 particle surface is covered by MOX as it is degraded. Evidently, a decrease in the photocatalytic degradation rate is to be expected with increasing irradiation time (Haque and Muneer, 2007). A concentration dependency of the reaction rate constant k_1 is observed and consequently the apparent first-order reaction kinetics are abandoned. To compare different conditions, initial degradation rates ($\mu\text{mol L}^{-1} \text{min}^{-1}$) are determined by fitting the following function to the experimental data (dashed lines Fig. 2.8a) and taking the tangent in $t = 0$ (Eq. 2.8).

$$f(x) = a \cdot e^{-b \cdot x} \quad (2.8)$$

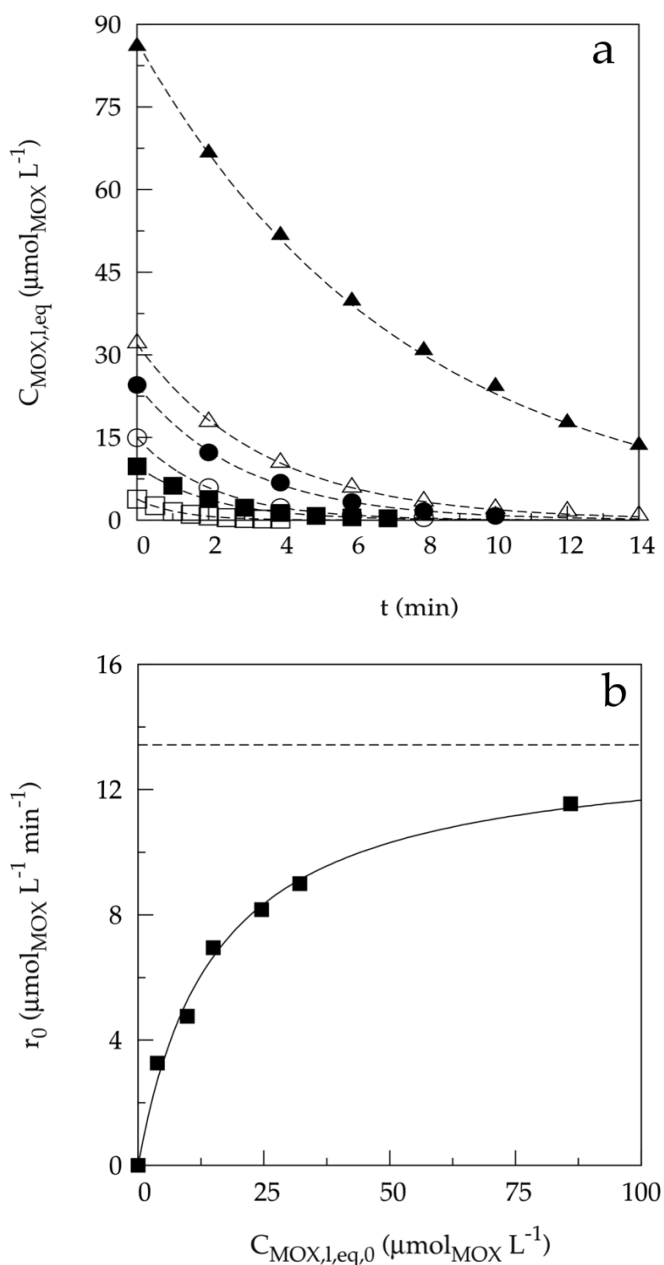


Fig. 2.8 (a) Photocatalytic degradation of (\blacktriangle) 124.6, (\triangle) 62.3, (\bullet) 49.9, (\circ) 37.4, (\blacksquare) 24.9, and (\square) 12.5 $\mu\text{mol} \text{L}^{-1}$; (b) Initial degradation rate, r_0 ($\mu\text{mol} \text{L}^{-1} \text{min}^{-1}$) as a function of initial equilibrium MOX concentration, $C_{\text{MOX},l,\text{eq},0}$ ($\mu\text{mol} \text{L}^{-1}$) deduced from Fig. 2.9a.

Initial degradation rates for the photocatalytic degradation of MOX as a function of the initial equilibrium MOX concentration ($C_{\text{MOX},l,\text{eq},0}$) are shown in Fig. 2.8b. The Langmuir-Hinshelwood (LH) kinetics, see Eq. 2.9, is the most commonly used kinetic expression to explain the kinetics of heterogeneous photocatalytic processes of various organics by TiO_2 (Demeestere et al., 2007; Kumar et al., 2008):

$$r_0 = -\frac{dC_{\text{MOX},l,\text{eq},0}}{dt} = \frac{k_r K_{\text{LH}} C_{\text{MOX},l,\text{eq},0}}{1 + K_{\text{LH}} C_{\text{MOX},l,\text{eq},0}} \quad (2.9)$$

where r_0 is the initial degradation rate, $C_{\text{MOX},l,\text{eq},0}$ the MOX concentration in the liquid phase after equilibrium ($\mu\text{mol L}^{-1}$), k_r the reaction rate coefficient ($\mu\text{mol L}^{-1} \text{min}^{-1}$), and K_{LH} the LH adsorption coefficient ($\text{L } \mu\text{mol}^{-1}$). The LH equation fits the experimental well (full line, $R^2 = 0.998$). The linear transformation of Eq. 2.9 gives a rate coefficient, k_r , and an adsorption coefficient, K_{LH} , both with its 95% confidence interval, of $13.4 \pm 1.9 \mu\text{mol L}^{-1} \text{min}^{-1}$ and $0.066 \pm 0.008 \text{ L } \mu\text{mol}^{-1}$, respectively. In literature, a rather wide range of k_r and K_{LH} values are observed for the photocatalytic removal of FQ compounds ($k_r = 19.7 \mu\text{mol L}^{-1} \text{min}^{-1}$ and $K_{\text{LH}} = 0.014 \text{ L } \mu\text{mol}^{-1}$ for FLU; $k_r = 0.75 \mu\text{mol L}^{-1} \text{min}^{-1}$ and $K_{\text{LH}} = 0.05 \text{ L } \mu\text{mol}^{-1}$ for OFL; $k_r = 1.1 \mu\text{mol L}^{-1} \text{min}^{-1}$ and $K_{\text{LH}} = 0.3 \text{ L } \mu\text{mol}^{-1}$ for OFL). This is possibly due to the different reaction conditions applied during the photocatalytic experiments (Palominos et al., 2008; Hapeshi et al., 2010; Michael et al., 2010).

The initial degradation rate increases from 3.2 to 11.6 $\mu\text{mol L}^{-1} \text{min}^{-1}$ with increasing initial equilibrium MOX concentrations from 3.8 to 86.0 $\mu\text{mol L}^{-1}$, respectively. At higher $C_{\text{MOX},l,\text{eq},0}$ concentrations, the initial degradation rate levels off since the complete coverage of the semiconductor surface is approached. The maximum initial degradation rate of 13.4 $\mu\text{mol L}^{-1} \text{min}^{-1}$ is theoretically attained when the MOX monolayer is formed, which is visualized by the dashed line in Fig. 2.8b. A similar trend is noticed for the P25 mediated photocatalytic degradation of NOR and OFL (Haque and Muneer, 2007; Michael et al., 2010).

2.2.2.2 Catalyst concentration and stirring speed

Preliminary suspension experiments revealed that sedimentation occurs for TiO₂ P25 catalyst concentrations varying from 0.25-8 g L⁻¹ under the slowest stirring regime, 2.3 rps (Fig. 2.9).

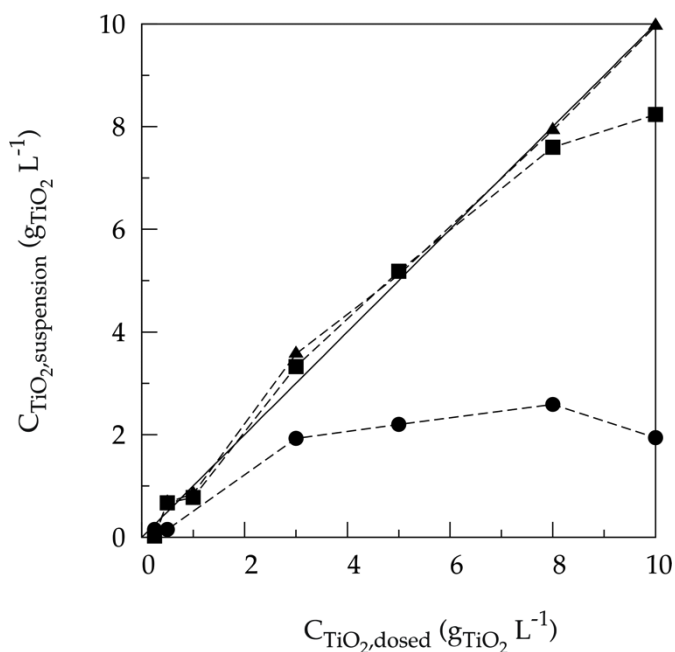


Fig. 2.9 Suspended over added amount of TiO₂ catalyst (g L⁻¹) as a function of stirring speeds 13.2 rps (▲), 7.9 rps (■) and 2.3 rps (●) at pH 7.0, 298 K and 60 mL min⁻¹ air sparging. Dashed lines are plotted to guide the eye. The full line is the first bisector which states full suspension of the added catalyst (n = 1).

No sedimentation is observed using stirring speeds greater than 7.9 rps. Degradation experiments with the lowest stirring speed are not performed due to the inefficient use of catalyst.

It is worth noticing that the initial equilibrium concentration of MOX in the liquid phase ($C_{\text{MOX}, \text{l}, \text{eq}, 0}$) is not the same for every catalyst concentration because of the higher fraction of adsorbed MOX at higher catalyst concentrations, see Fig. 2.10a interrupted dashed lines. Therefore, it is difficult to compare solely the effect of the investigated variable catalyst concentration due to the fact that changing

initial equilibrium concentrations in the liquid phase also alters the initial MOX degradation rate r_0 (see Section 2.2.2.1).

A possible solution is to express the degradation of MOX in total moles of MOX in the reactor as a function of time. Adsorption experiments performed with different catalyst concentrations and the same initial MOX concentration enable the calculation of the amount of MOX adsorbed on TiO_2 for every $C_{\text{MOX},\text{leq},t}$ during a degradation experiment. Degradation curves are now expressed as the total amount of moles MOX left in the reactor, both in liquid phase and adsorbed phase, as function of time, see Fig. 2.10b. The initial photocatalytic degradation rate of MOX deduced at $t = 0$ is denoted as r_0^* . This procedure is from now on applied for all the operational variables studied in this chapter.

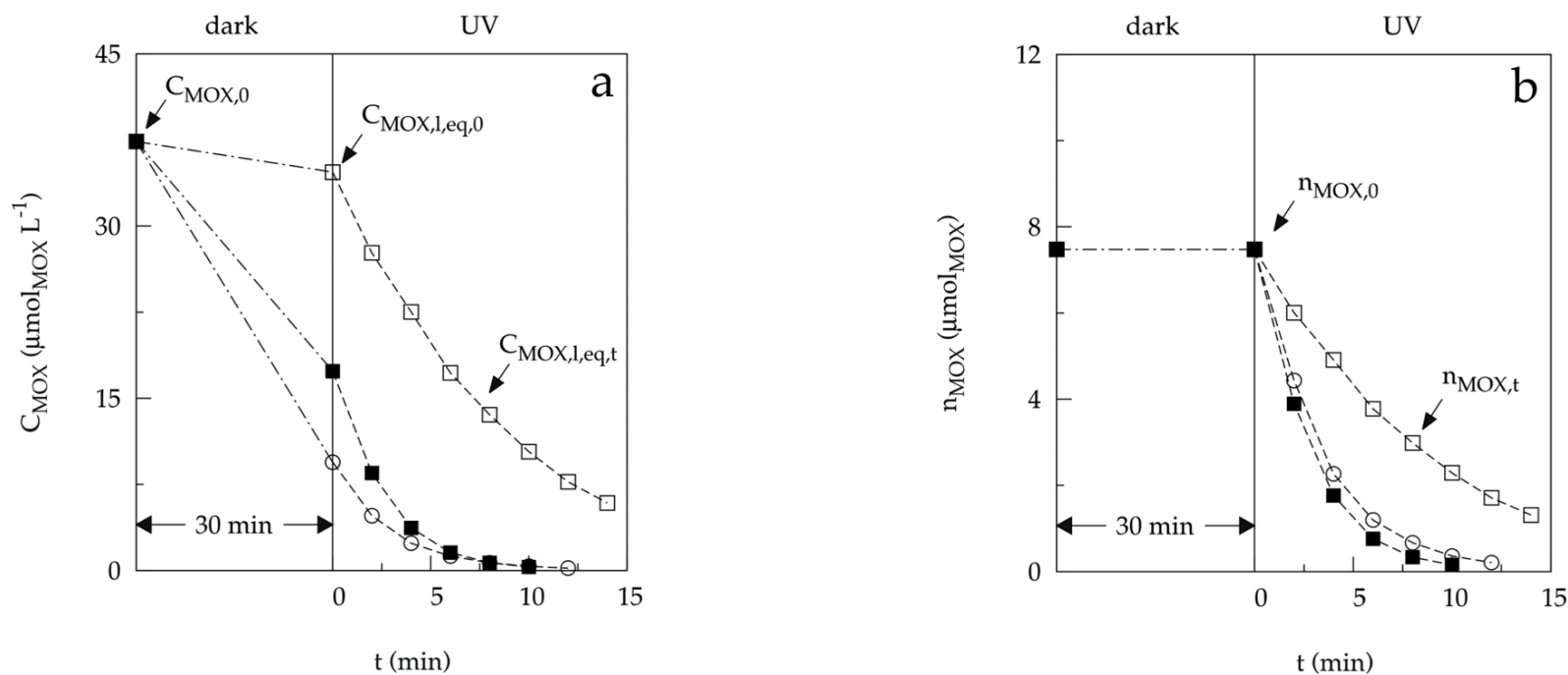


Fig. 2.10 (a) Concentration profile of aqueous MOX in the dark period and in the UV period for the catalyst loadings (\square) 0.25 g L⁻¹, (\blacksquare) 3 g L⁻¹ and (\circ) 8 g L⁻¹; (b) The total amount of moles of MOX present in the reactor in the dark period and in the UV period for the catalyst loadings (\square) 0.25 g L⁻¹, (\blacksquare) 3 g L⁻¹ and (\circ) 8 g L⁻¹. Initial degradation rates, r_0^* ($\mu\text{mol L}^{-1} \text{min}^{-1}$), are determined by plotting the tangent at $t = 0$, this is after adsorption-desorption equilibration in the dark period.

Using the initial degradation rates as determined in Fig. 2.10b, the effect of the photocatalyst concentration on r_0^* is examined, see Fig. 2.11.

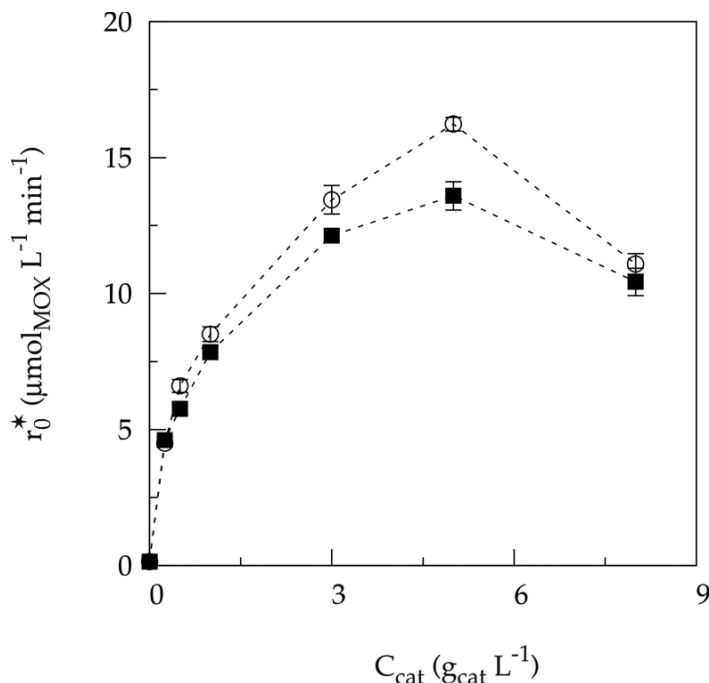
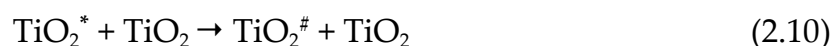


Fig. 2.11 Initial degradation rate, r_0^* ($\mu mol L^{-1} min^{-1}$) as a function of catalyst loading ($g L^{-1}$) for the stirring speeds (■) 7.9 rps and (○) 13.2 rps ($n = 3$). Dashed lines are plotted to guide the eye.

An optimal catalyst loading of $5 g L^{-1} TiO_2$ is observed for both stirring speeds. A more vigorous stirring regime results in a higher initial degradation rate probably due to the increase in turbulence. Dosing more catalyst to the reaction solution below the optimal loading results in a higher initial degradation rate for both stirring speeds. This may be attributed to the higher amount of total active surface area, i.e., a larger number of active surface sites and a more pronounced light absorption when the added catalyst mass increases (Wei et al., 2009). It is assumed that the geometric catalyst surface area and the absorption of light by TiO_2 are limiting factors when working below the optimal catalyst loading (Evgenidou et al., 2005a).

Above the optimal catalyst loading, the initial degradation rate decreases with higher catalyst concentrations. Different factors may influence the degradation rate when working above optimal conditions: (a) increased turbidity and opacity of the solution with scattering phenomena reducing the light transmission through the solution (shielding effect) (Mehrotra et al., 2003), (b) agglomeration of the catalyst due to particle-particle interactions resulting in the loss of active surface sites (Michael et al., 2010), (c) a higher catalyst dosage results in a lower degree of surface coverage, and (d) deactivation of the originally activated TiO_2 particles through collision with ground state catalyst particles, see Eq. 2.10:



where TiO_2^* is the TiO_2 with active species adsorbed on the surface and $\text{TiO}_2^\#$ the ground state form of TiO_2 (Neppolian et al., 2002).

The dependency of the optimal TiO_2 loading on both the photoreactor geometry and the nature of the compound, makes it difficult to compare different optimum catalyst loadings obtained in different studies. Optimal catalyst concentrations reported in literature for Degussa TiO_2 P25 range from 0.1-5.0 g L⁻¹ (Qourzal et al., 2005).

2.2.2.3 Oxygen concentration

The effect of sparging pure oxygen, pure air, nitrogen and passive diffusion (no sparging) of ambient air on the initial degradation rate of the photocatalytic degradation of MOX is presented in Fig. 2.12.

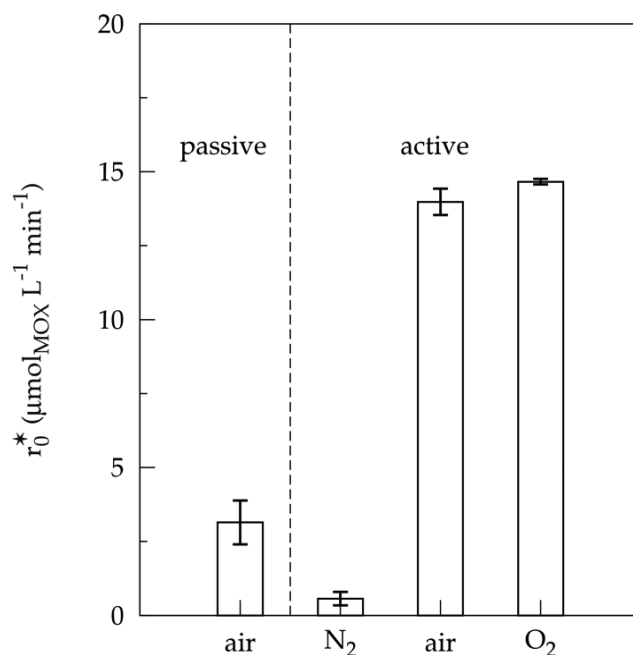


Fig. 2.12 Initial degradation rate, r_0^* ($\mu\text{mol L}^{-1} \text{min}^{-1}$) as a function of oxygen supply (20% passive, 0%, 20% and 100%, $n = 3$). The active part is sparged with a flow of 60 mL min^{-1} , the passive part is not sparged but kept open to the atmosphere during reaction.

MOX degrades significantly slower under N_2 sparging compared to pure oxygen and air. Since oxygen free environments inhibit the photocatalytic degradation of organic compounds completely, there is probably still a residual amount of oxygen available in the reaction solution being responsible for the observed slow MOX degradation rate under N_2 sparging (McMurray et al., 2006). Oxygen adsorbed on the surface of TiO_2 prevents the recombination process by trapping the CB electrons with the formation of superoxide radical ions, $\text{O}_2^{\bullet-}$.

The formation of this superoxide radical ion can result in the formation of more reactive oxygen species like peroxide radicals (Xekoukoulotakis et al., 2011). Oxygen has no negative effect on the adsorption of the compound since the reduction reaction takes place at a different location from where oxidation occurs (Chong et al., 2010).

Comparing the sparging of dry air and pure oxygen a 5% increase in the initial degradation rate of MOX is observed when applying pure oxygen. The same trend is noticed during the degradation of other organic compounds using heterogeneous photocatalysis (McMurray et al., 2006; Malato et al., 2009; Chong et al., 2010). The use of ambient air is therefore a promising alternative for future applications in photocatalytic degradation reactions.

Sparging the solution during the photocatalytic degradation is nonetheless necessary. Experiments performed with passive diffusion of ambient air show that the oxygen diffusion is too slow to prevent the electron-hole recombination process. The initial degradation rate decreases with 77% in comparison to active air diffusion due to the slow oxygen diffusion towards the reaction solution.

2.2.2.4 Temperature

Adsorption experiments performed under temperatures ranging from 278 up to 338 K show that the adsorption of MOX decreases with a rising solution temperature. The enthalpy of the MOX adsorption on TiO₂ is calculated to amount -16.8 ± 1.9 kJ mol⁻¹ by using the van't Hoff equation, which is an indirect method to calculate thermodynamic adsorption parameters at solid–solution interfaces (Fig. 2.13a).

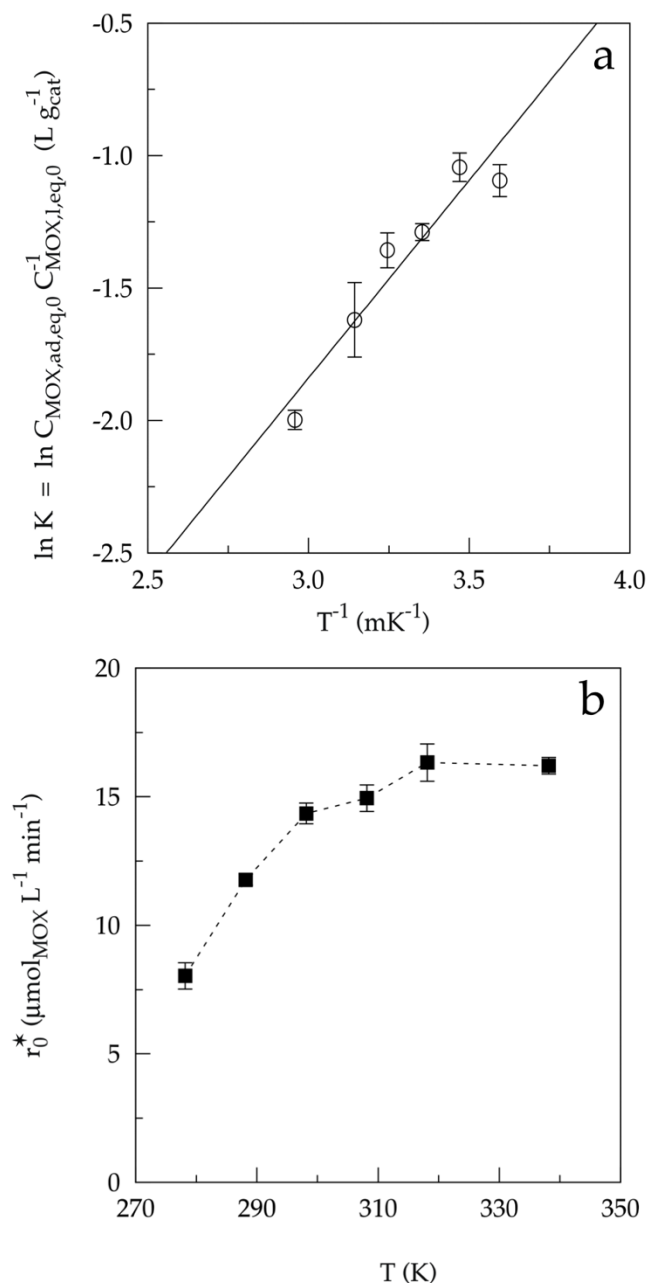


Fig. 2.13 (a) Linearisation of the van't Hoff equation for the temperature range 278-338 K ($n = 3$); (b) Initial degradation rate, r_0^* ($\mu\text{mol L}^{-1} \text{min}^{-1}$), of MOX as a function of reaction temperature ($n = 3$). Dashed line is plotted to guide the eye.

The negative value of the adsorption enthalpy, ΔH° , indicates the exothermic nature of the process. The magnitude gives an idea about the type of adsorption, which is mainly physical or chemical. Physisorption processes usually have energies in the range of 10-40 kJ mol^{-1} while higher adsorption enthalpies of 100-500 kJ mol^{-1} suggest chemisorption (Parga et al., 2009; Berger and Bhowan, 2011).

The calculated adsorption enthalpy of MOX in this study indicates the physisorbed nature of the adsorption process on TiO₂. Similar values are obtained for phenol adsorption on activated carbon and cyanide adsorption on TiO₂ (Cañizares et al., 2006; Parga et al., 2009).

The influence of the applied reaction temperature on the initial degradation rate of MOX is presented in Fig. 2.13b. Two regions can be defined, which are probably the result of two counter effects, namely the decreasing MOX adsorption at higher temperatures and the faster diffusion and reaction kinetics with increasing temperature. Below a reaction temperature of 298 K the increase in diffusion rate and kinetics have the upper hand, resulting in a higher initial degradation rate with an increasing temperature. Above 298 K a leveling off appears and the expected increase of the initial degradation rate with increasing temperature is possibly compensated by the decrease in MOX adsorption (Evgenidou et al., 2005b; Tsai et al., 2009; Herrmann, 2010), the decrease in oxygen solubility with higher working temperatures (Malato et al., 2009; Geng and Duan, 2010), and/or the faster recombination of charge carriers (Rideh et al., 1997; Chong et al., 2010). According to Geng and Duan (2010), the oxygen concentration can decrease from 13 to 5 mg O₂ L⁻¹ with temperatures ranging from 278 to 338 K. The importance of oxygen is discussed in the previous paragraph.

2.2.2.5 Effect of radical inhibitors

Two scavengers, ISO and KI, were added to the reaction solution in order to capture reactive species during a photocatalytic reaction. Adsorption experiments for different scavenger concentrations of ISO and KI show that no interference is noticed for the applied KI concentrations up to 3.74 mmol L⁻¹ and that ISO did not interfere up to a concentration of 37.4 mmol L⁻¹. Applying higher KI and ISO concentrations interferes with MOX adsorption. To compare the photocatalytic

degradation reaction of MOX with and without the addition of scavenger, degradation reactions are performed only in these cases where no interference with the MOX adsorption is noticed.

2.2.2.5.1 Isopropanol

ISO is known to be a good hydroxyl radical scavenger with a reaction constant (k) of $1.9 \times 10^9 \text{ L mol}^{-1} \text{ s}^{-1}$ and is used to discriminate between direct oxidation with positive 'holes' and the degradation with hydroxyl radicals in solution (Chen et al., 2005; Palominos et al., 2008; Zhang et al., 2008). Though direct oxidation of short aliphatic alcohols by photogenerated 'holes' occurs, it was considered negligible because they have a very weak adsorption on TiO_2 surfaces in aqueous media (Chen et al., 2005). Different concentrations of ISO were dosed to evaluate the effect on the heterogeneous photocatalytic degradation of MOX, see Fig. 2.14.

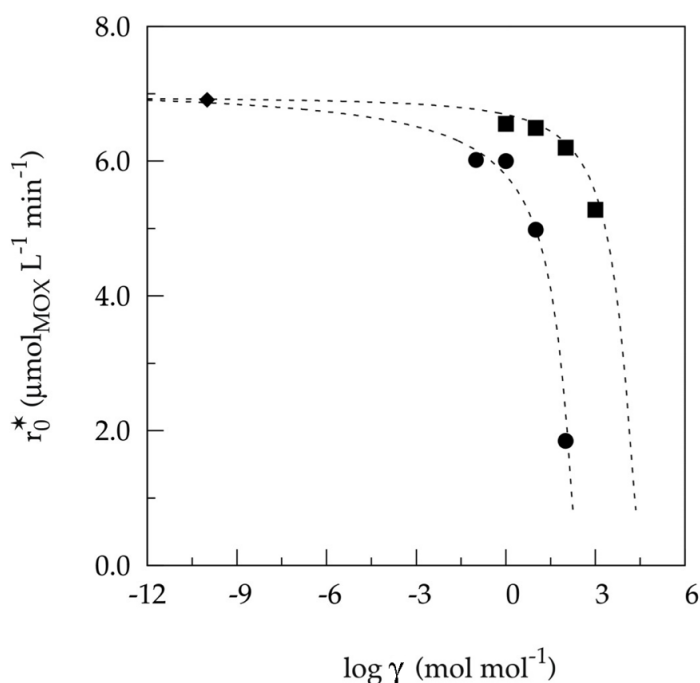


Fig. 2.14 Initial degradation rate, r_0^* ($\mu\text{mol L}^{-1} \text{min}^{-1}$), of MOX as a function of different (■) ISO and (●) KI concentrations expressed as the ratio γ . Initial degradation rate with no added scavenger is presented with (◆). Dashed lines are plotted to guide the eye.

The bimolecular rate constant of MOX with a hydroxyl radical is estimated to be $1.38 \times 10^{10} \text{ L mol}^{-1} \text{ s}^{-1}$, which is the mean value of the lowest (NOR) and highest (CIP) value of FQs found in literature (An et al., 2010a; An et al., 2010b). Dividing the reaction rates of ISO and MOX with hydroxyl radicals, Eq. 2.11 is deduced:

$$\kappa_{\text{ISO}} = \frac{r_{0,\text{ISO}}}{r_{0,\text{MOX}}} = \frac{k_{0,\text{ISO}} C_{0,\text{ISO}} C_{\text{HO}\cdot}}{k_{0,\text{MOX}} C_{0,\text{MOX}} C_{\text{HO}\cdot}} = 0.14 \frac{C_{0,\text{ISO}}}{C_{0,\text{MOX}}} = 0.14 \gamma_{\text{ISO}} \quad (2.11)$$

with κ_{ISO} the ratio of the reaction rate of ISO and MOX with hydroxyl radicals and γ_{ISO} the ratio of ISO over MOX concentration. Altering the ISO to MOX concentration ratio within the experimental ranges applied in this study results in a κ_{ISO} from 0.14-140. A first significant decrease of the initial degradation rate was noticed at $\gamma_{\text{ISO}} = 100$. Here, the initial degradation rate of ISO with hydroxyl radicals is 14 times higher than the one of MOX due to its higher concentration. At $\gamma_{\text{ISO}} = 1000$ a drop of only 25% in initial degradation rate was noticed. This relatively small decrease in initial degradation rate with a high scavenger concentration can be an indication that hydroxyl radicals in solution have a moderate contribution in the photocatalytic degradation reaction mechanism of MOX. ISO concentrations above $\gamma_{\text{ISO}} = 1000$ negatively influence the adsorption process of MOX up to 40% which makes the decrease in initial degradation rate a combination of inhibition and lowered MOX adsorption.

2.2.2.5.2 Potassium iodide

The iodide ion is used to evaluate the contribution of both photogenerated 'holes' and hydroxyl radicals, bimolecular rate constant k of $1.1 \times 10^{10} \text{ L mol}^{-1} \text{ s}^{-1}$ (Buxton et al., 1988), in the photocatalytic degradation of MOX. VB 'holes' and hydroxyl radicals are easily captured by I^- (Martin et al., 1995; Ishibashi et al., 2000; Chen et

al., 2005). Different concentrations of KI were applied during the heterogeneous photocatalytic degradation of MOX, see Fig. 2.14.

Applying an γ_{KI} of 100 a decrease of 80% in the initial degradation rate can be noticed. When applying KI concentrations above $\gamma_{\text{KI}} = 100$ a negative influence on the adsorption process of MOX up to 75% is noticed which makes the decrease in initial degradation rate a combination of inhibition and lowered MOX adsorption as noticed with ISO. The greater inhibition of the reaction through KI compared to ISO at lower scavenger concentrations gives an indication that photogenerated 'holes' play a more important role in the photodegradation of MOX under UV-A light irradiation than hydroxyl radicals (Ishibashi et al., 2000; Giraldo et al., 2010).

Relevant contribution estimates are obtained for the different active species during the photocatalytic degradation of MOX at different scavenger concentrations. Knowing that ISO scavenges hydroxyl radicals and KI both 'holes' and hydroxyl radicals, one can calculate the minimum percentage of 'holes' and hydroxyl radicals which participate in the photocatalytic degradation of MOX. If 100% is the total amount of reactive species, then the abstraction of the 'holes' and hydroxyl radicals result in the amount of non-captured radicals (NCR), which can be 'holes', hydroxyl radicals and ROS. More radicals are captured with increasing scavenger concentrations. The results in Table 2.3 indicate that photocatalytic 'holes' and hydroxyl radicals are the two reactive species which are probably responsible for the greatest part in the photocatalytic breakdown of MOX, 63% and 24%, respectively.

Table 2.3 Percentage of inhibition due to the scavengers KI and ISO, and the percentage of contribution for the photocatalytic ‘holes’ and hydroxyl radicals during the photocatalytic degradation of MOX, with γ (mol mol⁻¹) the ratio scavenger over MOX concentration

Inhibition percentage		Inhibition percentage		Percentage of contribution		
γ_{KI}	KI (%) ^a	γ_{ISO}	ISO (%) ^a	h ⁺ (%) ^b	HO [•] (%) ^b	NCR (%) ^b
0	0	0	0	0	0	100
0.1	12.9 ± 0.2	0.1	n.d. ^c	n.d.	n.d.	n.d.
1	13.1 ± 0.2	1	5.1 ± 0.1	8.0 ± 0.2	5.1 ± 0.1	86.9 ± 0.2
10	27.9 ± 0.3	10	6.0 ± 1.1	21.9 ± 1.1	6.0 ± 1.1	72.1 ± 1.6
100	73.3 ± 1.1	100	10.3 ± 0.1	63.0 ± 1.1	10.3 ± 0.1	26.7 ± 1.1
1000	n.d.	1000	23.6 ± 0.2	n.d.	23.6 ± 0.2	n.d.
100	73.3 ± 1.1	1000	23.6 ± 0.2	63.0 ± 1.1	23.6 ± 0.2	13.4 ± 1.1

^a 95% confidence intervals; ^b standard deviations are based on on error propagation; ^c not determined.

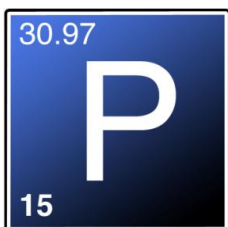
Since KI and ISO are not used to scavenge ROS during the photocatalytic degradation of MOX, they are enclosed in the NCR and results in the fact that ROS are probably responsible for equal or less than 14% of the photocatalytic degradation. These radicals have therefore a minor contribution in the reaction pathway of the antibiotic MOX (Chen et al., 2005; Yang et al., 2010b).

2.2.3 Conclusions

New data and insights are obtained for the TiO₂ mediated heterogeneous photocatalytic degradation of MOX by investigating a wide set of operational variables. The photocatalytic degradation of MOX can be described by the Langmuir-Hinshelwood kinetics and an optimal catalyst loading is observed at 5.0 g L⁻¹ with a higher initial degradation rate at a higher stirring speed (13.2 rps). Applying pure oxygen (60 mL min⁻¹) during sparging does not result in a major increase in initial degradation rate comparing to pure air, but aeration is nonetheless necessary since passive diffusion of oxygen from the ambient air to the solution is too slow. The small increase (< 10% at 338 K) in initial degradation

rate above 298 K is a clear indication that ambient temperature is sufficient for the photocatalytic degradation reaction of MOX.

Estimated amounts of the different reactive species during the photocatalytic degradation of MOX are obtained using two scavengers at different concentrations. Photogenerated 'holes' have a minimum contribution of 63% in the photocatalytic degradation of MOX. This indicates that 'holes' are mainly responsible for the oxidation of MOX and that only a small amount of the degradation can be attributed to hydroxyl radicals, i.e., 24%. The amount of non-captured radicals reveal that ROS like superoxide radicals, have a negligible part in the photocatalytic degradation pathway of MOX, i.e., $\leq 13\%$.



art III

Identification of moxifloxacin photocatalytic degradation products

Redrafted from:

Van Doorslaer, X., Demeestere, K., Heynderickx, P.M., Caussyn, M., Van Langenhove, H., Deolieghere, F., Vermeulen, A., Dewulf, J., 2013. Applied Catalysis B-Environmental 138-139, 333-341.

3.1 Introduction

Results in Part II show that heterogeneous photocatalysis has potential to remove FQ compounds from water matrices. Doll and Frimmel (2004), however, reported that the application of AOPs is not cost efficient when full mineralization is strived for. As a result, it is preferred to partially degrade the pollutants with the formation of less hazardous DPs.

Therefore, the main goal of this chapter is to gain new insights in the photocatalytic degradation of MOX, by primarily focusing on the molecular composition of the water phase during this reaction. Identification of the main photocatalytic DPs of MOX is performed with the elucidation of a possible initial photocatalytic degradation pathway, and the effect of pH is evaluated on this matter.

Analysis and identification of photocatalytic DPs is not straightforward due to their unknown structures, occurrence at low concentrations, and the lack of commercially available chemical standards for structure elucidation. However, it can be assumed that initial photocatalytic DPs have some structural resemblance with the mother compound. Different identification methodologies for the chemical analysis of DPs during AOP treatment can be applied, as explained in detail by De Witte et al. (2011). In this work, liquid chromatography coupled to HRMS is used in combination with UV-vis spectrum determination. Therefore, according to the classification proposed by De Witte et al. (2011), the identification level of DPs presented in this work can be defined as 'full identification'.

3.2 Material and methods

3.2.1 Chemicals and experimental setup

Water (LC-MS grade), methanol (LC-MS grade) and formic acid (LC-MS grade) are provided by Biosolve (The Netherlands). Other chemicals are reported in Part II.

UV-A mediated photocatalytic degradation of MOX is performed according to the experimental setup and methodology described in Part II, with applied operational conditions listed in Table 0.1. The rather high initial MOX concentration is chosen to enable the detection of both mother compound and its DPs with the applied analytical instruments without any (selective) preconcentration steps.

Aqueous samples of 1 mL are taken at 0, 0', 5, 15, 25, 35, 45, 55, 65, 75, 85, 95, 105, 115, 125, 135 and 145 min of photocatalytic degradation time. With the sample taken at 0 min reaction time, representing the solution before catalyst addition, and 0' min reaction time, representing the starting point for the reaction after adsorption-desorption equilibrium.

A preliminary photolytic experiment under the same reaction conditions showed that the amount of photolytic MOX degradation was below 5% (data not shown). This indicates that the amount of photolytic DPs is negligible and that all the detected DPs are from a photocatalytic nature.

3.2.2 Analytic methods

3.2.2.1 TOC and MOX determination

The total organic carbon content (TOC) of the photocatalytic reaction samples is analyzed using a Shimadzu TOC analyzer equipped with a non-dispersive infrared detector. TOC values of demineralized water with and without catalyst are taken into account as background TOC values. MOX analysis is performed using the HPLC-PDA procedure described in Chapter 2.1.

3.2.2.2 Degradation product identification

The different DPs are analyzed by HPLC-ESI-MS. The HPLC is equipped with a Luna C18(2) column (150 mm × 2.0 mm, 3 μm, Phenomenex, USA), maintained at 35°C, and a binary mobile phase consisting of 0.1% formic acid in water and 0.1% formic acid in methanol is used. The mobile phase flow rate was 170 μL min⁻¹ and starts with one minute isocratic 10% organic phase, which then rises to 60% in twenty minutes and to 100% in the following five minutes. It was kept constant for 10 min before returning to the starting condition in 1 min. It was then equilibrated for 20 min prior to the next run. The MS detection ($m/z = 149.5-450.5$) is performed on a Thermo Finnigan double focusing magnetic sector MAT95XP-TRAP high resolution mass spectrometer (Finnigan, Bremen, Germany) equipped with an electrospray ionization (ESI) source in positive-ion mode. The spray voltage was 3 kV with nitrogen as sheath gas at 4 bars and a capillary temperature of 250°C.

Low resolution (LRMS) magnetic scan is used during the initial analysis of the photocatalytic samples taken at preset reaction times. To elucidate the molecular composition of the measured DPs, high resolution measurements are performed, with a mass resolution of 10,000 (10% valley definition, corresponding to

20,000 mass resolution at full width at half maximum (FWHM)), on the sample taken at the reaction time where most DPs with an ion intensity greater than 10^5 μV were observed during low resolution modus. Polyethylene glycols (PEG) were used as HRMS internal mass calibration standards for determination of the accurate mass and chemical formula of the DPs. Given the molecular formula of protonated MOX ($\text{C}_{21}\text{H}_{25}\text{O}_4\text{N}_3\text{F}$), chemical formulae containing 0-21 carbon atoms, 0-30 hydrogen atoms, 0-10 oxygen atoms, 0-3 nitrogen atoms, and 0-1 fluorine atoms were taken into account for identification of DPs.

3.3 Results and Discussion

3.3.1 Degree of MOX mineralization

The residual MOX and TOC concentrations in the liquid phase during the photocatalytic degradation of a $124.6 \mu\text{mol L}^{-1}$ MOX solution are plotted as a function of degradation time at neutral reaction conditions in Fig. 3.1.

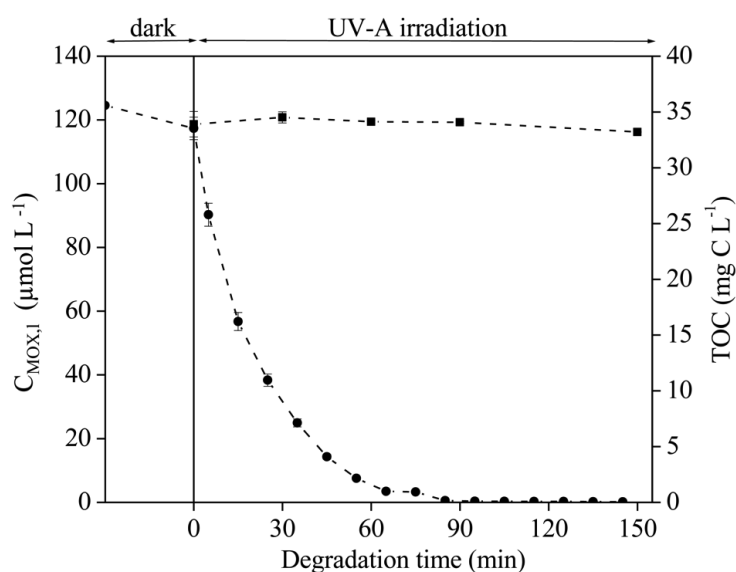


Fig. 3.1 Residual MOX concentration $C_{\text{MOX},1}$ ($\mu\text{mol L}^{-1}$; ●) and TOC (mg C L^{-1} ; ■) in the liquid phase as a function of photocatalytic treatment time ($n = 3$).

After 90 min, the residual liquid MOX concentration drops below the LOD and no significant mineralization ($p = 0.90$), represented by TOC removal, is measured, even after 145 min of treatment. This indicates the presence of different photocatalytic DPs, which still reside in the reaction solution.

3.3.2 Identification of degradation products

A large number of DPs are detected in the photocatalytic reaction samples and the time course of the HPLC-MS peak areas associated with these products, together with the residual MOX concentration in solution, are presented in Fig. 3.2. Since no analytical standards are available for DP quantification, chromatographic peak areas are used. A supporting analysis of 8 commercially available FQ standards with different R₁/R₇ substituents showed a response factor variation of less than 22% (data not given), which indicates that the peak areas of the different DPs are most probably a good measure for their relative order of magnitude in occurrence in the photocatalytic reaction mixture.

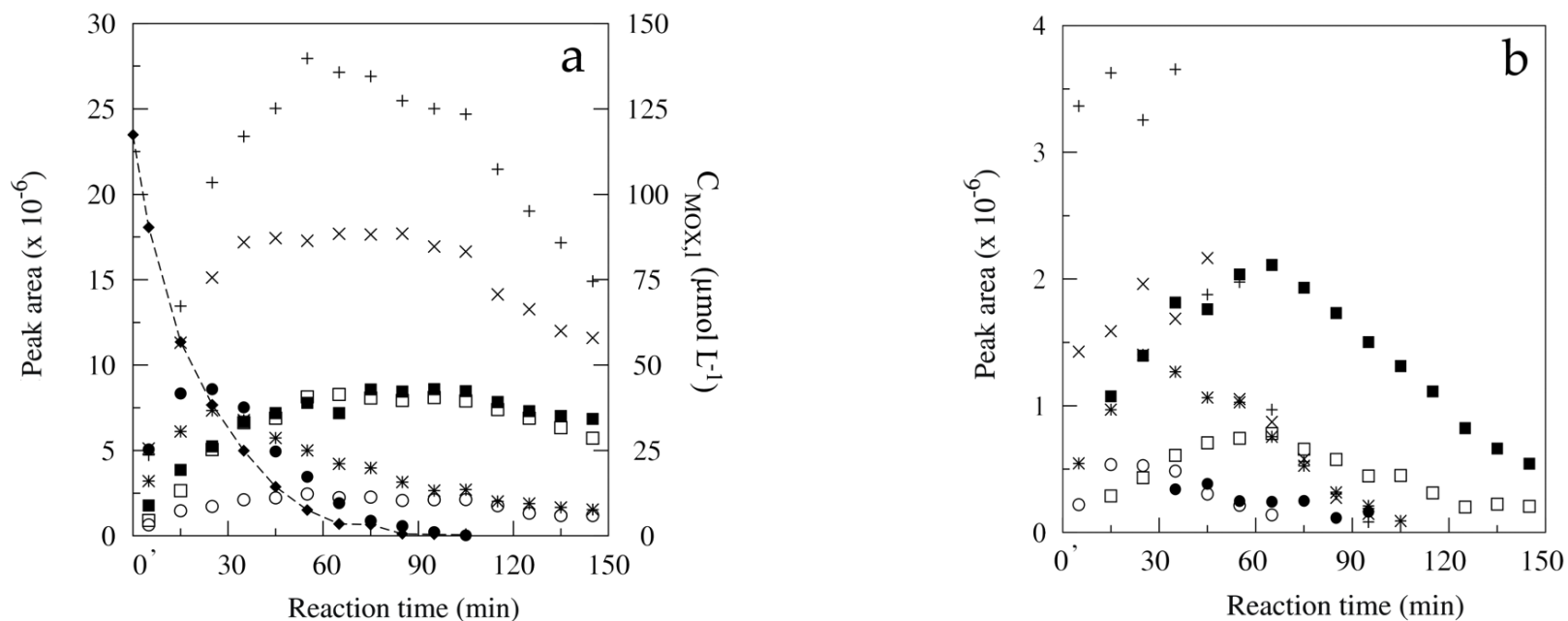


Fig. 3.2 (a) Integrated peak areas of the major products in the liquid phase during the photocatalytic degradation of MOX. Nominal masses (Da) and chromatographic retention time (t_R : min) are (+) 292, t_R : 23.46; (○): 306, t_R : 23.43; (■): 306, t_R : 22.11; (×): 320, t_R : 20.87; (●): 417, t_R : 16.00; (□): 429, t_R : 17.16 and (*): 429, t_R : 12.11 (left y-axis), with (◆): the liquid concentration of MOX ($C_{\text{MOX},l}$ $\mu\text{mol L}^{-1}$) during photocatalytic degradation (6% adsorption; $n = 1$; right y-axis). Dashed line is plotted to guide the eye; (b) Integrated peak areas of the minor products the liquid phase during the photocatalytic degradation of MOX with nominal masses (Da) and chromatographic retention time (t_R : min) are (+): 399, t_R : 15.89; (×): 399, t_R : 17.19; (*): 399, t_R : 20.52; (□) 415, t_R : 10.74; (■): 415, t_R : 14.38; (○): 415, t_R : 17.40 and (●): 415, t_R : 21.46 ($n = 1$).

Similar figures for pH 3.0 and 10.0 can be found in Addendum C. At pH 7.0, fourteen different DPs with a signal-to-noise ratio (S/N) higher than ten are clearly detected during low resolution analysis with several of them having the same nominal mass but different chromatographic retention times. High resolution measurements were performed for reaction solution samples taken at 95 min for pH 3.0, 65 min for pH 7.0 and 35 min for pH 10.0. The selected time at pH 10.0 allowed to perform a HRMS analysis on additional peaks corresponding to a mass of 417 Da. Measured masses ($[M+H]^+$) and molecular compositions are presented in Table 3.1. Similar DPs are identified for all investigated pH levels. All detected compounds show a limited change in the UV-spectrum compared to MOX (Fig. 3.3).

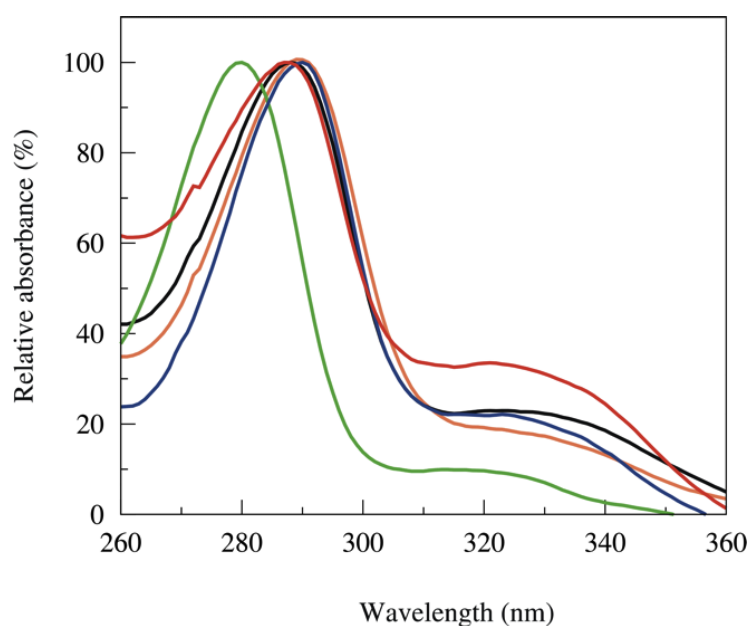


Fig. 3.3 Relative absorbance (%) of MOX and some of its photocatalytic DPs, with ■ : MOX; ■ : 417 Da, $t_R = 14.32$ min; ■ : 415 Da, $t_R = 14.38$ min; ■ : 429 Da, $t_R = 11.89$ min; ■ : 292 Da, $t_R = 23.46$ min.

Table 3.1 Determination of DPs ^a of MOX after photocatalytic degradation at pH = 3.0, 7.0, and 10.0 determined by HPLC and LR and HR mass spectrometry (n = 1)

LR MS				HR MS						
Nominal mass	t _R ^b (min)	t _R ^b (min)	t _R ^b (min)	[M+H] ⁺ measured	[M+H] ⁺ measured	[M+H] ⁺ measured	DBE ^d	Molecular formula	Difference with MOX	No. ^a
(Da)	pH 3.0	pH 7.0	pH 10.0	pH 3.0 (error ^c (ppm))	pH 7.0 (error ^c (ppm))	pH 10.0 (error ^c (ppm))				
292	23.27	23.46	23.40	293.09304 (-0.59)	293.09047 (2.93)	293.09296 (-0.86)	9.0	C ₁₄ H ₁₄ O ₄ N ₂ F	-7C 11H	12
306	22.46	22.11	22.02	no HR-MS	307.07148 (-3.25)	no HR-MS	10.0	C ₁₄ H ₁₂ O ₅ N ₂ F	-7C 13H +O	10
	23.30	23.43	23.33	no HR-MS	307.10788 (-3.20)	no HR-MS	9.0	C ₁₅ H ₁₆ O ₄ N ₂ F	-6C 9H N	8
320	20.68	20.87	20.75	321.08792 (-0.65)	321.08824 (0.35)	321.08815 (0.07)	10.0	C ₁₅ H ₁₄ O ₅ N ₂ F	-6C 11H +O	11
399	15.73	15.89	15.85 *	400.16774 (2.57)	400.16801 (3.25)	no HR-MS	12.0	C ₂₁ H ₂₃ O ₄ N ₃ F	-2H	6
	16.78	n.d.	16.44	no HR-MS	no HR-MS	400.16882 (5.27)	12.0	C ₂₁ H ₂₃ O ₄ N ₃ F	-2H	6
	n.d.	17.19	17.16	no HR-MS	400.16806 (3.37)	400.16873 (5.00)	12.0	C ₂₁ H ₂₃ O ₄ N ₃ F	-2H	6
	n.d.	n.d.	17.57	no HR-MS	no HR-MS	no HR-MS				
	20.09	20.52	20.40 *	no HR-MS	400.16799 (3.20)	no HR-MS	12.0	C ₂₁ H ₂₃ O ₄ N ₃ F	-2H	6
401	16.34	16.49	16.53	402.18303 (1.66)	402.18413 (4.40)	402.18289 (1.31)	11.0	C₂₁H₂₅O₄N₃F		MOX
415	10.52*	10.74	10.58	no HR-MS	no HR-MS	no HR-MS				
	14.17	14.38	14.32	416.16137 (-0.62)	416.16150 (-0.3)	no HR-MS	12.0	C ₂₁ H ₂₃ O ₅ N ₃ F	-2H +O	7
	16.94	17.40	17.28	no HR-MS	no HR-MS	no HR-MS				
	n.d.	21.46	21.40	no HR-MS	no HR-MS	no HR-MS				
	n.d.	n.d.	24.30	no HR-MS	no HR-MS	no HR-MS				
417	n.d.	n.d.	24.98	no HR-MS	no HR-MS	no HR-MS				
	13.70 *	13.91 *	13.76	no HR-MS	no HR-MS	418.17917 (4.53)	11.0	C ₂₁ H ₂₅ O ₅ N ₃ F	+O	1-5
	14.23 *	14.47 *	14.32	no HR-MS	no HR-MS	no HR-MS				
	n.d.	n.d.	15.23	no HR-MS	no HR-MS	418.17776 (1.16)	11.0	C ₂₁ H ₂₅ O ₅ N ₃ F	+O	1-5
	15.60	16.00	15.85	418.17582 (-3.48)	418.17722 (-0.14)	418.17997 (6.44)	11.0	C ₂₁ H ₂₅ O ₅ N ₃ F	+O	1-5
n.d.	n.d.	17.60	no HR-MS	no HR-MS	no HR-MS					
429	11.89	12.11	n.d.	no HR-MS	430.14151 (1.44)	no HR-MS	13.0	C ₂₁ H ₂₁ O ₆ N ₃ F	-4H +2O	9
	14.41	n.d.	14.92	no HR-MS	no HR-MS	no HR-MS				
	16.95	17.16	16.79	no HR-MS	430.14062 (0.63)	no HR-MS	13.0	C ₂₁ H ₂₁ O ₆ N ₃ F	-4H +2O	9

^a Numbering according to the proposed pathway in Fig. 3.4; ^b HPLC retention time based on MS detection; ^c Difference between measured and theoretical mass; ^d Double Bond Equivalent;

* 3 < S/N < 10; n.d.: S/N < 3

A large absorbance peak between 270 and 290 nm with a shoulder between 310 and 330 nm indicates that the quinolone core is unaffected and, by consequence, degradation occurs at the R₇ substituent (Langlois et al., 2005). This statement is supported by the fact that all detected DPs retain at least two nitrogen atoms as well as the fluorine atom. Structures are proposed based on the molecular formula, double bond equivalent (DBE) and molecular composition of the mother compound. Compounds 1, 2, 7, 9, 11 and 12 are analogous to previously reported FQ degradation products using oxidation techniques, such as ozonation, photolysis, biodegradation and electrochemical oxidation (Burhenne et al., 1997; Wetzstein et al., 1997; Karl et al., 2006; Calza et al., 2008; De Witte et al., 2008; An et al., 2010a; Guinea et al., 2010; Paul et al., 2010; Hubicka et al., 2012). Compounds 2, 7 and 9 have been earlier identified during MOX photocatalysis (Sturini et al., 2012b), but it is the first time that compounds 1, 3, 4, 5, 6, 8, 10, 11 and 12 are reported as MOX degradation products during heterogeneous photocatalysis.

Based on all identified reaction products, a pathway for the photocatalytic degradation of MOX is proposed in Fig. 3.4. Considering Table 3.1, up to five different DPs with a mass of 417 Da are detected during MOX photocatalysis. Chromatographic retention times indicate that they consist of five different structures and HRMS analysis shows a net gain of one oxygen atom compared to MOX. Compounds 1-5, as shown in Fig. 3.4, are all plausible structures for these detected DPs. Among them, compounds 1 and 2 represent a ring cleavage of the cyclopropyl group or a random addition of a hydroxyl group, while compounds 3-5 have a ring cleavage on the (4a*S*,7a*S*)-octahydro-6*H*-pyrrolo[3,4-*b*]pyridin-6-yl, R₇, group. Hubicka et al.(2012) observed a similar MOX degradation product with a ring opening on the R₇ group during photolytic treatment.

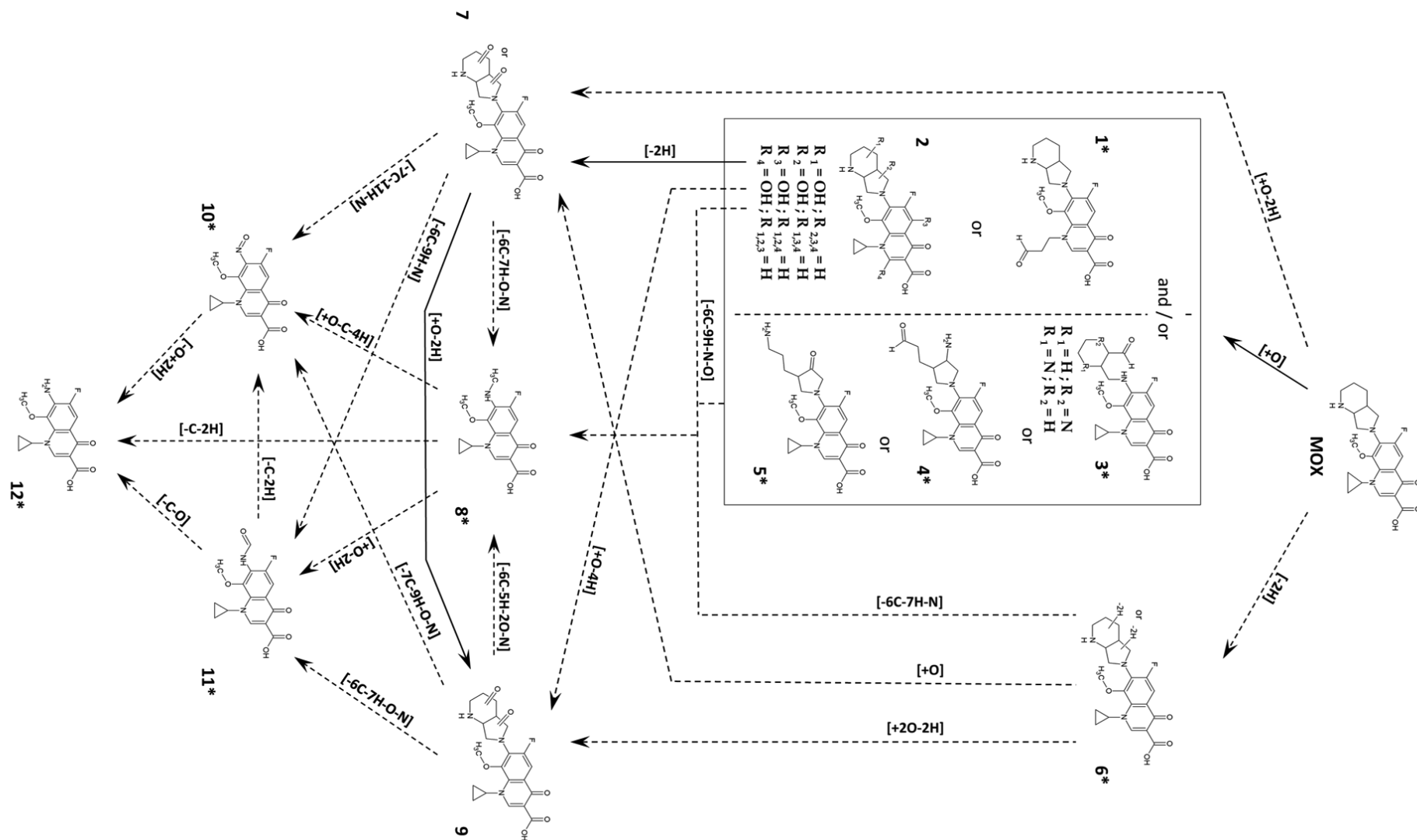


Fig. 3.4 Proposal of the initial photocatalytic degradation pathway of MOX. Compounds marked with * are newly identified MOX photocatalytic DPs. Dashed lines are newly proposed possible degradation routes, in addition to the full lines described in literature (Sturini et al., 2012b). Multiple plausible structures are proposed for compounds 6, 7 and 9 due to the unknown exact location of the double bond and keto functions, respectively.

Together with compound 6, formation of a double bond on the R₇ substituent, and compound 7, formation of a keto group on the R₇ substituent, these are probably the primary reaction products formed during photocatalytic degradation of MOX. Further oxidation can lead to the formation of a double keto group like compound 9 or the further degradation of the substituent resulting in compound 8. Degradation from compounds 8, 10 and 11 includes oxidation, reduction and demethylation reactions, eventually resulting in compound 12, which contains only the MOX quinolone moiety.

Using ab initio molecular orbital calculations, De Witte et al. (2009) investigated where the most reactive centra for LEVO, a similar FQ, are positioned. From these calculations it could be concluded that the C₂ carbon and the N'₁ nitrogen are the most reactive centra in this molecule, with C₂ being a suitable site for hydroxyl radical attack, see Fig. C.3. Since no degradation at the quinolone moiety has been observed, one might conclude that the effect of hydroxyl radicals is negligible and that the main degradation mechanism occurs through reaction with 'holes' or via direct charge injection as proposed by Paul et al. (2007).

However, in Chapter 2.2 it is observed that hydroxyl radicals contribute for about 24% in the degradation of MOX under UV-A irradiation using the same catalyst concentration. DPs formed by hydroxyl radical attack may be less stable, rapidly degrading into lower molecular weight compounds or are not easily detected by the applied HPLC-HRMS methodology (Paul et al., 2010). This might also explain why, so far, only two photocatalytic DPs, resulting from a ring opening at the quinolone moiety are observed in literature (Calza et al., 2008; An et al., 2010a). Since no pH dependency is noticed in the main type of DPs formed, the suggested pathway can be acknowledged as a general pathway for all pH levels.

Nevertheless a pH effect is observed in the time profiles of the reaction products (Fig. 3.2, Fig. B.1, and Fig. B.2). The relative importance of the identified compounds in the liquid phase as a function of pH, in terms of maximum peak area observed during photocatalytic degradation, is presented in Fig. 3.5.

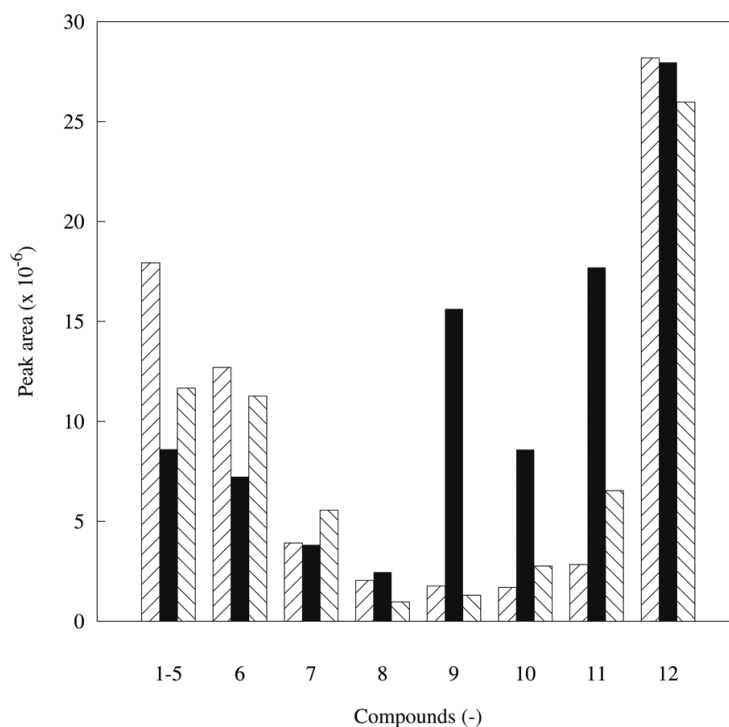
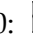




Fig. 3.5 Maximum LRMS peak areas detected in the liquid phase of compounds 1-12 during photocatalytic degradation of MOX as a function of pH 3.0:  ; 7.0:  ; and 10.0:  (n = 1).

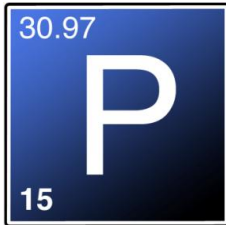
Among the investigated pH levels, compounds 8, 9, 10 and 11 show the highest occurrence at neutral conditions. On the other hand, compounds 1-5, 6 and 7 show higher peak areas at pH 3.0 and 10.0 compared to pH 7.0. No significant pH influence on the formation of compound 12 could be observed. A clear shift in maximum abundance from ‘weakly’ oxidized DPs at pH 3.0 and 10.0 towards more oxidized DPs in neutral conditions is noticed.

A possible reason for this difference could be the influence of pH on the reaction speeds in the pathway favoring specific reactions or slowing down others, creating ‘bottle-necks’. Another possible explanation can be found in the complex

nature of the photocatalytic process itself. The photocatalytic degradation reaction of MOX takes place in the liquid phase and at the catalyst surface and is greatly influenced by pH. It has been shown in Chapter 2.1 that the adsorption of FQs on a TiO₂ catalyst surface is higher at neutral conditions indicating that surface reactions are more pronounced. The pH dependent adsorption of MOX together with the formation of DPs, which probably have a similar pH dependent adsorption behavior, could contribute to the different distribution of DPs.

3.4 Conclusions

No significant mineralization is observed after 145 min of photocatalytic treatment, even though MOX is completely removed after 90 min of degradation time. Using HPLC-HRMS, 14 different MOX degradation products are detected in the photocatalytic reaction solutions. Structure elucidation showed no degradation of the base quinolone moiety and no defluorination. Time profiles of the different DPs reveal that the solution pH influences the abundance of the different DPs in the water phase during reaction. Nonetheless, the same types of photocatalytic DPs are observed at all pH levels. In addition, a new pathway is proposed with the different identified DPs, resulting in a better understanding of the initial photocatalytic degradation mechanism of MOX.



art IV

Biological endpoints: residual antibacterial activity and algal growth inhibition

Redrafted from:

Van Doorslaer, X., Demeestere, K., Heynderickx, P.M., Caussyn, M., Van Langenhove, H., Devlieghere, F., Vermeulen, A., Dewulf, J., 2013. Applied Catalysis B-Environmental 138-139, 333-341.

and

Van Doorslaer, X., Haylamicheal, I.D., Dewulf, J., Van Langenhove, H., Janssen, C., Demeestere, K., 2014. Chemosphere doi:10.1016/j.chemosphere.2014.03.048.

4.0 Introduction

Different DPs are identified during photocatalytic treatment in Part III. As a result of their structural similarity with MOX, it cannot be excluded that these DPs can still exert biological activity. It is therefore important to not solely evaluate an AOP treatment on a compound removal basis, as presented in Part II, but also for its capability in removing biological activity. The following two approaches to quantify residual biological activity of photocatalytic reaction solutions are used: residual antibacterial activity determination and ecotoxicity tests.

Antibacterial activity can be assessed by means of bacterial growth measurements in both liquid media or on agar plates (De Witte et al., 2010). In studies focusing on AOP treatment of antibiotic solutions, mainly agar diffusion methods using the test bacterial species *Escherichia coli* are performed (De Bel et al., 2009; De Witte et al., 2009; Paul et al., 2010; Nasuhoglu et al., 2012; Rodrigues-Silva et al., 2013). However, literature on residual antibacterial activity of FQs after a photocatalytic treatment, and information on DP activity is scarce.

Therefore, in Chapter 4.1, agar diffusion tests are performed for a representative set of bacteria to (i) determine the reduction in residual antibacterial activity during a photocatalytic treatment of MOX at different pH levels, and (ii) to assess the antibacterial activity of the photocatalytic DPs present in the reaction solution.

Ecotoxicity test procedures are available for many aquatic organisms, but since microalgae are the basis of the food web in aquatic ecosystems, they are often used as indicators for xenobiotic pollution (Martins et al., 2012;

Gonzalez-Pleiter et al., 2013). So far, ecotoxicity data for the most recent generation FQ antibiotics, such as MOX, are scarce or missing, making their risk assessment difficult. It is also unclear to what extent their photocatalytic DPs contribute to the reaction solution's toxicity.

Therefore, in Chapter 4.2, algal growth inhibition experiments, using the fresh water alga *Pseudokirchneriella subcapitata* as a non-target organism, are performed (i) to determine the 72-h algal growth inhibition of MOX compared with that of the previous generation fluoroquinolone CIP as a reference, and (ii) to evaluate the effect of a heterogeneous photocatalytic treatment on the toxicity of a MOX solution. Also, the contribution of both MOX and its photocatalytic DPs to the overall reaction solution's toxicity is investigated, and the effect of chemical transformation on cell permeation and biological activity is discussed to better understand the residual ecotoxicity.

4.1 Residual antibacterial activity of a MOX solution after photocatalytic treatment

4.1.1 Materials and methods

4.1.1.1 Chemicals and experimental setup

Nutrient agar (NA), Tryptone soy agar (TSA) and brain heart infusion (BHI) are purchased from OXOID LTD (UK). NaCl (99.5%) used in the physiological solution is provided by Sigma-Aldrich.

Degradation experiments were performed in triplicate according to the experimental procedure described in Chapter 2.1, and are separately evaluated for residual antibacterial activity.

Photocatalytic samples are analyzed for MOX using the HPLC-PDA setup described in Chapter 2.1.

4.1.1.2 Antibacterial activity

Non-pathogenic bacteria *Escherichia coli* LMG 8223 (G^-), *Staphylococcus carnosus* LFMFP 163 (G^+), *Streptococcus mutans* LMG 14558T (G^+) and *Klebsiella pneumoniae* LMG 2095 (G^-) were used.

The sensitivity of the selected bacteria to MOX is tested through agar diffusion tests using a concentration range of 12.46, 7.48, 2.49, 1.25, 0.75 and 0.07 $\mu\text{mol L}^{-1}$ of the pure substance MOX. Agar diffusion tests are performed using pour plates consisting of 2.8% NA and for all investigated bacteria the same initial cell

density is applied (10^8 cells mL^{-1} broth). The NA is buffered by peptones present in the NA mix. Wells of 0.64 cm diameter were cut manually in the agar.

To evaluate the residual antibacterial activity during the photocatalytic degradation of MOX at pH 3.0, 7.0 and 10.0, samples of 2 mL are taken at 0, 0', 2, 4, 6, 8, 10, 12 and 14 min degradation time, filtered over a 0.22 μm disk filter and 1/3 diluted before dosing 20 μL in the wells. Inhibition zone diameters of both experiments are measured after 48 h incubation at 37°C in aerobic conditions with a digital slide gauge. The inhibition zone at 0' min degradation time represents 100% residual inhibition. Netto inhibition zone diameters (corrected for drill hole diameter) measured after X min of photocatalytic degradation time are divided by the netto inhibition zone diameter at 0' min degradation time and expressed as residual percentage of antibacterial activity.

4.1.2 Results and Discussion

As demonstrated in Part III, MOX is subject to photocatalytic degradation, and mineralization is incomplete. The efficiency of the photocatalytic treatment is not solely defined by the chemical degradation of MOX, but also by the reduction of the residual antibacterial activity of the reaction solution. Therefore, agar diffusion tests are performed with a selection of bacteria from the antibacterial spectrum of MOX. In a first step, the sensitivity of the bacteria strains is evaluated using a concentration range of MOX (0-12.46 $\mu\text{mol L}^{-1}$). The dosis-response curve of MOX for the selected bacteria is presented in Fig. 4.1 (full symbols). In a second step, agar diffusion tests are performed on photocatalytic samples. The inhibition zone diameters resulting from the samples of the photocatalytically treated solution at pH 7.0 are also plotted in Fig. 4.1 (open symbols).

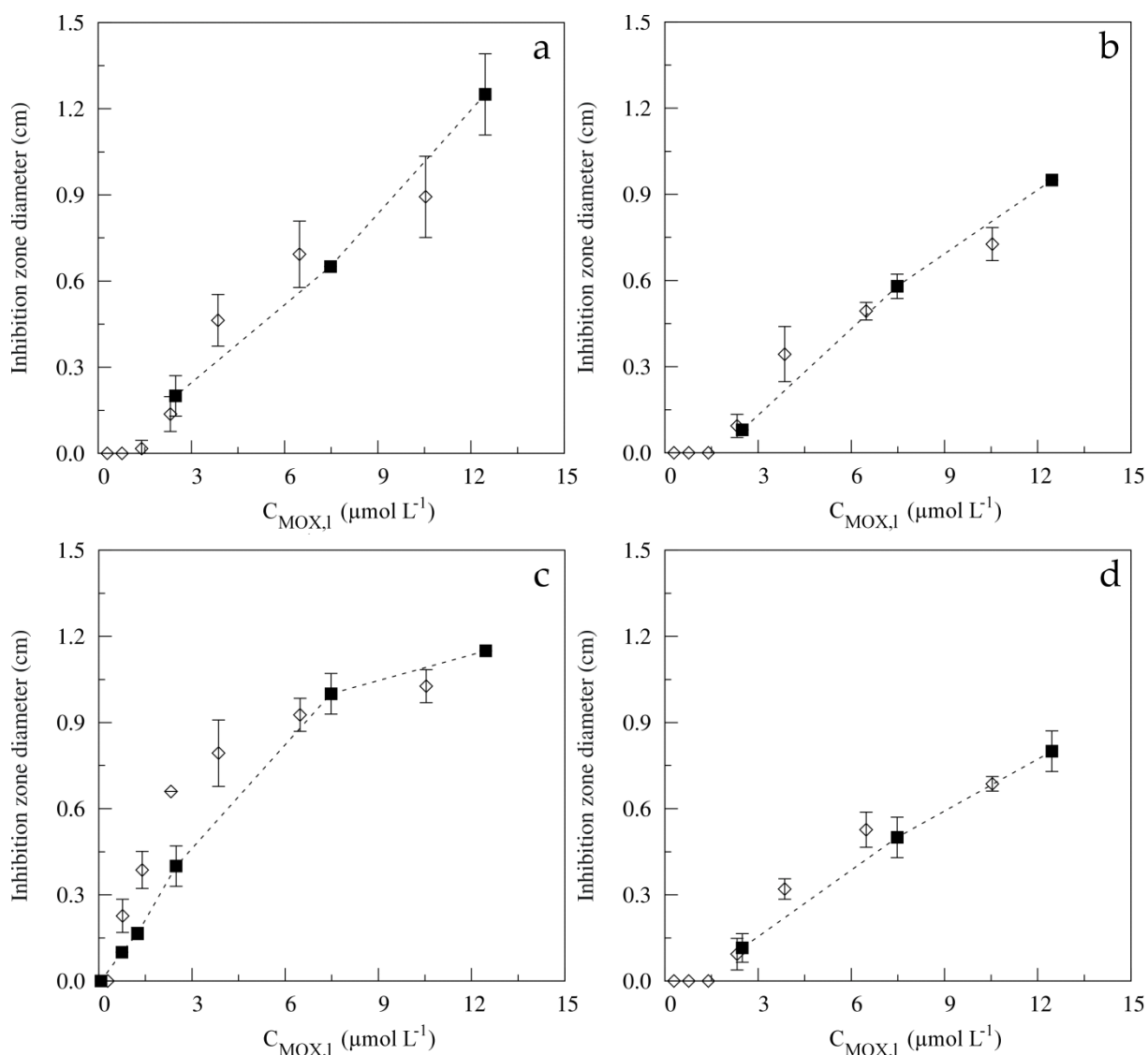


Fig. 4.1 Inhibition zone diameters ($n = 3$) as a function of MOX concentrations 0.07, 0.75, 1.25, 2.49, 7.48 and 12.46 $\mu\text{mol L}^{-1}$ (■) for *K. pneumoniae* (a), *S. mutans* (b), *E. coli* (c), and *S. carnosus* (d) together with the inhibition zone diameters as a function of the MOX concentration of the 1/3 diluted photocatalytic degradation samples (◇) after 12, 10, 8, 6, 4, 2, and 0' min of degradation time ($n = 3$). Dashed line is plotted to guide the eye.

For *K. pneumoniae*, *S. carnosus* and *S. mutans* similar inhibition zone diameters are attained for a given standard MOX concentration and a similar MOX concentration during photocatalytic degradation. This correlation indicates that the mother compound is the main descriptor for the residual antibacterial activity. A similar trend is noticed for the fluoroquinolones LEVO and CIP; the residual antibacterial activity of the photocatalytically treated solutions correlated

well with the residual amount of mother compound in solution (Paul et al., 2010; Nasuhoglu et al., 2012). For *E. coli*, the observed inhibition zone diameters resulting from the photocatalytic samples are slightly higher than the inhibition zone diameters for a given MOX concentration between 0-8 $\mu\text{mol L}^{-1}$ MOX (Fig. 4.1). This may indicate that *E. coli* is more sensitive to the formed DPs of MOX.

In a third step, the residual percentage of inhibition, based on the measured inhibition zone diameters, for the selected bacteria during photocatalytic degradation of MOX at pH 3.0, 7.0 and 10.0 is compared (Table 4.1).

Table 4.1 Percentage of residual antibacterial activity based on inhibition zone diameters versus photocatalytic degradation time at pH 3.0, 7.0, and 10.0 for *K. pneumoniae* (G⁻), *S. mutans* (G⁺), *E. coli* (G⁻) and *S. carnosus* (G⁺). Time 0' representing the starting point for the reaction after adsorption-desorption equilibrium. Photocatalytic reaction samples were 1/3 diluted before addition of 20 µL. Inhibition diameters were measured after an aerobic incubation of 48 h at 37°C (n= 3)

Species	pH	Reaction time (min)							
		0'	2	4	6	8	10	12	14
<i>K. pneumoniae</i>	3.0	100.0	96.1 ± 1.6	90.3 ± 2.9	77.5 ± 9.7	70.1 ± 14.9	64.8 ± 14.5	54.1 ± 17.1	49.4 ± 21.3
	7.0	100.0	77.3 ± 3.2	51.6 ± 3.7	16.1 ± 9.3	- ^a	-	-	-
	10.0	100.0	88.6 ± 0.4	78.0 ± 2.2	72.5 ± 6.4	61.5 ± 6.9	54.0 ± 6.7	48.2 ± 11.0	32.9 ± 9.6
<i>S. mutans</i>	3.0	100.0	95.8 ± 4.1	89.0 ± 6.1	82.6 ± 1.1	75.0 ± 7.8	72.8 ± 11.3	63.3 ± 7.5	53.7 ± 7.4
	7.0	100.0	68.0 ± 2.0	46.8 ± 10.1	13.1 ± 6.6	-	-	-	-
	10.0	100.0	93.4 ± 0.4	76.5 ± 4.3	64.5 ± 4.3	53.3 ± 5.2	40.4 ± 4.2	27.8 ± 5.9	15.4 ± 6.5
<i>E. coli</i>	3.0	100.0	93.3 ± 5.8	91.6 ± 5.9	84.7 ± 7.6	88.3 ± 3.1	86.2 ± 4.0	79.3 ± 7.5	77.9 ± 5.5
	7.0	100.0	90.2 ± 0.6	77.0 ± 7.1	64.4 ± 3.7	37.6 ± 5.1	21.9 ± 4.5	-	-
	10.0	100.0	98.4 ± 2.7	93.0 ± 6.2	89.5 ± 1.1	82.5 ± 6.5	77.1 ± 5.4	71.7 ± 8.4	60.4 ± 2.0
<i>S. carnosus</i>	3.0	100.0	87.4 ± 3.2	81.9 ± 1.4	74.0 ± 2.4	70.7 ± 3.9	72.8 ± 6.4	61.5 ± 12.0	41.3 ± 18.5
	7.0	100.0	76.6 ± 7.2	46.7 ± 6.3	13.4 ± 7.7	-	-	-	-
	10.0	100.0	90.8 ± 3.5	81.1 ± 3.3	66.2 ± 3.0	44.3 ± 12.2	37.7 ± 8.5	28.9 ± 8.6	14.0 ± 10.6

^a below visual detection

Photographs of the inhibition zones for *S. carnosus* for the investigated pH levels are illustrated in Fig. 4.2. After 12 min of photocatalytic treatment of MOX at pH 7.0 no residual antibacterial activity is noticed for all investigated bacteria, while residual activity is still observed after 14 min of reaction under acidic and alkaline conditions. This is probably due to the slower photocatalytic degradation rate of MOX at these pH levels as discussed in Chapter 2.1.

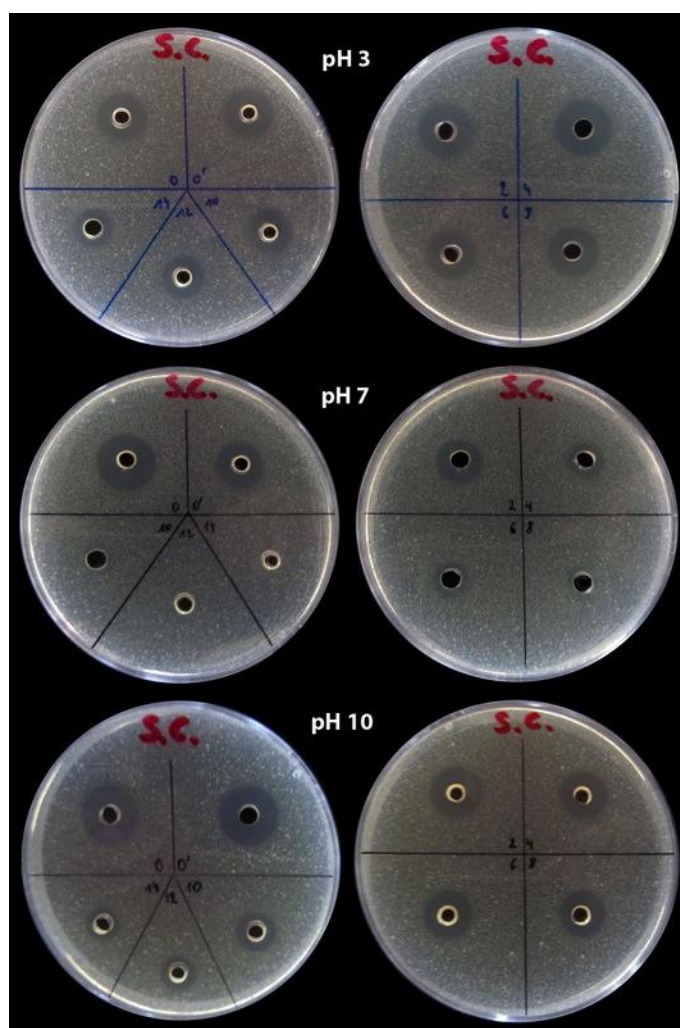


Fig. 4.2 Agar diffusion tests for *Staphylococcus carnosus* for reaction samples taken after 0, 0', 2, 4, 6, 8, 10, 12 and 14 min of photocatalytic treatment at pH 3.0, 7.0 and 10.0. Inhibition diameters are measured after an aerobic incubation of 48 h at 37°C.

All DPs observed during photocatalytic degradation of MOX retain the quinolone structure, see Part III. This quinolone core contains a carboxyl and a keto group which are considered to be essential for the antibacterial activity since they are necessary for the FQ-DNA gyrase binding (Chu and Fernandes, 1989). Hence, the degradation of this moiety could be supposed to be necessary to reduce the antibacterial activity. Therefore, we could expect higher inhibition zone diameters resulting from the photocatalytic degradation samples comparing to the inhibition zone diameters resulting from the MOX concentration range, but this was not the case as demonstrated in Fig. 4.1. Transformation and/or degradation of the auxiliary groups, such as the R₇ group, can also significantly decrease the antibacterial activity (Sharma et al., 2009). Chu and Fernandes (1989) reported that quinolones with a large substituent at the R₇ position have a higher activity than the ones with a smaller group at that position. This is also shown by Wetzstein et al. (1999) who have found that desethylene CIP is 100 fold less active than its mother compound against *E. coli* and that the base quinolone core of CIP has less than 3% of the antibacterial activity compared to CIP. A similar compound retaining only the MOX quinolone moiety is also identified during photocatalytic treatment of MOX (Compound 12, Fig. 3.4). Next to the altered activity, a reduced binding affinity with DNA topoisomerases is achieved because the R₇ substituent is an important factor for target selection by quinolones (Alovero et al., 2000).

Overall, the evaluation of the antibacterial activity of a single DP is difficult to determine. It is more relevant to evaluate the potential of a photocatalytic treatment technique through the assessment of the overall bacterial inhibition after a given reaction time. Since a different trend in decrease of antibacterial activity has been noticed for the investigated bacteria, the importance to evaluate

the efficiency of a degradation process in real applications for a large variety of bacterial species has to be emphasized. According to Lemaire et al. (2011), a different sensitivity is not only noticed between different species, but also between different strains of one bacterial species. Therefore, conclusions for one bacterial species have to be made with caution, keeping in mind the interspecies variation of sensitivity.

4.1.3 Conclusions

Linking inhibition zone diameters resulting from a MOX concentration range with the inhibition zone diameters of photocatalytic samples shows that the residual concentration of mother compound in solution correlates well with the residual antibacterial activity for all investigated bacterial species. *E. coli* is slightly more sensitive towards the formed DPs since in a higher inhibition zone diameter is observed for the photocatalytic reaction samples. Heterogeneous photocatalysis is very effective in reducing the antibacterial activity at pH 7.0 with no observed residual antibacterial activity for the four investigated bacterial species after 12 min of degradation time. Photocatalysis is therefore a promising technique to degrade the antibiotic MOX and to reduce its biological activity in wastewater effluents.

4.2 Ecotoxicity of a MOX solution after photocatalytic treatment towards a green alga non-target organism

4.2.1 Materials and methods

4.2.1.1 Chemicals

The following chemicals are used for the preparation of OECD guideline mineral stock solutions. $\text{MgCl}_2 \cdot 6\text{H}_2\text{O}$ (98-101%), $\text{CaCl}_2 \cdot 2\text{H}_2\text{O}$ (Analar Normapur), $\text{MgSO}_4 \cdot 7\text{H}_2\text{O}$ (Ph Eur grade), $\text{FeCl}_3 \cdot 6\text{H}_2\text{O}$ (Analar Normapur), $\text{MnCl}_2 \cdot 4\text{H}_2\text{O}$ (99.99%) are supplied by VWR BDH Prolabo. Analytical grade reagents ZnCl_2 , $\text{CoCl}_2 \cdot 6\text{H}_2\text{O}$, $\text{CuCl}_2 \cdot 2\text{H}_2\text{O}$ and $\text{Na}_2\text{MoO}_4 \cdot 2\text{H}_2\text{O}$ are provided by Merck and NH_4Cl ($\geq 99.5\%$), KH_2PO_4 ($\geq 99.0\%$), $\text{Na}_2\text{EDTA} \cdot 2\text{H}_2\text{O}$ ($\geq 97.0\%$), H_3BO_3 (99.7%), NaHCO_3 ($\geq 99.7\%$) by Sigma-Aldrich.

4.2.1.2 Algal toxicity of MOX and its photocatalytic degradation mixture: growth inhibition tests

Samples for the algal growth inhibition tests are taken after 0, 30, 60, 90 and 150 min of photocatalytic treatment performed according the methodology described in Part II (operational variables mentioned in Table 0.1). The reaction solutions are filtered over a 5-13 μm filter paper (VWR international), followed by a refined filtration over a 0.22 μm disk filter (Merck millipore, Germany), and stored at 4°C. Each reaction sample is also analyzed for MOX using the HPLC-PDA procedure applied in Chapter 2.1.

The 72-h algal growth inhibition cuvette test is performed according to the OECD guideline 201 (OECD, 2011). The fresh water alga *Pseudokirchneriella subcapitata* is purchased from the Culture Collection of Algae and Protozoa (CCAP, www.ccap.ac.uk). Four days prior to the start of each growth inhibition experiment, a new algal culture is prepared and allowed to grow on a shaking table at $20 \pm 1^\circ\text{C}$ under continuous illumination (5200 lux).

Growth inhibition tests with pure CIP (MP Biomedicals Inc.) and MOX are performed using five concentrations between 0.25 and 10 mg L⁻¹, prepared in OECD algal growth medium. To determine growth inhibition effects caused by the photocatalytically treated solution, being a mixture of MOX and/or DPs, each sample is diluted at five concentration levels expressed as a reaction solution dilution percentage (% solution). Phosphate buffer is used as the dilution medium to ensure the same phosphate level in all sample dilutions and nutrients are added to the same concentration as in the OECD algal growth medium. In both cases, preliminary range finding tests are performed to ensure a good spreading of the test concentrations/dilutions.

Three replicate cuvettes, inoculated with 10⁴ algal cells mL⁻¹, and a background correction (no algae) are prepared for each test concentration/dilution. A control in OECD algae growth medium is added to evaluate the validity of the test results. At regular times, the vitality of the algal culture is checked with the reference compound potassium dichromate. Incubation is done in cuvettes for 72 h at 298 K under continuous illumination (3000 lux) and slightly opened to ensure gas exchange. Every 24 h, light absorption was measured at 670 nm using a Jenway spectrophotometer to quantify the algal cell density (after background correction).

4.2.1.3 Calculations and statistics

The average specific growth rate between day 0 and day 3, μ_{0-3} (d^{-1}), and the growth rate inhibition, I (%), are calculated according to Eq. 4.1-4.2:

$$\mu_{0-3,C} = (\ln(B_{3d}) - \ln(B_{0d})) / (t_3 - t_0) \quad (4.1)$$

$$I = (\mu_{0-3,C} - \mu_{0-3,T}) / \mu_{0-3,C} \cdot 100 \quad (4.2)$$

with B_{0d} and B_{3d} the algal cell density (cells mL^{-1}) at day 0 (t_0) and day 3 (t_3), respectively; and $\mu_{0-3,C}$ and $\mu_{0-3,T}$ the average specific growth rate (d^{-1}) in the control and test solution.

A log-logistic regression model Eq. 4.3 is used to determine the EC-50 of the test solutions and their associated 95% confidence intervals (STATISTICA 7, StatSoft, Inc., 2004).

$$\mu_{0-3,T} = \mu_{0-3,C} / \left(1 + \left(\frac{x}{\exp(a)} \right)^{\ln(\frac{1}{9}) / b - a} \right) \quad (4.3)$$

with a and b representing \ln (EC-50) and \ln (EC-10), respectively; whereas x gives the concentration ($mg L^{-1}$) of CIP or MOX (Section 4.2.2.2) and the dilution of the reaction solution expressed in % solution (Section 4.2.2.3). Calculated EC-50s, indicating a 50% algal growth rate inhibition compared to the control, are expressed in the same units. In cases that the average specific growth rate inhibition was less than 50%, a one-way ANOVA ($\alpha = 0.05$) test is conducted to determine the absence or presence of toxic effects. Normality of data was checked using the Shapiro-Wilk test before applying parametric statistical tests. Variance homogeneity tests are conducted before using one-way ANOVA.

4.2.2 Results and Discussion

4.2.2.1 Test validity and internal quality control

All data obtained from the toxicity tests were first checked for validity using the OECD algal toxicity test validity criteria (OECD, 2011) before estimating the EC-50 (Fig. 4.3). The validity tests showed that all the toxicity data comply with the OECD guidelines. Moreover, the performance of the test organism *P. subcapitata* and the reproducibility of test results were assessed by determining the EC-50 of the reference toxicant potassium dichromate. The experimentally determined EC-50 of potassium dichromate, 1.040 mg L^{-1} [1.036-1.045], was in the same order of magnitude as those reported in literature (Halling-Sørensen et al., 2000; Paixao et al., 2008), showing a good algal performance and assurance of test reproducibility.

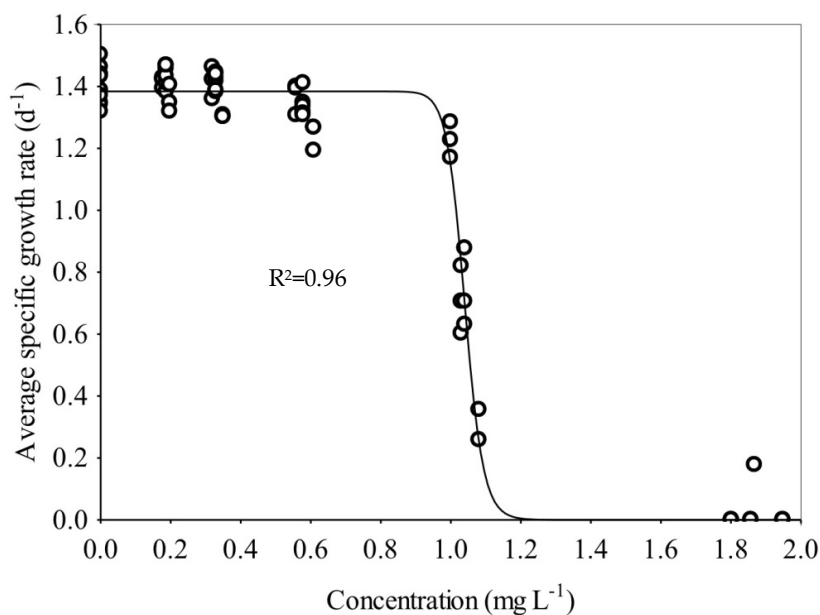


Fig. 4.3 A concentration-response curve of *P. subcapitata* exposed to $\text{K}_2\text{Cr}_2\text{O}_7$. The solid line is plotted using the log-logistic model for EC-50 determination ($n = 3$).

4.2.2.2 Algal toxicity of pure MOX and CIP

The dose-response curves plotted in Fig. 4.4 clearly show that MOX causes a more pronounced growth inhibition effect on *P. subcapitata* than the previous generation CIP.

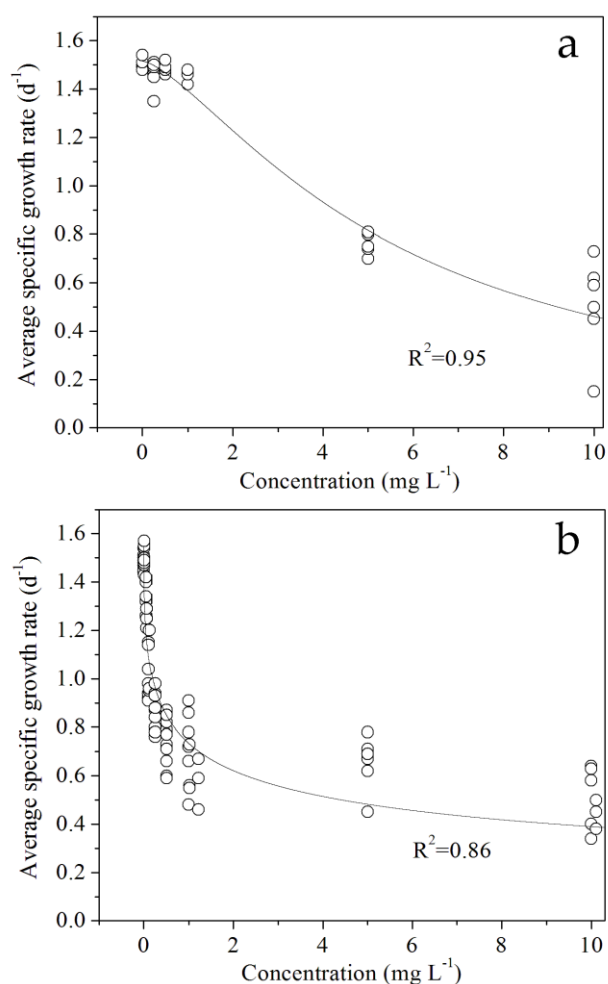


Fig. 4.4 Dose-response curves for the green alga *P. subcapitata* exposed to a FQ concentration range of 0.25-10 mg L⁻¹ (a) CIP (n = 5) and (b) MOX (n = 2). The solid lines are plotted using the log-logistic model.

A broader comparison is given in Table 4.2, summarizing the EC-50 values calculated from the data in Fig. 4.4 using Eq. 4.3, with reported EC-50 values of different FQ generations for the same algal species.

Table 4.2 Fluoroquinolone EC-50 values (mg L⁻¹), with 95% confidence interval, for the alga *Pseudokirchneriella subcapitata*

FQ	Gen. ^a	Use	Protocol	EC-50 [95% CI]	Reference
FLU	1	Vet ^b	n.d.a. ^f	5.0 [4.8, 5.2]	Robinson et al. (2005)
ENRO	n.d. ^c	Vet	n.d.a.	3.1 [2.6, 3.6]	Robinson et al. (2005)
CIP	2	Hum ^d	n.d.a.	18.7 [16.2, 21.2]	Robinson et al. (2005)
			OECD no. 201 (1984)	2.97 [2.41, 3.66]	Halling-Sørensen et al. (2000)
			OECD no. 201 (2006)	4.83 [3.44, 7.32]	Martins et al. (2012)
			OECD no. 201 (2011)	5.57 [4.86, 6.38]	This study
LOME	2	Hum	n.d.a.	22.7 [19.9, 25.5]	Robinson et al. (2005)
OFL	2	Hum	n.d.a.	12.1 [10.4, 13.7]	Robinson et al. (2005)
			ISO no. 8692 (1989)	1.4 [1.1, 1.8]	Isidori et al. (2005)
LEVO	2	Hum	n.d.a.	7.4 [6.4, 8.4]	Robinson et al. (2005)
MOX	3	Hum	OECD no. 201 (2011)	0.78 [0.56, 1.09]	This study
CLINA ^e	n.d.	Hum	n.d.a.	1.1 [0.93, 1.3]	Robinson et al. (2005)

^a generation; ^b veterinary; ^c no data in European classification system (Adriaenssens et al., 2011); ^d human; ^e Clinafloxacin; ^f no data available.

The number of studies reporting ecotoxicity data of FQs towards *P. subcapitata* is limited and EC-50 values for the same compound vary by a factor of up to 10. Different protocols have been used which might contribute to variability in the obtained data. Nevertheless, the table shows that the EC-50 of MOX (0.78 [0.56, 1.09] mg L⁻¹) as determined in this study is the lowest one among all reported FQ data; and is a factor of 7 lower than that of CIP (5.57 [4.86, 6.38] mg L⁻¹). The CIP EC-50 is determined using exactly the same experimental procedure and setup, and is of the same order than that recently reported by Martins et al. (2012), who also followed the OECD guideline 201.

4.2.2.3 Photocatalytic degradation: moxifloxacin removal and algal growth inhibition

Average 72-h algal growth rates in different dilutions (0-100%) of reaction solutions sampled at 0 min (i.e. after adsorption-desorption equilibrium) and after 30, 60, 90 and 150 min of photocatalytic treatment are presented in Fig. 4.5a. EC-50 values increase from 5.5% to 38.2% solution in the first 60 min, clearly showing that the solution's toxicity decreases with longer treatment times. Although the growth rate inhibition is less than 50% after 90 and 150 min, there is still residual toxicity since the algal growth rate in the 100% reaction solution is significantly ($p < 0.05$) lower than that in the control (0% solution).

To better understand the contribution of both MOX and its DPs to algal toxicity, Fig. 4.5b compares at different treatment times (i) measured (black bar) growth rate inhibition of the 100% reaction solutions with (ii) growth rate inhibition calculated (grey bar) from the residual MOX concentration using the MOX toxicity data plotted in Fig. 4.5a (at 0 min).

The difference between both bars is an estimate for the toxicity caused by the DPs mixture. Photocatalytic treatment reduces the algal growth rate inhibition from 72% to 14% over a time span of 150 min, with an increased contribution of DPs at longer irradiation times. As long as MOX is present in the reaction solution (≤ 60 min), it is the main actor for algal growth inhibition. Nevertheless, growth rate inhibition at 90 min (when MOX is below its detection limit) still amounts 1/3 of that at 0 min. This shows that the entire mixture of DPs has a lower toxicity on the algal culture compared to MOX, but that their effect cannot be neglected.

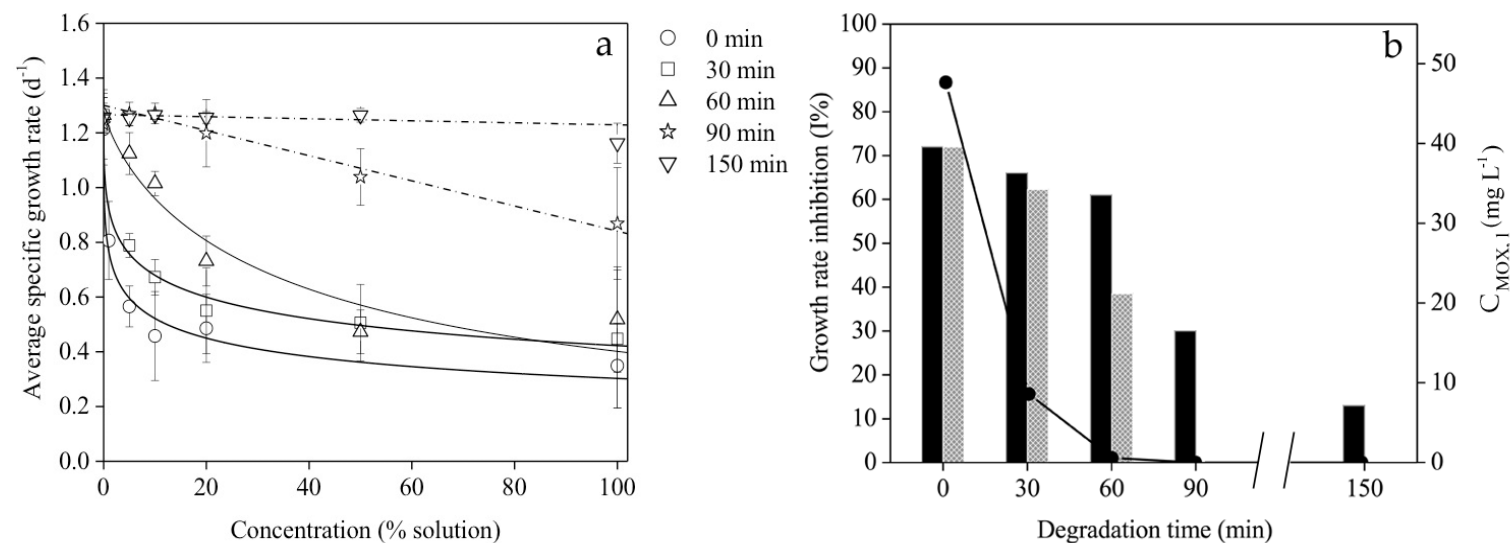


Fig. 4.5 (a) Dose-response plots for reaction mixtures sampled after 0, 30, 60, 90 and 150 min of photocatalytic treatment ($124.6 \mu\text{mol L}^{-1}/50 \text{ mg L}^{-1}$). Solid lines are fitted with the log-logistic model and broken lines are drawn to guide the eye; (b) Average growth rate inhibition (I %) measured in the 100% reaction solutions (black bar, MOX and/or DPs) and calculated from the residual MOX concentration (grey bar, DPs not included) as a function of degradation time with the residual aqueous MOX concentration (\bullet , mg L^{-1} ; right y-axis).

4.2.2.4 Identified degradation products: structural characteristics and possible impact on biological activity and cell permeation

The lower toxicity of the DP mixture formed through photocatalytic treatment (Fig. 4.5b) can result from (i) a decreased biological activity and/or (ii) a diminished cell membrane permeation of the DPs. It is reported that transformation and/or degradation of the auxiliary groups such as the R₇ group can significantly decrease the FQ biological activity (Chu and Fernandes, 1989; Wetzstein et al., 1999; Alovero et al., 2000). Looking at FQ cell permeation, three different transportation mechanisms have to be considered: (i) passive diffusion through the lipid bilayer, (ii) porin channel transport, and (iii) self-promoted uptake. The latter, however, has been disputed for MOX (Lindner et al., 2002). Diffusion through the lipid bilayer is limited to lipophilic uncharged molecules (Fresta et al., 2002), whereas porin mediated transport is favored for zwitterion species (Chapman and Georgopapadakou, 1988; Mahendran et al., 2010).

Most of the identified photocatalytic DPs have an increased hydrophilicity by either the complete loss (292 Da), fragmentation (306 Da and 320 Da) or transformation (417 Da, 429 Da, and 415 Da) of the diazobicyclo group (Table 3.1). Exceptions are DP 417 Da with a ring opening of the R₁ substituent and DP 399 Da which gained a double bond. Based on Fig. 3.2, their occurrence in the photocatalytically treated reaction solution is estimated to be rather low compared with the other DPs, particularly at longer irradiation times. Due to the increase in hydrophilicity of most DPs, the passive diffusion of their uncharged structures through the cell membrane might be decreased when compared with uncharged MOX. Moreover, transformations at the R₁/R₇ substituent can alter the acid-base speciation (i.e. mainly the ratio of uncharged versus zwitterionic form at the neutral pH conditions of our experiments), and thus porin mediated

transport (Schmitt-Kopplin et al., 1999; Langlois et al., 2005). Further research is needed, however, to better understand to what extent a change in acid-base speciation may affect the overall cell permeation process.

4.2.3 Conclusions

The ecotoxicity of two FQ antibiotics is determined using a 72-h growth rate inhibition test with *P. subcapitata* as a non-target model organism. As far as we know, this provides the first reported EC-50 for MOX towards this green alga, showing a toxicity which is 7 times higher than that of its previous generation FQ family member CIP.

Applying a UV-A heterogeneous photocatalytic treatment on a MOX solution results in an algal growth inhibition decrease from 72% to 14% after 150 min of treatment. A combined interpretation of both the chemical analytical (Part III) and ecotoxicological data (this Part) revealed that as long as MOX is present in the reaction solution, it is the main contributor for algal growth inhibition. However, the fact that growth rate inhibition is still observed in treated solutions - from which MOX has been removed below its detection limit - also indicates that DPs may not be neglected in toxicity assessment. Structural analysis suggests mainly transformations at the R₇ substituent resulting in a decreased lipophilicity and a possible altered acid-base speciation. This may explain their lower biological activity and cell membrane permeation, which is supportive for the observed decrease in toxicity during photocatalytic MOX degradation.



art V

Heterogeneous photocatalysis of moxifloxacin
in hospital effluent:

effect of selected matrix constituents

Redrafted from:

Van Doorslaer, X., Dewulf, J., De Maerschalk, J., Van Langenhove, H., Demeestere, K., 2014. Submitted to Chemical Engineering Journal.

5.1 Introduction

Current research on photocatalytic water treatment for pharmaceutical removal is mostly performed in demineralized water matrices, and focuses mainly on reactor optimization, reaction kinetics and DP identification (Homem and Santos, 2011). Since antibiotics are frequently detected in hospital wastewaters and WWTP effluents (Santos et al., 2010; Verlicchi et al., 2010), research in real effluent matrices is necessary to evaluate the applicability of a photocatalytic treatment technique.

A transition from synthetic matrices towards applications in effluent waters is ongoing (Vasconcelos et al., 2009b; Michael et al., 2010; Homem and Santos, 2011; Dimitroula et al., 2012; Sousa et al., 2012; Prieto-Rodriguez et al., 2013). Still, it is difficult, however, to fully understand and quantify the effect of an effluent matrix on a photocatalytic process, since little studies so far investigated photocatalytic antibiotic removal in both effluent and demineralized water in the same experimental setup. Next to that, no specific research is performed to clarify how and to what extent different types of effluent matrix components affect the different steps of a heterogeneous photocatalysis process.

In this Part, the effect of selected inorganic and organic effluent water constituents on both the adsorption-desorption equilibrium and photocatalytic degradation of MOX is investigated in a systematic approach. Focus is put on suspended particulate matter (SPM), chloride anions and inorganic carbon (IC), and different types of dissolved organic matter (DOM). Adsorption-desorption equilibria and initial degradation rates in (un)filtered hospital effluent waters and

in demineralized water enriched with different amounts of the selected matrix compounds are determined. To conclude, it is estimated to what extent the combined effect of the studied matrix constituents can explain the observed difference between photocatalytic removal in demineralized and hospital effluent water.

5.2 Materials and methods

5.2.1 Chemicals and experimental setup

Chloride and bicarbonate anions are added to the reaction solution using NaCl (Sigma Aldrich, > 99.5%) and NaHCO₃ (Chem-Lab, 99-100.5%). Humic acid sodium salt (HA), bovine serum albumin (BSA), alginic acid sodium salt, Suwannee River Fulvic Acid Standard I (FA) and Suwannee River natural organic matter (SRNOM) are provided by Sigma Aldrich and International Humic substances Society, USA.

Hospital effluent water has been sampled at the settling tank effluent side of the WWTP of the Maria Middelaes hospital (Ghent, Belgium). Grab samples were collected in amber glass bottles and stored in the dark at 4°C for maximum 48 h without acidification. The Maria Middelaes hospital uses a biologic WWTP consisting of two activated sludge reservoirs of 201 m³ with a total effluent flow of 250 m³ d⁻¹. Effluent characteristics and company specific discharge levels are presented in Table 5.1.

Table 5.1 Characteristics of the hospital Maria Middelaes WWTP effluent water (range and average from 12/2011-07/2013, n = 20) and discharge concentration regulations

Parameter	Unit	Range ^b	Average	Legislation ^c
pH	-	7.0-7.7	7.3	6.5 < x < 9.0
COD	mg L ⁻¹	14.0-48.0	30.4	120
SPM	mg L ⁻¹	0.8-31.2	7.8	60
Chloride	mg L ⁻¹	464-745	600	800
N _{tot}	mg L ⁻¹	5.9-29.9	14.0	15
(NO ₂ + NO ₃) - N	mg L ⁻¹	0.2-18.0	5.4	n.a. ^d
P _{total}	mg L ⁻¹	0.7-5.0	2.0	2
AOX	mg L ⁻¹	0.4-0.7	0.6	1

^a n = number of measurements; ^b determined by Eco Process Assistance (EPAS, Nazareth, Belgium); ^c discharge levels imposed by the Belgian authorities; ^d not available; COD: chemical oxygen demand; AOX: adsorbable organohalogens

Each photocatalytic degradation experiment consisted of two phases: (i) dark adsorption of MOX and/or matrix constituents on the catalyst surface, and (ii) photocatalytic degradation after switching on the UV light. The amount of MOX adsorption is expressed by an adsorption coefficient K_d (L kg⁻¹) by measuring the liquid phase MOX concentration initially added in the reaction solution and that after adsorption-desorption equilibrium. Experimental setup, methodology, and initial degradation rate, r_0 (μmol L⁻¹ min⁻¹), calculation are described in Part II. Reaction conditions applied during photocatalytic degradations are mentioned in Table 0.1.

Effluent water is not buffered due to the formation of precipitation, but is brought to pH 7.0 using NaOH or HCl after spiking with MOX. In the case of filtered effluent water, spiking is performed after filtration. After catalyst addition solutions are stirred under complete darkness for 30 min during experiments in demineralized water; for four hours when demineralized water spiked with in/organic constituents is used; and for eight hours in the experiments performed

with (un)filtered hospital effluent, to attain adsorption-desorption equilibrium.

Extra pH adjustments to pH 7.0 are performed in the hospital effluent during sampling.

Preliminary photolytic MOX experiments in both demineralized and effluent water showed no significant ($p > 0.05$) degradation in the time interval (0-14 min) during which photocatalytic degradation is performed in this study.

5.2.2 Analytical methods

MOX is analyzed using the HPLC-PDA procedure described in Part II. A blank run of the hospital effluent is performed and no absorption is noticed at the quantification wavelength of MOX.

A Shimadzu VCPN TOC analyzer (Japan) is used to determine the TOC and IC of the hospital effluent samples, and DOM stock solutions. The amount of organic matter adsorption on TiO_2 , in the absence of MOX, is determined by analyzing the TOC of the reaction solution before catalyst addition and after adsorption-desorption equilibrium on the catalyst surface ($t = 30$ min). TOC values of demineralized water and demineralized water with catalyst are taken into account as background TOC values.

The concentration of SPM in hospital effluent samples is determined by weighing a $0.2 \mu\text{m}$ filter (Merck Millipore, Germany) on a micro-scale balance, which has been pre-rinsed with demineralized water and oven dried, before and after filtering 500 mL effluent water.

5.2.3 Experimental approach

The different setups used during the heterogeneous photocatalysis experiments of MOX and the corresponding 'results and discussion' sections are shown in Fig. 5.1.

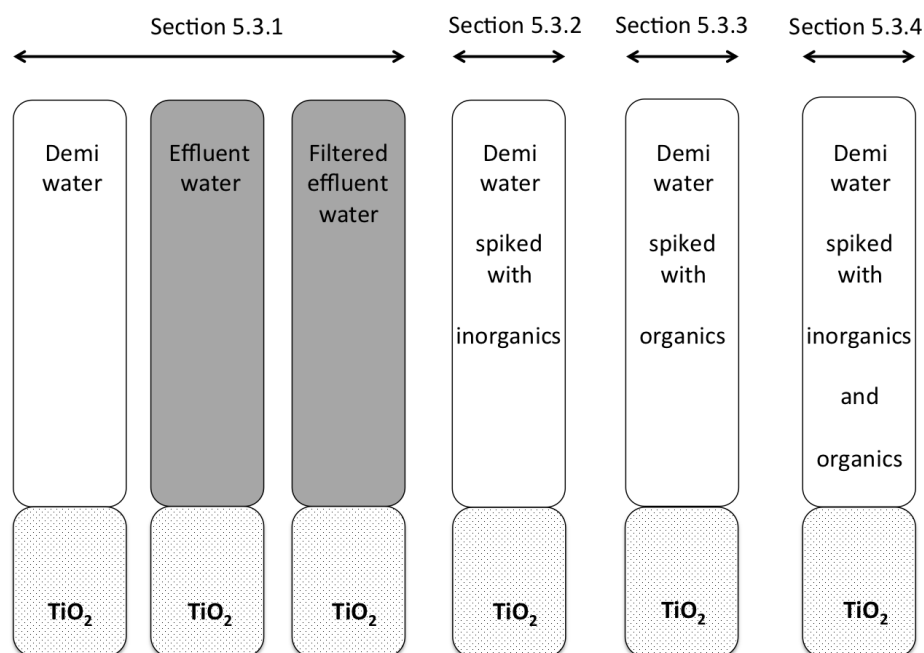


Fig. 5.1 Experimental strategy applied to investigate the effect of hospital effluent constituents.

Eight different hospital effluent waters, sampled at four different days in the period December 2012-August 2013 (Table 5.2), have been used to compare MOX photocatalysis in (un)filtered hospital and demineralized water (Section 5.3.1).

Table 5.2 Effluent characteristics TOC, IC, and SPM for different unfiltered and filtered effluent samples from the Maria Middelaers hospital WWTP

	Effluent water Maria Middelaers ^d								
	Unit	Effluent 1	Effluent 2	Effluent 3	Effluent 4a ^c	Effluent 4b ^c	Effluent 4c ^c	Effluent 4d ^c	Effluent 4e ^c
Sample date	-	10/12/2012	24/06/2013	06/08/2013	13/08/2013	13/08/2013	13/08/2013	13/08/2013	13/08/2013
TOC (TOC filtered) ^b	mg C L ⁻¹	14.5	6.4 (6.1)	4.0 (3.9)	7.5 (6.3)	12.6 (5.9)	6.8 (6.2)	7.4 (5.5)	6.6 (6.0)
IC (IC filtered) ^b	mg C L ⁻¹	55.1	34.2 (33.2)	36.5 (36.1)	28.8 (28.9)	28.3 (28.5)	27.0 (26.9)	26.6 (26.3)	26.9 (26.0)
SPM	mg L ⁻¹	n.d. ^a	1.8	1.3	5.0	15.6	3.0	6.8	3.4

^a not determined; ^b filtered over a 0.2 µm filter; ^c samples taken at 9:00 (4a), 11:00 (4b), 13:00 (4c), 15:00 (4d), and 16:30 (4e); ^d effluent characterization is performed the day of sampling

Inorganics (Section 5.3.2) used in this study are chloride anions and IC. Chloride concentrations ranging up to hundreds of milligrams per liter are frequently detected in hospital effluents around the world, and the effluent water of the Maria Middelaes hospital is no exception (Table 5.1) (Emmanuel et al., 2004; Verlicchi et al., 2010). Therefore, chloride anions are added in demineralized water to a concentration of 200-800 mg Cl⁻ L⁻¹. The upper limit of 800 mg Cl⁻ L⁻¹ is specifically chosen since it is the maximum effluent concentration regulated for the Maria Middelaes hospital imposed by the Belgian authorities (Table 5.1). IC is mainly present in effluent water as bicarbonate and is added to the reaction solution using sodium bicarbonate at a IC concentrations of 25-250 mg C L⁻¹ (Van Den Hende et al., 2011).

The effect of dissolved organic compounds is studied in two phases (Section 5.3.3). A first part consists of dosing HA to a TOC concentration ranging from 3.6 to 40.0 mg C L⁻¹. Taking in mind a constant COD TOC⁻¹ ratio of 3 for most effluent waters (Emmanuel et al., 2004), the upper TOC value approximates the imposed discharge limit of the hospital WWTP (Table 5.1). In a second part, the effect of different types of organic constituents is studied. Effluent water has a complex composition of organic material and contains different organic fractions like biopolymers, fulvic and humic substances, among others (Huber et al., 2011). Model organic compounds HA, BSA, alginate, FA and SRNOM are used and are dosed to the same TOC concentration as measured in effluent 1 (Table 5.2). The combined effect of inorganics and organics (Section 5.3.4) is investigated by dosing 600 mg L⁻¹ Cl⁻, 25 mg C L⁻¹ IC and 7.3 mg C L⁻¹ HA to the reaction solution.

5.3 Results and Discussion

5.3.1 Photocatalytic degradation of MOX in (un)filtered hospital effluent water

The initial photocatalytic degradation rate of MOX, r_0 ($\mu\text{mol L}^{-1} \text{min}^{-1}$), in the different unfiltered (NF) and filtered (F) hospital effluent water samples is compared to that in demineralized water in Fig. 5.2.

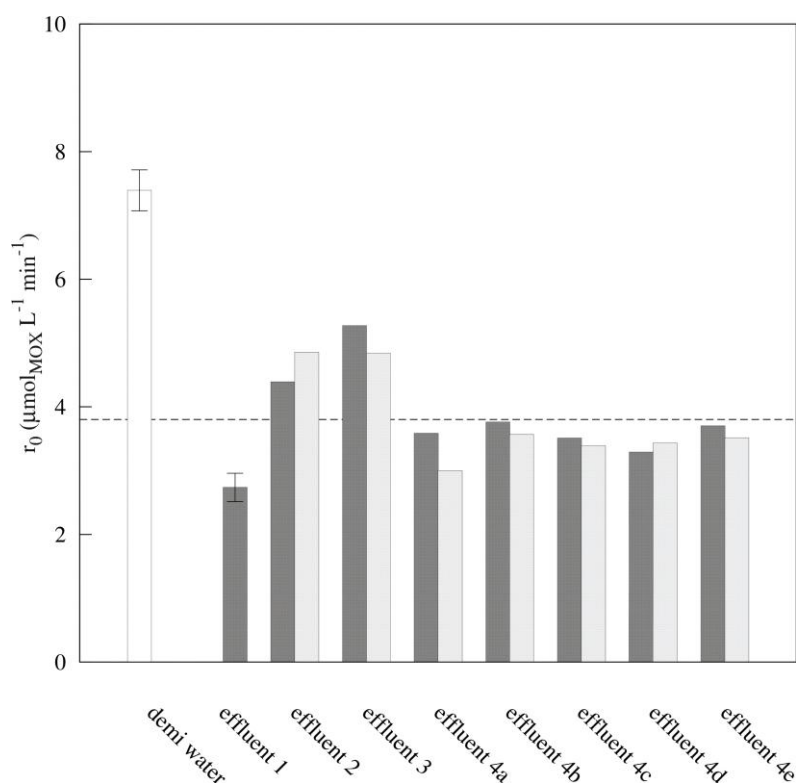


Fig. 5.2 Initial photocatalytic degradation rate of MOX, r_0 ($\mu\text{mol L}^{-1} \text{min}^{-1}$), in demineralized water (white, $n = 3$), unfiltered (dark grey, $n = 1$; except for effluent 1 where $n = 3$) and filtered (light grey, $n = 1$) effluent waters. Dashed line is the average initial degradation rate of MOX in the unfiltered effluents ($r_0 = 3.8 \mu\text{mol L}^{-1} \text{min}^{-1}$; $n = 8$).

Three points of attention need to be addressed. First, it can be observed that the initial photocatalytic degradation rate of MOX in (un)filtered effluent ($r_{0,\text{eff}}$: 2.7-5.3 $\mu\text{mol L}^{-1} \text{min}^{-1}$) is on the average a factor of 2 lower compared to that in demineralized water ($r_{0,\text{demi}}$: $7.4 \pm 0.3 \mu\text{mol L}^{-1} \text{min}^{-1}$). Second, a variation of up to a factor of about 2 is noticed among the effluent waters, although this is less pronounced when samples of the same day are compared (4a-4e). The highest inhibition in r_0 (compared to $r_{0,\text{demi}}$) is measured in effluent 1, which has also the highest load of both TOC and IC of all effluent samples (Table 5.2). Third, no statistical difference ($p = 0.365$, $n = 7$) could be observed between unfiltered and filtered effluent water, indicating that SPM has a negligible effect on the photocatalytic degradation process.

In order to understand the difference between demineralized and effluent water, MOX adsorption experiments on TiO_2 are performed in both matrices. The adsorption coefficient of MOX in demineralized water, $K_{\text{d,demi}}$: $184 \pm 3 \text{ L kg}^{-1}$, is higher compared to that in unfiltered and filtered effluent water, $K_{\text{d,NF eff}}$: 70-167 L kg^{-1} and $K_{\text{d,F eff}}$: 42-100 L kg^{-1} , respectively, which may support the slower photocatalytic degradation in effluent water. On the other hand, an average decrease in adsorption by a factor of 1.4 occurs when effluent water is filtered, showing that SPM increases MOX adsorption although no significant difference in r_0 is noticed (Fig. 5.2). This indicates that effects on the adsorption-desorption equilibrium are not solely responsible for the degradation rate inhibition in effluent waters.

5.3.2 Effect of inorganic constituents

The effects of chloride anions and IC on the adsorption-desorption coefficient and initial photocatalytic degradation rate of MOX are presented in Fig. 5.3a and Fig. 5.3b, respectively.

An inhibition of the degradation rate by a factor of 1.1 is observed in the presence of 200 mg Cl⁻ L⁻¹ and no additional decrease occurs at higher chloride concentrations. Chloride anions clearly interfere in the MOX adsorption, with a decrease in K_d values by a factor of 2.3 to 6.8 at 200-800 mg Cl⁻ L⁻¹. This effect on adsorption is even more pronounced than that observed in effluent water, having a similar Cl⁻ content (Table 5.1), although the initial MOX degradation rate is more than 2 times lower in the effluent matrix compared to that in chloride enriched demineralized water.

A similar trend can be observed for IC. Although bicarbonate at high concentrations (250 mg C L⁻¹) causes a clear drop (3.1 times) in the MOX adsorption-desorption coefficient, the initial degradation rate is only affected by a factor of 1.2. Moreover, effluent 1, which has an IC content of 55 mg C L⁻¹ (Table 5.2), inhibits the degradation rate 3.6 times more compared to the demineralized water enriched with an equal amount of IC, 50 mg C L⁻¹.

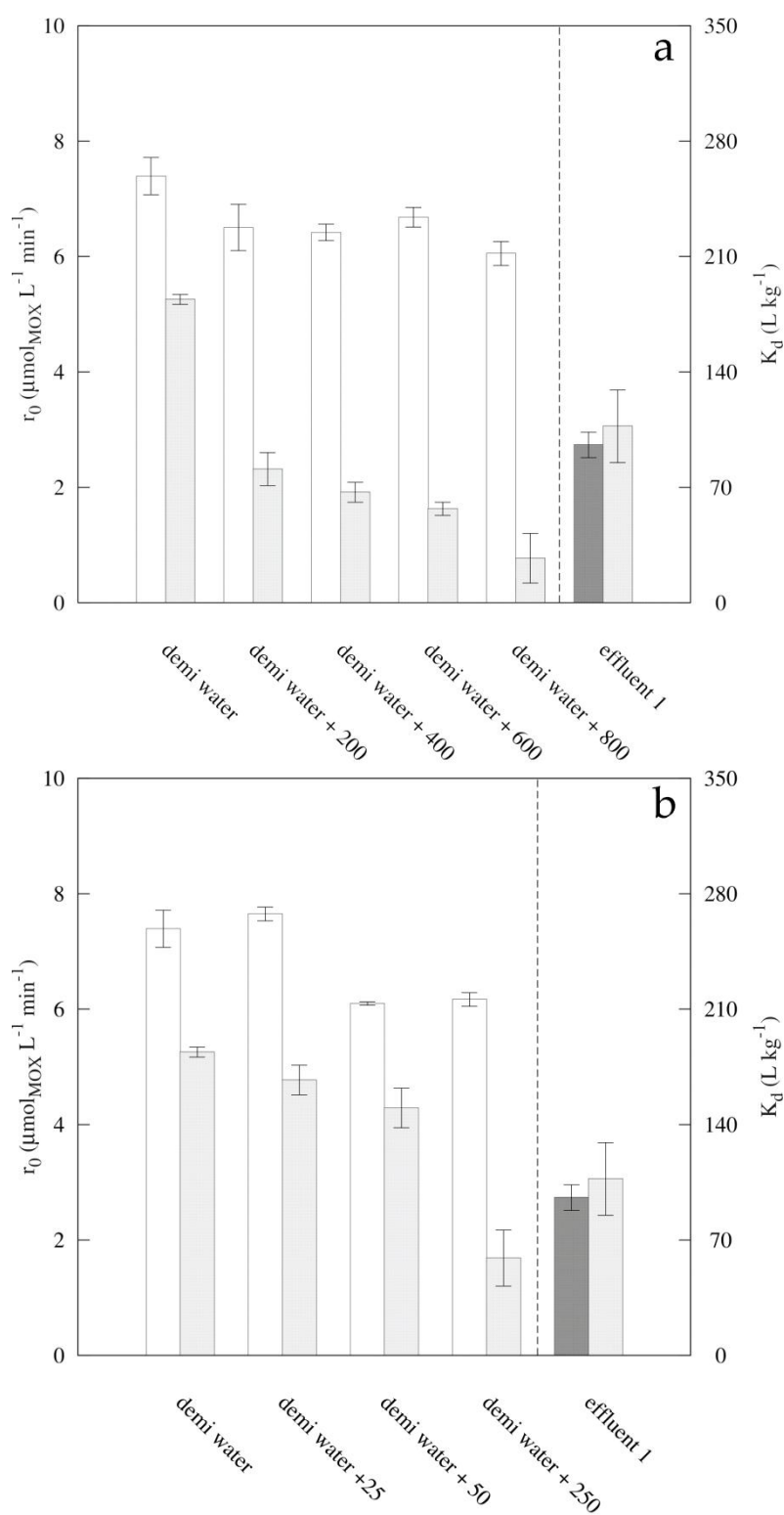


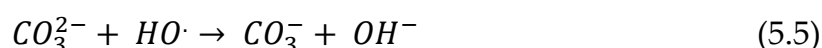
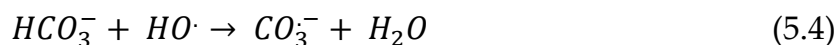
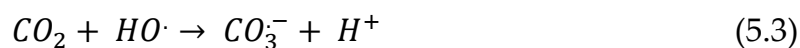
Fig. 5.3 Initial photocatalytic degradation rate of MOX, r_0 ($\mu\text{mol} \text{min}^{-1} \text{L}^{-1}$), in demineralized water enriched with a (a) chloride anion concentration between 0 and 800 $\text{mg} \text{Cl}^- \text{L}^{-1}$ and (b) IC concentration between 0 and 250 $\text{mg} \text{C} \text{L}^{-1}$ (white, $n = 3$), and in effluent 1 (dark grey, $n = 3$). Light grey bars represent the MOX adsorption coefficients, K_d ($\text{L} \text{kg}^{-1}$) ($n = 3$).

In literature, there are two main hypotheses concerning the effect of chloride anions and IC on a photocatalytic process. It is suggested that both species compete with organic compounds for the same adsorption sites on the catalyst surface, decreasing the amount of adsorbed pollutant (Chen et al., 1997). Also, Guillard et al. (2005) explain that the inhibitory effect of chloride on the photocatalytic degradation of methylene blue is due to the formation of an inorganic layer on the catalyst surface, which interferes with the adsorption of organic pollutants. Yang et al. (2005) suggest that, apart from adsorption effects, also catalyst deactivation is possible by the presence of chloride anions through the formation of TiCl complexes. However, Kormann et al. (1991) report that this is only significant at low pH. Although catalyst deactivation is not investigated as such in this work, its effect cannot be excluded because of the high chloride concentrations that are used during the photocatalytic experiments.

Second, it is suggested that chloride anions can scavenge reactive species although there is yet no consensus regarding this aspect. According to Buxton et al. (1988) and Rauf and Ashraf (2009), chloride ions can scavenge hydroxyl radicals with a high rate constant, i.e. $4.3 \cdot 10^9 \text{ L mol}^{-1} \text{ s}^{-1}$, and scavenging reactions can occur on the catalyst surface as well as in the reaction solution according to Eqs. 5.1-5.2:



On the other hand, Herrmann and Pichat (1980) noticed that Cl^- is inert in a photocatalytic treatment process and that no scavenging occurs. Scavenging reactions between active species and IC are reported in (Buxton et al., 1988; Guillard et al., 2005) according to Eqs. 5.3-5.5:



Our results indicate that adsorption inhibition of MOX by chloride and bicarbonate anions is significant and cannot be neglected. Based on the results obtained in Part II, investigating the effect of pH on both adsorption and degradation, it could be expected that less MOX adsorption should result in slower degradation rates. The observed effects of chloride and IC on r_0 are, however, rather small certainly when compared to the drop in r_0 when MOX is degraded in hospital effluent. This indicates that (i) scavenging by Cl^- and IC has no direct negative effect on the photocatalytic degradation rate; and (ii) apart from the studied inorganic matrix compounds and adsorption process, also other constituents and processes may play a crucial role in heterogeneous photocatalysis in effluent water.

5.3.3 Effect of organic constituents

5.3.3.1 Effect of humic acid

Humic substances belong to the most significant components of organic matter in natural water and effluents. Therefore, the effect of HA at TOC concentrations between 3.6 and 40.0 mg C L⁻¹ on the adsorption-desorption coefficient and initial

photocatalytic degradation rate of MOX is investigated, and results are shown in Fig. 5.4.

The addition of HA into demineralized water clearly has a two-fold effect on the photocatalytic process. First, an increasing HA concentration causes an inhibitory effect on the initial MOX photocatalytic degradation rate. This effect becomes statistical significant ($p < 0.05$) at TOC concentrations greater than 3.6 mg C L⁻¹ and a maximum decrease by a factor 2.8 is observed at 40.0 mg C L⁻¹. In the latter case, the drop in r_0 is similar as noticed in effluent 1, even though the TOC content in effluent 1 is 3 times lower.

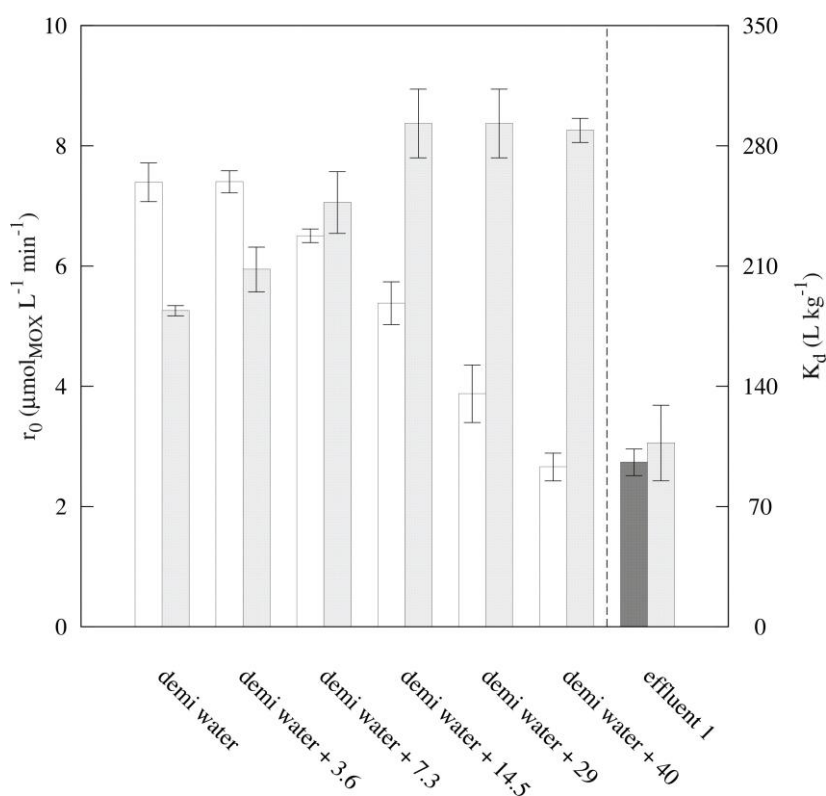


Fig. 5.4 Initial photocatalytic degradation rate of MOX, r_0 ($\mu\text{mol L}^{-1} \text{min}^{-1}$) in demineralized water, enriched with HA at TOC concentrations between 0 and 40.0 mg C L⁻¹ (white, $n = 3$), and in effluent water 1 (dark grey, $n = 3$). Light grey bars represent the MOX adsorption coefficients, K_d (L kg^{-1})($n = 3$).

Second, the adsorption-desorption coefficient of MOX increases with a rising HA concentration, ranging from 184 L kg⁻¹ in demineralized water without HA up to 293 L kg⁻¹ at 14.5-40.0 mg C L⁻¹. In Fig. 5.5, the amount of TOC adsorbed on TiO₂ in the absence of MOX is plotted at different equilibrium TOC concentrations for HA in demineralized water.

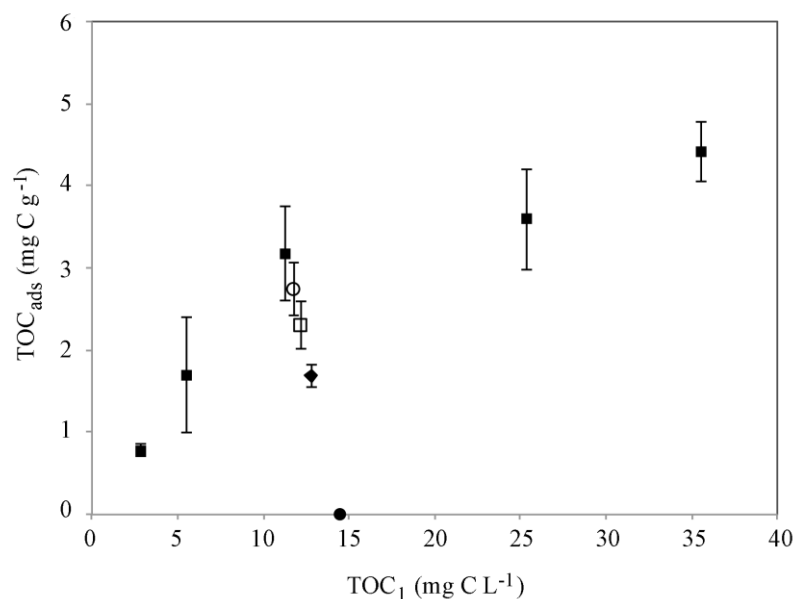


Fig. 5.5 Adsorption data of HA (■), FA (◇), BSA (○), SRNOM (◆) and alginate (●) on TiO₂. TOC_{ads} (mg C g⁻¹) is the TOC of the organic matter adsorbed per gram of catalyst; TOC₁ (mg C L⁻¹) is the TOC of the organic matter in solution (demineralized water) at equilibrium (n = 3)

At lower HA concentrations (≤ 14.5 mg C L⁻¹), being the range in which $K_{d,MOX}$ increases at increasing HA concentration (Fig. 5.4), an increase in HA adsorption is noticed (Fig. 5.5). At higher HA concentrations, no significant differences ($p > 0.05$) are measured for both $K_{d,MOX}$ (Fig. 5.4) and adsorbed HA (Fig. 5.5). This strongly indicates that HA adsorption on TiO₂ favors the removal of MOX from the liquid phase through sorption processes. This might be surprising since a decrease in MOX adsorption due to competition of HA and MOX for the same adsorption sites could be expected.

Rav-Acha and Rebhun (1992) investigated the adsorption of organic solutes on mineral surfaces in aqueous medium in the presence of humic substances, and they report the occurrence of the following interactions: (i) adsorption of the organic solute on the mineral surface; (ii) adsorption of the organic solute on solid mineral-humic complexes (i.e. mineral surface covered by humic substances); (iii) binding of the organic solute to dissolved humic substances to form aqueous solute-humate complexes; (iv) adsorption of solute-humate complexes on the mineral surface; (v) desorption of organic solutes due to solubilization effects by dissolved humic substances and/or competition for sorbent sites. To explain the observed increase in MOX adsorption in the presence of HA (Fig. 5.4), a partitioning scheme based on the interactions reported by Rav-Acha and Rebhun (1992) is proposed in Fig. 5.6.

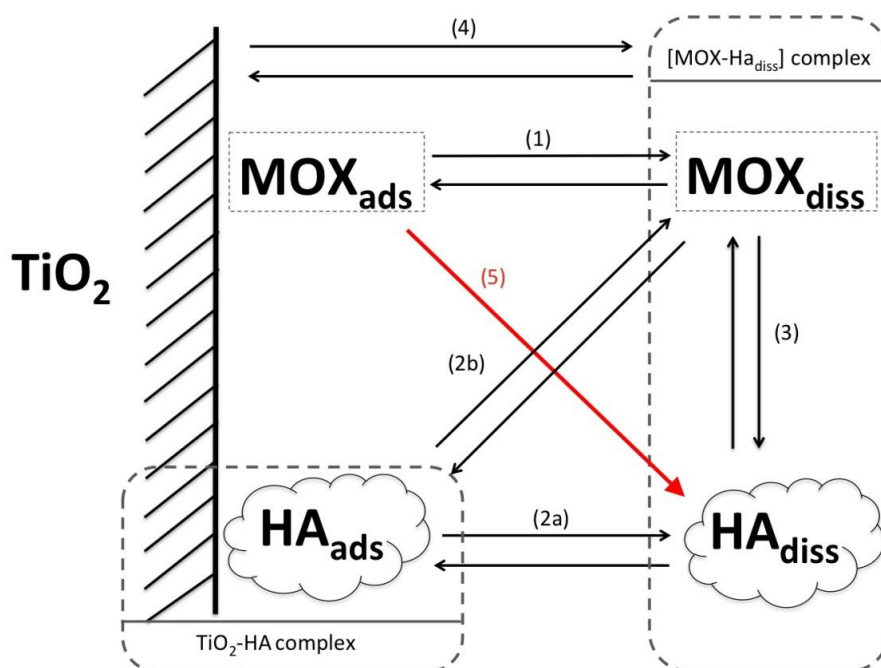


Fig. 5.6 Partitioning scheme of MOX and HA in an aqueous system containing a TiO_2 catalyst, with (1) MOX adsorption-desorption equilibrium; (2a) HA adsorption-desorption equilibrium; (2b) partitioning of MOX between the liquid phase and the TiO_2 -HA complex; (3) interaction between dissolved HA and MOX in the liquid phase; (4) adsorption of $[\text{MOX-HA}_{\text{diss}}]$ complex on the TiO_2 surface; (5) desorption of MOX due to solubilization effects by dissolved HA (based on Rav-Acha and Rebhun (1992)).

It is clear that MOX can adsorb directly on the catalyst surface (equilibrium 1 in Fig. 5.6). Although this can occur through different types of interactions, pH dependent charge-charge interactions are calculated to be the determining factor (Part II). Fig. 5.5 shows that also HA adsorbs on the catalyst surface (equilibrium 2a in Fig. 5.6), hereby forming a TiO_2 -HA solid complex. Although this could lead to competitive sorption effects, it is also possible that dissolved MOX sorbs onto this TiO_2 -HA complex (equilibrium 2b). Next, according to Ravacha and Rebhun (1992) and Carmosini and Lee (2009), dissolved MOX and HA may interact with each other (equilibrium 3), resulting into the formation of a $[\text{MOX-HA}]_{\text{diss}}$ complex that might adsorb on the catalyst surface (equilibrium 4). Finally, possible desorption of MOX from the TiO_2 surface by solubilization in dissolved HA should be taken into consideration (Fig. 5.6: process 5) (Ravacha and Rebhun, 1992).

Overall, results in Fig. 5.4 clearly indicate that in the investigated TiO_2 -MOX-HA system, competitive adsorption and solubilization processes are not the main interactions but are dominated by increased adsorption of dissolved MOX on TiO_2 -HA complexes and/or the sorption of aqueous MOX-HA complexes on the TiO_2 surface. Since this increased adsorption cannot explain the decrease in initial MOX degradation rate during photocatalysis at increasing HA concentration, it is clear that also other effects play a crucial role. Plausible explanations are (i) inhibition through decreased accessibility of MOX for reactive species or their scavenging by HA (Wiszniewski et al., 2002), and/or (ii) absorption of a fraction of the UV light by the chromophore groups of HA making it less available for the catalyst (Wiszniewski et al., 2002; Ahmed et al., 2011).

5.3.3.2 Effect of different types of DOM

Apart from the amount of organic matter present in the aqueous matrix, also its nature might be an important parameter affecting photocatalytic processes in DOM loaded matrices. Fig. 5.7 therefore presents the effect of HA, FA, BSA, alginate and SRNOM on the adsorption-desorption coefficient and initial photocatalytic degradation rate of MOX. The different types of organic matter have been dosed at a constant TOC loading of 14.5 mg C L^{-1} , being the same as that measured in effluent 1.

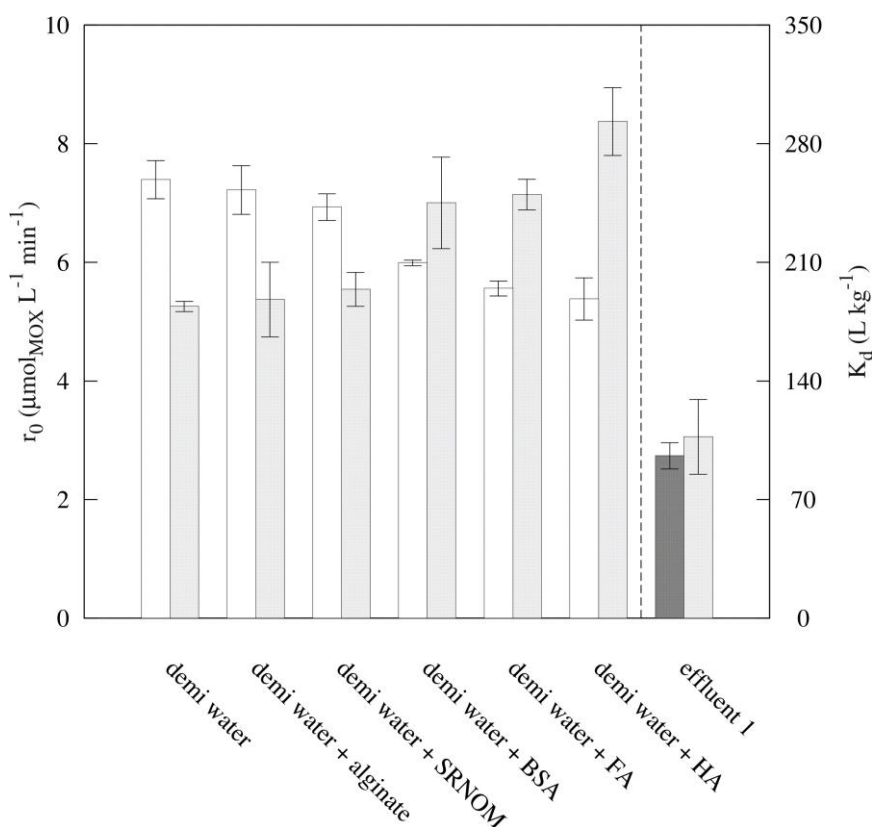


Fig. 5.7 Initial photocatalytic degradation rate of MOX, r_0 ($\mu\text{mol min}^{-1} \text{ L}^{-1}$) in demineralized water spiked with different types of organic matter (white, $n = 3$) at a constant TOC level of 14.5 mg C L^{-1} , and in effluent 1 (dark grey, $n = 3$). The light grey bars represent the MOX adsorption coefficients, K_d (L kg^{-1}) ($n = 3$).

It is clear that, at this constant TOC level, none of the different organic model substances affect the photocatalytic process to the same extent as effluent 1. For alginate and SRNOM, even no significant impact on both the adsorption and

initial photocatalytic degradation rate of MOX is noticed, compared to that in demineralized water. Addition of BSA, FA and HA causes a decrease in r_0 values by a factor 1.2 to 1.4, respectively, whereas the adsorption-desorption coefficient increased 1.3 to 1.6 times. Comparing the results obtained in effluent 1 with that in HA-enriched demineralized water, it can be seen that the adsorption-desorption coefficient and initial degradation rate in effluent are a factor of respectively 3 and 2 lower.

Similar as was noticed in Fig. 5.4, the most pronounced drop in degradation rate in DOM-loaded demineralized water occurs when the increase in adsorption is the highest. Fig. 5.7 and Fig. 5.5 also show that the highest increase in MOX adsorption is observed for those OM compounds that have the highest affinity for the TiO_2 surface, i.e. HA, FA and BSA. This supports the explanation that MOX adsorption is favored by the formation of TiO_2 -OM complexes (equilibria 2a and 2b in Fig. 5.6), but that at the same time the OM scavenges the formed reactive species and/or part of the UV light leading to slower MOX degradation.

5.3.4 Combined effect of inorganic and organic constituents

In order to compare the effect of all investigated matrix constituents on both the adsorption-desorption equilibrium and initial photocatalytic degradation rate with each other, Fig. 5.8 plots the K_d and r_0 values obtained in each experimental setup ($K_{d,i}$ and $r_{0,i}$) versus those in demineralized water ($K_{d,demi}$ and $r_{0,demi}$).

The data related to inorganic and organic enriched demineralized water and those related to the real effluent samples are given a color code, respectively red, blue and green.

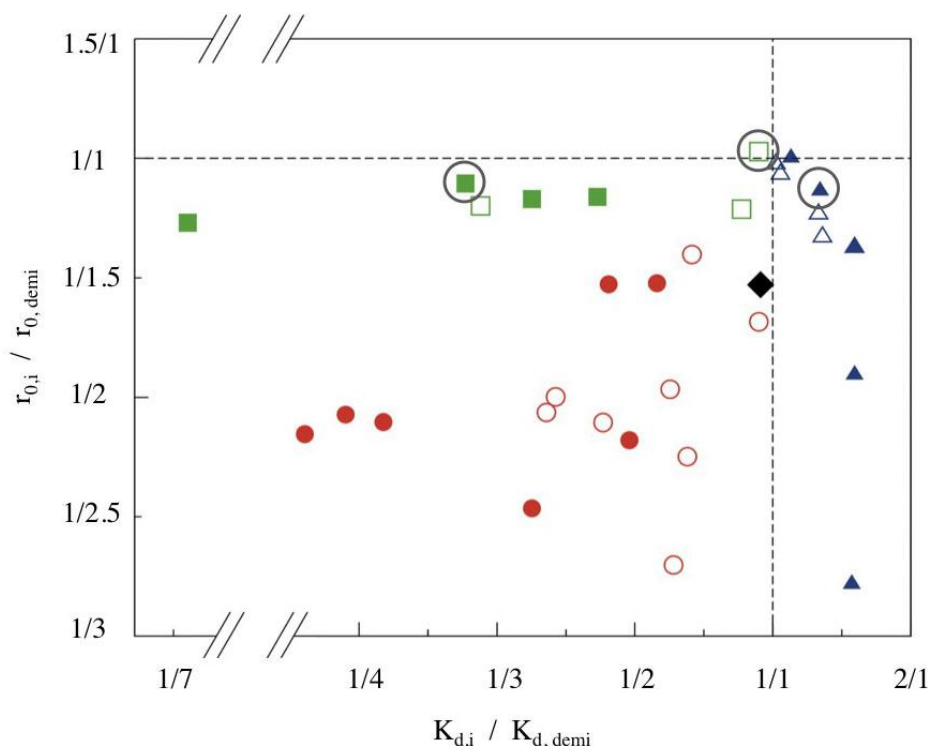


Fig. 5.8 Ratio between both the K_d and r_0 values obtained in demineralized water as a reference on the one hand, and that obtained in unfiltered effluent (\circ), filtered effluent (\bullet), and demineralized water spiked with Cl^- (\blacksquare), IC (\square), HA (\blacktriangle), different DOM (\triangle) and $\text{Cl}^- + \text{HA} + \text{IC}$ (\blacklozenge) on the other hand. Standard deviations are smaller than 10% and are not plotted for a better overview.

In all experimental setups, a slower photocatalytic degradation has been observed compared to that in demineralized water, apart from some exceptions where no significant difference is noticed. This inhibitory effect on r_0 (up to a factor of 2.8 difference with $r_{0,demi}$) is the most pronounced for the real hospital effluent water (red) and for demineralized water enriched with the highest concentrations of organic constituents (blue), whereas the effect for inorganics (green) is in all cases lower than a factor of 1.2. In terms of adsorption, there is clear differentiation between (i) the effluents and inorganic-enriched demineralized waters, both showing a suppressing effect on the MOX adsorption; and (ii) the demineralized water enriched with organics, increasing the K_d values.

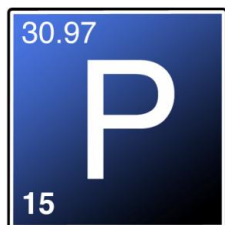
The average chloride, IC and TOC content in the sampled hospital effluents amount 600 mg Cl⁻ L⁻¹ (Table 5.1), 33 mg C L⁻¹ IC and 8.2 mg C L⁻¹ TOC (Table 5.2), respectively. The data points of enriched demineralized water that correspond the best to these conditions are encircled in Fig. 5.8, showing that individual inorganic or organic matrix constituents added at these concentration levels inhibit the degradation rate only to a limited extent (< factor of 1.1), which indicates that a combined effect takes place in real effluent.

Heterogeneous photocatalysis of MOX in demineralized water spiked with a mixture of 600 mg Cl⁻ L⁻¹, 25 mg C L⁻¹ IC and 7.3 mg C L⁻¹ HA - being similar to real concentrations in hospital effluent (encircled in Fig. 5.8) - is performed in triplicate (Fig. 5.8, diamond). The obtained initial photocatalytic degradation rate of MOX ($r_{0,combined} = 4.8 \pm 0.2 \mu\text{mol L}^{-1} \text{min}^{-1}$) is a factor of 1.5 lower than that obtained in demineralized water, and a factor of 1.3 higher than the average r_0 obtained in (un)filtered effluent. This means that 70% of the inhibitory effect that hospital effluent causes on the initial MOX degradation rate can be explained by the selected matrix constituents, showing their high relevance for photocatalytic treatment in real water matrices. The average drop in K_d value in the effluent is much more pronounced than that in the mixture-enriched demineralized water where the added inorganic and organic constituents most probably counteract each other. Therefore, apart from the fact that the investigated matrix compounds are shown to be of major importance in heterogeneous photocatalytic processes, it cannot be excluded that also other matrix constituents play an additional role deserving further research.

5.4 Conclusions

Through a systematic research approach, new insights have been gained in the effect that SPM and selected inorganic and organic matrix constituents have on heterogeneous photocatalysis of MOX in hospital effluent water. It proves that MOX degradation is about 2 times slower in a hospital effluent matrix than in demineralized water. Comparing photocatalytic MOX degradation in both filtered and unfiltered effluent water shows no significant inhibitory effect of SPM on the degradation rate. In contrast, both inorganics like chloride anions and bicarbonates, and organic matrix constituents like HA, FA and BSA all cause a drop in degradation rate, although this inhibitory effect is the most pronounced (up to a factor of 2.8 at a TOC of 40 mg C L⁻¹) in the presence of organic matrix compounds. This cannot solely be explained by adsorption effects since the addition of inorganic compounds results into a MOX adsorption-desorption equilibrium coefficient being up to 6.8 times lower than in demineralized water; whereas organic matrix constituents like HA favor MOX adsorption (up to factor of 1.6), most probably due the formation of HA-TiO₂ complexes. This indicates the importance of also other processes on photocatalytic MOX degradation, like scavenging of or reduced accessibility to reactive species and/or UV light shielding in DOM loaded waters.

Overall, the combined effect of a realistic mixture of the selected matrix constituents explains about 70% of the average inhibition that a real hospital effluent water matrix causes on the MOX photocatalytic degradation rate, showing their high relevance for photocatalytic treatment in real practice applications.



Part VI

General Discussion and Perspectives

6.1 Scientific overview, Progress & Discussion

In 2008, when starting this study, only very few data concerning heterogeneous photocatalysis of FQ compounds in water were available. At that time, the focus was mainly on the degradation of second generation FQs in demineralized water with a moderate interest for the effect of operational variables (Haque and Muneer, 2007; Paul et al., 2007; Calza et al., 2008). Since the start of this work, it is observed that the focus of recent literature shifted towards identification of DPs and toxicity determination of photocatalytic reaction solutions (Table 6.1).

This work contributes to the knowledge on heterogeneous photocatalysis for FQ degradation through different ways. First, by selecting a latest generation target FQ compound, MOX, for which no photocatalytic data were available. Second, by going beyond the available knowledge on FQ photocatalysis observed in literature, using different research approaches. Attention has been paid on the FQ adsorption mechanism, operational variables, and degradation mechanism (**Part II**), DP identification (**Part III**), toxicity determination using bacteria and green algae (**Part IV**), and application in real effluent matrices (**Part V**).

In the following paragraphs, the main results on each of the aforementioned items are discussed in the context of recent literature.

Table 6.1 Progress of research focusing on the heterogeneous photocatalytic degradation of FQ compounds

Matrix	Catalyst	FQ compound	Research focus	References
Double distilled water	P25	NOR	Parameter study: pH, C_{cat}^b , C_{FQ}^c	Haque and Muneer (2007)
Demineralized water	Hombikat UV100, P25	CIP, ENRO, FLU, NOR	Adsorption Parameter study: pH, C_{oxygen}^d Scavenger study Degradation products	Paul et al. (2007)
HPLC-grade water	P25	OFL, CIP	Degradation products Toxicity: <i>Vibrio fischeri</i>	Calza et al. (2008)
Demineralized water	P25	FLU	Degradation products Toxicity: <i>Escherichia coli</i> Scavenger study	Palominos et al. (2008)
Distilled water	P25	FLU	Degradation products Toxicity: <i>Vibrio fischeri</i>	Sirtori et al. (2009)
Hospital effluent water	P25	CIP	Degradation profile	Vasconcelos et al. (2009b)
Milli-Q-water	P25	NOR, LEVO, LOME	Degradation products	An et al. (2010a)
Milli-Q-water	P25	CIP	Parameter study: pH, C_{cat} Degradation products	An et al. (2010b)

Ultrapure water			Parameter study: pH, C_{cat} , C_{FQ}	
Groundwater	P25	OFL	Toxicity: <i>Daphnia magna</i>	Hapeshi et al. (2010)
Secondary effluent water			Matrix effects	
Secondary effluent water	P25	OFL	Parameter study: pH, C_{cat} , C_{FQ} Toxicity: <i>Daphnia magna</i>	Michael et al. (2010)
Demineralized water	Hombikat UV100	CIP	Degradation profile Degradation products Toxicity: <i>Escherichia coli</i>	Paul et al. (2010)
n.d. ^a	P25	CIP	Degradation profile	Gad-Allah et al. (2011)
Demineralized water	P25	CIP, MOX	Parameter study: UV-A/C, pH Adsorption	Van Doorslaer et al. (2011)
Demineralized water	P25	OFL, NOR, CIP, ENRO	Parameter study: pH, C_{cat} , C_{FQ} Toxicity: <i>Bacillus subtilis</i>	Li et al. (2012c)
Reversed osmosis water	P25	LEVO	Degradation profile Toxicity: <i>Escherichia coli</i> <i>Pseudomonas fluorescens</i>	Nasuhoglu et al. (2012)
Demineralized water	Hombikat UV100	OFL	Adsorption	Paul et al. (2012)
Surface water	P25	CIP, DANO, ENRO, LEVO, MOX, MARBO	Degradation profile Degradation products	Sturini et al. (2012b)

Demineralized water	P25	MOX	Parameter study: C_{cat}, C_{FQ}, T^e, C_{oxygen} Scavenger study	Van Doorslaer et al. (2012)
Demineralized water	Anatase	OFL	Adsorption Degradation profile Degradation products	Van Wieren et al. (2012)
Demineralized water	P25	MOX	Degradation products Toxicity: <i>Escherichia coli</i> <i>Klebsiella pneumoniae</i> <i>Staphylococcus carnosus</i> <i>Streptococcus mutans</i>	Van Doorslaer et al. (2013)
Milli-Q-water	n.d.	OFL	Degradation products	Vasquez et al. (2013)
Hospital effluent water	P25	MOX	Matrix effects Adsorption	Van Doorslaer et al. (2014) ^f
Demineralized water	P25	MOX	Degradation products Toxicity: <i>Pseudokirchneriella subcapitata</i>	Van Doorslaer et al. (2014)

^a no data; ^b catalyst concentration; ^c initial FQ concentration; ^d oxygen concentration; ^e temperature; bold: contributions to scientific literature by this author; ^f submitted.

6.2 Photocatalytic mechanisms: adsorption and reactive species

6.2.1 Adsorption-desorption equilibrium

A first research goal was to obtain a deeper understanding of the **adsorption process** on a TiO_2 catalyst, since only Paul et al. (2007) briefly reported procentual concentration decrease of CIP after dark adsorption at different pH levels. However, no partition coefficients, or discussion on the relationship between the pH dependent adsorption and the amphoteric nature of FQs is presented.

Here, new insights on the FQ adsorption-desorption equilibrium are gained by performing adsorption experiments at different pH levels, with attention for the pH dependent FQ speciation and catalyst surface charges. Our results show that the reaction solution pH influences the amount of MOX and CIP adsorption, which is favored at neutral conditions due to the large amount of charge-charge interactions between both the catalyst surface charges and the FQ ion species. At acid and alkaline conditions, repulsive forces of the FQ compounds and the catalyst surface impede adsorption. In addition, partition coefficients for the different FQ species are calculated, which reveal that FQ cations ($\text{CIP}^+ K_d = 527 \text{ L kg}_{\text{cat}}^{-1}$; $\text{MOX}^+ K_d = 691 \text{ L kg}_{\text{cat}}^{-1}$) and zwitterions ($\text{CIP}^{\text{Z}/0} K_d = 68 \text{ L kg}_{\text{cat}}^{-1}$; $\text{MOX}^{\text{Z}/0} K_d = 69 \text{ L kg}_{\text{cat}}^{-1}$) mainly participate in the FQ adsorption process on the TiO_2 catalyst surface.

Van Wieren et al. (2012) observed during adsorption experiments of OFL on a TiO_2 catalyst that adsorption is stimulated at conditions where the substrate surface is positive and the drug is zwitterionic or cationic, confirming the results obtained in this study. However, a strong electrostatic (physisorption) or surface complexation (chemisorption) mechanism of OFL on TiO_2 is suggested due to the low (< 2%) extractability of the mother compound from the catalyst surface, which is not in compliance with our results where a weak and reversible physisorption is proposed due to the low adsorption enthalpy ($-16.8 \text{ kJ mol}^{-1}$) for MOX calculated in Part II (Parga et al., 2009; Berger and Bhowan, 2011). In addition, modeling the adsorption of OFL on TiO_2 in a more recent paper by Paul et al. (2012) showed that zwitterionic FQ adsorption involves the deprotonated carboxylate group and the adjacent carbonyl group ruling out the participation of the cation FQ species during FQ adsorption on a TiO_2 surface, which is in contrast with the results obtained in this work (Fig. 6.1).

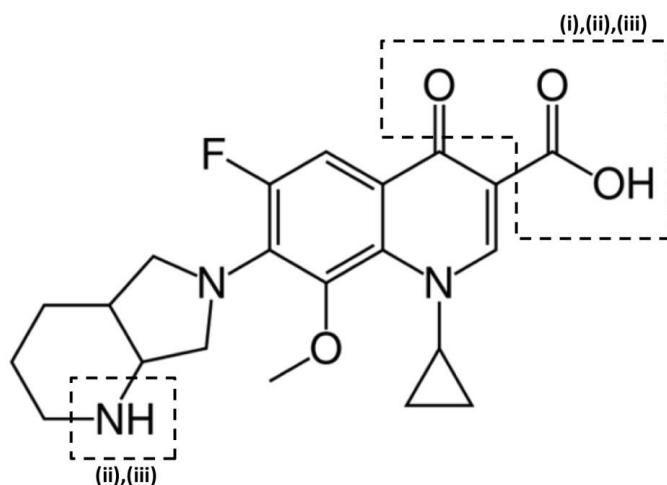


Fig. 6.1 Possible interaction sites of MOX with a TiO_2 catalyst surface, based on results from: (i) Paul et al. (2012), (ii) Van Wieren et al. (2012) and (iii) results obtained in this work.

Although the importance of zwitterionic species is not questioned, adsorption studies performed in this work show the highest adsorption at pH 5.0, where CIP and MOX are more than 95% present as cations, indicating that cations do

contribute to the adsorption on TiO₂. Even though there is no consensus regarding the interaction sites of FQs, it can be concluded that both zwitter and cations are important for the adsorption of FQ compounds on a TiO₂ catalyst.

6.2.2 Reactive species

In a next step, the contribution of different **reactive species** during a photocatalytic treatment are tentatively quantified using the **radical scavengers** ISO and KI at different concentrations (3.73-3740 μM). Photocatalytic degradation of MOX mainly occurs through direct surface mediated oxidation via photo-induced 'holes' (ca. 63%), and to a lesser extent via hydroxyl radicals in solution (ca. 24%). Paul et al. (2007) evaluated the contribution of hydroxyl radicals during photocatalytic degradation of CIP, using 1 M ethanol as hydroxyl radical scavenger, while Palominos et al. (2008) focused on 'holes' (KI), hydroxyl radicals (ISO) and superoxide anions (benzoquinone) during photocatalytic degradation of FLU. In accordance with this study, it is concluded that surface reactions are the dominant reaction mechanism for TiO₂ mediated FQ degradation, but no quantification of reactive species was performed.

Moreover, in this study it is observed that KI and ISO at concentrations of 3.74 mM and 37.4 mM influenced MOX adsorption. Both researchers did not perform an evaluation of the effect of these scavengers on the FQ adsorption and applied concentrations that are double (Palominos et al., 2008), or even 30 times higher (Paul et al., 2007) than the highest scavenger concentrations applied here. Spiking scavengers at these high concentrations could result in overestimated inhibitions due to a decreased adsorption, which is shown to be of major importance during FQ photocatalysis (Part II).

Main messages:

FQ compounds dominantly adsorb on a TiO₂ catalyst surface by reversible electrostatic interactions, with the highest affinity for cationic and zwitterionic FQ species.

Relative contributions of reactive species during the photocatalytic degradation of MOX are determined, indicating that photo-induced 'holes' are mainly responsible for FQ degradation.

6.3 Photocatalytic degradation of MOX: effect of process parameters

A second research goal was to evaluate the effect of different operational variables on the photocatalytic degradation of MOX. In literature, research mainly focused on a selected and rather limited group of variables such as pH, catalyst concentration and initial FQ concentration. Therefore, a more extended and systematic operational variables study has been performed. The effect of pH, UV-A/C irradiation, initial FQ concentration, catalyst concentration, stirring speed, temperature, and oxygen concentration in the gas flow sparged through the reaction solution is evaluated on both the adsorption-desorption equilibrium and photocatalytic degradation rate. The operational variable having the most noticeable effect on the photocatalytic degradation rate is the reaction solution pH, with optimum results obtained at neutral conditions. A decrease in half-life times from 8 and 10 min at pH 3.0 and 10.0, towards 3 min at pH 7.0 is observed for UV-A mediated MOX photocatalysis. Similar results are obtained for CIP, and are confirmed in Paul et al. (2007) and in a more recent research performed by An et al. (2010a). In addition, by linking the FQ adsorption with the

degradation data, it is concluded that the photocatalytic degradation rate is strongly determined by the pH dependent FQ adsorption on the TiO₂ catalyst surface. This once again indicates the importance of surface induced degradation reactions.

It is also observed that the aqueous MOX concentration after adsorption-desorption equilibrium has an effect on the initial MOX degradation rate r_0 . Moreover, after adsorption-desorption equilibrium different MOX concentrations are measured dependent on the catalyst concentration for the same initial MOX dosage. As a result, it is difficult to solely assess the impact of the catalyst concentration on the degradation rate. To overcome this problem, a new approach is proposed for calculating initial degradation rates by presenting the total amount of moles in the reaction solution. As such, the initial photocatalytic degradation rate is represented as r_0^* . The difference between r_0 and r_0^* is that the first is based on the amount of moles in the liquid phase, while the latter is calculated from the total amount of moles present in the reaction solution (both solid and liquid phase), hereby taking into account adsorption-desorption data from Section 6.2.1.

Main messages:

Different operational variables are studied for the TiO₂ P25 mediated photocatalytic degradation rate of MOX, with pH having the most pronounced effect. Optimal reaction conditions for photocatalytic MOX degradation are at neutral pH and ambient temperature under continuous air sparging.

A new approach is proposed for calculating initial degradation rates where instead of liquid concentrations, the total amount of moles present in the reaction solution is used.

6.4 Degradation products

Degradation product identification is one of the most investigated research topics in FQ photocatalysis (Table 6.1). Although pH dependent DP formation is clearly observed during ozonation of CIP (De Witte et al., 2008) no studies are found, which evaluate the effect of pH on DP formation for a photocatalytic treatment. Reaction solutions after photocatalytic degradation at pH 3.0, 7.0 and 10.0 are analyzed using HPLC coupled to HRMS, resulting in the detection of 13, 14 and 20 different MOX degradation products.

Identified DPs structures show that photocatalytic degradation of MOX occurred at the R₇ substituent, with no observed defluorination and ring opening of the quinolone basic structure. Eight structures are reported here for the first time. The relative occurrence of the different DPs as a function of degradation time show a shift from 'weakly' oxidized DPs at pH 3.0 and 10.0 towards more oxidized DPs at neutral conditions. Nonetheless, the same types of photocatalytic DPs are observed at all investigated pH levels. Based on all identified DPs, a pathway for the photocatalytic degradation of MOX is proposed.

In literature, so far, only one study reports the photocatalytic degradation of MOX in river water with the identification of DPs and pathway proposal (Sturini et al., 2012b). Almost half of the DPs identified reported in that study are defluorinated, which is not observed in our results. Moreover, several papers including this study report that the R₇ substituent is the main target for photocatalytic transformation (Paul et al., 2007; Paul et al., 2010; Sturini et al., 2012b), but ring cleavage of the FQ basic quinolone moiety of

CIP by heterogeneous photocatalysis is also noticed (Calza et al., 2008; An et al., 2010a). The previous shows that, although research on FQ photocatalytic DPs is ongoing, divergent structures are identified. This could be due to the application of different process parameters during degradation experiments and/or the use of other analytical techniques. Moreover, full identification of DPs is challenging since analytical standards for the proposed DP structures are lacking.

Main messages:

Photocatalytic degradation of MOX occurred at the R₇ substituent with no observed defluorination and ring opening of the quinolone base structure. Eight DPs structure proposals are reported for the first time.

Reaction solution pH affects the relative occurrence of the DPs in solution, which can be important for ecotoxicity purposes for the reason that some products may impose greater toxic effects than others.

6.5 Biological endpoints

Biological effects of a FQ containing photocatalytic reaction solution gained more interest since 2009, with increased efforts to determine residual antibacterial activity and *Daphnia magna* immobilization (Table 6.1).

It is observed in literature that agar diffusion tests are mainly performed using the test organism *E. coli* (Table 6.1) and that, so far, only Paul et al. (2010) and Nasuhoglu et al. (2012) assessed the contribution of DPs after photocatalytic treatment of a CIP and LEVO solution. This shows the need for more research on other species since observations cannot be generalized for all

bacteria and, even within the same genus, differences in sensitivity are observed (Lemaire et al., 2011).

Therefore, residual antibacterial activity of MOX is determined by means of agar diffusion tests for four relevant bacterial species. The contribution of DPs is determined by comparing inhibition zone diameters resulting from the photocatalytic samples with inhibition zone diameters for a given range of MOX concentrations. Results show that degradation of the mother compound is a good indicator for residual activity removal, and that DPs do not significantly contribute to the reaction solution's ecotoxicity. Nevertheless, caution is required since a variation in sensitivity towards DPs is observed for one of the investigated bacterial species, namely *E. coli*. Parent compound related antibacterial activity reduction is not only observed during photocatalytic treatment of FQs (Li et al., 2012c; Paul et al., 2010), but also for ozonation of FQs (De Witte et al., 2008) and other antibiotic classes like β -lactams, tetracyclines etc. (Dodd et al., 2009).

FQ ecotoxicity is mainly evaluated by *Vibrio fischeri* fluorescence tests (Table 6.1). In this study, it is the first time that algal growth rate inhibition tests using the green alga *Pseudokirchneriella subcapitata* are performed to assess FQ ecotoxicity during a photocatalytic treatment, and this with a particular focus on DP toxicity. The application of algae as indicator species is relevant since they are the basis of the food chain, and are more sensitive towards FQ pollution than other higher organisms like *Daphnia magna* (Table A.1). A reduction in algal growth rate inhibition is observed and the combined interpretation of both the chemical analytical and ecotoxicological data reveal that also here, as long as MOX is present in the reaction solution it is the main contributor for algal growth

inhibition (62-100%). However, when MOX is removed below its detection limit, 1/3 of the original growth rate inhibition is still observed in treated solutions, indicating that DPs may not be neglected in toxicity assessment.

Main messages:

Photocatalytic degradation is capable of removing biological activity like antibacterial activity and ecotoxicological effects.

MOX is the main contributor for residual biological activity, and DPs are less toxic compared to the FQ mother compound.

No significant DP antibacterial activity is observed for the investigated bacteria, but caution is required. Algal growth inhibition tests show that *P. subcapitata* is sensitive towards photocatalytic DPs.

6.6 From synthetic to real environmental matrices: degradation in the effluent of a hospital WWTP

A last research goal was to elaborate on the application of heterogeneous photocatalysis in **real effluent matrices**. Heterogeneous photocatalytic FQ degradation performed in effluent water is only performed by a few researchers (Table 6.1). Moreover, photocatalytic degradation of CIP in a hospital effluent water matrix is only reported by Vasconcelos et al. (2009b), but no comparison with photocatalytic CIP degradation in demineralized water is made, and no discussion about the inhibition of effluent constituents on both FQ adsorption and photocatalytic degradation is given.

Hence, the latter is investigated in this study and it is shown that TiO₂ mediated photocatalytic degradation of MOX is two times faster in demineralized water than in hospital effluent water. Filtering effluent waters did not significantly influence photocatalytic degradation rates indicating the negligible effect of SPM. The addition of inorganic ions like chloride anions and bicarbonates mainly inhibited FQ adsorption (up to 6.8 times) by competition for adsorption sites on the catalyst surface, but inhibited the photocatalytic degradation rate only to a small extent (by a factor 1.2). Dissolved organic matter like FA and HA on the other hand favored FQ adsorption (by a factor of 1.6), possibly due to the formation of organic-TiO₂ complexes. However, the addition of these organic compounds inhibited the photocatalytic degradation rate of MOX up to a factor of 1.3 to 1.4, respectively. Inhibitory effects resulting from these organic compounds are most probably a combination of scavenging of reactive species, reduced accessibility of the target compound for reactive species, and/or UV light shielding. Spiking demineralized water with both inorganics and organics at relevant effluent concentrations could explain 70% of the inhibition obtained by the hospital effluent matrix, showing the relevance of the studied effluent components.

Main messages:

MOX photocatalysis is 2 times slower in hospital effluent than in demineralized water.

SPM has a negligible effect on the photocatalytic degradation rate of MOX.

Inorganics inhibit MOX adsorption, and to a lesser extent its degradation rate.

Organics enhance MOX adsorption but inhibit its photocatalytic degradation.

The studied set of (in)organics (Cl⁻, IC, HA) can explain about 70% of the degradation rate inhibition obtained in effluent water.

Overall, it can be concluded that heterogeneous photocatalysis is a promising technique for remediation of FQ polluted wastewaters since optimal degradation rates are obtained at neutral pH and ambient temperatures which are viable for practical implementation. In order to fully understand the potential of heterogeneous photocatalysis in real applications, further research is needed to make the transition from lab scale experiments using synthetic matrices towards pilot and full-scale applications treating real effluent matrices, which is discussed in Section 6.7 and 6.8.

In the following paragraphs, experimental values obtained in this study and in literature are discussed within the context of the application potential of heterogeneous photocatalysis as a tertiary treatment technique for the effluent water of the Maria Middelares hospital, described in Part V.

To remove 90% of the MOX at adsorption-desorption equilibrium (reached after 5 min) with $0.5 \text{ g L}^{-1} \text{ TiO}_2$, a residence time of 14 min is needed (Part II). Taking into account that the degradation in hospital effluent water was 2 times slower compared to demineralized water, a residence time of about 30 min is estimated. This is most probably an overestimation since it is based on an initial concentration of $15 \text{ mg L}^{-1} \text{ MOX}$. In real hospital waters, FQ concentrations range between ng L^{-1} and $\mu\text{g L}^{-1}$ (median: $3.5 \mu\text{g L}^{-1}$, 75th percentile: $15 \mu\text{g L}^{-1}$; 25th percentile: 385 ng L^{-1} ; see Part I), which will result in lower treatment times. Literature concerning photocatalytic FQ degradation at such low concentrations is scarce, and only Miranda-García et al. (2010) and Sturini et al. (2012b) reported FQ photocatalysis at $\mu\text{g L}^{-1}$ concentrations under solar irradiation. Sturini et al. (2010) photocatalytically degraded a mixture of 6 FQs at $50 \mu\text{g L}^{-1}$ in a river water matrix. About 90% of the FQs at adsorption-desorption equilibrium is degraded after 12 min of solar irradiation in the presence of $0.5 \text{ g L}^{-1} \text{ TiO}_2$.

Miranda-García et al. (2010) investigated the photocatalytic degradation of a mixture of 15 pharmaceuticals, including OFL and FLU, at $100 \mu\text{g L}^{-1}$ in a solar compound parabolic concentrator photocatalytic reactor. After 10 min of solar irradiation at $0.005 \text{ g L}^{-1} \text{ TiO}_2$, which is a 1000 times lower, no OFL could be detected, and 90% of FLU is degraded after 20 min. Most of the other pharmaceuticals were removed for 90% after 70 min of treatment at this low catalyst concentration. The authors indicate that increasing the TiO_2 concentration to its optimal catalyst concentration of 0.2 g L^{-1} would reduce the necessary treatment time.

Treatments times in operational pilot scale ozonation plants, e.g. 22 min at the WWTP of Lausanne (Margot et al., 2013), 20 min at the Marienhospital Gelsenkirchen (Pills, 2009), 5-20 min at the WWTP in Cham (Microzon, 2014), and at least 10 min at the WWTP in Regensdorf Switzerland (Hollender et al., 2009), are of the same order of magnitude as obtained for the photocatalytic treatment of the FQ mixtures. Taking into account the advantages of heterogeneous photocatalysis over ozonation (see Section 6.7), it can be said that heterogeneous photocatalysis can be a competitive tertiary treatment technique.

The Maria Middelaes hospital discharges on the average $250 \text{ m}^3 \text{ d}^{-1}$ resulting in a reactor volume of around 5 m^3 with the estimated treatment time of 30 min. Reactor volumes of the ozonation pilot plants are of similar volume, ranging between 1.2 m^3 to 129 m^3 . This shows that the implementation of this technique at existing WWTP facilities is possible if enough surface area is available. Moreover, the presence of tertiary treatment techniques coupled to conventional WWTPs will gain importance and their implementation should be included in the design phase of new WWTPs.

6.7 Challenges

In this study, it is shown that heterogeneous photocatalysis has potential to treat FQ polluted water. However, it is important to evaluate this technique's strengths and weaknesses for future applications and competitiveness with other remediation techniques.

UV mediated heterogeneous photocatalysis has advantages over other advanced oxidation techniques. First of all, TiO_2 is a cheap catalyst (around 20 € kg^{-1} ; Muñoz, 2006), not toxic, and commercially available. Also, no addition of toxic and/or extra chemicals is needed to attain pollutant degradation, as is necessary with ozonation and Fenton based degradation techniques. However, there are challenges that need to be addressed to increase the applicability and the competitiveness of this advanced oxidation technique. Here, items related to reactor design, catalyst modification, and the application of solar heterogeneous photocatalysis are discussed.

Research on the degradation of organic pollutants using heterogeneous photocatalysis is mainly performed in slurry reactors. This poses limitations for practical implementation since it is not easy to separate the TiO_2 particles (less than 0.5 μm for agglomerates and generally 10-100 nm for elementary particles (Pichat, 2013)) from the suspension, and membrane filtration techniques are necessary to retain the photocatalyst in the reactor (Mozia, 2010). Decantation is another possibility for catalyst separation, but large settling tanks are needed

due to the slow decantation of TiO₂ particles, and an additional filtration step is still necessary to remove residual particles (Fernández-Ibáñez et al., 2003).

As a solution for the separation problem, research is performed on the development and performance of TiO₂ coatings on different inert supports like glass, ceramics, quartz, silica gel, polymer membranes, etc. (Mozia, 2010; Shan et al., 2010). A good support must be UV transparent; has strong bonds with the TiO₂ surface without interfering the degradation properties; has a high specific surface; is resistant to oxidation; promotes the contact between the contaminant and the photocatalyst; and is chemically inert (Shan et al., 2010; Miranda-García et al., 2011). Coating of TiO₂ gives the advantage that the catalyst is easily removed from the reaction solution. However, problems associated with immobilized systems include the loss of reactive surface area, and a longer average diffusion path of the pollutant to the photocatalyst surface (Malato et al., 2009). The photocatalyst film thickness, which is in the 100 nm to 1.2 µm range (Pichat, 2013; Wu et al., 2013), may also affect the photocatalytic activity by influencing the light absorption and internal mass transfer. If the catalytic film is too thick, light penetration and access to the catalyst material at deeper regions near the support material will be limited (Alexiadis and Mazzarino, 2005; McCullagh et al., 2011). On the other hand, if the film is too thin, very little of the incident light will be absorbed (Butterfield et al., 1997).

Most authors agree that, for the moment, the best photocatalytic degradation results are obtained in slurry reactors (Malato et al., 2009; Li et al., 2010; Pichat, 2013).

Another challenge in heterogeneous photocatalysis concerns the catalyst's activity and life span. Deactivation of a catalyst during water treatment has not been extensively investigated, and contradictory results are reported in literature. Miranda-García et al. (2010) observed a photoactivity decrease of TiO₂ coated beads after 5 cycles of photocatalytic degradation of a pharmaceutical mixture containing 15 different compounds, most possibly caused by the adsorption of DPs on the catalyst surface. On the other hand, Wang et al. (2013) stated that TiO₂ microsphere particles can be reused for photocatalytic reactions in a slurry reactor for more than 50 times without significant loss of activity (compounds not specified). Doll and Frimmel (2005) continuously used TiO₂ in a cross flow microfiltration reactor and did not observe a significant reduction in activity after a few days of pharmaceutical (clofibric acid and carbamazepine) degradation. However, Carbonaro et al. (2013) observed that inorganic and organic wastewater components contribute to catalyst deactivation upon treatment of effluent water spiked with 4 pharmaceutical compounds (acetaminophen, carbamazepine, iopromide, sulfamethoxazole) in a continuous flow reactor. Examining the immobilized TiO₂ surface showed slight discoloration, microcracks, and surface precipitates rich in Ca and Al. Considering a worst-case scenario, catalyst regeneration or replacement would be needed at a regular basis, significantly increasing the photocatalytic treatment operating costs. The lack of knowledge regarding catalyst deactivation reveals the need for research on catalyst surface deterioration after continuous treatment of effluent water.

Next to slurry and immobilized catalyst application, the catalyst morphology and electronic structure is of importance since, with the commonly used commercial TiO₂, UV light irradiation is necessary for photocatalyst activation. Nowadays, the application of TiO₂ mediated photocatalysis using solar light

irradiation is of great interest and, given that only 5% of the solar flux incident at the earth's surface lies in the UV spectral region, TiO_2 is rather inefficient when sunlight is used as irradiation source. Therefore, research is ongoing to increase the absorption spectrum of photocatalysts towards the visible light region by means of nonmetal doping (N, S, C, B, ...), metal doping (Cu, Co, Mn, Fe, ...), codoping (metal/nonmetal: Ni-B, nonmetal/nonmetal: N-C, N-F), noble metal deposition (Ag, Pt, Au), composites (TiO_2/CdS , TiO_2/WO_3), ... (Zaleska, 2008; Daghri et al., 2013; Pichat, 2013). This enhanced absorption spectrum would make heterogeneous photocatalysis applicable without UV light irradiance, reducing energy costs. This could be an important improvement since electricity amounts 60% of the operating costs for a photocatalytic reactor (Oller et al., 2011). However, it is not easy to create a modified catalyst that absorbs in the visible light spectrum, without reduced photocatalytic activity compared to an unmodified (commercially available) TiO_2 catalyst (Lazar et al., 2012). This shows the need for further research in the catalyst synthesis domain.

Next to catalyst modification, research is performed on the development of solar reactors for the application of heterogeneous photocatalysis in wastewater treatment (Fig. 6.2). The most famous research center regarding solar photocatalysis is Plataforma Solar de Almeria, Spain. There, research is performed on the degradation of pharmaceuticals using TiO_2 as a slurry or a coating, either on the inner side of the pyrex tubes or on glass beads (Miranda-García et al., 2010). Promising results are obtained with 3.3 g of coated TiO_2 on glass beads placed in a photoreactor tube of 2 L, with a complete removal of 15 pharmaceuticals ($100 \mu\text{g L}^{-1}$ each) in 120 min of solar irradiation.



Fig. 6.2 (Top) Solar photocatalytic reactors at Plataforma Solar de Almeria, Spain, (Bottom) TiO_2 coated glass spheres with Ø 5 mm (pictures taken by author).

Zooming in on FQs, OFL was completely removed after 5 min of treatment, which is 7 times lower compared to the treatment time obtained in this study at $0.5 \text{ g L}^{-1} \text{ TiO}_2$ and $15 \text{ mg L}^{-1} \text{ MOX}$ (35 min). The main disadvantage of such reactor designs is the large surface area to volume ratio, e.g. 100 m^2 for treating 1 m^3 wastewater (Malato et al., 2009). Therefore, it is still unclear if this technique can be up scaled for WWTP effluent remediation applications.

6.8 Perspectives

Perspectives for research in the field of heterogeneous photocatalysis are given in this section, dealing with aspects on (i) the catalyst level, (ii) reactor configuration, and (iii) application potential.

Photocatalytic research on FQ remediation mainly focuses on the application of TiO₂ P25 because it is widely investigated and considered as a reference catalyst for other catalysts like the commercially available Hombikat UV100, P90, Kronos vlp7000, and self modified ones. All these catalysts have different properties such as specific surface area, crystallinity, and particle size, which influence their adsorption capacity and photocatalytic activity.

It would therefore be interesting to perform controlled catalyst synthesis to evaluate the effect of these structural properties on the photocatalytic activity.

In a next step, catalyst mixtures can be investigated, since combining different properties can be of use to degrade a wider range of micropollutants. Also, recent developments in TiO₂ coatings give the opportunity to design experiments where catalyst deactivation and reuse can be assessed. Repetitive degradation of different pharmaceutical test compounds can reveal the importance of catalyst deactivation during continuous photocatalytic degradation. In addition, investigating structural changes of the catalyst surface by X-ray diffraction or scanning electron microscope analysis can give more insights why this effect occurs.

Another interesting topic for future research is the application of UV-leds. Since electricity is the main cost for photocatalytic AOPs, it would reduce the energy demand significantly. The reduction in electricity consumption using a UV-led system (when compared to an equivalent UV-output mercury lamp) can reach up to 50-75% (Phoseon, 2009; Lazar et al., 2012). Other advantages of UV-leds are the higher energy efficiency, they are mercury free, and can be designed to emit a specific wavelength of interest (PeakLED).

Experiments performed in this work provide insights in the photocatalytic degradation of single FQ antibiotic contaminants in both demineralized and hospital effluent water. However, in real effluent waters a large variety of pharmaceutical compounds can be detected at lower concentrations as applied here (Verlicchi et al., 2012a). It would therefore be interesting to perform photocatalytic degradation experiments on a mixture of pharmaceuticals at environmental relevant concentrations, and evaluate both acute and chronic residual toxicity of the reaction solution for test species of different trophic levels.

In this context, it is also recommended to perform further research on the formation of transformation and by-products during heterogeneous treatment of real matrices. The formation of chlorine, chlorinated and brominated by-products is observed after electrolytic oxidation of micropollutants in a reverse osmosis concentrate, hereby inducing a higher ecotoxicity (Radjenovic et al., 2011). So far, no studies on heterogeneous photocatalysis investigated the formation of chlorinated or brominated by-products and degradation products after treatment of secondary effluents, showing the need for further research on this matter.

Heterogeneous photocatalysis can have an application in different approaches for wastewater treatment. This technique can be positioned as a post-treatment of a secondary WWTP effluent to increase biodegradation and reduce toxicity of these refractory compounds. Tertiary effluents can either be (i) recycled back to the biological reactor, (ii) coupled to a sand filter and/or granulated activated carbon filter, (iii) coupled to an extra biological polishing step, or (iv) discharged. Not only centralized WWTP effluents can be treated, also more locally situated sources such as hospital and pharmaceutical bulk drug producer effluents can be remediated.

Moreover, heterogeneous photocatalysis can be implemented in short-cycled water reuse systems, as practiced in Koksijde (Belgium), Singapore, and Windhoek (Namibia) (Verstraete and Vlaeminck, 2011). Here, wastewater is considered as 'used' water from which energy, nutrients, and water itself are recovered. Before water is acceptable for reuse, pathogens and other organic micropollutants need to be eliminated, for which reverse osmosis (RO) can be used (Bagastyo et al., 2011; Verstraeten and Vlaeminck, 2011; Garcia et al., 2013). As a result of the RO process, the retentate can contain high concentrations of contaminants, and further treatment of the RO concentrate with AOP technologies is an opportunity to reduce the pharmaceutical pollution load towards the aquatic environment. Heterogeneous photocatalysis can be addressed as a remediation technique since, in literature, already promising results are reported for photocatalytic RO concentrate treatment (Westerhoff et al., 2009; Zhou et al., 2011; Martínez et al., 2013).

Apart from tertiary effluent water treatment and water reuse systems, the application of heterogeneous photocatalysis as an advanced oxidation technique can be of great interest for the production of safe drinking water. Safe drinking water is a problem that many third world countries have to deal with every day. A commonly used practice to remove pathogens from polluted water is solar disinfection (SODIS), which is the exposure of plastic bottles filled with contaminated water to direct sunlight for at least 6 hours. Approximately 4 million people in 32 different countries are dependent of this technique to obtain safe drinking water (Belgiorno et al., 2011). In most cases, users do not wait until complete disinfection is achieved due to the long necessary treatment time. Therefore, improved treatment methods are requested, which are cheap, easy to use, and effective at removing pathogenic bacteria. Recent research focuses on the

application of solar mediated photocatalytic reactors for large-scale water disinfection (Malato et al., 2009; Alrousan et al., 2012; Fisher et al., 2013). Next to that, heterogeneous photocatalysis is coupled with SODIS by coating PET bottles with a thin layer of TiO₂ or by the insertion of a catalyst rod (Meichtry et al., 2007; 3M, 2012). It would be of interest to evaluate the performance of this technique, not only for its disinfection capacity but also for its pharmaceutical and other organic (micro)pollutant removal efficiencies.

Taking heterogeneous photocatalysis out of earth's boundaries, its possible application for water treatment in space missions, where water reuse is also of major importance, could be evaluated. This is especially of interest when humankind wants to travel further than the moon, e.g. in Mars missions planned in the near future, where re-supply through cargo is no option. Biological Life Cycle Support systems like BIOS-3, CELSS, Moon PALACE and MELISSA use combined biological and physical-chemical technology for the cycling of oxygen, carbon, nutrients and water during space missions (Klanjscek and Legovic, 2001; Manukovsky et al., 2005; Hendrickx and Mergaey, 2007) (Fig. 6.3).

The presence of pharmaceuticals in this closed circuit can hamper its stability and efficiency (Pycke, 2009), resulting in the necessity of physical-chemical techniques for water reclamation during long space travels (Van Oostveldt et al., 2010). At present times, urine and faeces of sick astronauts are separately collected and discharged in transport vessels, which disintegrate upon return in earth's atmosphere. This approach is not feasible with long space travels due to large amount of waste creation, supporting the necessity of waste treatment and water purification techniques.

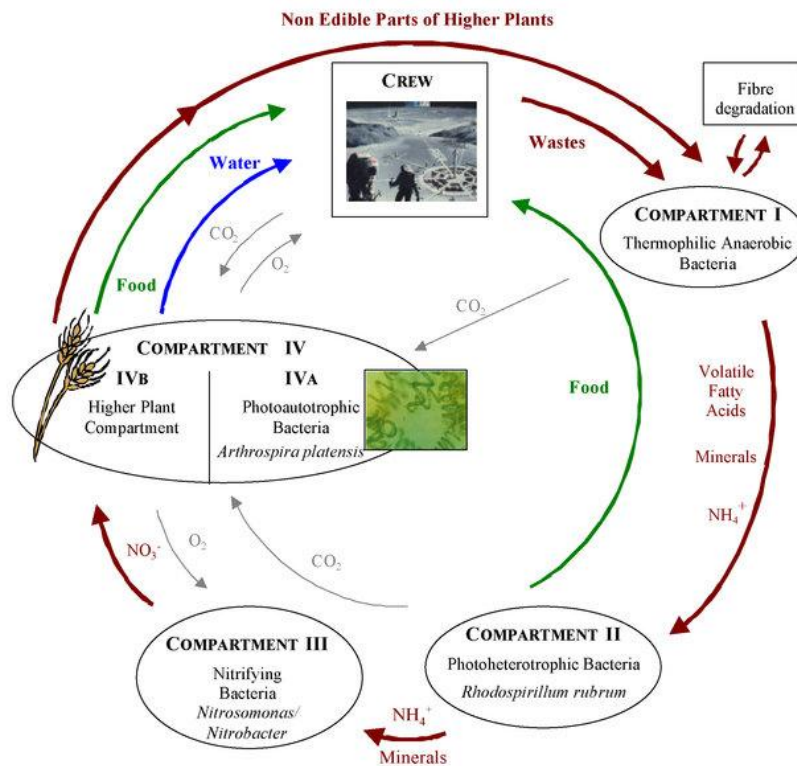


Fig. 6.3 MELiSSA loop: The four compartments of the cycle in the European Space Agency's Micro-Ecological Life Support System Alternative project (ESA, 2013).

AOP technologies can be complementary to the traditional MELiSSA system in removing pharmaceuticals, metabolites, and by inactivating bacteria present in liquid waste streams. Apart from other techniques like UV/H₂O₂, also heterogeneous photocatalysis offers potential since no extra chemicals are necessary (like in the Fenton reaction) and no toxic reactants, like ozone, are used that are not favorable in confined and unventilated areas. Therefore, UV mediated photocatalysis could be an interesting path of research for the remediation of polluted water in space.

Summary

Fluoroquinolones are antibiotic compounds, which are frequently detected in WWTP effluent waters at concentrations ranging from ng L^{-1} up to $\mu\text{g L}^{-1}$, and in some extreme cases even up to mg L^{-1} . The continuous input and long environmental life times of these biologically active components can promote bacterial resistance and induce toxic effects on aquatic organisms.

Part I provides a literature overview of the different sources, pathways, and environmental occurrence of FQ antibiotics. The main route of these emerging micropollutants to the environment is via WWTP effluents, since their biorecalcitrant nature results in an inefficient removal by conventional wastewater treatment techniques. Hence, FQs are detected in different environmental matrices like surface waters, WWTP effluent waters, soils, biota, etc.

Due to the low biodegradability of FQs, additional physical-chemical removal techniques are necessary to degrade these compounds before they are released into the environment. In this work, the AOP heterogeneous photocatalysis is studied, and the basic principles of this degradation technique are described in **Part I**.

In **Part II**, the UV-A and UV-C induced photolysis and heterogeneous photocatalysis of the FQ compounds CIP and MOX were investigated. Experiments showed that reaction pH is of main importance for FQ degradation with both processes. UV-A photolysis was slow for both FQs in the entire investigated pH range ($t_{1/2,CIP} \leq 46$ min; $t_{1/2,MOX} \leq 115$ min at $3.0 \leq \text{pH} \leq 10.0$), while UV-C photolysis was faster with half-life times of 9 min at pH 7.0 for CIP, and 11 min at pH 10.0 for MOX. The fastest removal, however, is obtained at pH 7.0 in the presence of TiO_2 as a photocatalyst ($t_{1/2,CIP,UV-A} = 5$ min, $t_{1/2,CIP,UV-C} = 4$ min, $t_{1/2,MOX,UV-A} = 3$ min, $t_{1/2,MOX,UV-C} = 3$ min). Both the difference in half-life times between photolysis and heterogeneous photocatalysis, and the observed pH dependency indicate that surface reactions are crucial during heterogeneous photocatalysis. A positive relationship is noticed between the FQ degradation rate and the fraction of FQ adsorbed onto the catalyst surface, with the latter being strongly pH dependent. Adsorption experiments reveal that FQ adsorption is favored at neutral pH and explanations are proposed based on the amphoteric nature of the FQ molecules, and the pH dependent catalyst surface charge. With the use of reported pK_a values and experimental adsorption data, partition ratios were calculated for the different FQ species. These indicate that mainly the single positively charged and zwitter FQ ion participate in the adsorption process, explaining the highest photocatalytic degradation at neutral pH.

Next to the effect of the reaction solution pH and UV light source, other operational variables like the initial pollutant concentration, catalyst concentration, stirring speed, oxygen concentration of the gas flow sparged through the reaction solution, and temperature were investigated. An optimal MOX degradation is attained at a catalyst concentration of 5 g L^{-1} , 298 K, and

air sparging, resulting in an initial degradation rate of $16.2 \pm 0.3 \mu\text{mol L}^{-1} \text{min}^{-1}$ and a half-life time of $t_{1/2} = 1.6 \text{ min}$. In addition, a deeper insight in the photocatalytic degradation mechanism of MOX is obtained through the estimation of the contribution of different reactive species during the photocatalytic MOX degradation. This is investigated by using two scavengers at different concentrations. The role of hydroxyl radicals was monitored using ISO, and the participation of oxidative 'holes' in the reaction mechanism was evaluated by the addition of iodine anions. The scavenger study indicates that 'holes' are the dominant reactive species, contributing up to 63%, and that hydroxyl radicals participate for about 24% in the photocatalytic degradation of MOX. Reactive oxygen species created by CB electrons are probably of lower importance, < 13%, during the photocatalytic degradation of MOX.

Even though complete mother compound removal was obtained during photocatalytic degradation, no significant mineralization was measured, which indicates the presence of DPs. In **Part III**, HPLC coupled to HRMS is used to determine the accurate mass of the measured DPs. Eight types of DPs were identified at all investigated pH levels, and a general initial photocatalytic degradation pathway was proposed. The photocatalytic degradation of MOX did not take place at the quinolone core, and defluorination is not observed. Photocatalytically induced modifications mainly occur at the diazobicyclo-substituent as ring opening, oxidation into carbonyl groups, and hydroxylation. Time profiles of the different DPs revealed that the solution pH influences their relative abundance during reaction, but the observed DPs types show no pH dependency.

In **Part IV**, the heterogeneous photocatalytic removal efficiency was evaluated with respect to residual biological activity. First, residual antibacterial activity of the photocatalytic reaction solutions was evaluated against *E. coli*, *S. carnosus*, *S. mutans* and *K. pneumoniae* by means of agar diffusion tests. A reduction in residual antibacterial activity is noticed at all investigated pH levels, with a complete inactivation at neutral pH after 12 min of UV-A mediated photocatalytic treatment with 1 g L⁻¹ TiO₂. Although the residual antibacterial activity is mainly determined by the residual MOX concentration in solution, a different sensitivity towards DPs is observed for the studied bacterial species.

Secondly, ecotoxic effects towards the green alga organism *Pseudokirchneriella subcapitata* were investigated using algal growth rate inhibitions tests. Photocatalytic treatment of MOX in aqueous solution decreased the average algal growth rate inhibition from 71% to 15% after 150 min reaction time. Combined chemical and toxicological analysis shows that as long as MOX is present in the reaction solution, it is the main actor for growth inhibition. However, the contribution of the DPs to the overall reaction solution's toxicity cannot be overlooked.

In **Part V**, the application of photocatalysis in real effluent water was assessed. TiO₂ mediated photocatalysis of MOX in hospital effluent water shows to be 2 times slower than in demineralized water. Since little knowledge existed about to what extent different types of effluent matrix components affect heterogeneous photocatalytic processes, the effect of SPM and selected inorganic and organic matrix constituents on both the adsorption-desorption equilibrium and initial photocatalytic degradation rate of MOX in water were investigated. Regarding adsorption, the most pronounced effect is observed when inorganics, i.e. chloride anions and IC, are added into demineralized water

(reference matrix), hereby decreasing adsorption 3 times at 600 mg Cl⁻ L⁻¹. Organic constituents like HA, FA, and BSA favor MOX adsorption (by a factor of 1.6 at 15 mg C L⁻¹ TOC), which might be explained by the formation of TiO₂-organic matter complexes. Despite this opposite effect in adsorption, both inorganics and organics cause a drop in photocatalytic degradation rate, with the highest effect observed for HA and FA (factor of 1.3-1.4). This is most probably because of scavenging of, or limited accessibility to reactive species and/or light shielding. Overall, a mixture of the investigated matrix constituents at effluent concentration levels can explain about 70% of the inhibitory effect that hospital effluent causes on the MOX degradation, showing their high relevance for photocatalytic treatment of real water matrices.

An overall discussion focusing on the scientific results and progress with respect to FQ heterogeneous photocatalysis is given in **Part VI**. In addition, challenges and perspectives for this AOP are presented.

Samenvatting

Fluorchinolonen (FQ) zijn antibiotica die vaak aangetroffen worden in het effluent water van waterzuiveringsinstallaties bij concentraties van ng L^{-1} tot $\mu\text{g L}^{-1}$ én in sommige extreme gevallen zelfs tot mg L^{-1} . De continue lozing en lange verblijftijd in het milieu van deze biologisch actieve componenten kunnen negatieve effecten op natuurlijke ecosystemen veroorzaken zoals o.a. bacteriële resistentie vorming en toxiciteit op aquatische organismen.

Hoofdstuk I geeft een overzicht van de verschillende bronnen van FQ antibiotica, routes, en hun voorkomen in het milieu. Hoofdzakelijk komen deze antibiotica in het milieu via waterzuiveringsinstallaties, daar conventionele waterzuiveringstechnieken niet in staat zijn deze bio-recalcitrante micropolluenten efficiënt af te breken. Hierdoor worden deze componenten in verschillende natuurlijke matrices gedetecteerd onder andere oppervlaktewater, bodem, biota, enz.

De lage biodegradeerbaarheid van deze polluenten toont aan dat additionele fysisch-chemische zuiveringstechnieken noodzakelijk zijn voor een meer adequate degradatie. In dit doctoraat wordt gefocust op heterogene fotokatalyse als geavanceerde oxidatietechnologie om FQ polluenten te verwijderen uit water.

Geavanceerde oxidatietechnologiën en het principe van heterogene fotokatalyse worden eveneens uiteengezet in Hoofdstuk I.

In **Hoofdstuk II** werden UV-A en UV-C geïnduceerde fotolyse en fotokatalyse van CIP en MOX onderzocht. Resultaten tonen aan dat de reactie pH een belangrijke factor is voor beide processen. Fotolyse onder UV-A instraling was traag over het volledige onderzochte pH bereik ($t_{1/2,CIP} \leq 46$ min; $t_{1/2,MOX} \leq 115$ min bij $3.0 \leq \text{pH} \leq 10.0$). Fotolyse bij UV-C instraling was sneller met een halfwaardetijd van 9 min voor CIP bij pH 7.0, 11 min voor MOX bij pH 10.0.

De snelste verwijdering werd echter verkregen onder neutrale pH omstandigheden in de aanwezigheid van TiO_2 als katalysator ($t_{1/2,CIP,UV-A} = 5$ min, $t_{1/2,CIP,UV-C} = 4$ min; $t_{1/2,MOX,UV-A} = 3$ min; $t_{1/2,MOX,UV-C} = 3$ min). Het verschil in halfwaardetijden voor fotolyse en fotokatalyse in combinatie met het waargenomen pH effect, geeft aan dat oppervlaktereacties van groot belang zijn tijdens heterogene fotokatalyse. Een positieve relatie tussen FQ verwijdering en de sterk pH afhankelijk adsorptie werd opgemerkt. Een verhoogde adsorptie op TiO_2 werd waargenomen onder neutrale pH. Dit kan verklaard worden aan de hand van de amfoterische aard van de FQ componenten en de pH afhankelijke ladingstoestand van de katalysator. Gebruikmakend van gerapporteerde pK_a waarden en de experimentele adsorptiedata werden partitie verhoudingen berekend voor de verschillende FQ ladingstoestanden. Resultaten tonen aan dat voornamelijk het eenwaardig positief geladen ion en het zwitterion participeren in het adsorptie proces, wat op zijn beurt de sterkste adsorptie rond neutrale pH kan verklaren.

Naast het effect van pH werden ook andere procesparameters zoals initiële FQ concentratie, katalysatorconcentratie, zuurstofconcentratie van het

instromende gas en reactietemperatuur onderzocht. Een optimale fotokatalytische MOX degradatie werd verkregen onder neutrale omstandigheden bij een katalysatorconcentratie van 5 g L^{-1} , 298 K en bij luchtdoorborreling, resulterend in een initiële degradatie snelheid van $16,2 \pm 0,3 \mu\text{mol L}^{-1} \text{ min}^{-1}$ en een halfwaardetijd van $t_{1/2} = 1,6 \text{ min}$.

Inzichten in het fotokatalytische degradatiemechanisme werden verkregen door het inschatten van de bijdrage van verschillende reactieve species, dit door middel van twee verschillende radicaalvangers bij variërende concentraties. Hydroxylradicalen werden gevangen door de toevoeging van isopropanol. De bijdrage van oxidatieve 'gaten' werd geëvalueerd door de toevoeging van iodide anionen. Uit de resultaten kan afgeleid worden dat 'gaten' de dominante reactieve species zijn en tot 63% bijdragen aan de fotokatalytische degradatie van MOX. Hydroxylradicalen participeren voor ongeveer 24%, en reactieve zuurstofspecies geproduceerd door de geleidingsband elektronen zijn relatief minder belangrijk (< 13%).

De verwaarloosbare mineralisatie tijdens de fotokatalytische degradatie van MOX is een indicatie voor de aanwezigheid van verschillende degradatieproducten. In **Hoofdstuk III** werd HPLC gekoppeld aan HRMS ingezet om de accurate massa te bepalen van de gedetecteerde degradatieproducten. Acht types degradatieproducten werden geïdentificeerd bij zure, neutrale en basische omstandigheden. Hiermee werd een algemene afbraakroute voorgesteld. Uit de moleculaire structuur van de degradatieproducten kon opgemerkt worden dat er geen fotokatalytische degradatie aan de chinolon basisstructuur plaatsvond, ook defluorinatie werd niet vastgesteld. Fotokatalytisch geïnduceerde modificaties vonden voornamelijk plaats op de diazobicyclo-substituent,

onder de vorm van ringopening, oxidatie naar carbonylgroepen en hydroxylering. Tijdsprofielen van de verschillende degradatieproducten tonen aan dat de pH hun relatieve voorkomen beïnvloedt, hoewel dezelfde types reactieproducten werden gedetecteerd.

Naast de verwijderingsefficiëntie werd heterogene fotokatalyse van MOX in **Hoofdstuk IV** ook geëvalueerd naar residuele biologische activiteit. Eerst werd aan de hand van agar-diffusie testen de residuele antibacteriële activiteit van de fotokatalytische reactie-oplossing getest voor de bacteriën *E. coli*, *S. carnosus*, *S. mutans* en *K. pneumoniae*. Een reductie in residuele antibacteriële activiteit werd opgemerkt bij alle onderzochte pH-waarden, met een complete verwijdering onder neutrale omstandigheden na 12 min fotokatalytische behandeling met UV-A belichting en een katalysator concentratie van 1 g L⁻¹. Hoewel de residuele antibacteriële activiteit hoofdzakelijk werd bepaald door de residuele MOX concentratie in oplossing, werd een verschillende gevoeligheid voor degradatieproducten opgemerkt onder de bestudeerde bacteriën.

Ten tweede werd de ecotoxiciteit voor de groene alg, *Pseudokirchneriella subcapitata*, onderzocht; dit gebruikmakend van groeisnelheid inhibitie testen. Fotokatalytische behandeling van een MOX oplossing resulteerde in een daling van de groeisnelheid inhibitie van 71% naar 15% na 150 min behandeling. Een gecombineerde interpretatie van zowel de chemische als biologische analyses tonen aan dat de groeisnelheid inhibitie hoofdzakelijk veroorzaakt wordt zolang MOX in de oplossing aanwezig is. Niettegenstaande kan het aandeel van de fotokatalytische degradatieproducten in de veroorzaakte groei-inhibitie niet verwaarloosd worden.

In **Hoofdstuk V** werd heterogene fotokatalyse van MOX geëvalueerd in reële effluent matrices. Fotokatalytische degradatie uitgevoerd in hospitaal effluent water was tweemaal trager dan deze in gedemineraliseerd water. Door het gebrek aan kennis betreffende het effect van verschillende matrix componenten op de adsorptie en op het fotokatalytische degradatieproces werd het effect van gesuspendeerd materiaal en een selectie van anorganische en organische componenten op zowel het adsorptie-desorptie evenwicht als de initiële degradatiesnelheid onderzocht. FQ adsorptie werd voornamelijk geïnhibeed door de toevoeging van anorganische componenten zoals chloride-ionen en anorganische koolstof. In tegenstelling tot anorganische componenten bevorderen organische componenten zoals huminezuren, fulvinezuren en runderalbumine de MOX adsorptie; dit waarschijnlijk door complexvorming van het organisch materiaal met het katalysator oppervlak. Zowel anorganische als organische componenten inhiberen de fotokatalytische degradatie met de grootste inhibitie opgemeten bij additie van humine - en fulvinezuren. Deze inhibitie kan te wijten zijn aan het vangen van reactieve species door het organisch materiaal, aan een gehinderde bereikbaarheid van MOX voor de reactieve species en/of aan absorptie van UV licht door deze organische stoffen. Globaal gezien kan de toediening van zowel anorganische als organische componenten, bij effluent relevante concentraties, ongeveer 70% van de inhibitie geobserveerd tijdens een fotokatalytische MOX degradatie in hospitaal effluent verklaren. Dit duidt de relevantie aan van bovengenoemde componenten voor een fotokatalytische behandeling van effluent water.

Tot slot omvat **Hoofdstuk VI** een globale discussie over de verworven resultaten en wetenschappelijke vooruitgang van FQ heterogene fotokatalyse. Ook zijn de uitdagingen en perspectieven voor deze AOP als waterzuiveringstechniek besproken.

Addendum A

Table A.1 Ecotoxicity data of the in the environment detected FQ compounds

FQ	Taxonomic group	F/S	Test organism	Test type	EC-50 [95% CI] Reported in mg L ⁻¹	Reference
CIP	B	S	<i>V. fischeri</i>	Bioluminescence assay, 30 min	11.5 [n.d.a]	Martins et al. (2012)
	CB	F	<i>M. aeruginosa</i>	Growth inhibition test, 5 d	0.017 [0.014, 0.020]	Robinson et al. (2005)
				Growth and reproduction test, 5 d	0.005 [0.004, 0.006]	Halling-Sørensen et al. (2000)
	CB	F	<i>A. flos-aquae</i>	Growth inhibition test, 72 h	0.0363 [0.0226, 0.0597]	Ebert et al. (2011)
	Alga	F	<i>P. subcapitata</i>	Growth inhibition test, 72 h	18.7 [16.2, 21.2]	Robinson et al. (2005)
				Growth inhibition test, 72 h	2.97 [2.41, 3.66]	Halling-Sørensen et al. (2000)
				Growth inhibition test, 96 h	4.83 [3.44, 7.32]	Martins et al. (2012)
				Growth inhibition test, 72 h	5.57 [4.86, 6.38]	This study
	Alga	F	<i>C. vulgaris</i>	Growth inhibition test, 96h	20.6 [n.d.a]	Nie et al. (2008)
	Alga	F	<i>S. capricornutum</i>	Growth inhibition test	2.97 [2.41, 3.66]	Halling-Sørensen et al. (2000)
	Plant	F	<i>L. minor</i>	Growth inhibition test, 7 d	0.413 [0.114, 1.84]	Ebert et al. (2011)
				Growth inhibition test, 7 d	3.75 [n.d.a]	Martins et al. (2012)
				Growth inhibition test, 7 d	0.203 [0.041, 0.364]	Robinson et al. (2005)
	Plant	F	<i>L. gibba</i>	Wet mass production test, 7d	0.698 [0.447, 0.919]	Brain et al. (2008)
	Crust	F	<i>D. magna</i>	Acute immobilization test, 48 h	65.3 [54.9, 79.1]	Martins et al. (2012)
				Acute toxicity test	> 60	Halling-Sørensen et al. (2000)
	Fish	F	<i>B. rerio</i>	Acute fish toxicity test	> 100	Halling-Sørensen et al. (2000)
	Fish	F	<i>G. holbrooki</i>	Fish acute toxicity test, 96 h	> 60	Martins et al. (2012)

ENRO	B	S	<i>V. fischeri</i>	Bioluminescence assay, 5 min	425 [n.d.a]	Park and Choi (2008)
				Bioluminescence assay, 15 min	326.8 [n.d.a]	
	CB	F	<i>M. aeruginosa</i>	Growth inhibition test, 5 d	0.049 [0.041, 0.056]	Robinson et al. (2005)
	CB	F	<i>A. flos-aquae</i>	Growth inhibition test, 72 h	0.465 [0.387, 0.562]	Ebert et al. (2011)
	Alga	F	<i>P. subcapitata</i>	Growth inhibition test, 72 h	3.1 [2.6, 3.6]	Robinson et al. (2005)
	Alga	F	<i>D. subcapitatus</i>	Growth inhibition test, 72 h	0.028 [0.024, 0.035]	Ebert et al. (2011)
	Plant	F	<i>L. minor</i>	Growth inhibition test, 7 d	0.322 [0.028, 4.24]	Ebert et al. (2011)
				Growth inhibition test, 7 d	0.114 [0.084, 0.143]	Robinson et al. (2005)
	Crust	F	<i>D. magna</i>	Acute toxicity test, 24 h	131.7 [107.9, 155.3]	Park and Choi (2008)
				Acute toxicity test, 48 h	56.7 [46.78, 66.6]	
				Chronic immobilization test, 21 d	11.47 [6.25, 16.71]	
	Crust	F	<i>M. macrocopa</i>	Acute toxicity test, 24 h	285.7 [176.87, 394.5]	Park and Choi (2008)
				Acute toxicity test, 48 h	>200	
				Chronic toxicity test, 8 d	>15	
Fish	F	<i>O. latipes</i>	Fish acute toxicity test, 48 h	>100	Park and Choi (2008)	
			Fish acute toxicity test, 96 h	>100		
LOME	B	S	<i>V. fischeri</i>	Bioluminescence assay, 24 h	0.0224 [0.0222, 0.00227]	Backhaus et al. (2000)
	CB	F	<i>M. aeruginosa</i>	Growth inhibition test, 5 d	0.186 [0.172, 0.20]	Robinson et al. (2005)
	Alga	F	<i>P. subcapitata</i>	Growth inhibition test, 72 h	22.7 [19.9, 25.5]	Robinson et al. (2005)
	Plant	F	<i>L. minor</i>	Growth inhibition test, 7 d	0.106 [0.045, 0.167]	Robinson et al. (2005)
	Plant	F	<i>L. gibba</i>	Wet mass production test, 7d	0.097 [0.057, 0.136]	Brain et al. (2008)

OFL	<i>B</i>	<i>F</i>	<i>V. fischeri</i>	Bioluminescence assay, 24 h	0.0136 [0.0129, 0.0143]	Backhaus et al. (2000)
	<i>CB</i>	<i>F</i>	<i>M. aeruginosa</i>	Growth inhibition test, 5 d	0.021 [0.018, 0.024]	Robinson et al. (2005)
	<i>Alga</i>	<i>F</i>	<i>P. subcapitata</i>	Growth inhibition test, 72 h	12.1 [10.4, 13.7]	Robinson et al. (2005)
				Growth inhibition test, 48 h	1.44 [1.08, 1.80]	Isidori et al. (2005)
	<i>Plant</i>	<i>F</i>	<i>L. gibba</i>	Wet mass production test, 7d	0.532 [0.378, 0.686]	Brain et al. (2008)
	<i>Plant</i>	<i>F</i>	<i>L. minor</i>	Growth inhibition test, 7 d	0.126 [0.052, 0.201]	Robinson et al. (2005)
	<i>Crust</i>	<i>F</i>	<i>D. magna</i>	Acute toxicity test, 24 h	31.75 [25.04, 40.26]	Isidori et al. (2005)
	<i>Crust</i>	<i>F</i>	<i>T. platyurus</i>	Acute toxicity test, 24 h	33.98 [25.66, 45.00]	Isidori et al. (2005)
	<i>Crust</i>	<i>F</i>	<i>C. dubia</i>	Acute toxicity test, 48 h	17.41 [10.49, 28.89]	Isidori et al. (2005)
	<i>Rotif</i>	<i>F</i>	<i>B. calyciflorus</i>	Acute toxicity test, 24 h	29.88 [26.67, 33.46]	Isidori et al. (2005)
SARA	<i>CB</i>	<i>F</i>	<i>M. aeruginosa</i>	Growth inhibition test, 7d	0.015 [0.009, 0.023]	Holten Lützhøft et al. (1999)
	<i>Alga</i>	<i>F</i>	<i>S. capricornutum</i>	According to ISO 8692	16 [9.8, 25]	Holten Lützhøft et al. (1999)
	<i>Alga</i>	<i>S/F</i>	<i>R. salina</i>	According to ISO 8692	24 [11, 52]	Holten Lützhøft et al. (1999)
LEVO	<i>B</i>	<i>S</i>	<i>V. fischeri</i>	Bioluminescence assay, 30 min	1150 [n.d.a]	El Najjar et al. (2013)
	<i>CB</i>	<i>F</i>	<i>M. aeruginosa</i>	Growth inhibition test, 5 d	0.0079 [0.0064, 0.0094]	Robinson et al. (2005)
	<i>Alga</i>	<i>F</i>	<i>P. subcapitata</i>	Growth inhibition test, 72 h	7.4 [6.4, 8.4]	Robinson et al. (2005)
	<i>Plant</i>	<i>F</i>	<i>L. minor</i>	Growth inhibition test, 7 d	0.051 [0.0086, 0.094]	Robinson et al. (2005)
	<i>Plant</i>	<i>F</i>	<i>L. gibba</i>	Wet mass production test, 7d	0.185 [0.120, 0.251]	Brain et al. (2008)

FLU	B	S	<i>V. fischeri</i>	Bioluminescence assay, 24 h	0.0190 [0.0188, 0.0193]	Backhaus et al. (2000)
				Bioluminescence assay, 30 min	11.45-16.05	Lalumera et al. (2004)
	CB	F	<i>M. aeruginosa</i>	Growth inhibition test, 5 d	1.96 [1.76, 2.16]	Robinson et al. (2005)
				Growth inhibition test, 7d	0.159 [0.066, 0.382]	Holten Lützhøft et al. (1999)
	Alga	F	<i>P. subcapitata</i>	Growth inhibition test, 72 h	5.00 [4.80, 5.20]	Robinson et al. (2005)
	Alga	S/F	<i>R. salina</i>	According to ISO 8692	18 [10, 31]	Holten Lützhøft et al. (1999)
	Alga	F	<i>S. capricornutum</i>	According to ISO 8692	5 [1.6, 16]	Holten Lützhøft et al. (1999)
	Plant	F	<i>L. minor</i>	Growth inhibition test, 7 d	2.47 [1.65, 3.30]	Robinson et al. (2005)
	Crust	S	<i>A. salina</i>	Acute toxicity test, 24 h	476.8 [91.6, 2480]	Migliore et al. (1997)
Acute toxicity test, 24 h				307.7 [80.9,6114]		
Acute toxicity test, 24 h				96.35 [38.9, 238.8]		
NOR	B	S	<i>V. fischeri</i>	Bioluminescence assay, 24 h	0.022 [0.0217, 0.0224]	Backhaus et al. (2000)
	Alga	F	<i>S. obliquus</i>	Growth inhibition test, 96h	38.49 [n.d.a]	Nie et al. (2009)
	Plant	F	<i>L. gibba</i>	Wet mass production test, 7d	0.913 [0.630, 1.195]	Brain et al. (2008)
MOX	Alga	F	<i>P. subcapitata</i>	Growth inhibition test, 72 h	0.78 [0.56, 1.09]	This study
	Alga	F	<i>D. subspicatus</i>	Growth inhibition test, 72 h	>25	Bayer (2014)
	Crust	F	<i>D. magna</i>	Acute toxicity, 48 h	>91	Bayer (2014)
	Fish	F	<i>D. rerio</i>	Acute fish toxicity, 96 h	>91.8	Bayer (2014)

B: bacteria; CB: cyanobacteria; Crust: crustaceae; Rotif: rotifer; F: fresh water; S: saline water; EC-50: median effect concentration; CI: confidence interval; *Anabaena flos-aquae*, *Artemia salina*, *Brachionus calyciflorus*, *Brachydanio rerio*, *Ceriodaphnia dubia*, *Chlorella vulgaris*, *Daphnia magna*, *Danio rerio*, *Desmodesmus subcapitatus*, *Gambusia holbrooki*, *Lemna gibba*, *Lemna minor*, *Microcystis aeruginosa*, *Moina macrocopa*, *Oryzias latipes*, *Pseudokirchneriella subcapitata*, *Rhodomonas salina*, *Scenedesmus obliquus*, *Selenastrum capricornutum*, *Thamnocephalus platyurus*, *Vibrio fischeri*; n.d.a: no data available.

Addendum B

B.1 Governing equations for the partition ratios

B.1.1 Basic equations

The calculation of the partition ratios of the FQs moxifloxacin (MOX) and ciprofloxacin (CIP), both denoted as 'A', in a buffered aqueous system, containing a titania photocatalyst is discussed in detail. The component, being present in its positive (3+), (2+) and (+), zwitterionic/non-charged (Z/0) and negative (-) forms, is distributed between the liquid phase (aq) and the photocatalyst surface by adsorption (ad). The adsorption of component A in its different forms is given by Eqs. B.1 to B.5 and the corresponding partition ratios are defined by Eqs. B.6 to B.10:



$$K_1 = \frac{C_{A_{ad}^{3+}}}{C_{A_{aq}^{3+}}} \quad (\text{B.6})$$

$$K_2 = \frac{C_{A_{ad}^{2+}}}{C_{A_{aq}^{2+}}} \quad (\text{B.7})$$

$$K_3 = \frac{C_{A_{ad}^+}}{C_{A_{aq}^+}} \quad (\text{B.8})$$

$$K_4 = \frac{C_{A_{ad}^{Z/0}}}{C_{A_{aq}^{Z/0}}} \quad (\text{B.9})$$

$$K_5 = \frac{C_{A_{ad}^-}}{C_{A_{aq}^-}} \quad (\text{B.10})$$

The concentration in the aqueous phase and the concentration of adsorbed species are written in mol L⁻¹ and mol kg_{cat}⁻¹, so that the partition ratio is expressed in L kg_{cat}⁻¹. The pH and the concentrations of the positive, zwitterionic/non-charged form and negative ions in the aqueous phase are related by means of the pK_a values (Fig. B.1) in Eqs. B.11 to B.14:

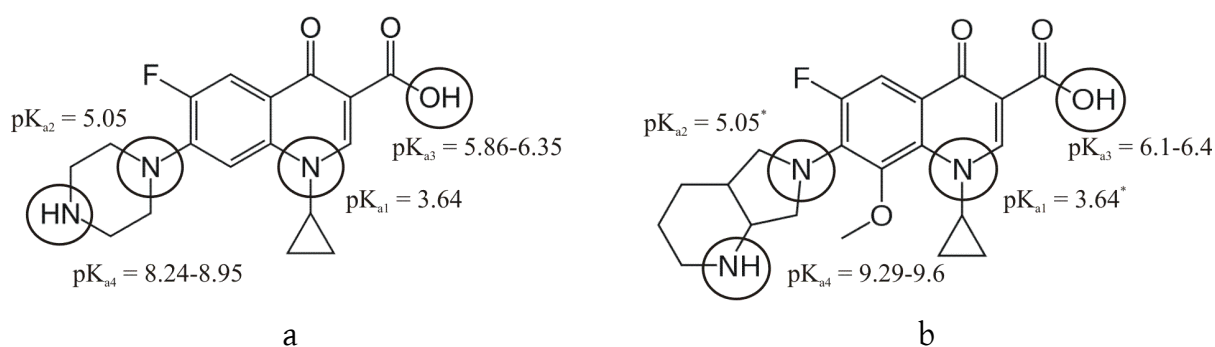


Fig. B.1 Molecular structure of (a) CIP and (b) MOX with range of pK_a values (MacGowan, 1999; Lin et al., 2004; Langlois et al., 2005; De Witte et al., 2007; Neves et al., 2007; Lorenzo et al., 2008). The pK_a values marked with "*" are not yet mentioned in literature, but are assumed to be equal to CIP pK_a values due to a similar structure.

$$pH = pK_{a1} + \log \frac{C_{A_{aq}^{2+}}}{C_{A_{aq}^{3+}}} \quad (B.11)$$

$$pH = pK_{a2} + \log \frac{C_{A_{aq}^+}}{C_{A_{aq}^{2+}}} \quad (B.12)$$

$$pH = pK_{a3} + \log \frac{C_{A_{aq}^{Z/0}}}{C_{A_{aq}^+}} \quad (B.13)$$

$$pH = pK_{a4} + \log \frac{C_{A_{aq}^-}}{C_{A_{aq}^{Z/0}}} \quad (B.14)$$

The fraction S of component A, adsorbed on the catalyst, is defined by Eq. B.15:

$$S = \frac{C_{A_{ad}^{3+}} + C_{A_{ad}^{2+}} + C_{A_{ad}^+} + C_{A_{ad}^{Z/0}} + C_{A_{ad}^-}}{C_{A,0}} \frac{m_{cat}}{V} \quad (B.15)$$

The mole balance for component A is given by Eq. B.16:

$$VC_{A,0} = V(C_{A_{aq}^{3+}} + C_{A_{aq}^{2+}} + C_{A_{aq}^+} + C_{A_{aq}^{Z/0}} + C_{A_{aq}^-}) + m_{cat}(C_{A_{ad}^{3+}} + C_{A_{ad}^{2+}} + C_{A_{ad}^+} + C_{A_{ad}^{Z/0}} + C_{A_{ad}^-}) \quad (B.16)$$

B.1.2 Main equations

In this section, a different pH level is indicated by an index i. From Eqs. B.11 to B.14 concentrations of species A in the aqueous phase are related by Eqs. B.17 to B.20:

$$C_{A_{aq,i}^{2+}} = C_{A_{aq,i}^{3+}} 10^{pH_i - pK_{a1}} \quad (B.17)$$

$$C_{A_{aq,i}^+} = C_{A_{aq,i}^{2+}} 10^{pH_i - pK_{a2}} \quad (B.18)$$

$$C_{A_{aq,i}^{Z/0}} = C_{A_{aq,i}^+} 10^{pH_i - pK_{a3}} \quad (B.19)$$

$$C_{A_{aq,i}^-} = C_{A_{aq,i}^{Z/0}} 10^{pH_i - pK_{a4}} \quad (B.20)$$

Using Eqs. B.17 to B.20, all aqueous concentrations can be written as function of the pK_a values and the concentration $C_{A_{aq,i}^+}$. For simplicity, the substitution

$\delta_{i,j} = 10^{pH_i - pK_{a,j}}$ with $j = 1 \dots 4$ and $i = 1 \dots 5$ is adopted:

$$C_{A_{aq,i}^{3+}} = \frac{C_{A_{aq,i}^{2+}}}{10^{pH_i - pK_{a1}}} = \frac{C_{A_{aq,i}^+}}{10^{pH_i - pK_{a2}}} \frac{1}{10^{pH_i - pK_{a1}}} = \frac{C_{A_{aq,i}^+}}{\delta_{i,1} \delta_{i,2}} \quad (B.21)$$

$$C_{A_{aq,i}^{2+}} = \frac{C_{A_{aq,i}^+}}{10^{pH_i - pK_{a2}}} = \frac{C_{A_{aq,i}^+}}{\delta_{i,2}} \quad (B.22)$$

$$C_{A_{aq,i}^{Z/0}} = C_{A_{aq,i}^+} 10^{pH_i - pK_{a3}} = \delta_{i,3} C_{A_{aq,i}^+} \quad (B.23)$$

$$C_{A_{aq,i}^-} = C_{A_{aq,i}^{Z/0}} 10^{pH_i - pK_{a4}} = C_{A_{aq,i}^+} 10^{pH_i - pK_{a3}} 10^{pH_i - pK_{a4}} = \delta_{i,3} \delta_{i,4} C_{A_{aq,i}^+} \quad (B.24)$$

Combining Eqs. B.6 to B.10 and B.16 gives Eq. B.25:

$$C_{A,0,i} = C_{A_{aq,i}^{3+}} \left(1 + \frac{m_{cat}}{V} K_1\right) + C_{A_{aq,i}^{2+}} \left(1 + \frac{m_{cat}}{V} K_2\right) + C_{A_{aq,i}^+} \left(1 + \frac{m_{cat}}{V} K_3\right) + C_{A_{aq,i}^{Z/0}} \left(1 + \frac{m_{cat}}{V} K_4\right) + C_{A_{aq,i}^-} \left(1 + \frac{m_{cat}}{V} K_5\right) \quad (B.25)$$

With the substitution $K'_q = \frac{m_{cat}}{V} K_q$, $q = 1 \dots 5$, and the substitution of Eqs. B.21 to

B.24 into Eq. B.25, Eq. B.26 is obtained:

$$C_{A,0,i} = \frac{C_{A_{aq,i}^+}}{\delta_{i,1} \delta_{i,2}} (1 + K'_1) + (1 + K'_2) + C_{A_{aq,i}^+} (1 + K'_3) + C_{A_{aq,i}^+} \delta_{i,3} (1 + K'_4) + C_{A_{aq,i}^+} \delta_{i,3} \delta_{i,4} (1 + K'_5) \quad (B.26)$$

Solving Eq. B.26 for $C_{A_{aq,i}^+}$ gives Eq. B.27:

$$C_{A_{aq,i}^+} = \frac{C_{A,0,i}}{\frac{1 + K'_1}{\delta_{i,1} \delta_{i,2}} + \frac{1 + K'_2}{\delta_{i,2}} + 1 + K'_3 + (1 + K'_4) \delta_{i,3} + (1 + K'_5) \delta_{i,3} \delta_{i,4}} \quad (B.27)$$

Substitution of Eq. B.27 into Eqs. B.21 to B.24 gives Eqs. B.28 to B.31 for the concentrations of the positive, zwitterionic/non-charged form and negative ion concentrations in the liquid phase:

$$C_{A_{aq,i}^{3+}} = \frac{\frac{C_{A,0,i}}{\delta_{i,1}\delta_{i,2}}}{\frac{1+K'_1}{\delta_{i,1}\delta_{i,2}} + \frac{1+K'_2}{\delta_{i,2}} + 1 + K'_3 + (1+K'_4)\delta_{i,3} + (1+K'_5)\delta_{i,3}\delta_{i,4}} \quad (\text{B.28})$$

$$C_{A_{aq,i}^{2+}} = \frac{\frac{C_{A,0,i}}{\delta_{i,2}}}{\frac{1+K'_1}{\delta_{i,1}\delta_{i,2}} + \frac{1+K'_2}{\delta_{i,2}} + 1 + K'_3 + (1+K'_4)\delta_{i,3} + (1+K'_5)\delta_{i,3}\delta_{i,4}} \quad (\text{B.29})$$

$$C_{A_{aq,i}^{Z/0}} = \frac{\delta_{i,3}C_{A,0,i}}{\frac{1+K'_1}{\delta_{i,1}\delta_{i,2}} + \frac{1+K'_2}{\delta_{i,2}} + 1 + K'_3 + (1+K'_4)\delta_{i,3} + (1+K'_5)\delta_{i,3}\delta_{i,4}} \quad (\text{B.30})$$

$$C_{A_{aq,i}^-} = \frac{\delta_{i,3}\delta_{i,4}C_{A,0,i}}{\frac{1+K'_1}{\delta_{i,1}\delta_{i,2}} + \frac{1+K'_2}{\delta_{i,2}} + 1 + K'_3 + (1+K'_4)\delta_{i,3} + (1+K'_5)\delta_{i,3}\delta_{i,4}} \quad (\text{B.31})$$

Summation of Eqs. B.27 to B.31 gives Eq. B.32, after division by $C_{A,0,i}$ on both hand sides and the use of Eqs. B.15 and B.16:

$$1 - S_i = \frac{\frac{1}{\delta_{i,1}\delta_{i,2}} + \frac{1}{\delta_{i,2}} + 1 + \delta_{i,3} + \delta_{i,3}\delta_{i,4}}{\frac{1+K'_1}{\delta_{i,1}\delta_{i,2}} + \frac{1+K'_2}{\delta_{i,2}} + 1 + K'_3 + (1+K'_4)\delta_{i,3} + (1+K'_5)\delta_{i,3}\delta_{i,4}} \quad (\text{B.32})$$

Elaborating Eq. B.32 gives Eqs. B.33, $i = 1..5$, which can be solved towards the unknown partition ratios K'_1 , K'_2 , K'_3 , K'_4 and K'_5 :

$$\frac{K'_1}{\delta_{i,1}\delta_{i,2}} + \frac{K'_2}{\delta_{i,2}} + K'_3 + \delta_{i,3}K'_4 + \delta_{i,3}\delta_{i,4}K'_5 = \frac{S_i}{1-S_i} \left(\frac{1}{\delta_{i,1}\delta_{i,2}} + \frac{1}{\delta_{i,2}} + 1 + \delta_{i,3} + \delta_{i,3}\delta_{i,4} \right) \quad (\text{B.33})$$

The partition ratios, as defined by Eqs. B.6 to B.10 are obtained by multiplication of the elements of the solution vector \underline{K}' , by the factor $\frac{V}{m_{cat}}$. A volume of $2.0 \cdot 10^{-1}$ L and an applied catalyst mass of $1.0 \cdot 10^{-4}$ kg_{cat} gives a factor of $2.0 \cdot 10^3$ L kg_{cat}⁻¹.

B.2 Estimation of the partition ratios

Five partition ratios, as given in Fig. B.1, are obtained by regression of Eq. B.33 to the experimental data, obtained in Chapter 2.1, using ODRpack (Boggs et al., 1987). Three replicate experiments are performed at five pH levels, so that fifteen responses ($n_{resp} = 15$) are applied in the fitting procedure. The objective function is defined by Eq. B.34, with L_l and R_l the left and the right hand side in Eq. B.33 for every experimental point l . Due to the difference in order of magnitude \underline{R}_l , normalisation is performed by setting $w_l = R_l^{-2}$ (Himmelblau, 1970):

$$S^* = \sum_{l=1}^{n_{resp}} w_l (R_l - L_l)^2 \quad (\text{B.34})$$

The objective function, S^* , is quadratic in the adsorption parameters, see Eqs. B.33 and B.34. Hence, the obtained minimum for this function is not dependent on the initial guesses for these parameters. The Levenberg-Marquardt method is used for minimization. Every parameter estimate is tested for its statistical significance using its individual t-value, given by Eq. B.35. A parameter is estimated significantly different from zero when its individual t value is higher than the corresponding tabulated value, given by $t_{tab}(n-p; 1-\alpha/2)$. A high individual t value indicates that the model calculations are very sensitive to the corresponding parameter. The corresponding confidence interval is obtained from Eq. B.36, with $V(\underline{b})_{ii}$ the diagonal element on row i of the covariance matrix, given by Eq. B.37. The element on row i and column j of Jacobian matrix, \underline{J} , represents the partial

derivative of response i with respect to parameter j for the reaction conditions of experiment k at the final parameter values.

$$(t_i)_{calc} = \frac{b_i}{\sqrt{V(\underline{b})_{ii}}} \quad (\text{B.35})$$

$$b_i - t_{tab}(n - p, 1 - \frac{\alpha}{2})\sqrt{V(\underline{b})_{ii}} \leq \beta_i \leq b_i + t_{tab}(n - p, 1 - \frac{\alpha}{2})\sqrt{V(\underline{b})_{ii}} \quad (\text{B.36})$$

$$\underline{\underline{V}}(\underline{b}) = (\underline{\underline{J}}^T \underline{\underline{J}})^{-1} \quad (\text{B.37})$$

The global significance of the non-isothermal regression is expressed by Fisher's F test, F_{calc} (Boggs et al., 1987). In this test, the regression sum of squares and the residual sum of squares (RSSQ), S^* , are compared. For a tabulated value of $F_{sig,tab} = 3.6$, a calculated $F_{calc} = 100$ is obtained. Hence, the model is found to be globally significant. Correlation between parameter estimates i and j is verified by means of the binary correlation coefficient, $\rho_{i,j}$, vide Eq. B.38. Absolute values close to unity indicate a strong correlation between the estimates of parameter i and j . A threshold value for very strong correlation is 0.95. In this case, changing parameter i would result in a similar change for parameter j , without altering the RSSQ. In other words, no meaningful parameters are obtained.

$$\rho_{i,j} = \frac{V(\underline{b})_{i,j}}{\sqrt{V(\underline{b})_{i,i} V(\underline{b})_{j,j}}} \quad (\text{B.38})$$

B3 Photo(cata)lytic MOX and CIP degradation profiles

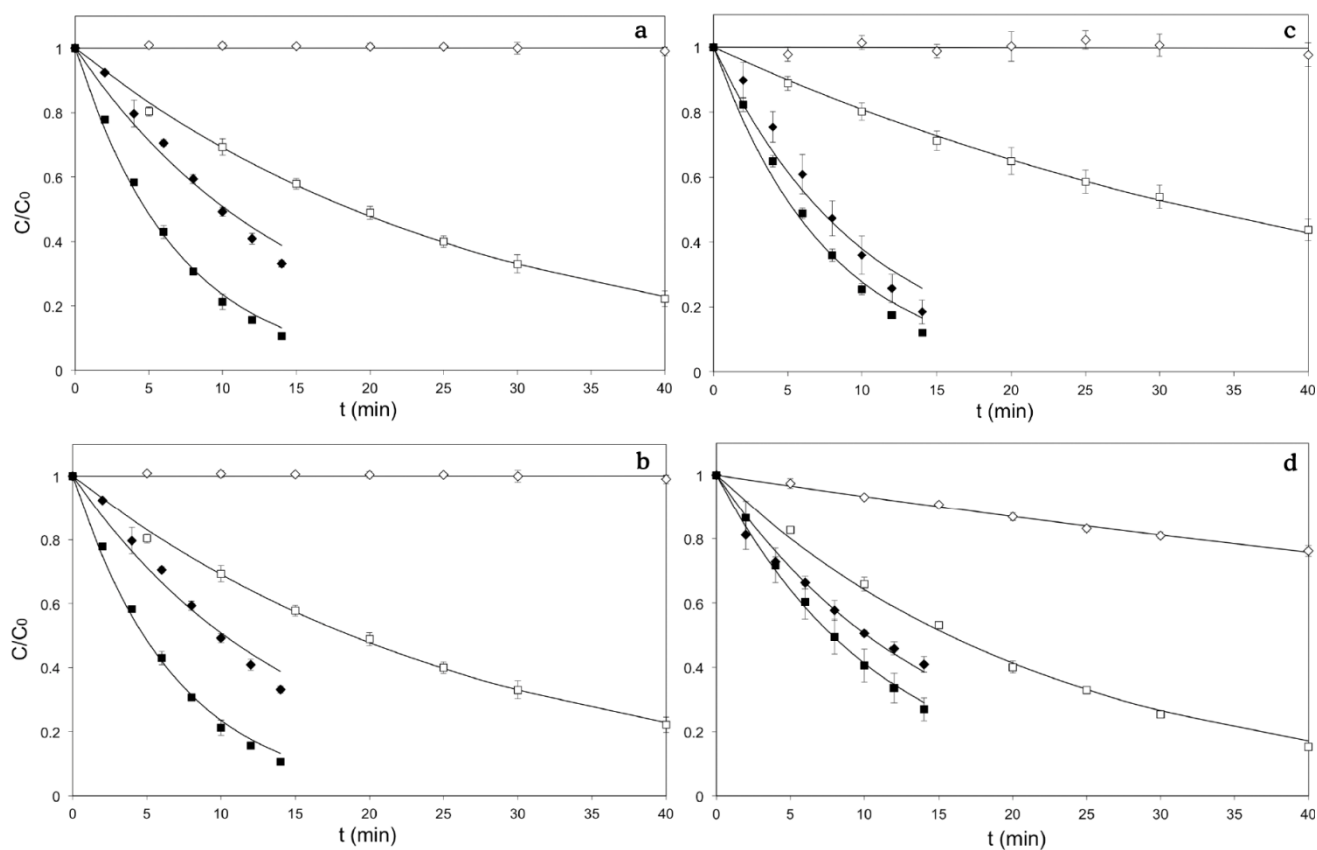


Fig. B.2 Photolytic and photocatalytic degradation of MOX at (a) pH 3.0 and (b) pH 10.0 and CIP at (c) pH 3.0 and (d) pH 10.0, with UV-A (\diamond), UV-C (\square), UV-A TiO₂ (\blacklozenge) and UV-C TiO₂ (\blacksquare) ($n = 3$). Full lines are obtained by regression of Eq. 2.1 to the experimental data.

Addendum C

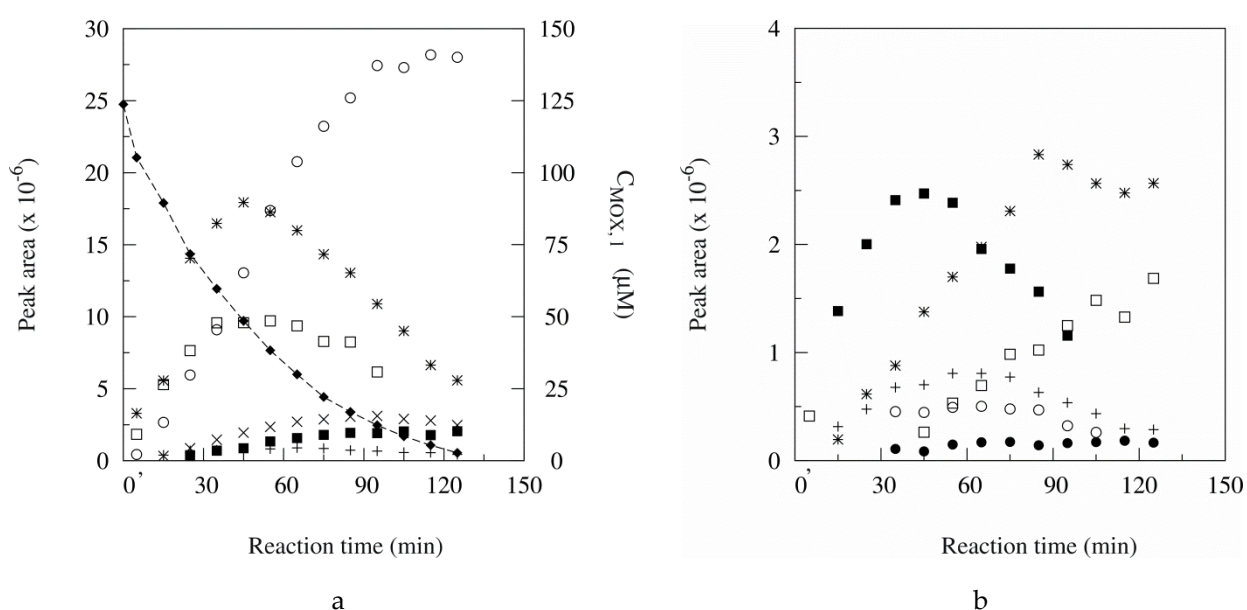


Fig. C.1 (a) Integrated peak areas of the major products in the liquid phase during the photocatalytic degradation of MOX at pH 3.0. Nominal masses (Da) and chromatographic retention time (t_R ; min) are (○) 292, t_R : 23.27 min; (□): 399, t_R : 15.73; (×): 415, t_R : 14.17; (■) 306, t_R : 23.30; (*): 417, t_R : 15.60 and (+): 429, t_R : 11.89 (left y-axis), with (◆): the liquid concentration ($C_{MOX,1}$ $\mu\text{mol L}^{-1}$) of MOX during photocatalytic degradation ($n = 1$; < 1% adsorption; right y-axis). Dashed line is plotted to guide the eye; (b) Integrated peak areas of the minor products in the liquid phase during the photocatalytic degradation of MOX with nominal masses (Da) and chromatographic retention time (t_R ; min) (□) 306, t_R : 22.46; (*): 320, t_R : 20.68; (■): 399, t_R : 16.78; (○): 399, t_R : 20.09; (+) 415, t_R : 16.94 and (●): 429, t_R : 16.95 ($n = 1$).

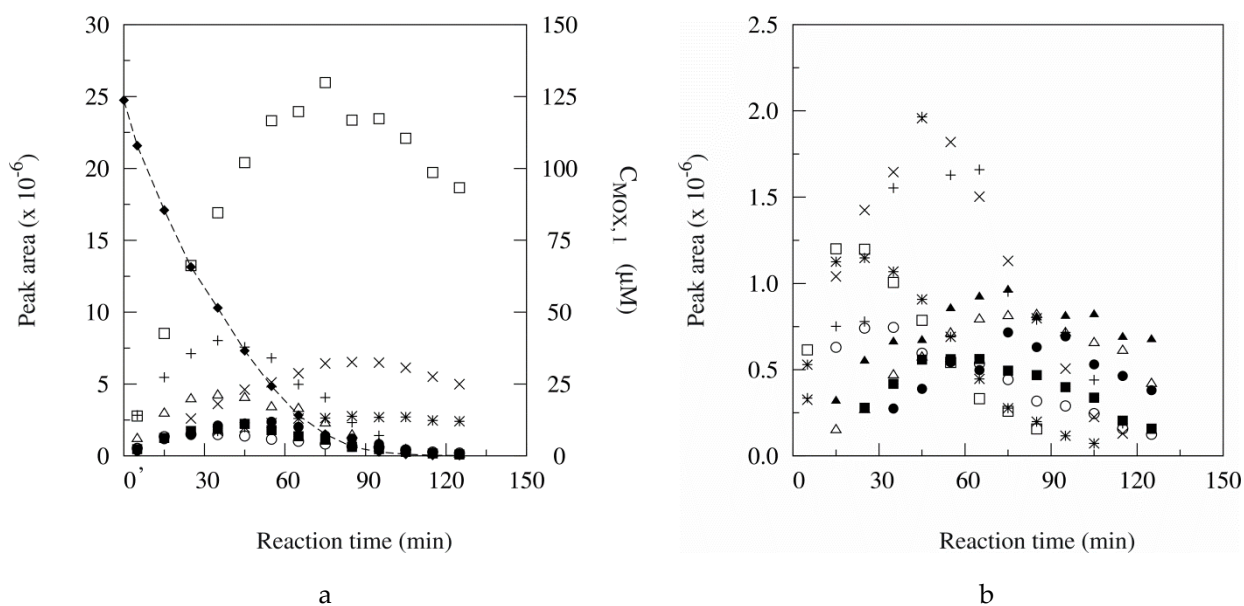


Fig. C.2 (a) Integrated peak areas of the major products in the liquid phase during the photocatalytic degradation of MOX at pH 10.0. Nominal masses (Da) and chromatographic retention time (t_R ; min) are (□) 292, t_R : 23.40 min; (+) 399, t_R : 16.44; (×) 320, t_R : 20.75; (△) 417, t_R : 15.85; (※) 306, t_R : 22.02; (●) 417, t_R : 15.23; (■) 399, t_R : 17.16 and (○) 415, t_R : 24.98 (left y-axis), with (◆): the liquid concentration ($C_{\text{MOX},1}$ $\mu\text{mol L}^{-1}$) of MOX during photocatalytic degradation ($n = 1$; < 1% adsorption; right y-axis). Dashed line is plotted to guide the eye; (b) Integrated peak areas of the minor products in the liquid phase during the photocatalytic degradation of MOX with nominal masses (Da) and chromatographic retention time (t_R ; min) (+) 417, t_R : 14.32; (×) 417, t_R : 13.76; (□) 415, t_R : 17.28; (※) 417, t_R : 17.60; (○) 415, t_R : 24.30; (△): 415, t_R : 10.58; (▲) 306, t_R : 23.33; (●) 415, t_R : 14.32 and (■) 415, t_R : 21.40 ($n = 1$).

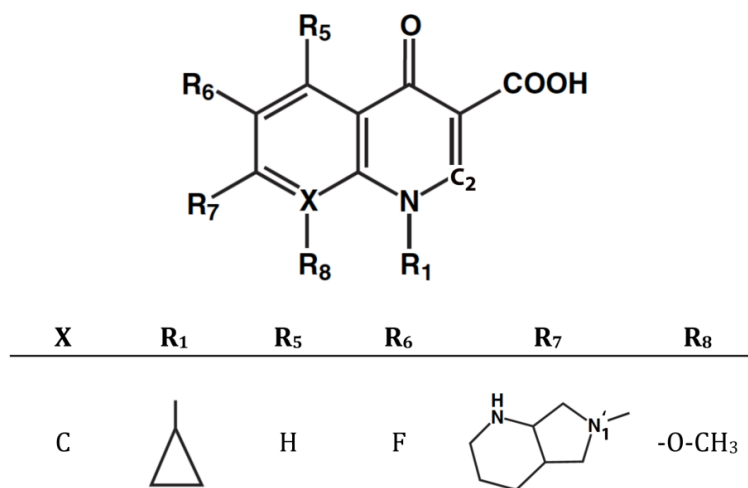


Fig. C.3 General molecular structure of the quinolone moiety with substituents for the fluoroquinolone MOX.

Bibliography

- Adachi, F., Yamamoto, A., Takakura, K.I., Kawahara, R., **2013**. Occurrence of fluoroquinolones and fluoroquinolone-resistance genes in the aquatic environment. *Science of the Total Environment* 444, 508-514.
- Adam, H.J., Schurek, K.N., Nichol, K.A., Hoban, C.J., Baudry, T.J., Laing, N.M., Hoban, D.J., Zhanel, G.G., **2007**. Molecular characterization of increasing fluoroquinolone resistance in *Streptococcus pneumoniae* isolates in Canada, 1997 to 2005. *Antimicrobial Agents and Chemotherapy* 5, 198-207.
- Adriaenssens, N., Coenen, S., Versporten, A., Muller, A., Minalu, G., Faes, C., Vankerckhoven, V., Aerts, M., Hens, N., Molenberghs, G., Goossens, H., **2011**. European Surveillance of Antimicrobial Consumption (ESAC): outpatient quinolone use in Europe (1997-2009). *Journal of Antimicrobial Chemotherapy* 66(6), 47-56.
- Aga, D.S., Batt, A.L., Bruce, I.B., **2006**. Evaluating the vulnerability of surface waters to antibiotic contamination from varying wastewater treatment plant discharges. *Environmental Pollution* 142, 295-302.
- Agrawal, N., Ray, R.S., Farooq, M., Pant, A.B., Hans, R.K., **2007**. Photosensitizing potential of ciprofloxacin at ambient level of UV radiation. *Photochemistry and Photobiology* 83, 1226-1236.
- Ahmed, S., Rasul, M.G., Brown, R., Hashib, M.A., **2011**. Influence of parameters on the heterogeneous photocatalytic degradation of pesticides and phenolic contaminants in wastewater: A short review. *Journal of Environmental Management* 92, 311-330.
- Al Aukidy, M., Verlicchi, P., Jelic, A., Petrovic, M., Barceló, D., **2012**. Monitoring release of pharmaceutical compounds: Occurrence and environmental risk assessment of two WWTP effluents and their receiving bodies in the Po Valley, Italy. *Science of the Total Environment* 438, 15-25.
- Albini, A., Monti, S., **2003**. Photophysics and photochemistry of fluoroquinolones. *Chemical Society Reviews* 32, 238-250.
- Alder, A.C., McArdell, C.S., Golet, M., Kohler, H.P.E., Molnar, E., Anh Pham Thi, N., Siegrist, H., Suter, M.J.F., Giger, W., **2004**. Environmental exposure of antibiotics in wastewaters, sewage sludge and surface waters in Switzerland. Chapter in: *Pharmaceuticals in the environment: Source, fate, effect, and risks*, Springer, Germany.

- Alexander, M., **2000**. Aging, bioavailability, and overestimation of risk from environmental pollutants. *Environmental Science & Technology* 34, 4259-4265.
- Alexiadis, A., Mazzarino, I., **2005**. Design guidelines for fixed-bed photocatalytic reactors. *Chemical Engineering and Processing* 44, 453-459.
- Alexy, R., Sommer, A., Lange, F.T., Kümmerer, K., **2006**. Local use of antibiotics and their input and fate in a small sewage treatment plant - significance of balancing and analysis on a local scale vs. nationwide scale. *Acta Hydrochimica et Hydrobiologica* 34, 587-592.
- Allen, H.K., Donato, J., Wang, H.H., Cloud-Hansen, K.A., Davies, J., Handelsman, J., **2010**. Call of the wild: Antibiotic resistance genes in natural environments. *Nature Reviews Microbiology* 8, 251-259.
- Alovero, F.L., Pan, X.S., Morris, J.E., Manzo, R.H., Fisher, L.M., **2000**. Engineering the specificity of antibacterial fluoroquinolones: Benzenesulfonamide modifications at C-7 of ciprofloxacin change its primary target in *Streptococcus pneumoniae* from topoisomerase IV to gyrase. *Antimicrobial Agents and Chemotherapy* 44(2), 320-325.
- Alrousan, D.M.A., Polo-López, M.I., Dunlop, P.S.M., Fernández-Ibáñez, P., Byrne, J.A., **2012**. Solar photocatalytic disinfection of water with immobilised titanium dioxide in re-circulating flow CPC reactors. *Applied Catalysis B-Environmental* 128, 126-134.
- An, T., Yang, H., Li, G., Song, W., Cooper, W.J., Nie, X., **2010a**. Kinetics and mechanism of advanced oxidation processes (AOPs) in degradation of ciprofloxacin in water. *Applied Catalysis B-Environmental* 94, 288-294.
- An, T., Yang, H., Song, W., Li, G., Luo, H., Cooper, W.J., **2010b**. Mechanistic considerations for the advanced oxidation treatment of fluoroquinolone pharmaceutical compounds using TiO₂ heterogeneous catalysis. *Journal of Physical Chemistry A* 114, 2569-2575.
- Andreozzi, R., Caprio, V., Insola, A., Marotta, R., **1999**. Advanced oxidation processes (AOP) for water purification and recovery. *Catalysis Today* 53, 51-59.
- Andreozzi, R., Raffaele, M., Nicklas, P., **2003**. Pharmaceuticals in STP effluents and their solar photodegradation in aquatic environment. *Chemosphere* 50, 1319-1330.
- Andreu, V., Blasco, C., Picó, Y., **2007**. Analytical strategies to determine quinolone residues in food and the environment. *Trac-Trends in Analytical Chemistry* 26, 534-556.
- Andriole, V.T., **1999**. The future of the quinolones. *Drugs* 58, 1-5.
- Appelbaum, P.C., Hunter, P.A., **2000**. The fluoroquinolone antibacterials: Past, present and future perspectives. *International Journal of Antimicrobial Agents* 16, 5-15.
- AQIS, **2007**. AQIS Imported Food Surveys. Australian Government; Quarantine and Inspection Service.
- Avisar, D., Primor, O., Gozlan, I., Mamane, H., **2009**. Sorption of sulfonamides and tetracyclines to montmorillonite clay. *Water, Air, & Soil Pollution* 209, 439-450.

- Avisar, D., Lester, Y., Mamane, H., **2010**. pH induced polychromatic UV treatment for the removal of a mixture of SMX, OTC and CIP from water. *Journal of Hazardous Materials* 175, 1068-1074.
- Babić, S., Ašperger, D., Mutavdžić, D., Horvat, A.J.M., Kaštelan-Macan, M., **2006**. Solid phase extraction and HPLC determination of veterinary pharmaceuticals in wastewater. *Talanta* 70, 732-738.
- Babić, S., Mutavdžić, D., Ašperger, D., Periša, M., Zrnčić, M., Horvat, A.J.M., Kaštelan-Macan, M., **2010**. Determination of multi-class pharmaceuticals in wastewater by liquid chromatography-tandem mass spectrometry (LC-MS-MS). *Analytical and Bioanalytical Chemistry* 398, 1185-1194.
- Babić, S., Periša, M., Škorić, I., **2013**. Photolytic degradation of norfloxacin, enrofloxacin and ciprofloxacin in various aqueous media. *Chemosphere* 91, 1635-1642.
- Backhaus, T., Scholze, M., Grimme, L.H., **2000**. The single substance and mixture toxicity of quinolones to the bioluminescent bacterium *Vibrio fischeri*. *Aquatic Toxicology* 49, 49-61.
- Bagastyo, A.Y., Radjenovic, J., Mu, Y., Rozendal, R.A., Batstone, D.J., Rabaey, K., **2011**. Electrochemical oxidation of reverse osmosis concentrate on mixed metal oxide (MMO) titanium coated electrodes. *Water Research* 45, 4951-4959.
- Ball, P., **2000**. Quinolone generations: Natural history or natural selection? *Journal of Antimicrobial Chemotherapy* 46, 17-24.
- Barron, L., Havel, J., Purcell, M., Szpak, M., Kelleher, B., Paull, B., **2009**. Predicting sorption of pharmaceuticals and personal care products onto soil and digested sludge using artificial neural networks. *Analyst* 134, 663-670.
- Batt, A.L., Aga, D.S., **2005**. Simultaneous analysis of multiple classes of antibiotics by ion trap LC/MS/MS for assessing surface water and groundwater contamination. *Analytical Chemistry* 77, 2940-2947.
- Batt, A.L., Bruce, I.B., Aga, D.S., **2006**. Evaluating the vulnerability of surface waters to antibiotic contamination from varying wastewater treatment plant discharges. *Environmental Pollution* 142, 295-302.
- Batt, A.L., Kim, S., Aga, D.S., **2007**. Comparison of the occurrence of antibiotics in four full-scale wastewater treatment plants with varying designs and operations. *Chemosphere* 68, 428-435.
- Bayer, **2014**. Safety data sheet Moxifloxacin HCl / Bay 12-8039. Bayer Healthcare.
- Belgiorno, V., Naddeo, V., Rizzo, L., **2011**. Water, wastewater, and soil treatment by Advanced Oxidation Processes (AOPs), SEED, Italy.
- BelVetSac, **2011**. <http://www.belvetsac.ugent.be/pages/home/>, last visited 25/01/2013.
- Berger, A.H., Bhowan, A.S., **2011**. Comparing physisorption and chemisorption solid sorbents for use separating CO₂ from flue gas using temperature swing adsorption. *Energy Procedia* 4, 562-567.

- Bernabeu, A., Vercher, R.F., Santos-Juanes, L., Simón, P.J., Lardín, C., Martínez, M.A., Vicente, J.A., González, R., Llosá, C., Arques, A., Amat, A.M., **2011**. Solar photocatalysis as a tertiary treatment to remove emerging pollutants from wastewater treatment plant effluents. *Catalysis Today* 161, 235-240.
- Blair, B.D., Crago, J.P., Hedman, C.J., Treguer, R.J.F., Magruder, C., Royer, L.S., Klaper, R.D., **2013**. Evaluation of a model for the removal of pharmaceuticals, personal care products, and hormones from wastewater. *Science of the Total Environment* 444, 515-521.
- Boelsteri, U.A., **2003**. *Mechanistic Toxicology: The molecular basis of how chemicals disrupt biological targets*, Taylor & Francis, New York.
- Boggs, P.T., Byrd, R.H., Schnabel, R.B., **1987**. A Stable and efficient algorithm for nonlinear orthogonal distance regression. *Siam Journal on Scientific and Statistical Computing* 8, 1052-1078.
- Bouki, C., Venieri, D., Diamadopoulos, E., **2013**. Detection and fate of antibiotic resistant bacteria in wastewater treatment plants: A review. *Ecotoxicology and Environmental Safety* 91, 1-9.
- Bound, J.P., Voulvoulis, N., **2005**. Household disposal of pharmaceuticals as a pathway for aquatic contamination in the United Kingdom. *Environmental Health Perspectives* 113, 1705-1711.
- Brain, R.A., Hanson, M.L., Solomon, K.R., Brooks, B.W., **2008**. Aquatic plants exposed to pharmaceuticals: Effects and risks. *Reviews of Environmental Contamination and Toxicology* 192, 67-115.
- Brooks, B.W., Huggett, D.B., **2013**. *Human pharmaceuticals in the environment: Current and future perspectives*. Springer, United states of America.
- Brown, K.D., Kulis, J., Thomson, B., Chapman, T.H., Mawhinney, D.B., **2006**. Occurrence of antibiotics in hospital, residential, and dairy, effluent, municipal wastewater, and the Rio Grande in New Mexico. *Science of the Total Environment* 366, 772-783.
- Burhenne, J., Ludwig, M., Nikoloudis, P., Spitteller, M., **1997**. Photolytic degradation of fluoroquinolone carboxylic acids in aqueous solution. 1: Primary photoproducts and half-lives. *Environmental Science and Pollution Research* 4(1), 10-15.
- Butterfield, I.M., Christensen, P.A., Hamnett, A., Shaw, K.E., Walker, G.M., Walker, S.A., Howarth, C.R., **1997**. Applied studies on immobilized titanium dioxide films as catalysts for the photoelectrochemical detoxification of water. *Journal of Applied Electrochemistry* 27, 385-395.
- Buxton, G.V., Greenstock, C.L., Helman, W.P., Ross, A.B., **1988**. Critical review of rate constants for reactions of hydrated electrons, hydrogen atoms and hydroxyl radicals (.OH/.O- in aqueous solution. *Journal of Physical and Chemical Reference Data* 17, 513-886.
- Cabeza, Y., Candela, L., Ronen, D., Teijon, G., **2012**. Monitoring the occurrence of emerging contaminants in treated wastewater and groundwater between 2008 and 2010. The Baix Llobregat (Barcelona, Spain). *Journal of Hazardous Materials* 239-240, 32-39.
- Calamari, D., Zuccato, E., Castiglioni, S., Bagnati, R., Fanelli, R., **2003**. Strategic survey of therapeutic drugs in the rivers Po and Lambro in Northern Italy. *Environmental Science & Technology* 37, 1241-1248.

- Calisto, V., Esteves, V.I., **2009**. Psychiatric pharmaceuticals in the environment. *Chemosphere* 77, 1257-1274.
- Calza, P., Medana, C., Carbone, F., Giancotti, V., Baiocchi, C., **2008**. Characterization of intermediate compounds formed upon photoinduced degradation of quinolones by high-performance liquid chromatography/high-resolution multiple-stage mass spectrometry. *Rapid Communications in Mass Spectrometry* 22, 1533-1552.
- Cañizares, P., Carmona, M., Baraza, O., Delgado, A., Rodrigo, M.A., **2006**. Adsorption equilibrium of phenol onto chemically modified activated carbon F400. *Journal of Hazardous Materials* 131, 243-248.
- Carballa, M., Fink, G., Omil, F., Lema, J.M., Ternes, T., **2008**. Determination of the solid-water distribution coefficient (K_d) for pharmaceuticals, estrogens and musk fragrances in digested sludge. *Water Research* 42, 287-295.
- Carbonaro, S., Sugihara, M.N., Strathmann, T.J., **2013**. Continuous-flow photocatalytic treatment of pharmaceutical micropollutants: Activity, inhibition, and deactivation of TiO₂ photocatalysts in wastewater effluent. *Applied Catalysis B-Environmental* 129, 1-12.
- Carlsson, G., Örn, S., Larsson, D.G.J., **2009**. Effluent from bulk drug production is toxic to aquatic vertebrates. *Environmental Toxicology and Chemistry* 28(12), 2656-2662.
- Carmosini, N., Lee, L.S., **2009**. Ciprofloxacin sorption by dissolved organic carbon from reference and bio-waste materials. *Chemosphere* 77, 813-820.
- Carp, O., Huisman, C.L., Reller, A., **2004**. Photoinduced reactivity of titanium dioxide. *Progress in Solid State Chemistry* 32, 33-177.
- Castiglioni, S., Bagnati, R., Calamari, D., Fanelli, R., Zuccato, E., **2005**. A multiresidue analytical method using solid-phase extraction and high-pressure liquid chromatography tandem mass spectrometry to measure pharmaceuticals of different therapeutic classes in urban wastewaters. *Journal of Chromatography A* 1092, 206-215.
- Castiglioni, S., Bagnati, R., Fanelli, R., Pomati, F., Calamari, D., Zuccato, E., **2006**. Removal of pharmaceuticals in sewage treatment plants in Italy. *Environmental Science & Technology* 40, 357-363.
- Chapman, J.S., Georgopadakou, N.H., **1988**. Routes of quinolone permeation in *Escherichia coli*. *Antimicrobial Agents and Chemotherapy* 32(4), 438-442.
- Chen, H.Y., Zahraa, O., Bouchy, M., **1997**. Inhibition of the adsorption and photocatalytic degradation of an organic contaminant in an aqueous suspension of TiO₂ by inorganic ions. *Journal of Photochemistry and Photobiology A: Chemistry* 108, 37-44.
- Chen, Y., Yang, S., Wang, K., Lou, L., **2005**. Role of primary active species and TiO₂ surface characteristic in UV-illuminated photodegradation of Acid Orange 7. *Journal of Photochemistry and Photobiology A: Chemistry* 172, 47-54.
- Chenxi, W., Spongberg, A.L., Witter, J.D., **2008**. Determination of the persistence of pharmaceuticals in biosolids using liquid-chromatography tandem mass spectrometry. *Chemosphere* 73, 511-518.

- Chiron, S., Fernandez-Alba, A., Rodriguez, A., Garcia-Cavo, E., **2000**. Pesticide chemical oxidation: State-of-the-art. *Water Research* 34, 366-377.
- Chong, M.N., Jin, B., Chow, C.W.K., Saint, C., **2010**. Recent developments in photocatalytic water treatment technology: A review. *Water Research* 44, 2997-3027.
- Christian, T., Schneider, R.J., Färber, H.A., Skutlarek, D., Meyer, M.T., Goldbach, H.E., **2003**. Determination of antibiotic residues in manure, soil, and surface waters. *Acta Hydrochimica et Hydrobiologica* 31, 36-44.
- Chu, D.T.W., Fernandes, P.B., **1989**. Structure-activity relationships of the fluoroquinolones. *Antimicrobial Agents and Chemotherapy* 33(2), 131-135.
- Coetsier, C.M., Spinelli, S., Lin, L., Roig, B., Touraud, E., **2009**. Discharge of pharmaceutical products (PPs) through a conventional biological sewage treatment plant: MECs vs PECs? *Environment International* 35, 787-792.
- Collignon, P., Powers, J.H., Chiller, T.M., Aidara-Kane, A., Aarestrup, F.M., **2009**. World Health Organization ranking of antimicrobials according to their importance in human medicine: a critical step for developing risk management strategies for the use of antimicrobials in food production animals. *Clinical Infectious Diseases* 49, 132-141.
- Conkle, J.L., Lattao, C., White, J.R., Cook, R.L., **2010**. Competitive sorption and desorption behavior for three fluoroquinolone antibiotics in a wastewater treatment wetland soil. *Chemosphere* 80, 1353-1359.
- Conley, J.M., Symes, S.J., Schorr, M.S., Richards, S.M., **2008**. Spatial and temporal analysis of pharmaceutical concentrations in the upper Tennessee river basin. *Chemosphere* 73, 1178-1187.
- Cordova-Kreylos, A.L., Scow, K.M., **2007**. Effects of ciprofloxacin on salt marsh sediment microbial communities. *Isme Journal* 1, 585-595.
- Cosa, G., **2004**. Photodegradation and photosensitization in pharmaceutical products: Assessing drug phototoxicity. *Pure and Applied Chemistry* 76(2), 263-275.
- Costanzo, S.D., Murby, J., Bates, J., **2005**. Ecosystem response to antibiotics entering the aquatic environment. *Marine Pollution Bulletin* 51, 218-223.
- Cui, J., Zhang, K., Huang, Q., Yu, Y., Peng, X., **2011**. An indirect competitive enzyme-linked immunosorbent assay for determination of norfloxacin in waters using a specific polyclonal antibody. *Analytica Chimica Acta* 688, 84-89.
- Daghrir, R., Drogui, P., Robert, D., **2013**. Modified TiO₂ for environmental photocatalytic applications: A review. *Industrial & Engineering Chemistry Research* 52, 3581-3599.
- Dalkmann, P., Broszat, M., Siebe, C., Willaschek, E., Sakinc, T., Huebner, J., Amelung, W., Grohmann, E., Siemens, J., **2012**. Accumulation of pharmaceuticals, Enterococcus, and resistance genes in soils irrigated with wastewater for zero to 100 years in central Mexico. *Plos One* 7 (9), 1-9.

- De Bel, E., Dewulf, J., De Witte, B., Van Langenhove, H., Janssen, C., **2009**. Influence of pH on the sonolysis of ciprofloxacin: Biodegradability, ecotoxicity and antibiotic activity of its degradation products. *Chemosphere* 77, 291-295.
- De la Cruz, N., Giménez, J., Esplugas, S., Grandjean, D., de Alencastro, L.F., Pulgarín, C., **2012**. Degradation of 32 emergent contaminants by UV and neutral photo-fenton in domestic wastewater effluent previously treated by activated sludge. *Water Research* 46, 1947-1957.
- De Morgen, **2012**. Dieren slikken opnieuw meer antibiotica. Article published on 02/10/2012.
- De Standaard, **2012**. 1 miljoen meer doosjes antibiotica verkocht. Article published on 24/02/2012.
- De Witte, B., Dewulf, J., Demeestere, K., De Ruyck, M., Van Langenhove, H., **2007**. Critical points in the analysis of ciprofloxacin by high-performance liquid chromatography. *Journal of Chromatography A* 1140, 126-130.
- De Witte, B., Dewulf, J., Demeestere, K., De Vyvere, V., De Wispelaere, P., Van Langenhove, H., **2008**. Ozonation of ciprofloxacin in water: HRMS identification of reaction products and pathways. *Environmental Science & Technology* 42, 4889-4895.
- De Witte, B., Dewulf, J., Demeestere, K., Van Langenhove, H., **2009a**. Ozonation and advanced oxidation by the peroxone process of ciprofloxacin in water. *Journal of Hazardous Materials* 161, 701-708.
- De Witte, B., Van Langenhove, H., Hemelsoet, K., Demeestere, K., De Wispelaere, P., Van Speybroeck, V., Dewulf, J., **2009b**. Levofloxacin ozonation in water: Rate determining process parameters and reaction pathway elucidation. *Chemosphere* 76, 683-689.
- De Witte, B., Van Langenhove, H., Demeestere, K., Saerens, K., De Wispelaere, P., Dewulf, J., **2010**. Ciprofloxacin ozonation in hospital wastewater treatment plant effluent: Effect of pH and H₂O₂. *Chemosphere* 78, 1142-1147.
- De Witte, B., Van Langenhove, H., Demeestere, K., Dewulf, J., **2011**. Advanced oxidation of pharmaceuticals: Chemical analysis and biological assessment of degradation products. *Critical Reviews in Environmental Science and Technology* 41, 215-242.
- Deblonde, T., Cossu-Leguille, C., Hartemann, P., **2011**. Emerging pollutants in wastewater: A review of the literature. *International Journal of Hygiene and Environmental Health* 214, 442-448.
- Demeestere, K., Dewulf, J., Van Langenhove, H., Sercu, B., **2003**. Gas-solid adsorption of selected volatile organic compounds on titanium dioxide Degussa P25. *Chemical Engineering Science* 58, 2255-2267.
- Demeestere, K., Dewulf, J., Van Langenhove, H., **2007**. Heterogeneous photocatalysis as an advanced oxidation process for the abatement of chlorinated, monocyclic aromatic and sulfurous volatile organic compounds in air: State of the art. *Critical Reviews in Environmental Science and Technology* 37, 489-538.

- Dimitroula, H., Daskalaki, V.M., Frontistis, Z., Kondarides, D.I., Panagiotopoulou, P., Xekoukoulotakis, N.P., Mantzavinos, D., **2012**. Solar photocatalysis for the abatement of emerging micro-contaminants in wastewater: Synthesis, characterization and testing of various TiO₂ samples. *Applied Catalysis B-Environmental* 117-118, 283-291.
- Dinh, Q.T., Alliot, F., Moreau-Guigon, E., Eurin, J., Chevreuil, M., Labadie, P., **2011**. Measurement of trace levels of antibiotics in river water using on-line enrichment and triple-quadrupole LC-MS/MS. *Talanta* 85, 1238-1245.
- Dodd, M.C., Kohler, H.P.E., Von Gunten, U., **2009**. Oxidation of antibacterial compounds by ozone and hydroxyl radical: Elimination of biological activity during aqueous ozonation processes. *Environmental Science & Technology* 43, 2498-2504.
- Dolar, D., Gros, M., Rodriguez-Mozaz, S., Moreno, J., Comas, J., Rodriguez-Roda, I., Barceló, D., **2012**. Removal of emerging contaminants from municipal wastewater with an integrated membrane system, MBR-RO. *Journal of Hazardous Materials* 239-240, 64-69.
- Doll, T.E., Frimmel, F.H., **2004**. Kinetic study of photocatalytic degradation of carbamazepine, clofibrac acid, iomeprol and iopromide assisted by different TiO₂ materials - determination of intermediates and reaction pathways. *Water Research* 38, 955-964.
- Doll, T.E., Frimmel, F.H., **2005**. Cross-flow microfiltration with periodical back-washing for photocatalytic degradation of pharmaceutical and diagnostic residues-evaluation of the long-term stability of the photocatalytic activity of TiO₂. *Water Research* 39, 847-854.
- Dorival-García, N., Zafra-Gómez, A., Navalón, A., González, J., Vílchez, J.L., **2012**. Removal of quinolone antibiotics from wastewaters by sorption and biological degradation in laboratory-scale membrane bioreactors. *Science of the Total Environment* 442, 317-328.
- Dorival-García, N., Zafra-Gómez, A., Cantarero, S., Navalón, A., Vílchez, J.L., **2013a**. Simultaneous determination of 13 quinolone antibiotic derivatives in wastewater samples using solid-phase extraction and ultra performance liquid chromatography-tandem mass spectrometry. *Microchemical Journal* 106, 323-333.
- Dorival-García, N., Zafra-Gómez, A., Navalón, A., González, J., Hontoria, E., Vílchez, J.L., **2013b**. Removal and degradation characteristics of quinolone antibiotics in laboratory-scale activated sludge reactors under aerobic, nitrifying and anoxic conditions. *Journal of Environmental Management* 120, 75-83.
- Drakopoulos, A.I., Ioannou, P.C., **1997**. Spectrofluorimetric study of the acid-base equilibria and complexation behavior of the fluoroquinolone antibiotics ofloxacin, norfloxacin, ciprofloxacin and pefloxacin in aqueous solution. *Analytica Chimica Acta* 354, 197-204.
- Drillia, P., Stamatelatos, K., Lyberatos, G., **2005**. Fate and mobility of pharmaceuticals in solid matrices. *Chemosphere* 60, 1034-1044.
- Drugbank, <http://www.drugbank.ca/drugs/DB01208>, last visited 03/02/2014.
- Du, L.F., Liu, W.K., **2012**. Occurrence, fate, and ecotoxicity of antibiotics in agro-ecosystems: A review. *Agronomy for Sustainable Development* 32, 309-327.

- Dufresne, G., Fouquet, A., Forsyth, D., Tittlemier, S.A., **2007**. Multiresidue determination of quinolone and fluoroquinolone antibiotics in fish and shrimp by liquid chromatography/tandem mass spectrometry. *Journal of AOAC International* 90(2), 604-612.
- Duong, H.A., Pham, N.H., Nguyen, H.T., Hoang, T.T., Pham, H.V., Pham, V.C., Berg, M., Giger, W., Alder, A.C., **2008**. Occurrence, fate and antibiotic resistance of fluoroquinolone antibacterials in hospital wastewaters in Hanoi, Vietnam. *Chemosphere* 72, 968-973.
- Ebert, I., Bachmann, J., Kühnen, U., Küster, A., Kussatz, C., Maletzki, D., Schlüter, C., **2011**. Toxicity of the fluoroquinolone antibiotics enrofloxacin and ciprofloxacin to photoautotrophic aquatic organisms. *Environmental Toxicology and Chemistry* 30(12), 2786-2792.
- EC, **2012**. http://europa.eu/rapid/press-release_IP-12-88_en.htm, last visited 10/02/2014.
- EC, **2013**. www.europarl.europa.eu/news/en/news-room/content/20130701IPR14760/html/Surface-waters-12-new-controlled-chemicals-three-pharmaceuticals-on-watch-list, last visited 10/02/2014.
- ECDC, **2010**. www.ecdc.europa.eu/en/healthtopics/antimicrobial_resistance/pages/index.aspx, last visited 08/01/2014.
- Efpia, **2013**. www.efpia.eu/uploads/Figures_Key_Data_2013.pdf, last visited 13/02/2014.
- El Najjar, N.H., Deborde, M., Journal, R., Leitner, N.K.V., **2013**. Aqueous chlorination of levofloxacin: Kinetic and mechanistic study, transformation product identification and toxicity. *Water Research* 47, 121-129.
- Elmolla, E.S., Chaudhuri, M., **2010**. Photocatalytic degradation of amoxicillin, ampicillin and cloxacillin antibiotics in aqueous solution using UV/TiO₂ and UV/H₂O₂/TiO₂ photocatalysis. *Desalination* 252, 46-52.
- EMA, <http://www.ema.europa.eu/ema>, last visited 03/02/2014.
- Emmanuel, E., Keck, G., Blanchard, J.M., Vermande, P., Perrodin, Y., **2004**. Toxicological effects of disinfections using sodium hypochlorite on aquatic organisms and its contribution to AOX formation in hospital wastewater. *Environment International* 30, 891-900.
- EOS, 2012. Die-hard bacteriën. Article published on 12/07/2012.
- ESA, <http://ecls.esa.int/ecls/?p=newmelissaloop>, last visited 23/01/2014.
- ESAC, **2010**. www.ecdc.europa.eu/en/publications/Publications/1111_SUR_AMR_data.pdf, last visited 25/01/2014.
- Escher, B.I., Baumgartner, R., Koller, M., Treyer, K., Lienert, J., McArdell, C.S., **2011**. Environmental toxicology and risk assessment of pharmaceuticals from hospital wastewater. *Water Research* 45, 75-92.
- Esplugas, S., Bila, D.M., Krause, L.G.T., Dezotti, M., **2007**. Ozonation and advanced oxidation technologies to remove endocrine disrupting chemicals (EDCs) and pharmaceuticals and personal care products (PPCPs) in water effluents. *Journal of Hazardous Materials* 149, 631-642.

- EUROSTAT, <http://epp.eurostat.ec.europa.eu/portal/page/portal/eurostat/home/>, last visited 02/03/2014.
- Evgenidou, E., Fytianos, K., Poullos, I., **2005a**. Photocatalytic oxidation of dimethoate in aqueous solutions. *Journal of Photochemistry and Photobiology A: Chemistry* 175, 29-38.
- Evgenidou, E., Fytianos, K., Poullos, I., **2005b**. Semiconductor-sensitized photodegradation of dichlorvos in water using TiO₂ and ZnO as catalysts. *Applied Catalysis B-Environmental* 59, 81-89.
- Fatta-Kassinos, D., Meric, S., Nikolaou, A., **2011**. Pharmaceutical residues in environmental waters and wastewater: Current state of knowledge and future research. *Analytical and Bioanalytical Chemistry* 399, 251-275.
- FDA, <http://www.fda.gov/ucm/groups/fdagov-public/@fdagov-av-gen/documents/document/ucm072389.pdf>, last visited 03/02/2014.
- Feitosa-Felizzola, J., Chiron, S., **2009**. Occurrence and distribution of selected antibiotics in a small Mediterranean stream (Arc river, Southern France). *Journal of Hydrology* 364, 50-57.
- Fent, K., Weston, A.A., Caminada, D., **2006**. Ecotoxicology of human pharmaceuticals. *Aquatic Toxicology* 76, 122-159.
- Ferdig, M., Kaleta, A., Buchberger, W., **2005**. Improved liquid chromatographic determination of nine currently used (fluoro)quinolones with fluorescence and mass spectrometric detection for environmental samples. *Journal of Separation Science* 28, 1448-1456.
- Fernández-Ibáñez, P., Blanco, J., Malato, S., de las Nieves, F.J., **2003**. Application of the colloidal stability of TiO₂ particles for recovery and reuse in solar photocatalysis. *Water Research* 37, 3180-3188.
- Fick, J., Söderstrom, H., Lindberg, R.H., Phan, C., Tysklind, M., Larsson, D.G.J., **2009**. Contamination of surface, ground, and drinking water from pharmaceutical production. *Environmental Toxicology and Chemistry* 28(12), 2522-2527.
- Fisk, P., **2013**. *Chemical Risk Assessment: A manual for REACH*. Wiley, United Kingdom
- Figueroa-Diva, R.A., Vasudevan, D., MacKay, A.A., **2010**. Trends in soil sorption coefficients within common antimicrobial families. *Chemosphere* 79, 786-793.
- Fisher, M.B., Keane, D.A., Fernández-Ibáñez, P., Colreavy, J., Hinder, S.J., McGuigan, K.G., Pillai, S.C., **2013**. Nitrogen and copper doped solar light active TiO₂ photocatalysts for water decontamination. *Applied Catalysis B-Environmental* 130-131, 8-13.
- Foo, K.Y., Hameed, B.H., **2009**. An overview of landfill leachate treatment via activated carbon adsorption process. *Journal of Hazardous Materials* 171, 54-60.
- Fresta, M., Guccione, S., Beccari, A.R., Furneri, P.M., Puglisi, G., **2002**. Combining molecular modeling with experimental methodologies: Mechanisms of membrane permeation and accumulation of ofloxacin. *Bioorganic & Medicinal Chemistry* 10, 3871-3889.

- Gad-Allah, T.A., Ali, M.E.M., Badawy, M.I., **2011**. Photocatalytic oxidation of ciprofloxacin under simulated sunlight. *Journal of Hazardous Materials* 186, 751-755.
- Gao, L., Shi, Y., Li, W., Niu, H., Liu, J., Cai, Y., **2012a**. Occurrence of antibiotics in eight sewage treatment plants in Beijing, China. *Chemosphere* 86, 665-671.
- Gao, L., Shi, Y., Li, W., Liu, J., Cai, Y., **2012b**. Occurrence, distribution and bioaccumulation of antibiotics in the Haihe river in China. *Journal of Environmental Monitoring* 14, 1247-1254.
- Garcia, N., Moreno, J., Cartmell, E., Rodriguez-Roda, I., Judd, S., **2013**. The application of microfiltration-reverse osmosis/nanofiltration to trace organics removal for municipal wastewater reuse. *Environmental Technology* 34, 3183-3189.
- Gavrilescu, M., Caliman, F.A., **2009**. Pharmaceuticals, personal care products and endocrine disrupting agents in the environment - A review. *Clean-Soil, Air, Water* 37, 277-303.
- Ge, L., Chen, J., Wei, X., Zhang, S., Qiao, X., Cai, X., Xie, Q., **2010a**. Aquatic photochemistry of fluoroquinolone antibiotics: Kinetics, pathways, and multivariate effects of main water constituents. *Environmental Science & Technology* 44, 2400-2405.
- Ge, L., Chen, J., Zhang, S., Cai, X., Wang, Z., Wang, C., **2010b**. Photodegradation of fluoroquinolone antibiotic gatifloxacin in aqueous solutions. *Chinese Science Bulletin* 55(15), 1495-1500.
- Geng, M., Duan, Z., **2010**. Prediction of oxygen solubility in pure water and brines up to high temperatures and pressures. *Geochimica et Cosmochimica Acta* 74, 5631-5640.
- Ghosh, G.C., Okuda, T., Yamashita, N., Tanaka, H., **2009**. Occurrence and elimination of antibiotics at four sewage treatment plants in Japan and their effects on bacterial ammonia oxidation. *Water Science and Technology* 59(4), 779-786.
- Giguère, S., Prescott, J.F., Dowling, P.M., **2013**. *Antimicrobial therapy in veterinary medicine*, Fifth Edition, John Wiley & Sons, United States of America.
- Ginebreda, A., Muñoz, I., López de Alda, M., Brix, R., López-Doval, J., Barceló, D., **2010**. Environmental risk assessment of pharmaceuticals in rivers: Relationships between hazard indexes and aquatic macroinvertebrate diversity indexes in the Llobregat river (NE Spain). *Environment International* 36, 153-162.
- Giraldo, A.L., Peñuela, G.A., Torres-Palma, R.A., Pino, N.J., Palominos, R.A., Mansilla, H.D., **2010**. Degradation of the antibiotic oxolinic acid by photocatalysis with TiO₂ in suspension. *Water Research* 44, 5158-5167.
- Girardi, C., Greve, J., Lamshoeft, M., Fetzer, I., Miltner, A., Schaeffer, A., Kaestner, M., **2011**. Biodegradation of ciprofloxacin in water and soil and its effects on the microbial communities. *Journal of Hazardous Materials* 198, 22-30.
- Glaze, W.H., Kang, J.W., Chapin, D.H., **1987**. The chemistry of water treatment processes involving ozone, hydrogen peroxide, and ultraviolet radiation. *Ozone Science and Engineering* 9, 335-352.

- Golet, E.M., Alder, A.C., Hartmann, A., Ternes, T.A., Giger, W., **2001**. Trace determination of fluoroquinolone antibacterial agents in solid-phase extraction urban wastewater by and liquid chromatography with fluorescence detection. *Analytical Chemistry* 73, 3632-3638.
- Golet, E.M., Alder, A.C., Giger, W., **2002a**. Environmental exposure and risk assessment of fluoroquinolone antibacterial agents in wastewater and river water of the Glatt valley watershed, Switzerland. *Environmental Science & Technology* 36(17), 3645-3651.
- Golet, E.M., Strehler, A., Alder, A.C., Giger, W., **2002b**. Determination of fluoroquinolone antibacterial agents in sewage sludge and sludge-treated soil using accelerated solvent extraction followed by solid-phase extraction. *Analytical Chemistry* 74, 5455-5462.
- Golet, E.M., Xifra, I., Siegrist, H., Alder, A.C., Giger, W., **2003**. Environmental exposure assessment of fluoroquinolone antibacterial agents from sewage to soil. *Environmental Science & Technology* 37(15), 3243-3249.
- González-Pleiter, M., Gonzalo, S., Rodea-Palomares, I., Leganés, F., Rosal, R., Boltes, K., Marco, E., Fernández-Piñas, F., **2013**. Toxicity of five antibiotics and their mixtures towards photosynthetic aquatic organisms: Implications for environmental risk assessment. *Water Research* 47, 2050-2064.
- Gottschall, N., Topp, E., Metcalfe, C., Edwards, M., Payne, M., Kleywegt, S., Russell, P., Lapen, D.R., **2012**. Pharmaceutical and personal care products in groundwater, subsurface drainage, soil, and wheat grain, following a high single application of municipal biosolids to a field. *Chemosphere* 87, 194-203.
- Gracia-Lor, E., Sancho, J.V., Serrano, R., Hernández, F., **2012**. Occurrence and removal of pharmaceuticals in wastewater treatment plants at the Spanish Mediterranean area of Valencia. *Chemosphere* 87, 453-462.
- Grave, K., Greko, C., Kvaale, M.K., Torren-Edo, J., Mackay, D., Muller A., Moulin, G., **2012**. Sales of veterinary antibacterial agents in nine European countries during 2005-09: Trends and patterns. *Journal of Antimicrobial Chemotherapy* 67, 3001-3008.
- Gros, M., Petrović, M., Barceló, D., **2007**. Wastewater treatment plants as a pathway for aquatic contamination by pharmaceuticals in the Ebro river basin (Northeast Spain). *Environmental Toxicology and Chemistry* 26(8), 1553-1562.
- Gros, M., Petrović, M., Barceló, D., **2009**. Tracing pharmaceutical residues of different therapeutic classes in environmental waters by using liquid chromatography/quadrupole-linear ion trap mass spectrometry and automated library searching. *Analytical Chemistry* 81, 898-912.
- Gros, M., Petrović, M., Ginebreda, A., Barceló, D., **2010**. Removal of pharmaceuticals during wastewater treatment and environmental risk assessment using hazard indexes. *Environment International* 36, 15-26.
- Grung, M., Källqvist, T., Sakshaug, S., Skurtveit, S., Thomas, K.V., **2008**. Environmental assessment of Norwegian priority pharmaceuticals based on the EMEA guideline. *Ecotoxicology and Environmental Safety* 71, 328-340.
- Guillard, C., Puzenat, E., Lachheb, H., Houas, A., Herrmann, J.M., **2005**. Why inorganic salts decrease the TiO₂ photocatalytic efficiency. *International Journal of Photoenergy* 7, 1-9.

- Guinea, E., Antonio Garrido, J., María Rodríguez, R., Cabot, P.L., Arias, C., Centellas, F., Brillas, E., **2010**. Degradation of the fluoroquinolone enrofloxacin by electrochemical advanced oxidation processes based on hydrogen peroxide electrogeneration. *Electrochimica Acta* 55, 2101-2115.
- Gulkowska, A., He, Y.H., So, M.K., Yeung, L.W.Y., Leung, H.W., Giesy, J.P., Lam, P.K.S., Martin, M., Richardson, B.J., **2007**. The occurrence of selected antibiotics in Hong Kong coastal waters. *Marine Pollution Bulletin* 54, 1287-1293.
- Gulkowska, A., Leung, H.W., So, M.K., Taniyasu, S., Yamashita, N., Yeung, L.W.Y., Richardson, B.J., Lei, A.P., Giesy, J.P., Lam, P.K.S., **2008**. Removal of antibiotics from wastewater by sewage treatment facilities in Hong Kong and Shenzhen, China. *Water Research* 42, 395-403.
- Halling-Sørensen, B., Lützhøft, H.C.H., Andersen, H.R., Ingerslev, F., **2000**. Environmental risk assessment of antibiotics: Comparison of mecillinam, trimethoprim and ciprofloxacin. *Journal of Antimicrobial Chemotherapy* 46, 53-58.
- Hamad, B., **2010**. The antibiotics market. *Nature Reviews Drug Discovery* 9, 675.
- Han, F., Kambala, V.S.R., Srinivasan, M., Rajarthnam, D., Naidu, R., **2009**. Tailored titanium dioxide photocatalysts for the degradation of organic dyes in wastewater treatment: A review. *Applied Catalysis A-General* 359, 25-40.
- Hapeshi, E., Achilleos, A., Vasquez, M.I., Michael, C., Xekoukoulotakis, N.P., Mantzavinos, D., Kassinos, D., **2010**. Drugs degrading photocatalytically: Kinetics and mechanisms of ofloxacin and atenolol removal on titania suspensions. *Water Research* 44, 1737-1746.
- Haque, M.M., Muneer, M., **2007**. Photodegradation of norfloxacin in aqueous suspensions of titanium dioxide. *Journal of Hazardous Materials* 145, 51-57.
- Hari, A.C., Paruchuri, R.A., Sabatini, D.A., Kibbey, T.C.G., **2005**. Effects of pH and cationic and nonionic surfactants on the adsorption of pharmaceuticals to a natural aquifer material. *Environmental Science & Technology* 39, 2592-2598.
- Hartmann, A., Alder, A.C., Koller, T., Widmer, R.M., **1998**. Identification of fluoroquinolone antibiotics as the main source of umuC genotoxicity in native hospital wastewater. *Environmental Toxicology and Chemistry* 17(3), 377-382.
- Hatchard, C.G., Parker, C.A., **1956**. A new sensitive chemical actinometer. II. potassium ferrioxalate as a standard chemical actinometer. *Proceedings of the Royal Society of London. Series A, Mathematical and Physical Sciences* 235, 518-536.
- He, X., Wang, Z., Nie, X., Yang, Y., Pan, D., Leung, A.W., Cheng, Z., Yang, Y., Li, K., Chen, K., **2012**. Residues of fluoroquinolones in marine aquaculture environment of the Pearl river delta, South China. *Environmental Geochemistry and Health* 34, 323-335.
- Hendrickx, L., Mergaey, M. **2007**. From the deep sea to the stars: human life support through minimal communities. *Current opinion in microbiology* 10, 231-237.
- Hernández-Borrell, J., Montero, M.T., **1997**. Calculating microspecies concentration of zwitterion amphoteric compounds: Ciprofloxacin as example. *Journal of Chemical Education* 74(11), 1311-1314.

- Herrmann, J.M., Pichat, P., **1980**. Heterogeneous photocatalysis - oxidation of halide-ions by oxygen in ultraviolet irradiated aqueous suspension of titanium-dioxide. *Journal of the Chemical Society-Faraday Transactions I* 76, 1138-1146.
- Herrmann, J.M., **1999**. Heterogeneous photocatalysis: Fundamentals and applications to the removal of various types of aqueous pollutants. *Catalysis Today* 53, 115-129.
- Herrmann, J.M., **2005**. Heterogeneous photocatalysis: State of the art and present applications. *Topics in Catalysis* 34, 49-65.
- Herrmann, J.M., **2010**. Photocatalysis fundamentals revisited to avoid several misconceptions. *Applied Catalysis B-Environmental* 99, 461-468.
- Het Nieuwsblad, **2012a**. Ziekenhuisbacterie MRSA krijgt concurrentie. Article published on 17/11/2012.
- Het Nieuwsblad, **2012b**. België koploper in antibiotica gebruik. Article published on 17/11/2012.
- Hey, G., **2013**. Application of chemical oxidation processes for the removal of pharmaceuticals in biologically treated wastewater. PhD dissertation Lund University. <http://lup.lub.lu.se/luur/download?func=downloadFile&recordOId=3412268&fileOId=3412272>, last visited on 02/05/2014.
- Himmelblau, D.M., **1970**. *Process analysis by statistical methods*, Wiley, Unites States of America.
- HLN, **2012**. België blijft meeste antibiotica bij dieren gebruiken. Article published on 23/01/2012.
- Hollender, J., Zimmermann, S.G., Koepke, S., Krauss, M., McArdell, C.S., Ort, C., Singer, H., von Gunten, U., Siegrist, H., **2009**. Elimination of organic micropollutants in a municipal wastewater treatment plant upgraded with a full-scale post-ozonation followed by sand filtration. *Environmental Science & Technology* 43, 7862-7869.
- Holmström, K., Gräslund, S., Wahlström, A., Pongshompoo, S., Bengtsson, B.E., Kautsky, N., **2003**. Antibiotic use in shrimp farming and implications for environmental impacts and human health. *International Journal of Food Science and Technology* 38, 255-266.
- Holten Lützhøft, H.C., Halling-Sørensen, B., Jørgensen, S.E., **1999**. Algal toxicity of antibacterial agents applied in Danish fish farming. *Archives of Environmental Contamination and Toxicology* 36, 1-6.
- Homem, V., Santos, L., **2011**. Degradation and removal methods of antibiotics from aqueous matrices - A review. *Journal of Environmental Management* 92, 2304-2347.
- Howard, P.H., Meylan, W.M., **1997**. Prediction of physical properties, transport, and degradation for environmental fate and exposure assessments. *Quantitative Structure-Activity Relationships in Environmental Sciences - VII*. Chen, F., Schürmann, G., Eds., SETAC Press, Pensacola, FL, 185-205.
- Hruska, K., Franek, M., **2012**. Sulfonamides in the environment: A review and a case report. *Veterinari Medicina* 57, 1-35.

- Hu, X., Zhou, Q., Luo, Y., **2010**. Occurrence and source analysis of typical veterinary antibiotics in manure, soil, vegetables and groundwater from organic vegetable bases, Northern China. *Environmental Pollution* 158, 2992-2998.
- Hu, X., He, K., Zhou, Q., **2012**. Occurrence, accumulation, attenuation and priority of typical antibiotics in sediments based on long-term field and modeling studies. *Journal of Hazardous Materials* 225, 91-98.
- Huang, Z.Y., Huang, H.P., Cai, R.X., Lin, Z.X., Korenaga, T., Zeng, Y.E., **1997**. Fluorescence investigation of some fluoroquinolones in various media: Ground-state acid-base equilibria. *Analytical Sciences* 13, 77-80.
- Huber, S.A., Balz, A., Abert, M., Pronk, W., **2011**. Characterisation of aquatic humic and non-humic matter with size-exclusion chromatography - organic carbon detection - organic nitrogen detection (LC-OCD-OND). *Water Research* 45, 879-885.
- Hubicka, U., Krzek, J., Zuromska, B., Walczak, M., Zylewski, M., Pawlowski, D., **2012**. Determination of photostability and photodegradation products of moxifloxacin in the presence of metal ions in solutions and solid phase. Kinetics and identification of photoproducts. *Photochemical & Photobiological Sciences* 11, 351-357.
- Hurum, D.C., Agrios, A.G., Gray, K.A., Rajh, T., Thurnauer, M.C., **2003**. Explaining the enhanced photocatalytic activity of Degussa P25 mixed-phase TiO₂ using EPR. *Journal of Physical Chemistry B* 107, 4545-4549.
- Hyland, K.C., Dickenson, E.R.V., Drewes, J.E., Higgins, C.P., **2012**. Sorption of ionized and neutral emerging trace organic compounds onto activated sludge from different wastewater treatment configurations. *Water Research* 46, 1958-1968.
- Ishibashi, K., Fujishima, A., Watanabe, T., Hashimoto, K., **2000**. Quantum yields of active oxidative species formed on TiO₂ photocatalyst. *Journal of Photochemistry and Photobiology A: Chemistry* 134, 139-142.
- Isidori, M., Lavorgna, M., Nardelli, A., Pascarella, L., Parrella, A., **2005**. Toxic and genotoxic evaluation of six antibiotics on non-target organisms. *Science of the Total Environment* 346, 87-98.
- Jain, S., Kumar, P., Vyas, R.K., Pandit, P., Dalai, A.K., **2013**. Occurrence and removal of antiviral drugs in environment: A review. *Water, Air, & Soil Pollution* 224, 1409-1428.
- Jarnheimer, P.A., Ottoson, J., Lindberg, R., Stenström, T.A., Johansson, M., Tysklind, M., Winner, M.M., Olsen, B., **2004**. Fluoroquinolone antibiotics in a hospital sewage line; Occurrence, distribution and impact on bacterial resistance. *Scandinavian Journal of Infectious Diseases* 36, 752-755.
- Jia, A., Wan, Y., Xiao, Y., Hu, J., **2012**. Occurrence and fate of quinolone and fluoroquinolone antibiotics in a municipal sewage treatment plant. *Water Research* 46, 387-394.
- Jones, O.A.H., Voulvoulis, N., Lester, J.N., **2004**. Potential ecological and human health risks associated with the presence of pharmaceutically active compounds in the aquatic environment. *Critical Reviews in Toxicology* 34(4), 335-350.

- Joss, A., Keller, E., Alder, A.C., Göbel, A., McArdell, C.S., Ternes, T., Siegrist, H., **2005**. Removal of pharmaceuticals and fragrances in biological wastewater treatment. *Water Research* 39, 3139-3152.
- Juan-García, A., Font, G., Picó, Y., **2007**. Simultaneous determination of different classes of antibiotics in fish and livestock by CE-MS. *Electrophoresis* 28, 4180-4191.
- Kan, C.A., Petz, M., **2000**. Residues of veterinary drugs in eggs and their distribution between yolk and white. *Journal of Agricultural and Food Chemistry* 48, 6397-6403.
- Kar, S., Roy, K., **2010**. First report on interspecies quantitative correlation of ecotoxicity of pharmaceuticals. *Chemosphere* 81, 738-747.
- Karci, A., Balcioglu, I.A., **2009**. Investigation of the tetracycline, sulfonamide, and fluoroquinolone antimicrobial compounds in animal manure and agricultural soils in Turkey. *Science of the Total Environment* 407, 4652-4664.
- Karl, W., Schneider, J., Wetzstein, H.G., **2006**. Outlines of an "exploding" network of metabolites generated from the fluoroquinolone enrofloxacin by the brown rot fungus *Gibeophyllum striatum*. *Applied Microbiology and Biotechnology* 71, 101-113.
- Karthikeyan, K.G., Meyer, M.T., **2006**. Occurrence of antibiotics in wastewater treatment facilities in Wisconsin, USA. *Science of the Total Environment* 361, 196-207.
- Kassinis, D., Klavarioti, M., Mantzavinos, D., **2009**. Removal of residual pharmaceuticals from aqueous systems by advanced oxidation processes. *Environment International* 35, 402-417.
- Kelly, B.C., Gobas, F., **2001**. Bioaccumulation of persistent organic pollutants in lichen-caribou-wolf food chains of Canada's Central and Western Arctic. *Environmental Science & Technology* 35, 325-334.
- Kemper, N., **2008**. Veterinary antibiotics in the aquatic and terrestrial environment. *Ecological Indicators* 8, 1-13.
- Kim, K.H., Ihm, S.K., **2011**. Heterogeneous photocatalytic wet air oxidation of refractory organic pollutants in industrial wastewaters: A review. *Journal of Hazardous Materials* 186, 16-34.
- Klamerth, N., Miranda, N., Malato, S., Agüera, A., Fernandez-Alba, A.R., Maldonado, M.I., Coronado, J.M., **2009**. Degradation of emerging contaminants at low concentrations in MWTPs effluents with mild solar photo-Fenton and TiO₂. *Catalysis Today* 144, 124-130.
- Klanjscek, T., Legovic, T., **2001**. Toward a closed life support system for interplanetary missions. *Ecological modelling* 138, 41-54.
- Klauson, D., Babkina, J., Stepanova, K., Krichevskaya, M., Preis, S., **2010**. Aqueous photocatalytic oxidation of amoxicillin. *Catalysis Today* 151, 39-45.
- Klavarioti, M., Mantzavinos, D., Kassinis, D., **2009**. Removal of residual pharmaceuticals from aqueous systems by advanced oxidation processes. *Environment International* 35, 402-417.

- Knapp, C.W., Cardoza, L.A., Hawes, J.N., Wellington, E.M.H., Larive, C.K., Graham, D.W., **2005**. Fate and effects of enrofloxacin in aquatic systems under different light conditions. *Environmental Science & Technology* 39, 9140-9146.
- Köck-Schulmeyer, M., Ginebreda, A., Postigo, C., López-Serna, R., Pérez, S., Brix, R., Llorca, M., López de Alda, M., Petrović, M., Munné, A., Tirapu, L., Barceló, D., **2011**. Wastewater reuse in Mediterranean semi-arid areas: The impact of discharges of tertiary treated sewage on the load of polar micro pollutants in the Llobregat river (NE Spain). *Chemosphere* 82, 670-678.
- Kolpin, D.W., Furlong, E.T., Meyer, M.T., Thurman, E.M., Zaugg, S.D., Barber, L.B., Buxton, H.T., **2002**. Pharmaceuticals, hormones, and other organic wastewater contaminants in U.S. streams, 1999-2000: A national reconnaissance. *Environmental Science & Technology* 36, 1202-1211.
- Kormann, C., Bahnemann, D.W., Hoffmann, M.R., **1991**. Photolysis of chloroform and other organic-molecules in aqueous TiO₂ suspensions. *Environmental Science & Technology* 25, 494-500.
- Kumar, K.V., Porkodi, K., Rocha, F., **2008**. Langmuir-Hinshelwood kinetics - A theoretical study. *Catalysis Communications* 9, 82-84.
- Kümmerer, K., Henninger, A., **2003**. Promoting resistance by the emission of antibiotics from hospitals and households into effluent. *Clinical Microbiology and Infection* 9, 1203-1214.
- Kümmerer, K., **2008**. *Pharmaceuticals in the Environment. Sources, fate, effects and risks*. Springer, Germany.
- Kümmerer, K., **2009a**. The presence of pharmaceuticals in the environment due to human use - present knowledge and future challenges. *Journal of Environmental Management* 90, 2354-2366.
- Kümmerer, K., **2009b**. Antibiotics in the aquatic environment - A review - Part I. *Chemosphere* 75, 417-434.
- Kümmerer, K., **2009c**. Antibiotics in the aquatic environment - A review - Part II. *Chemosphere* 75, 435-441.
- Lai, H.T., Lin, J.J., **2009**. Degradation of oxolinic acid and flumequine in aquaculture pond waters and sediments. *Chemosphere* 75, 462-468.
- Lalumera, G.M., Calamari, D., Galli, P., Castiglioni, S., Crosa, G., Fanelli, R., **2004**. Preliminary investigation on the environmental occurrence and effects of antibiotics used in aquaculture in Italy. *Chemosphere* 54, 661-668.
- Länge, R., Dietrich, D., **2002**. Environmental risk assessment of pharmaceutical drug substances – conceptual considerations. *Toxicology Letters* 131, 97-104.
- Langlois, M.H., Montagut, M., Dubost, J.P., Grellet, J., Saux, M.C., **2005**. Protonation equilibrium and lipophilicity of moxifloxacin. *Journal of Pharmaceutical and Biomedical Analysis* 37, 389-393.
- Larsson, D.G.J., de Pedro, C., Paxeus, N., **2007**. Effluent from drug manufactures contains extremely high levels of pharmaceuticals. *Journal of Hazardous Materials* 148, 751-755.

- Lazar, M.A, Varghese, S., Nair, S.S., **2012**. Photocatalytic water treatment by titanium dioxide: Recent updates. *Catalysts* 2, 572-601.
- Le, T.X., Munekage, Y., **2004**. Residues of selected antibiotics in water and mud from shrimp ponds in mangrove areas in Viet Nam. *Marine Pollution Bulletin* 49, 922-929.
- Leal, R.M.P., Figueira, R.F., Tornisielo, V.L., Regitano, J.B., **2012**. Occurrence and sorption of fluoroquinolones in poultry litters and soils from São Paulo State, Brazil. *Science of the Total Environment* 432, 344-349.
- Leal, R.M.P., Alleoni, L.R.F., Tornisielo, V.L., Regitano, J.B., **2013**. Sorption of fluoroquinolones and sulfonamides in 13 Brazilian soils. *Chemosphere* 92, 979-985.
- Lemaire, S., Tulkens, P.M., Van Bambeke, F., **2011**. Contrasting effects of acidic pH on the extracellular and intracellular activities of the anti-Gram-positive fluoroquinolones moxifloxacin and delafloxacin against *Staphylococcus aureus*. *Antimicrobial Agents and Chemotherapy* 55(2), 649-658.
- Leung, H.W., Minh, T.B., Murphy, M.B., Lam, J.C.W., So, M.K., Martin, M., Lam, P.K.S., Richardson, B.J., **2012**. Distribution, fate and risk assessment of antibiotics in sewage treatment plants in Hong Kong, South China. *Environment International* 42, 1-9.
- Li, B., Zhang, T., Xu, Z., Fang, H.H.P., **2009**. Rapid analysis of 21 antibiotics of multiple classes in municipal wastewater using ultra performance liquid chromatography-tandem mass spectrometry. *Analytica Chimica Acta* 645, 64-72.
- Li, B., Zhang, T., **2010**. Biodegradation and adsorption of antibiotics in the activated sludge process. *Environmental Science & Technology* 44, 3468-3473.
- Li, G., Lv, L., Fan, H., Ma, J., Li, Y., Wan, Y., Zhao, X.S., **2010**. Effect of the agglomeration of TiO₂ nanoparticles on their photocatalytic performance in the aqueous phase. *Journal of Colloid and Interface Science* 348, 342-347.
- Li, Y.W., Wu, X.L., Mo, C.H., Tai, Y.P., Huang, X.P., Xiang, L., **2011**. Investigation of sulfonamide, tetracycline, and quinolone antibiotics in vegetable farmland soil in the Pearl river delta area, Southern China. *Journal of Agricultural and Food Chemistry* 59, 7268-7276.
- Li, W., Shi, Y., Gao, L., Liu, J., Cai, Y., **2012a**. Occurrence of antibiotics in water, sediments, aquatic plants, and animals from Baiyangdian lake in North China. *Chemosphere* 89, 1307-1315.
- Li, W., Shi, Y., Gao, L., Liu, J., Cai, Y., **2012b**. Investigation of antibiotics in mollusks from coastal waters in the Bohai Sea of China. *Environmental Pollution* 162, 56-62.
- Li, W., Guo, C., Su, B., Xu, J., **2012c**. Photodegradation of four fluoroquinolone compounds by titanium dioxide under simulated solar light irradiation. *Journal of Chemical Technology and Biotechnology* 87, 643-650.
- Li, W., Shi, Y., Gao, L., Liu, J., Cai, Y., **2013**. Occurrence and removal of antibiotics in a municipal wastewater reclamation plant in Beijing, China. *Chemosphere* 92, 435-444.

- Lillenberg, M., Yurchenko, S., Kipper, K., Herodes, K., Pihl, V., Sepp, K., Löhmus, R., Nei, L., **2009**. Simultaneous determination of fluoroquinolones, sulfonamides and tetracyclines in sewage sludge by pressurized liquid extraction and liquid chromatography electrospray ionization-mass spectrometry. *Journal of Chromatography A* 1216, 5949-5954.
- Lillenberg, M., Yurchenko, S., Kipper, K., Herodes, K., Pihl, V., Löhmus, R., Ivask, M., Kuu, A., Kutti, S., Litvin, S.V., Nei, L., **2010**. Presence of fluoroquinolones and sulfonamides in urban sewage sludge and their degradation as a result of composting. *International Journal of Environmental Science and Technology* 7(2), 307-312.
- Lin, C.E., Deng, Y.J., Liao, W.S., Sun, S.W., Lin, W.Y., Chen, C.C., **2004**. Electrophoretic behavior and pKa determination of quinolones with a piperazinyl substituent by capillary zone electrophoresis. *Journal of Chromatography A* 1051, 283-290.
- Lin, A.Y.C., Yu, T.H., Lin, C.F., **2008**. Pharmaceutical contamination in residential, industrial, and agricultural waste streams: Risk to aqueous environments in Taiwan. *Chemosphere* 74, 131-141.
- Lin, A.Y.C., Yu, T.H., Lateef, S.K., **2009**. Removal of pharmaceuticals in secondary wastewater treatment processes in Taiwan. *Journal of Hazardous Materials* 167, 1163-1169.
- Lindberg, R., Jarnheimer, P.A., Olsen, B., Johansson, M., Tysklind, M., **2004**. Determination of antibiotic substances in hospital sewage water using solid phase extraction and liquid chromatography/mass spectrometry and group analogue internal standards. *Chemosphere* 57, 1479-1488.
- Lindberg, R.H., Wennberg, P., Johansson, M.I., Tysklind, M., Andersson, B.A.V., **2005**. Screening of human antibiotic substances and determination of weekly mass flows in five sewage treatment plants in Sweden. *Environmental Science & Technology* 39(10), 3421-3429.
- Lindberg, R.H., Olofsson, U., Rendahl, P., Johansson, M.I., Tysklind, M., Andersson, B.A.V., **2006**. Behavior of fluoroquinolones and trimethoprim during mechanical, chemical, and active sludge treatment of sewage water and digestion of sludge. *Environmental Science & Technology* 40(3), 1042-1048.
- Lindner, B., Wiese, A., Brandenburg, K., Seydel, U., Dalhoff, A., **2002**. Lack of interaction of fluoroquinolones with lipopolysaccharides. *Antimicrobial Agents and Chemotherapy* 46(5), 1568-1570.
- LogKOW, <http://logkow.cisti.nrc.ca/logkow/index.jsp>, last visited 03/02/2014.
- López-Serna, R., Pérez, S., Ginebreda, A., Petrović, M., Barceló, D., **2010**. Fully automated determination of 74 pharmaceuticals in environmental and waste waters by online solid phase extraction-liquid chromatography-electrospray-tandem mass spectrometry. *Talanta* 83, 410-424.
- López-Serna, R., Petrović, M., Barceló, D., **2011**. Development of a fast instrumental method for the analysis of pharmaceuticals in environmental and wastewaters based on ultra high performance liquid chromatography (UHPLC)-tandem mass spectrometry (MS/MS). *Chemosphere* 85, 1390-1399.

- López-Serna, R., Jurado, A., Vázquez-Suñé, E., Carrera, J., Petrović, M., Barceló, D., **2013**. Occurrence of 95 pharmaceuticals and transformation products in urban groundwaters underlying the metropolis of Barcelona, Spain. *Environmental Pollution* 174, 305-315.
- Lorenzo, F., Navaratnam, S., Edge, R., Allen, N.S., **2008**. Primary photophysical properties of moxifloxacin - A fluoroquinolone antibiotic. *Photochemistry and Photobiology* 84, 1118-1125.
- Lu, S., Xuefei, Z., Yalei, Z., Guowei, G., **2009**. Occurrence and removal of fluoroquinolone antibiotics in a sewage treatment plant in Shanghai, China. *3rd International Conference on Bioinformatics and Biomedical Engineering (iCBBE 2009)*, 1-4.
- Luo, Y., Xu, L., Rysz, M., Wang, Y., Zhang, H., Alvarez, P.J.J., **2011**. Occurrence and transport of tetracycline, sulfonamide, quinolone, and macrolide antibiotics in the Haihe River Basin, China. *Environmental Science & Technology* 45, 1827-1833.
- MacGowan, A.P., **1999**. Moxifloxacin (Bay 12-8039): A new methoxy quinolone antibacterial. *Expert Opinion on Investigational Drugs* 8, 181-199.
- Mahendran, K.R., Kreir, M., Weingart, H., Fertig, N., Winterhalter, M., **2010**. Permeation of antibiotics through *Escherichia coli* OmpF and OmpC porins: Screening for influx on a single-molecule level. *Journal of Biomolecular Screening* 15, 302-307.
- Malato, S., Fernández-Ibáñez, P., Maldonado, M.I., Blanco, J., Gernjak, W., **2009**. Decontamination and disinfection of water by solar photocatalysis: Recent overview and trends. *Catalysis Today* 147, 1-59.
- Manukovsky, N.S., Kovalev, V.S., Somova, L.A., Gurevich, Y.L., Sadovsky, M.G., **2005**. Material balance and diet in bioregenerative life support systems: Connection with coefficient of closure. *Advances in space research* 35, 1563-1569.
- Margot, J., Kienle, C., Magnet, A., Weil, M., Rossi, L., de Alencastro, L.F., Abegglen, C., Thoney, D., Chèvre, N., Schärer, M., Barry, D.A., **2013**. Treatment of micropollutants in municipal wastewater: Ozone or powdered activated carbon? *Science of the Total Environment* 461-462, 480-498.
- Martin, J., Camacho-Muñoz, D., Santos, J.L., Aparicio, I., Alonso, E., **2012**. Occurrence of pharmaceutical compounds in wastewater and sludge from wastewater treatment plants: Removal and ecotoxicological impact of wastewater discharges and sludge disposal. *Journal of Hazardous Materials* 239, 40-47.
- Martin, S.T., Lee, A.T., Hoffmann, M.R., **1995**. Chemical mechanism of inorganic oxidants in the TiO₂/UV process: Increased rates of degradation of chlorinated hydrocarbons. *Environmental Science & Technology* 29, 2567-2573.
- Martinez, M., McDermott, P., Walker, R., **2006**. Pharmacology of the fluoroquinolones: A perspective for the use in domestic animals. *The Veterinary Journal* 172, 10-28.
- Martínez, F., López-Muñoz, M.J., Aguado, J., Melero, J.A., Arsuaga, J., Sotto, A., Molina, R., Segura, Y., Pariente, M.I., Revilaa, A., Cerro, L., Carenas, G., **2013**. Coupling membrane separation and photocatalytic oxidation processes for the degradation of pharmaceutical pollutants. *Water Research* 47, 5647-5658.

- Martins, A.F., Vasconcelos, T.G., Henriques, D.M., Frank, C.d.S., König, A., Kümmerer, K., **2008**. Concentration of ciprofloxacin in Brazilian hospital effluent and preliminary risk assessment: A case study. *Clean* 36(3), 264-269.
- Martins, N., Pereira, R., Abrantes, N., Pereira, J., Gonçalves, F., Marques, C.R., **2012**. Ecotoxicological effects of ciprofloxacin on freshwater species: Data integration and derivation of toxicity thresholds for risk assessment. *Ecotoxicology* 21, 1167-1176.
- Martinez Bueno, M.J., Agüera, A., Gómez, M.J., Hernando, M.D., García-Reyes, J.F., Fernández-Alba, A.R., **2007**. Application of liquid chromatography/quadrupole-linear ion trap mass spectrometry and time-of-flight mass spectrometry to the determination of pharmaceuticals and related contaminants in wastewater. *Analytical Chemistry* 79, 9372-9384.
- Martínez-Carballo, E., González-Barreiro, C., Scharf, S., Gans, O., **2007**. Environmental monitoring study of selected veterinary antibiotics in animal manure and soils in Austria. *Environment Pollution* 148, 570-579.
- Matsumoto, M., Kojima, K., Nagano, H., Matsubara, S., Yokota, T., **1992**. Photostability and biological activity of fluoroquinolones substituted at the 8 position after UV irradiation. *Antimicrobial Agents and Chemotherapy* 36(8), 1715-1719.
- Maul, J.D., Schuler, L.J., Belden, J.B., Whiles, M.R., Lydy, M.J., **2006**. Effects of the antibiotic ciprofloxacin on stream microbial communities and detritivorous macroinvertebrates. *Environmental Toxicology and Chemistry* 25, 1598-1606.
- McClellan, K., Halden, R.U., **2010**. Pharmaceuticals and personal care products in archived U.S. biosolids from the 2001 EPA national sewage sludge survey. *Water Research* 44, 658-668.
- McCullagh, C., Skillen, N., Adams, M., Robertson, P.K.J., **2011**. Photocatalytic reactors for environmental remediation: A review. *Journal of Chemical Technology and Biotechnology* 86, 1002-1017.
- McMurray, T.A., Dunlop, P.S.M., Byrne, J.A., **2006**. The photocatalytic degradation of atrazine on nanoparticulate TiO₂ films. *Journal of Photochemistry and Photobiology A: Chemistry* 182, 43-51.
- Mehrotra, K., Yablonsky, G.S., Ray, A.K., **2003**. Kinetic studies of photocatalytic degradation in a TiO₂ slurry system: Distinguishing working regimes and determining rate dependences. *Industrial & Engineering Chemistry Research* 42, 2273-2281.
- Meichtry, J.M., Lin, H.J., de la Fuente, L., Levy, I.K., Gautier, E.A., Blesa, M.A., Litter, M.I., **2007**. Low-cost TiO₂ photocatalytic technology for water potabilization in plastic bottles for isolated regions. Photocatalyst fixation. *Journal of Solar Energy Engineering-Transactions of the Asme* 129, 119-126.
- Mella, M., Fasani, E., Albin, A., **2001**. Photochemistry of 1-cyclopropyl-6-fluoro-1,4-dihydro-4-oxo-7-(piperazin-1-yl)quinoline-3-carboxylic acid (= ciprofloxacin) in aqueous solutions. *Helvetica Chimica Acta* 84, 2508-2519.
- Miao, X.S., Bishay, F., Chen, M., Metcalfe, C.D., **2004**. Occurrence of antimicrobials in the final effluents of wastewater treatment plants in Canada. *Environmental Science & Technology* 38(13), 3533-3541.

- Michael, I., Hapeshi, E., Michael, C., Fatta-Kassinos, D., **2010**. Solar fenton and solar TiO₂ catalytic treatment of ofloxacin in secondary treated effluents: Evaluation of operational and kinetic parameters. *Water Research* 44, 5450-5462.
- Michael, I., Rizzo, L., McArdell, C.S., Manaia, C.M., Merlin, C., Schwartz, T., Dagot, C., Fatta-Kassinos, D., **2013**. Urban wastewater treatment plants as hotspots for the release of antibiotics in the environment: A review. *Water Research* 47, 957-995.
- Michot, J.M., Seral, C., Van Bambeke, F., Mingeot-Leclercq, M.P., Tulkens, P.M., **2005**. Influence of efflux transporters on the accumulation and efflux of four quinolones (ciprofloxacin, levofloxacin, garenoxacin, and moxifloxacin) in J774 macrophages. *Antimicrobial Agents and Chemotherapy* 49, 2429-2437.
- MicroPoll, **2010**. http://www.pills-project.eu/daten/Vortraege_pdf/4_Schaerer.pdf, last visited 05/05/2014.
- Microzon, **2014**. www.labosafe.ch/brochures/brochure_microzon_en.pdf, last visited 12/02/2014.
- Miège, C., Choubert, J.M., Ribeiro, L., Eusèbe, M., Coquery, M., **2009**. Fate of pharmaceuticals and personal care products in wastewater treatment plants - Conception of a database and first results. *Environmental Pollution* 157, 1721-1726.
- Migliore, L., Civitareale, C., Brambilla, G., Di Delupis, G.D., **1997**. Toxicity of several important agricultural antibiotics to *Artemia*. *Water Research* 31, 1801-1806.
- Minh, T.B., Leung, H.W., Loi, I.H., Chan, W.H., So, M.K., Mao, J.Q., Choi, D., Lam, J.C.W., Zheng, G., Martin, M., Lee, J.H.W., Lam, P.K.S., Richardson, B.J., **2009**. Antibiotics in the Hong Kong metropolitan area: Ubiquitous distribution and fate in Victoria Harbour. *Marine Pollution Bulletin* 58, 1052-1062.
- Miranda-García, N., Maldonado, M.I., Coronado, J.M., Malato, S., **2010**. Degradation study of 15 emerging contaminants at low concentration by immobilized TiO₂ in a pilot plant. *Catalysis Today* 151, 107-113.
- Miranda-García, N., Suárez, S., Sánchez, B., Coronado, J.M., Malato, S., Maldonado, M.I., **2011**. Photocatalytic degradation of emerging contaminants in municipal wastewater treatment plant effluents using immobilized TiO₂ in a solar pilot plant. *Applied Catalysis B-Environmental* 103, 294-301.
- Mitani, K., Kataoka, H., **2006**. Determination of fluoroquinolones in environmental waters by in-tube solid-phase microextraction coupled with liquid chromatography-tandem mass spectrometry. *Analytica Chimica Acta* 562, 16-22.
- Mohamed, H.H., Bahnemann, D.W., **2012**. The role of electron transfer in photocatalysis: Facts and fiction. *Applied Catalysis B-Environmental* 128, 91-104.
- Mompelat, S., Thomas, O., Le Bot, B., **2011**. Contamination levels of human pharmaceutical compounds in French surface and drinking water. *Journal of Environmental Monitoring* 13, 2929-2939.

- Montesdeoca-Esponda, S., Sosa-Ferrera, Z., Santana-Rodriguez, J.J., **2012**. Combination of microwave-assisted micellar extraction with liquid chromatography tandem mass spectrometry for the determination of fluoroquinolone antibiotics in coastal marine sediments and sewage sludges samples. *Biomedical Chromatography* 26, 33-40.
- Monti, S., Sortino, S., Fasani, E., Albini, A., **2001**. Multifaceted photoreactivity of 6-fluoro-7-aminoquinolones from the lowest excited states in aqueous media: A study by nanosecond and picosecond spectroscopic techniques. *Chemistry - A European Journal* 7, 2185-2196.
- Morales-Muñoz, S., Luque-García, J.L., de Castro, M.D.L., **2004**. Continuous microwave-assisted extraction coupled with derivatization and fluorimetric monitoring for the determination of fluoroquinolone antibacterial agents from soil samples. *Journal of Chromatography A* 1059, 25-31.
- Morasch, B., Bonvin, F., Reiser, H., Grandjean, D., de Alencastro, L.F., Perazzolo, C., Chèvre, N., Kohn, T., **2010**. Occurrence and fate of micropollutants in the Vidy bay of lake Geneva, Switzerland. Part II: Micropollutant removal between wastewater and raw drinking water. *Environmental Toxicology and Chemistry* 29(8), 1658-1668.
- Mougin, C., Cheviron, N., Repincay, C., Hedde, M., Hernandez-Raquet, G., **2013**. Earthworms highly increase ciprofloxacin mineralization in soils. *Environmental Chemistry Letters* 11, 127-133.
- Moziá, S., **2010**. Photocatalytic membrane reactors (PMRs) in water and wastewater treatment. A review. *Separation and Purification Technology* 73, 71-91.
- Moziá, S., Brozek, P., Przepiorski, J., Tryba, B., Morawski, A.W., **2012**. Immobilized TiO₂ for phenol degradation in a pilot-scale photocatalytic reactor. *Journal of Nanomaterials*, doi:10.1155/2012/949764.
- Muñoz, I., **2006**. Life cycle assessment as a tool for green chemistry: Application to different Advanced Oxidation Processes for wastewater treatment. Doctoral thesis. Universitat Autònoma de Barcelona.
- Muñoz, I., Gómez-Ramos, M.J., Agüera, A., García-Reyes, J.F., Molina-Díaz, A., Fernández-Alba, A.R., **2009**. Chemical evaluation of contaminants in wastewater effluents and the environmental risk of reusing effluents in agriculture. *Trends in Analytical Chemistry* 28(6), 676-694.
- Musson, S.E., Townsend, T.G., **2009**. Pharmaceutical compound content of municipal solid waste. *Journal of Hazardous Materials* 162, 730-735.
- Naeslund, J., Hedman, J.E., Agestrand, C., **2008**. Effects of the antibiotic ciprofloxacin on the bacterial community structure and degradation of pyrene in marine sediment. *Aquatic Toxicology* 90, 223-227.
- Nageswara, R.R., Venkateswarlu, N., Narsimha, R., **2008**. Determination of antibiotics in aquatic environment by solid-phase extraction followed by liquid chromatography-electrospray ionization mass spectrometry. *Journal of Chromatography A* 1187, 151-164.
- Nakata, H., Kannan, K., Jones, P.D., Giesy, J.P., **2005**. Determination of fluoroquinolone antibiotics in wastewater effluents by liquid chromatography-mass spectrometry and fluorescence detection. *Chemosphere* 58, 759-766.

- Nasuhoglu, D., Rodayan, A., Berk, D., Yargeau, V., **2012**. Removal of the antibiotic levofloxacin (LEVO) in water by ozonation and TiO₂ photocatalysis. *Chemical Engineering Journal* 189-190, 41-48.
- Navrátilová, P., Borkovcová, I., Vyhnálková, J., Vorlová, L., **2011**. Fluoroquinolone Residues in Raw Cow's Milk. *Czech Journal of Food Sciences* 29(6) 641-646.
- Neppolian, B., Choi, H.C., Sakthivel, S., Arabindoo, B., Murugesan, V., **2002**. Solar/UV-induced photocatalytic degradation of three commercial textile dyes. *Journal of Hazardous Materials* 89, 303-317.
- Neugebauer, U., Szeghalmi, A., Schmitt, M., Kiefer, W., Popp, J., Holzgrabe, U., **2005**. Vibrational spectroscopic characterization of fluoroquinolones. *Spectrochimica Acta Part A: Molecular and Biomolecular Spectroscopy* 61, 1505-1517.
- Neves, P., Leite, A., Rangel, M., de Castro, B., Gameiro, P., **2007**. Influence of structural factors on the enhanced activity of moxifloxacin: A fluorescence and EPR spectroscopic study. *Analytical and Bioanalytical Chemistry* 387, 1543-1552.
- Nie, X., Wang, X., Chen, J., Zitko, V., An, T., **2008**. Response of the freshwater alga *Chlorella vulgaris* to trichloroisocyanuric acid and ciprofloxacin. *Environmental Toxicology and Chemistry* 27, 168-173.
- Nie, X., Gu, J., Lu, J., Pan, W., Yang, Y., **2009**. Effects of norfloxacin and butylated hydroxyanisole on the freshwater microalga *Scenedesmus obliquus*. *Ecotoxicology* 18, 677-684.
- Nowara, A., Burhenne, J., Spitteller, M., **1997**. Binding of fluoroquinolone carboxylic acid derivatives to clay minerals. *Journal of Agricultural and Food Chemistry* 45, 1459-1463.
- OECD, **2000**. Test No. 106: Adsorption-Desorption Using a Batch Equilibrium Method, OECD Guidelines for the Testing of Chemicals, Section 1. OECD Publishing.
- OECD, **2011**. Test No. 201: Freshwater Alga and Cyanobacteria, Growth Inhibition Test, OECD Guidelines for the Testing of Chemicals, Section 2. OECD Publishing.
- Ohlsen, K., Ternes, T., Werner, G., Wallner, U., Löffler, D., Ziebuhr, W., Witte, W., Hacker, J., **2003**. Impact of antibiotics on conjugational resistance gene transfer in *Staphylococcus aureus* in sewage. *Environmental Microbiology* 5(8), 711-716.
- Ohtani, B., Prieto-Mahaney, O.O., Li, D., Abe, R., **2010**. What is Degussa (Evonik) P25? Crystalline composition analysis, reconstruction from isolated pure particles and photocatalytic activity test. *Journal of Photochemistry and Photobiology A: Chemistry* 216, 179-182.
- Okay, O.S., Yediler, L.K., Karacik, B., **2012**. Determination of selected antibiotics in the Istanbul strait sediments by solid-phase extraction and high performance liquid chromatography. *Journal of Environmental Science and Health, Part A* 47, 1372-1380.
- Okuda, T., Yamashita, N., Tanaka, H., Matsukawa, H., Tanabe, K., **2009**. Development of extraction method of pharmaceuticals and their occurrences found in Japanese wastewater treatment plants. *Environment International* 35, 815-820.

- Oller, I., Malato, S., Sánchez-Pérez, J.A., **2011**. Combination of Advanced Oxidation Processes and biological treatments for wastewater decontamination-A review. *Science of the Total Environment* 409, 4141-4166.
- Olofsson, U., Brorström-Lundén, E., Kylin, H., Haglund, P., **2013**. Comprehensive mass flow analysis of Swedish sludge contaminants. *Chemosphere* 90, 28-35.
- Oloibiri, **2013**. Ozonation of biologically treated landfill leachate. Master's dissertation, Ghent University.
- Owens, R.C., Ambrose, P.G., **2000**. Clinical use of the fluoroquinolones. *Medical Clinics of North America* 84, 1447-1469.
- Paixao, S.M., Silva, L., Fernandes, A., O'Rourke, K., Mendonça, E., Picado, A., **2008**. Performance of a miniaturized algal bioassay in phytotoxicity screening. *Ecotoxicology* 17, 165-171.
- Pallo-Zimmerman, L.M., Byron, J.K., Graves, T.K., **2010**. Fluoroquinolones: Then and now. *Compendium: Continuing Education for Veterinarians*. www.vetlearn.com/compendium/.
- Palmisano, L., Sclafani, A., **1997**. Thermodynamics and kinetics for heterogeneous photocatalytic processes. *Heterogeneous photocatalysis*, Wiley & Sons, Chichester, 109-132.
- Palominos, R., Freer, J., Mondaca, M.A., Mansilla, H.D., **2008**. Evidence for hole participation during the photocatalytic oxidation of the antibiotic flumequine. *Journal of Photochemistry and Photobiology A: Chemistry* 193, 139-145.
- Palominos, R.A., Mondaca, M.A., Giraldo, A., Penuela, G., Perez-Moya, M., Mansilla, H.D., **2009**. Photocatalytic oxidation of the antibiotic tetracycline on TiO₂ and ZnO suspensions. *Catalysis Today* 144, 100-105.
- Papich, M.G., **2010**. *Saunders handbook of veterinary drugs: Small and large animal*. Elsevier Health Sciences, United States of America.
- Parga, J.R., Vázquez, V., Casillas, H.M., Valenzuela, J.L., **2009**. Cyanide detoxification of mining wastewaters with TiO₂ nanoparticles and its recovery by electrocoagulation. *Chemical Engineering & Technology* 32, 1901-1908.
- Park, H.R., Kim, T.H., Bark, K.M., **2002**. Physicochemical properties of quinolone antibiotics in various environments. *European Journal of Medicinal Chemistry* 37, 443-460.
- Park, S., Choi, K., **2008**. Hazard assessment of commonly used agricultural antibiotics on aquatic ecosystems. *Ecotoxicology* 17, 526-538.
- Paul, T., Miller, P.L., Strathmann, T.J., **2007**. Visible-light-mediated TiO₂ photocatalysis of fluoroquinolone antibacterial agents. *Environmental Science & Technology* 41, 4720-4727.
- Paul, T., Dodd, M.C., Strathmann, T.J., **2010**. Photolytic and photocatalytic decomposition of aqueous ciprofloxacin: Transformation products and residual antibacterial activity. *Water Research* 44, 3121-3132.

- Paul, T., Machesky, M.L., Strathmann, T.J., **2012**. Surface complexation of the zwitterionic fluoroquinolone antibiotic ofloxacin to nano-anatase TiO₂ photocatalyst surfaces. *Environmental Science & Technology* 46, 11896-11904.
- PeakLED, www.airmotionsystems.com/peak-led-uv-systems/, last visited 06/02/2014.
- Pena, A., Chmielova, D., Lino, C.M., Solich, P., **2007**. Determination of fluoroquinolone antibiotics in surface waters from Mondego river by high performance liquid chromatography using a monolithic column. *Journal of Separation Science* 30, 2924-2928.
- Peng, X., Wang, Z., Kuang, W., Tan, J., Li, K., **2006**. A preliminary study on the occurrence and behavior of sulfonamides, ofloxacin and chloramphenicol antimicrobials in wastewaters of two sewage treatment plants in Guangzhou, China. *Science of the Total Environment* 371, 314-322.
- Peng, X., Zhang, K., Tang, C., Huang, Q., Yu, Y., Cui, J., **2011**. Distribution pattern, behavior, and fate of antibacterials in urban aquatic environments in South China. *Journal of Environmental Monitoring* 13, 446-454.
- Phoseon, **2009**. www.phoseon.com/Documentation/UV-LED-Lamps-A-Viable-Alternative-for-UV-Inkjet.pdf, last visited 06/02/2014.
- Pichat, P., **2013**. Photocatalysis and water purification. From fundamentals to recent applications. Wiley-VCH, Germany.
- Picó, Y., Andreu, V., **2007**. Fluoroquinolones in soil - Risks and challenges. *Analytical Bioanalytical Chemistry* 387, 1287-1299.
- Pills, **2009**. www.pills-project.eu/, last visited 12/02/2014.
- Plósz, B.G., Lehnberg, K., Dott, W., Thomas, K.H., **2010**. An activated sludge model for xenobiotic organic micro-pollutants (ASM-X): Factors influencing the solid-liquid partitioning in wastewater treatment. 2nd IWA/WEF Wastewater Treatment Modeling Seminar: Conference Proceedings. International Water Association & Water Environment Federation, 297-305.
- Pomiès, M., Choubert, J.M., Wisniewski, C., Coquery, M., **2013**. Modelling of micropollutant removal in biological wastewater treatments: A review. *Science of the Total Environment* 443, 733-748.
- Prabhakaran, D., Sukul, P., Lamshöft, M., Maheswari, M.A., Zühlke, S., Spiteller, M., **2009**. Photolysis of difloxacin and sarafloxacin in aqueous systems. *Chemosphere* 77, 739-746.
- Prieto-Rodríguez, L., Miralles-Cuevas, S., Oller, I., Agüera, A., Puma, G.L., Malato, S., **2012**. Treatment of emerging contaminants in wastewater treatment plants (WWTP) effluents by solar photocatalysis using low TiO₂ concentrations. *Journal of Hazardous Materials* 211-212, 131-137.
- Prieto-Rodríguez, L., Oller, I., Klammerth, N., Agüera, A., Rodríguez, E.M., Malato, S., **2013**. Application of solar AOPs and ozonation for elimination of micropollutants in municipal wastewater treatment plant effluents. *Water Research* 47, 1521-1528.
- Pycke, B., **2009**. The fate and effects of micropollutants in a biological life support system. PhD thesis, University Ghent Belgium.

- Qiang, Z.M., Adams, C., **2004**. Potentiometric determination of acid dissociation constants (pKa) for human and veterinary antibiotics. *Water Research* 38, 2874-2890.
- Qourzal, S., Tamimi, M., Assabbane, A., Ait-Ichou, Y., **2005**. Photocatalytic degradation and adsorption of 2-naphthol on suspended TiO₂ surface in a dynamic reactor. *Journal of Colloid and Interface Science* 286, 621-626.
- Radjenović, J., Petrović, M., Barceló, D., **2007**. Analysis of pharmaceuticals in wastewater and removal using a membrane bioreactor. *Analytical and Bioanalytical Chemistry* 387, 1365-1377.
- Radjenović, J., Jelić, A., Petrović, M., Barceló, D., **2009**. Determination of pharmaceuticals in sewage sludge by pressurized liquid extraction (PLE) coupled to liquid chromatography-tandem mass spectrometry (LC-MS/MS). *Analytical and Bioanalytical Chemistry* 393, 1685-1695.
- Radjenovic, J., Escher, B.I., Rabaey, K., **2011**. Electrochemical degradation of the β -blocker metoprolol by Ti/Ru_{0.7}Ir_{0.3}O₂ and Ti/SnO₂-Sb electrodes. *Water Research* 45, 3205-3214.
- Ratola, N., Cincinelli, A., Alves, A., Katsoyiannis, A., **2012**. Occurrence of organic microcontaminants in the wastewater treatment process: A mini review. *Journal of Hazardous Materials* 239-240, 1-18.
- Rauf, M.A., Ashraf, S.S., **2009**. Fundamental principles and application of heterogeneous photocatalytic degradation of dyes in solution. *Chemical Engineering Journal* 151, 10-18.
- Rav-Acha, C., Rebhun, M., **1992**. Binding of organic solutes to dissolved humic substances and its effects on adsorption and transport in the aquatic environment. *Water Research* 26(12), 1645-1654.
- Renew, J.E., Huang, C.H., **2004**. Simultaneous determination of fluoroquinolone, sulfonamide, and trimethoprim antibiotics in wastewater using tandem solid phase extraction and liquid chromatography-electrospray mass spectrometry. *Journal of Chromatography A* 1042, 113-121.
- Reverté, S., Borrull, F., Pocurull, E., Marcé, R.M., **2003**. Determination of antibiotic compounds in water by solid-phase extraction-high-performance liquid chromatography-(electrospray) mass spectrometry. *Journal of Chromatography A* 1010, 225-232.
- Rideh, L., Wehrer, A., Ronze, D., Zoulalian, A., **1997**. Photocatalytic degradation of 2-chlorophenol in TiO₂ aqueous suspension: Modeling of reaction rate. *Industrial & Engineering Chemistry Research* 36, 4712-4718.
- Rizzo, L., Manaia, C., Merlin, C., Schwartz, T., Dagot, C., Ploy, M.C, Michael, I., Fatta-Kassinos, D., **2013**. Urban wastewater treatment plants as hotspots for antibiotic resistant bacteria and genes spread into the environment: A review. *Science of the Total Environment* 447, 345-360.
- Robinson, A.A., Belden, J.B., Lydy, M.J., **2005**. Toxicity of fluoroquinolone antibiotics to aquatic organisms. *Environmental Toxicology and Chemistry* 24(2), 423-430.
- Rodrigues-Silva, C., Maniero, M.G., Rath, S., Guimaraes, J.R., **2013**. Degradation of flumequine by photocatalysis and evaluation of antimicrobial activity. *Chemical Engineering Journal* 224, 46-52.
- Rosal, R., Rodríguez, A., Perdigón-Melón, J.A., Petre, A., García-Calvo, E., Gómez, M.J., Agüera, A., Fernández-Alba, A.R., **2010**. Occurrence of emerging pollutants in urban wastewater and their removal through biological treatment followed by ozonation. *Water Research* 44, 578-588.

- Rosen, J.E., Chen, D., Prahalad, A.K., Spratt, T.E., Schluter, G., Williams, G.M., **1997**. A fluoroquinolone antibiotic with a methoxy group at the 8 position yields reduced generation of 8-oxo-7,8-dihydro-2'-deoxyguanosine after ultraviolet-A irradiation. *Toxicology and Applied Pharmacology* 145, 381-387.
- Rosendahl, I., Siemens, J., Kindler, R., Groeneweg, J., Zimmermann, J., Czerwinski, S., Lamshöft, M., Laabs, V., Wilke, B.M., Vereecken, H., Amelung, W., **2012**. Persistence of the fluoroquinolone antibiotic difloxacin in soil and lacking effects on nitrogen turnover. *Journal of Environmental Quality* 41, 1275-1283.
- Ross, D.L., Elkinton, S.K., Riley, C.M., **1992**. Physicochemical properties of the fluoroquinolone antimicrobials III 1-octanol water partition-coefficients and their relationships to structure. *International Journal of Pharmaceutics* 88, 379-389.
- Rusu, A., Toth, G., Szocs, L., Kokosi, J., Kraszni, M., Gyeresi, A., Noszal, B., **2012**. Triprotic site-specific acid-base equilibria and related properties of fluoroquinolone antibacterials. *Journal of Pharmaceutical and Biomedical Analysis* 66, 50-57.
- Santos, L.H.M.L.M., Araújo, A.N., Fachini, A., Pena, A., Delerue-Matos, C., Montenegro, M.C.B.S.M., **2010**. Ecotoxicological aspects related to the presence of pharmaceuticals in the aquatic environment. *Journal of Hazardous Materials* 175, 45-95.
- Santos, L.H.M.L.M., Gros, M., Mozaz, S.R., Matos, C.D., Pena, A., Barceló, D., Conceição, M., Montenegro, M.C.B.S.M., **2013**. Contribution of hospital effluents to the load of pharmaceuticals in urban wastewaters: Identification of ecologically relevant pharmaceuticals. *Science of the Total Environment* 461-462, 302-316.
- Sapkota, A., Sapkota, A.R., Kucharski, M., Burke, J., McKenzie, S., Walker, P., Lawrence, R., **2008**. Aquaculture practices and potential human health risks: Current knowledge and future priorities. *Environment International* 34, 1215-1226.
- Schmitt-Kopplin, P., Burhenne, J., Freitag, D., Spiteller, M., Kettrup, A., **1999**. Development of capillary electrophoresis methods for the analysis of fluoroquinolones and application to the study of the influence of humic substances on their photodegradation in aqueous phase. *Journal of Chromatography A* 837, 253-265.
- Schwarzenbach, R.P., Escher, B.I., Fenner, K., Hofstetter, T.B., Johnson, C.A., von Gunten, U., Wehrli, B., **2006**. The challenge of micropollutants in aquatic systems. *Science* 313, 1072-1077.
- Seber, G.A.F., Lee, A.J., **2003**. *Linear regression analysis*, second ed., Wiley-Interscience, United States of America.
- Segura, P.A., García-Ac, A., Lajeunesse, A., Ghosh, D., Gagnon, C., Sauvé, S., **2007**. Determination of six anti-infectives in wastewater using tandem solid-phase extraction and liquid chromatography-tandem mass spectrometry. *Journal of Environmental Monitoring* 9, 307-313.
- Segura, P., François, M., Gagnon, C., Sauvé, S., **2009**. Review of the occurrence of anti-infectives in contaminated wastewaters and natural and drinking waters. *Environmental Health Perspectives* 117, 675-684.

- Seifrtová, M., Pena, A., Lino, C.M., Solich, P., **2008**. Determination of fluoroquinolone antibiotics in hospital and municipal wastewaters in Coimbra by liquid chromatography with a monolithic column and fluorescence detection. *Analytical and Bioanalytical Chemistry* 391, 799-805.
- Seifrtová, M., Nováková, L., Lino, C., Pena, A., Solich, P., **2009**. An overview of analytical methodologies for the determination of antibiotics in environmental waters. *Analytica Chimica Acta* 649, 158-179.
- Senta, I., Terzić, S., Ahel, M., **2008**. Simultaneous determination of sulfonamides, fluoroquinolones, macrolides and trimethoprim in wastewater and river water by LC-tandem-MS. *Chromatographia* 68, 747-758.
- Senta, I., Matosić, M., Jakopović, H.K., Terzić, S., Ćurko, J., Mijatović, I., Ahel, M., **2011**. Removal of antimicrobials using advanced wastewater treatment. *Journal of Hazardous Materials* 192, 319-328.
- Senta, I., Terzić, S., Ahel, M., **2013**. Occurrence and fate of dissolved and particulate antimicrobials in municipal wastewater treatment. *Water Research* 47, 705-714.
- Shan, A.Y., Ghazi, T.I.M., Rashid, S.A., **2010**. Immobilisation of titanium dioxide onto supporting materials in heterogeneous photocatalysis: A review. *Applied Catalysis A: General* 389, 1-8.
- Sharma, P.C., Jain, A., Jain, S., **2009**. Fluoroquinolone antibacterials: A review on chemistry, microbiology and therapeutic prospects. *Acta Poloniae Pharmaceutica* 66(6), 587-604.
- Shi, L., Zhou, X.F., Zhang, Y.L., Gu, G.W., **2009**. Simultaneous determination of 8 fluoroquinolone antibiotics in sewage treatment plants by solid-phase extraction and liquid chromatography with fluorescence detection. *Water Science and Technology* 59(4), 805-813.
- Shi, Y., Gao, L., Li, W., Liu, J., Cai, Y., **2012**. Investigation of fluoroquinolones, sulfonamides and macrolides in long-term wastewater irrigation soil in Tianjin, China. *Bulletin of Environmental Contamination and Toxicology* 89, 857-861.
- Silva, C.G., Wang, W., Faria, J.L., **2006**. Photocatalytic and photochemical degradation of mono-, di- and tri-azo dyes in aqueous solution under UV irradiation. *Journal of Photochemistry and Photobiology A: Chemistry* 181, 314-324.
- Sim, W.J., Lee, J.W., Oh, J.E., **2010**. Occurrence and fate of pharmaceuticals in wastewater treatment plants and rivers in Korea. *Environmental Pollution* 158, 1938-1947.
- Sim, W.J., Lee, J.W., Lee, E.S., Shin, S.K., Hwang, S.R., Oh, J.E., **2011**. Occurrence and distribution of pharmaceuticals in wastewater from households, livestock farms, hospitals and pharmaceutical manufactures. *Chemosphere* 82, 179-186.
- Singh, S., **2012**. Ozone treatment of municipal wastewater effluent for oxidation of emerging contaminants and disinfection. Master thesis University of Windsor. <http://scholar.uwindsor.ca/etd>, last visited on 02/05/2014.
- Sirtori, C., Zapata, A., Malato, S., Gernjak, W., Fernández-Alba, A.R., Agüera, A., **2009**. Solar photocatalytic treatment of quinolones: intermediates and toxicity evaluation. *Photochemical & Photobiological Sciences* 8, 644-651.

- Sludge Directive, <http://ec.europa.eu/environment/waste/sludge/>, last visited 25/02/2014.
- Sousa, M.A., Gonçalves, C., Vilar, V.J.P., Boaventura, R.A.R., Alpendurada, M.F., **2012**. Suspended TiO₂-assisted photocatalytic degradation of emerging contaminants in a municipal WWTP effluent using a solar pilot plant with CPCs. *Chemical Engineering Journal* 198-199, 301-309.
- Speltini, A., Sturini, M., Maraschi, F., Profumo, A., **2010**. Fluoroquinolone antibiotics in environmental waters: Sample preparation and determination. *Journal of Separation Science* 33, 1115-1131.
- Sponberg, A.L., Witter, J.D., **2008**. Pharmaceutical compounds in the wastewater process stream in Northwest Ohio. *Science of the Total Environment* 397, 148-157.
- Spurr, R.A., Myers, H., **1957**. Quantitative analysis of anatase-rutile mixtures with an X-ray diffractometer. *Analytical Chemistry* 29, 760-762.
- Stasinakis, A.S., **2012**. Review on the fate of emerging contaminants during sludge anaerobic digestion. *Bioresource Technology* 121, 432-440.
- Stevens-Garmon, J., Drewes, J.E., Khan, S.J., McDonald, J.A., Dickenson, E.R.V., **2011**. Sorption of emerging trace organic compounds onto wastewater sludge solids. *Water Research* 45, 3417-26.
- Stuer-Lauridsen, F., Birkved, M., Hansen, L.P., Lützhøft, H.C., Halling-Sørensen, B., **2000**. Environmental risk assessment of human pharmaceuticals in Denmark after normal therapeutic use. *Chemosphere* 40, 783-793.
- Sturini, M., Speltini, A., Pretali, L., Fasani, E., Profumo, A., **2009**. Solid-phase extraction and HPLC determination of fluoroquinolones in surface waters. *Journal of Separation Science* 32, 3020-3028.
- Sturini, M., Speltini, A., Maraschi, F., Rivagli, E., Profumo, A., **2010**. Solvent-free microwave-assisted extraction of fluoroquinolones from soil and liquid chromatography-fluorescence determination. *Journal of Chromatography A* 1217, 7316-7322.
- Sturini, M., Speltini, A., Maraschi, F., Profumo, A., Pretali, L., Fasani, E., Albini, A., **2012a**. Sunlight-induced degradation of soil-adsorbed veterinary antimicrobials Marbofloxacin and Enrofloxacin. *Chemosphere* 86, 130-137.
- Sturini, M., Speltini, A., Maraschi, F., Profumo, A., Pretali, L., Irastorza, E.A., Fasani, E., Albini, A., **2012b**. Photolytic and photocatalytic degradation of fluoroquinolones in untreated river water under natural sunlight. *Applied Catalysis B-Environmental* 119-120, 32-39.
- Sukul, P., Spittler, M., **2007**. Fluoroquinolone antibiotics in the environment. *Reviews of Environmental Contamination and Toxicology* 191, 131-162.
- Swedish EPA, **2002**. Aktionsplan för återföring av fosfor ur avlopp. The Swedish National Environmental Protection agency, Rapport 5214 (in Swedish). www.naturvardsverket.se/Documents/publikationer/620-5214-4.pdf.
- Takács-Novák, K., Józán, M., Hermecz, I., Szász, G., **1992**. Lipophilicity of antibacterial fluoroquinolones. *International Journal of Pharmaceutics* 79, 89-96.

- Takasu, H., Suzuki, S., Reungsang, A., Viet, P.H., **2011**. Fluoroquinolone (FQ) contamination does not correlate with occurrence of FQ-resistant bacteria in aquatic environments of Vietnam and Thailand. *Microbes and Environments* 26(2), 135-143.
- Takeda, N., Gotoh, M., Matsuoka, T., **2011**. Rapid screening method for quinolone residues in livestock and fishery products using immobilised metal chelate affinity chromatographic clean-up and liquid chromatography-fluorescence detection. *Food Additives and Contaminants Part A* 28(9), 1168-1174.
- Tamtam, F., Mercier, F., Le Bot, B., Eurin, J., Dinh, Q.T., Clément, M., Chevreuril, M., **2008**. Occurrence and fate of antibiotics in the Seine river in various hydrological conditions. *Science of the Total Environment* 393, 84-95.
- Tamtam, F., Mercier, F., Eurin, J., Chevreuril, M., Le Bot, B., **2009**. Ultra performance liquid chromatography tandem mass spectrometry performance evaluation for analysis of antibiotics in natural waters. *Analytical and Bioanalytical Chemistry* 393, 1709-1718.
- Tang, C., Yu, Y., Huang, Q., Peng, X., **2012**. Simultaneous determination of fluoroquinolone and tetracycline antibacterials in sewage sludge using ultrasonic-assisted extraction and HPLC-MS/MS. *International Journal of Environmental Analytical Chemistry* 92(12), 1389-1402.
- Teijon, G., Candela, L., Tamoh, K., Molina-Díaz, A., Fernández-Alba, A.R., **2010**. Occurrence of emerging contaminants, priority substances (2008/105/CE) and heavy metals in treated wastewater and groundwater at Depurbaix facility (Barcelona, Spain). *Science of the Total Environment* 408, 3584-3595.
- Terzić, S., Senta, I., Ahel, M., Gros, M., Petrović, M., Barceló, D., Müller, J., Knepper, T., Martí, I., Ventura, F., Jovančić, P., Jabučar, D., **2008**. Occurrence and fate of emerging wastewater contaminants in Western Balkan Region. *Science of the Total Environment* 399, 66-77.
- Tewari, S., Jindal, R., Kho, Y.L., Eo, S., Choi, K., **2013**. Major pharmaceutical residues in wastewater treatment plants and receiving waters in Bangkok, Thailand, and associated ecological risks. *Chemosphere* 91 (5), 697-704.
- Thi, T.T.H., Loan, T.C.T., Le, N.P., Dao, Q.P., Trinh, P.H., **2012**. Fate of fluoroquinolone antibiotics in Vietnamese coastal wetland ecosystem. *Wetlands Ecology and Management* 20, 399-408.
- Thiele-Bruhn, S., **2003**. Pharmaceutical antibiotic compounds in soils - A review. *Journal of Plant Nutrition and Soil Science* 166, 145-167.
- Thomas, K.V., Dye, C., Schlabach, M., Langford, K.H., **2007**. Source to sink tracking of selected human pharmaceuticals from two Oslo city hospitals and a wastewater treatment works. *Journal of Environmental Monitoring* 9, 1410-1418.
- Thuy, H.T.T., Nga, L.P., Loan, T.T.C., **2011**. Antibiotic contaminants in coastal wetlands from Vietnamese shrimp farming. *Environmental Science and Pollution Research* 18, 835-841.
- Tijani, J.O., Fatoba, O.O., Petrik, L.F., **2013**. A review of pharmaceuticals and endocrine-disrupting compounds: Sources, effects, removal, and detections. *Water, Air, & Soil Pollution* 224, 1770-1799.

- Tittlemier, S.A., Van de Riet, J., Burns, G., Potter, R., Murphy, C., Rourke, W., Pearce, H., Dufresne, G., **2007**. Analysis of veterinary drug residues in fish and shrimp composites collected during the Canadian Total Diet Study, 1993-2004. *Food Additives and Contaminants* 24, 14-20.
- Tolls, J., **2001**. Sorption of veterinary pharmaceuticals in soils: A review. *Environmental Science & Technology* 35, 3397-3406.
- Tong, C., Zhuo, X., Guo, Y., **2011a**. Occurrence and risk assessment of four typical fluoroquinolone antibiotics in raw and treated sewage and in receiving waters in Hangzhou, China. *Journal of Agricultural and Food Chemistry* 59, 7303-7309.
- Tong, A.Y.C., Peake, B.M., Braund, R., **2011b**. Disposal practices for unused medications in New Zealand community pharmacies. *Journal of Primary Health Care* 3, 197-203.
- Tong, A.Y.C., Braund, R., Warren, D.S., Peake, B.M., **2012**. TiO₂-assisted photodegradation of pharmaceuticals - A review. *Central European Journal of Chemistry* 10, 989-1027.
- Torniainen, K., Tammilehto, S., Ulvi, V., **1996**. The effect of pH, buffer type and drug concentration on the photodegradation of ciprofloxacin. *International Journal of Pharmaceutics* 132, 53-61.
- Tsai, W.T., Lee, M.K., Su, T.Y., Chang, Y.M., **2009**. Photodegradation of bisphenol-A in a batch TiO₂ suspension reactor. *Journal of Hazardous Materials* 168, 269-275.
- Turnipseed, S.B., Clark, S.B., Storey, J.M., Carr, J.R., **2012**. Analysis of veterinary drug residues in frog legs and other aquacultured species using liquid chromatography quadrupole time-of-flight mass spectrometry. *Journal of Agricultural and Food Chemistry* 60, 4430-4439.
- UNEP, **2007**. <http://www.unep.org/geo/geo4.asp>, last visited 30/01/2007.
- UNwater, www.unwater.org/downloads/Water_facts_and_trends.pdf, last visited 9/02/2014.
- Uslu, M.O., Yediler, A., Balcioğlu, I.A., Schulte-Hostede, S., **2008**. Analysis and sorption behavior of fluoroquinolones in solid matrices. *Water, Air, & Soil Pollution* 190, 55-63.
- Valcárel, Y., González Alonso, S., Rodríguez-Gil, J.L., Gil, A., Catalá, M., **2011**. Detection of pharmaceutically active compounds in the rivers and tap water of the Madrid Region (Spain) and potential ecotoxicological risk. *Chemosphere* 190, 55-63.
- Van Bambeke, F., Tulkens, P.M., **2009**. Safety profile of the respiratory fluoroquinolone moxifloxacin comparison with other fluoroquinolones and other antibacterial classes. *Drug Safety* 32(5), 359-378.
- Van Den Hende, S., Vervaeren, H., Saveyn, H., Maes, G., Boon, N., **2011**. Microalgal bacterial floc properties are improved by a balanced inorganic/organic carbon ratio. *Biotechnology and Bioengineering* 108, 549-558.
- Van Doorslaer, X., Demeestere, K., Heynderickx, P.M., Van Langenhove, H., Dewulf, J., **2011**. UV-A and UV-C induced photolytic and photocatalytic degradation of aqueous ciprofloxacin and moxifloxacin: Reaction kinetics and role of adsorption. *Applied Catalysis B-Environmental* 101, 540-547.

- Van Doorslaer, X., Heynderickx, P.M., Demeestere, K., Debevere, K., Van Langenhove, H., Dewulf, J., **2012**. TiO₂ mediated heterogeneous photocatalytic degradation of moxifloxacin: Operational variables and scavenger study. *Applied Catalysis B-Environmental* 111-112, 150-156.
- Van Doorslaer, X., Demeestere, K., Heynderickx, P.M., Caussyn, M., Van Langenhove, H., Devlieghere, F., Vermeulen, A., Dewulf, J., **2013**. Heterogeneous photocatalysis of moxifloxacin: Identification of degradation products and determination of residual antibacterial activity. *Applied Catalysis B-Environmental* 138-139, 333-341.
- Van Doorslaer, X., Haylamicheal, I.D., Dewulf, J., Van Langenhove, H., Janssen, C., Demeestere, K., **2014**. Heterogeneous photocatalysis of moxifloxacin in water: Chemical transformation and ecotoxicity. *Chemosphere* doi:10.1016/j.chemosphere.2014.03.048.
- Van Oostveldt, P., De Vos, W., Dieriks, B., **2010**. Interplanetary space travel and long-term habitation on Mars. *Journal of Cosmology* 12, 4113-4120.
- Van Wieren, E.M., Seymour, M.D., Peterson, J.W., **2012**. Interaction of the fluoroquinolone antibiotic, ofloxacin, with titanium oxide nanoparticles in water: Adsorption and breakdown. *Science of the Total Environment* 441, 1-9.
- Vargas, R., Núñez, O., **2009**. Hydrogen bond interactions at the TiO₂ surface: Their contribution to the pH dependent photo-catalytic degradation of p-nitrophenol. *Journal of Molecular Catalysis A: Chemical* 300, 65-71.
- Vasconcelos, T.G., Henriques, D.M., König, A., Martins, A.F., Kümmerer, K., **2009a**. Photo-degradation of the antimicrobial ciprofloxacin at high pH: Identification and biodegradability assessment of the primary by-products. *Chemosphere* 76, 487-493.
- Vasconcelos, T.G., Kümmerer, K., Henriques, D.M., Martins, A.F., **2009b**. Ciprofloxacin in hospital effluent: Degradation by ozone and photoprocesses. *Journal of Hazardous Materials* 169, 1154-1158.
- Vasquez, M.I., Hapeshi, E., Fatta-Kassinos, D., Kümmerer, K., **2013**. Biodegradation potential of ofloxacin and its resulting transformation products during photolytic and photocatalytic treatment. *Environmental Science and Pollution Research* 20, 1302-1309.
- Vasudevan, D., Bruland, G.L., Torrance, B.S., Upchurch, V.G., MacKay, A.A., **2009**. pH-dependent ciprofloxacin sorption to soils: Interaction mechanisms and soil factors influencing sorption. *Geoderma* 151, 68-76.
- Vazquez-Roig, P., Segarra, R., Blasco, C., Andreu, V., Picó, Y., **2010**. Determination of pharmaceuticals in soils and sediments by pressurized liquid extraction and liquid chromatography tandem mass spectrometry. *Journal of Chromatography A* 1217, 2471-2483.
- Vazquez-Roig, P., Andreu, V., Onghena, M., Blasco, C., Picó, Y., **2011**. Assessment of the occurrence and distribution of pharmaceuticals in a Mediterranean wetland (L'Albufera, Valencia, Spain) by LC-MS/MS. *Analytical and Bioanalytical Chemistry* 400, 1287-1301.
- Vazquez-Roig, P., Andreu, V., Blasco, C., Picó, Y., **2012**. Risk assessment on the presence of pharmaceuticals in sediments, soils and waters of the Pego-Oliva Marshlands (Valencia, Eastern Spain). *Science of the Total Environment* 440, 24-32.

- Verlicchi, P., Galletti, A., Petrovic, M., Barceló, D., **2010**. Hospital effluents as a source of emerging pollutants: An overview of micropollutants and sustainable treatment options. *Journal of Hydrology* 389, 416-428.
- Verlicchi, P., Al Aukidy, M., Zambello, E., **2012a**. Occurrence of pharmaceutical compounds in urban wastewater: Removal, mass load and environmental risk after a secondary treatment - A review. *Science of the Total Environment* 429, 123-155.
- Verlicchi, P., Al Aukidy, M., Galletti, A., Petrovic, M., Barceló, D., **2012b**. Hospital effluent: Investigation of the concentrations and distribution of pharmaceuticals and environmental risk assessment. *Science of the Total Environment* 430, 109-118.
- Verstraete, W., Vlaeminck, S.E., **2011**. ZeroWasteWater: Short-cycling of wastewater resources for sustainable cities of the future. *International Journal of Sustainable Development and World Ecology* 18(3), 253-264.
- Vieno, N.M., Tuhkanen, T., Kronberg, L., **2006**. Analysis of neutral and basic pharmaceuticals in sewage treatment plants and in recipient rivers using solid phase extraction and liquid chromatography-tandem mass spectrometry detection. *Journal of Chromatography A* 1134, 101-111.
- Vieno, N., Tuhkanen, T., Kronberg, L., **2007**. Elimination of pharmaceuticals in sewage treatment plants in Finland. *Water Research* 41, 1001-1012.
- Vijayabalan, A., Selvam, K., Velmurugan, R., Swaminathan, M., **2009**. Photocatalytic activity of surface fluorinated TiO₂-P25 in the degradation of Reactive Orange 4. *Journal of Hazardous Materials* 172, 914-921.
- Völgyi, G., Vizserálek, G., Takács-Novák, K., Avdeef, A., Tam, K.Y., **2012**. Predicting the exposure and antibacterial activity of fluoroquinolones based on physicochemical properties. *European Journal of Pharmaceutical Sciences* 47, 21-27.
- Volmer, D.A., Mansoori, B., Locke, S.J., **1997**. Study of 4-quinolone antibiotics in biological samples by short-column liquid chromatography coupled with electrospray ionization tandem mass spectrometry. *Analytical Chemistry* 69, 4143-4155.
- Vulliet, E., Cren-Olivé, C., **2011**. Screening of pharmaceuticals and hormones at the regional scale, in surface and groundwaters intended to human consumption. *Environmental Pollution* 159, 2929-2934.
- Walraven, N., Laane, R., **2009**. Assessing the discharge of pharmaceuticals along the Dutch coast of the North Sea. *Reviews of Environmental Contamination and Toxicology* 199, 1-18.
- Walters, E., McClellan, K., Halden, R.U., **2010**. Occurrence and loss over three years of 72 pharmaceuticals and personal care products from biosolids-soil mixtures in outdoor mesocosms. *Water Research* 44, 6011-6020.
- Wang, J.L., Xu, L.J., **2012**. Advanced oxidation processes for wastewater treatment: Formation of hydroxyl radical and application. *Critical Reviews in Environmental Science and Technology* 42 (2012) 251-325.

- Wang, C., Liu, H., Qu, Y., **2013**. TiO₂-based photocatalytic process for purification of polluted water: Bridging fundamentals to applications. *Journal of Nanomaterials*, <http://dx.doi.org/10.1155/2013/319637>.
- Watkinson, A.J., Murby, E.J., Costanzo, S.D., **2007**. Removal of antibiotics in conventional and advanced wastewater treatment: Implications for environmental discharge and wastewater recycling. *Water Research* 41, 4164-4176.
- Watkinson, A.J., Murby, E.J., Kolpin, D.W., Costanzo, S.D., **2009**. The occurrence of antibiotics in an urban watershed: From wastewater to drinking water. *Science of the Total Environment* 407, 2711-2723.
- Wegst-Uhrich, S.R., Navarro, D.A.G., Zimmerman, L., Aga, D.S., **2014**. Assessing antibiotic sorption in soil: A literature review and new case studies on sulfonamides and macrolides. *Chemistry Central Journal* 8:5.
- Wei, L., Shifu, C., Wei, Z., Sujuan, Z., **2009**. Titanium dioxide mediated photocatalytic degradation of methamidophos in aqueous phase. *Journal of Hazardous Materials* 164, 154-160.
- Westerhoff, P., Moon, H., Minakata, D., Crittenden, J., **2009**. Oxidation of organics in retentates from reverse osmosis wastewater reuse facilities. *Water Research* 43, 3992-3998.
- Wetzstein, H.G., Schmeer, N., Karl, W., **1997**. Degradation of the fluoroquinolone enrofloxacin by the brown rot fungus *Gloeophyllum striatum*: Identification of metabolites. *Applied and Environmental Microbiology* 63(11), 4272-4281.
- Wetzstein, H.G., Stadler, M., Tichy, H.V., Dalhoff, A., Karl, W., **1999**. Degradation of ciprofloxacin by basidiomycetes and identification of metabolites generated by the brown rot fungus *Gloeophyllum striatum*. *Applied and Environmental Microbiology* 65(4), 1556-1563.
- Williams, M., Ong, P.L., Williams, D.B., Kookana, R.S., **2009**. Estimating the sorption of pharmaceuticals based on their pharmacological distribution. *Environmental Toxicology and Chemistry* 28, 2572-2579.
- Wiszniewski, J., Robert, D., Surmacz-Gorska, J., Miksch, K., Weber, J.V., **2002**. Photocatalytic decomposition of humic acids on TiO₂; Part I: Discussion of adsorption and mechanism. *Journal of Photochemistry and Photobiology A: Chemistry* 152, 267-273.
- Wu, C.Y., Lee, Y.L., Lo, Y.S., Lin, C.J., Wu, C.H., **2013**. Thickness-dependent photocatalytic performance of nanocrystalline TiO₂ thin films prepared by sol-gel spin coating. *Applied Surface Science* 280, 737-744.
- WWTP USA, **2011**. www.globalmethane.org/expo-docs/canada13/mww_07_Toffey.pdf, last visited 22/02/2014.
- Xekoukoulotakis, N.P., Drosou, C., Brebou, C., Chatzisyneon, E., Hapeshi, E., Fatta-Kassinou, D., Mantzavinos, D., **2011**. Kinetics of UV-A/TiO₂ photocatalytic degradation and mineralization of the antibiotic sulfamethoxazole in aqueous matrices. *Catalysis Today* 161, 163-168.

- Xiao, Y., Chang, H., Jia, A., Hu, J., **2008**. Trace analysis of quinolone and fluoroquinolone antibiotics from wastewaters by liquid chromatography-electrospray tandem mass spectrometry. *Journal of Chromatography A* 1214, 100-108.
- Xu, W., Zhang, G., Li, X., Zou, S., Li, P., Hu, Z., Li, J., **2007a**. Occurrence and elimination of antibiotics at four sewage treatment plants in the Pearl river delta (PRD), South China. *Water Research* 41, 4526-4534.
- Xu, W., Zhang, G., Zou, S., Li, X., Liu, Y., **2007b**. Determination of selected antibiotics in the Victoria Harbour and the Pearl river, South China using high-performance liquid chromatography-electrospray ionization tandem mass spectrometry. *Environmental Pollution* 145, 672-679.
- Xu, W.H., Zhang, G., Wai, O.W.H., Zou, S.C., Li, X.D., **2009**. Transport and adsorption of antibiotics by marine sediments in a dynamic environment. *Journal of Soils and Sediments* 9, 364-373.
- Yan, C., Yang, Y., Zhou, J., Liu, M., Nie, M., Shi, H., Gu, L., **2013**. Antibiotics in the surface water of the Yangtze Estuary: Occurrence, distribution and risk assessment. *Environmental Pollution* 175, 22-29.
- Yang, S., Chen, Y., Lou, L., Wu, X., **2005**. Involvement of chloride anion in photocatalytic process. *Journal of Environmental Sciences* 17, 761-765.
- Yang, L.H., Ying, G.G., Su, H.C., Stauber, J.L., Adams, M.S., Binet, M.T., **2008**. Growth-inhibiting effects of 12 antibacterial agents and their mixtures on the freshwater microalga *Pseudokirchneriella subcapitata*. *Environmental Toxicology and Chemistry* 27, 1201-1208.
- Yang, J.F., Ying, G.G., Zhao, J.L., Tao, R., Su, H.C., Chen, F., **2010a**. Simultaneous determination of four classes of antibiotics in sediments of the Pearl rivers using RRLC-MS/MS. *Science of the Total Environment* 408, 3424-3432.
- Yang, H., Li, G., An, T., Gao, Y., Fu, J., **2010b**. Photocatalytic degradation kinetics and mechanism of environmental pharmaceuticals in aqueous suspension of TiO₂: A case of sulfa drugs. *Catalysis Today* 153, 200-207.
- Yang, X., Flowers, R.C., Weinberg, H.S., Singer, P.C., **2011**. Occurrence and removal of pharmaceuticals and personal care products (PPCPs) in an advanced wastewater reclamation plant. *Water Research* 45, 5218-5228.
- Yasojima, M., Nakada, N., Komori, K., Suzuki, Y., Tanaka, H., **2006**. Occurrence of levofloxacin, clarithromycin and azithromycin in wastewater treatment plant in Japan. *Water Science and Technology* 53, 227-233.
- Yurdakal, S., Loddò, V., Augugliaro, V., Berber, H., Palmisano, G., Palmisano, L., **2007**. Photodegradation of pharmaceutical drugs in aqueous TiO₂ suspensions: Mechanism and kinetics. *Catalysis Today* 129, 9-15.
- Zaleska, A., **2008**. Doped-TiO₂: A review. *Recent Patents on Engineering* 2, 157-164.
- Zhang, H.C., Huang, C.H., **2005**. Oxidative transformation of fluoroquinolone antibacterial agents and structurally related amines by manganese oxide. *Environmental Science & Technology* 39, 4474-4483.

- Zhang, H.C., Huang, C.H., **2007**. Adsorption and oxidation of fluoroquinolone antibacterial agents and structurally related amines with goethite. *Chemosphere* 66, 1502-1512.
- Zhang, X., Sun, D.D., Li, G., Wang, Y., **2008**. Investigation of the roles of active oxygen species in photodegradation of azo dye AO7 in TiO₂ photocatalysis illuminated by microwave electrodeless lamp. *Journal of Photochemistry and Photobiology A: Chemistry* 199, 311-315.
- Zhao, S., Jiang, H., Li, X., Mi, T., Li, C., Shen, J., **2007**. Simultaneous determination of trace levels of 10 quinolones in swine, chicken, and shrimp muscle tissues using HPLC with programmable fluorescence detection. *Journal of Agricultural Food and Chemistry* 55, 3829-3834.
- Zhao, L., Dong, Y.D., Wang, H., **2010**. Residues of veterinary antibiotics in manures from feedlot livestock in eight provinces of China. *Science of the Total Environment* 408, 1069-1075.
- Zhou, J., Xue, X., Chen, F., Zhang, J., Li, Y., Wu, L., Chen, L., Zhao, J., **2009**. Simultaneous determination of seven fluoroquinolones in royal jelly by ultrasonic-assisted extraction and liquid chromatography with fluorescence detection, *Journal of Separation Science* 32(7), 955-964.
- Zhou, T., Lim, T.T., Chin, S.S., Fane, A.G., **2011**. Treatment of organics in reverse osmosis concentrate from municipal wastewater reclamation plant: Feasibility test of advanced oxidation processes with/without pretreatment. *Chemical Engineering Journal* 166, 932-939.
- Zhou, L.J., Ying, G.G., Liu, S., Zhang, R.Q., Lai, H.J., Chen, Z.F., Pan, C.G., **2013**. Excretion masses and environmental occurrence of antibiotics in typical swine and dairy cattle farms in China. *Science of the Total Environment* 444, 183-195.
- Ziylan, A., Ince, N.H., **2011**. The occurrence and fate of anti-inflammatory and analgesic pharmaceuticals in sewage and fresh water: Treatability by conventional and non-conventional processes. *Journal of Hazardous Materials* 187, 24-36.
- Zorita, S., Martensson, L., Mathiasson, L., **2009**. Occurrence and removal of pharmaceuticals in a municipal sewage treatment system in the south of Sweden. *Science of the Total Environment* 407, 2760-2770.
- Zou, S., Xu, W., Zhang, R., Tang, J., Chen, Y., Zhang, G., **2011**. Occurrence and distribution of antibiotics in coastal water of the Bohai bay, China: Impacts of river discharge and aquaculture activities. *Environmental Pollution* 159, 2913-2920.
- Zuccato, E., Castiglioni, S., Fanelli, R., **2005**. Identification of the pharmaceuticals for human use contaminating the Italian aquatic environment. *Journal of Hazardous Materials* 122, 205-209.
- 3M, **2012**. <http://corporate.discovery.com/blog/2012/10/17/deepika-kurup-named-americas-top-young-scientist-in-2012-discovery-education-3m-young-scientist-challenge/>, last visited 11/02/2014.

Curriculum Vitae

Personal information

Last name: Van Doorslaer

First name: Xander

Date of birth: 4th of February 1985

Place of birth: Dendermonde

Address: Prinsemeers 51, 9200 Dendermonde

Civil status: not married ... yet

Telephone: +32(0) 472 88 11 98

Email: Xander.VanDoorslaer@UGent.be VanDoorslaer.Xander@Gmail.com

Education

2008-2014: PhD training at Faculty of Bioscience Engineering, Ghent University

Promotor: Prof. dr. ir. J. Dewulf and Prof. dr. ir. K. Demeestere

2011-2014: Opleiding tot milieucoördinator type A, Instituut Voor Permanente Vorming, Universiteit Gent

2003-2008: Bio-engineer in Chemistry, Faculty of Bioscience Engineering, Ghent University

Master thesis: Efficiëntie van seleniumbemesting bij grasland en maïs.

Promotor: Prof. dr. ir. F. Tack

1997-2003: Science-mathematics (8hours/week), Atheneum, Dendermonde

Professional experiences

2008-2014: PhD training Faculty of Bioscience Engineering, Department of Sustainable Organic Chemistry and Environmental Technology: assistant and doctoral researcher in Applied Biological Sciences.

Thesis: Advanced oxidation of fluoroquinolone antibiotics in water by heterogeneous photocatalysis.

Promoters: Prof. dr. ir. J. Dewulf and Prof. dr. ir. K. Demeestere

Teaching activities

Teaching practical exercises: Proceskunde I, Analyse van Micropolluenten, Chemische Analyse Technieken.

Elaboration of new practical exercises: Chemische Analyse Technieken.

Teaching during contact days for the course Milieucoördinator type A, Instituut Voor Permanente Vorming (IVPV), Ghent.

Tutor of 3 Master students Bio-engineering, 1 Master student Environmental Sanitation, 1 International Master student of Science in Environmental Technology and Engineering, and 1 Bachelor student Chemistry and Environment (Kaho Sint-Lieven, Department Ghent).

Peer-reviewed publications in international scientific journals

Van Doorslaer, X., Demeestere, K., Heynderickx, P.M., Van Langenhove, H., Dewulf, J., **2011**. UV-A and UV-C induced photolytic and photocatalytic degradation of aqueous ciprofloxacin and moxifloxacin: Reaction kinetics and role of adsorption. *Applied Catalysis B-Environmental* 101, 540-547.

Van Doorslaer, X., Heynderickx, P.M., Demeestere, K., Debevere, K., Van Langenhove, H., Dewulf, J., **2012**. TiO₂ mediated heterogeneous photocatalytic degradation of moxifloxacin: Operational variables and scavenger study. *Applied Catalysis B-Environmental* 111-112, 150-156.

Van der Weeën, P., Baetens, J.M., Verwaeren, J., Van Doorslaer, X., Heynderickx, P.M., Dewulf, J., De Baets, B., **2012**. Modeling the photocatalytic degradation of moxifloxacin by means of a stochastic cellular automaton. *Chemical Engineering Journal* 188, 181-190.

Van Doorslaer, X., Demeestere, K., Heynderickx, P.M., Caussyn, M., Van Langenhove, H., Devlieghere, F., Vermeulen, A., Dewulf, J., **2013**. Heterogeneous photocatalysis of moxifloxacin: Identification of degradation products and determination of residual antibacterial activity. *Applied Catalysis B-Environmental* 138-139, 333-341.

Van Doorslaer, X., Dewulf, J., De Maerschack, J., Van Langenhove, H., Demeestere, K., **2014**. Heterogeneous photocatalysis of moxifloxacin in hospital effluent: effect of selected matrix constituents. Submitted to *Chemical Engineering Journal*.

Van Doorslaer, X., Haylamicheal, I.D., Dewulf, J., Van Langenhove, H., Janssen, C., Demeestere, K., **2014**. Heterogeneous photocatalysis of moxifloxacin in water: chemical transformation and ecotoxicity. *Chemosphere* doi:10.1016/j.chemosphere.2014.03.048

Van Doorslaer, X., Dewulf, J., Van Langenhove, H., Demeestere, K., **2014**. Fluoroquinolone antibiotics: an emerging class of environmental micropollutants. In preparation.

Contributions to international conferences

Van Doorslaer, X., Demeestere, K., Heynderickx, P.M., Van Langenhove, H., Dewulf J., **2010**. UV-A and UV-C photolytic and photocatalytic degradation of ciprofloxacin and moxifloxacin: reaction kinetics and adsorption. Proceedings of the Advanced Oxidation Technologies for treatment of water, air, and soil conference (AOTs-16), 15/11/2010-18/11/2010, San Diego, California, USA. *Oral presentation by Van Doorslaer X.*

Van Doorslaer, X., Heynderickx, P.M., Demeestere, K., Van Langenhove, H., Dewulf, J., **2011**. TiO₂ mediated heterogeneous photocatalytic degradation of moxifloxacin: operational variables study. Proceedings of the Photocatalytic and Advanced Oxidation Technologies for the treatment of water, air, soil and surfaces conference (PAOT), 04/07/2011-08/07/2011, Gdansk, Poland. *Oral presentation by Van Doorslaer X.*

Van Doorslaer, X., Demeestere, K., Heynderickx, P.M., Caussyn, M., Van Langenhove, H., Devlieghere, F., Vermeulen, A., Dewulf, J., **2013**. Photocatalytic degradation of the antibiotic moxifloxacin: a deeper look at the degradation products and residual antibacterial activity. Proceedings of the 13th International Conference on Environmental Science and Technology (CEST), 05/09/2013-07/09/2013, Athens, Greece. *Oral presentation by Van Doorslaer X.*

Van Doorslaer, X., Demeestere, K., Heynderickx, P.M., Van Langenhove, H., Dewulf, J., **2013**. Photocatalytic removal of the fluoroquinolone moxifloxacin in water: mechanisms, ecologic effects, and application in a real matrix. Proceedings of the 3rd European conference on Environmental Applications of Advanced Oxidation Processes (EAAOP-3), 27/10/2013-30/10/2013, Almeria, Spain. *Oral presentation by Van Doorslaer X.*

Contribution to summer schools

Demeestere, K., Van Doorslaer, X., **2013**. Heterogeneous photocatalysis as an advanced oxidation technique to remove organic micropollutants from water. IMETE Summer School, 13/09/2013, Ghent, Belgium.

Oral presentation by Demeestere K. and Van Doorslaer X.

Study stages abroad

01/08/2009-14/09/2009: Stay at National Taiwan University, Department of Chemical Engineering, Taipei, Taiwan.



Fig. PhD The essential ingredients for a succesful PhD recipe. **P**atience, **H**ard work, and **D**edication.

